An investigation of the three-dimensional thermo/hydro/mechanical behaviour of large scale in-situ experiments

Troy Alexander Melhuish

Geoenvironmental Research Centre

Cardiff School of Engineering

Cardiff University

Thesis submitted in candidature for the degree of Doctor of Philosophy at Cardiff University

December 2004

ProQuest LLC
789 East Eisenhower Parkway
P.O. Box 1346
Ann Arbor, MI 48106-1346

DECLARATION

This work has not previously been accepted in substance for any degree and is not being concurrently submitted in candidature for any degree.

Signed ..... (candidate)

Date .....

STATEMENT 1

This thesis is the result of my own investigations, except where otherwise stated. Other sources are acknowledged by footnotes giving explicit references. A bibliography is appended.

Signed ..... (candidate)

Date .....

STATEMENT 2

I hereby give consent for my thesis, if accepted, to be made available for photocopying and for inter-library loan, and for the title and summary to be made available to outside organisations.

Signed .....(candidate)

Date .....

Acknowledgements

I would first like to thank SKB, AECL, the EPSRC and the University of Wales, Cardiff for providing the necessary resources and opportunity that allowed me to undertake this research.

I would also like to offer a special thank you to both of my supervisors, Dr. Peter Cleall and Prof. Hywel Thomas, for their advice, support and encouragement throughout the course of this research period. Their help is greatly appreciated.

My thanks also go to all of my friends and colleagues at the Geoenvironmental Research Centre, particularly Dr. Suresh Seetharam and Dr. Deping Ding for their technical assistance and cooperation at the various stages during this study.

The completion of this thesis has been greatly helped by the support and understanding of my family and my 'new' family. I am a very fortunate person indeed.

Finally, I would like to thank my wife, Sarah. Her optimism and unreserved love have helped me reach the top of the mountain.

Summary

This thesis presents an investigation of the three-dimensional thermo/hydro/mechanical behaviour of large scale in-situ experiments for the disposal of high-level nuclear waste. Two experiments are investigated in this work, which include principally the Prototype Repository Experiment and secondly the Tunnel Sealing Experiment.

A comprehensive numerical modelling exercise is performed in this investigation to study the coupled flow and deformation behaviour in the experiments. This is undertaken by applying the finite element modelling code COMPASS (COde for Modelling PArtially Saturated Soils) developed at Cardiff University. This is a mechanistic model which describes heat transfer, moisture migration, solute transport and air transfer in a material coupled with stress/strain behaviour. A standard finite element method is used for spatial discretisation and a finite difference method is used for temporal discretisation.

Due to the size and complexity of the experiments, sophisticated finite element models are analysed. To provide the facility to tackle highly computationally demanding simulations COMPASS has been developed via the application of iterative solution methods, parallel computing techniques and three-dimensional visualisation techniques.

In the simulation of the Prototype Repository experimental data was available concerning the thermal, hydraulic and mechanical fields, and therefore a systematic exercise to compare the results is presented. Key mechanisms seen in the experiment are captured in the analyses and the model simulates well both the thermal and hydraulic behaviour in the barrier materials. With respect to the deformation behaviour the model identifies important trends and provides reasonable agreement with the observed behaviour.

In the simulation of the Tunnel Sealing Experiment the behaviour of the clay bulkhead is investigated with a limited amount of experimental evidence available. Preliminary comparisons with the observed behaviour show that the thermal field is slightly over predicted. However, key trends in the mechanical response are identified and the hydraulic behaviour is captured reasonably well.

Contents

Chapter 3 Theoretical Formulation

Chapter 4 Finite Element Formulation and Computer Modelling

Chapter 5 The Prototype Repository Project

Chapter 6 Preliminary Results from the Prototype Repository Experiment

Chapter 7 Simulation of the Prototype Repository Experiment

Chapter 8 Simulation of the Tunnel Sealing Experiment

Notation

a	Constant used in equations (2.4), (2.5), (2.6) and (2.7)
A	Plastic modulus, defined in equation (3.137)
A_s	Defined in equation (3.115)
A_T	Defined in equation (3.116)
$\mathbf{A}$	Defined in equation (4.60)
b	Constant used in equations (2.4), (2.5), (2.6), (2.7) and (7.2)
b_x, b_y, b_z	Two-dimensional body forces
$\boldsymbol{b}$	Vector of body force
$\mathbf{B}$	Strain-displacement matrix, defined in equation (4.44)
c	Constant used in equations (2.4), (2.5), (2.6) and (2.7)
C	Corrected value, defined in equations (4.65) and (4.66)
C_{aa}	Defined in equation (3.67)
C_{al}	Defined in equation (3.65)
C_{aT}	Defined in equation (3.66)
C_{au}	Defined in equation (3.68)
C_{la}	Defined in equation (3.46)
C_{ll}	Defined in equation (3.44)
C_{lT}	Defined in equation (3.45)
C_{lu}	Defined in equation (3.47)
C_m	Compressive index with respect to suction, defined in equation (2.2)
C_{pda}	Specific heat capacity of dry air
C_{pl}	Specific heat capacity of liquid
C_{ps}	Specific heat capacity of solid particles
C_{pv}	Specific heat capacity of vapour
C_t	Compressive index with respect to net stress, defined in equation (2.2)
C_{Ta}	Defined in equation (3.91)
C_{Tl}	Defined in equation (3.89)
C_{TT}	Defined in equation (3.90)
C_{Tu}	Defined in equation (3.92)
C_{ua}	Defined in equation (3.144)

C_{ul}	Defined in equation (3.142)
C_{uT}	Defined in equation (3.143)
C_{uu}	Defined in equation (3.145)
$\mathbf{C}$	Defined in equation (4.60)
$\mathbf{C_{aa}}$	Defined in equation (4.35)
$\mathbf{C_{al}}$	Defined in equation (4.33)
$\mathbf{C_{aT}}$	Defined in equation (4.34)
$\mathbf{C_{au}}$	Defined in equation (4.36)
$\mathbf{C_{la}}$	Defined in equation (4.17)
$\mathbf{C_{ll}}$	Defined in equation (4.15)
$\mathbf{C_{lT}}$	Defined in equation (4.16)
$\mathbf{C_{lu}}$	Defined in equation (4.18)
$\mathbf{C_{Ta}}$	Defined in equation (4.26)
$\mathbf{C_{Tl}}$	Defined in equation (4.24)
$\mathbf{C_{TT}}$	Defined in equation (4.25)
$\mathbf{C_{Tu}}$	Defined in equation (4.27)
$\mathbf{C_{ua}}$	Defined in equation (4.56)
$\mathbf{C_{ul}}$	Defined in equation (4.54)
$\mathbf{C_{uT}}$	Defined in equation (4.55)
$\mathbf{C_{uu}}$	Defined in equation (4.57)
d	Constant used in equations (2.4), (2.5), (2.6) and (2.7)
D_{atms}	Molecular diffusivity of vapour through air
D_m	Coefficient of water content changes with respect to suction, defined in equation (2.3)
D_{MV}	Defined in equation (7.9)
D_l	Coefficient of water content changes with respect to net stress, defined in equation (2.3)
D_{TV}	Defined in equation (7.9)
$\boldsymbol{D}$	Elasticity matrix
$\boldsymbol{Dep}$	Elasto-plastic stress-strain matrix
e	Void ratio
e_s	Void ratio at saturation
e_0	Initial void ratio

E	Young's modulus
E_{ss}	Sink/source term
f	Flow area factor
F	Applied force
F_1	Yield function as defined in equation (3.121)
F_2	Yield function as defined in equation (3.123)
$\mathbf{f}_a$	Defined in equation (4.39)
$\mathbf{f}_l$	Defined in equation (4.22)
$\mathbf{f}_T$	Defined in equation (4.31)
$\mathbf{f}_u$	Defined in equation (4.58)
$\mathbf{F}_h$	Approximate heat flux normal to the boundary surface
g	Gravitational constant
G	Shear modulus
G_s	Specific weight
h	Relative humidity
H_c	Heat capacity of the soil
H_s	Henry's volumetric coefficient of solubility
i	Iteration level
J_a	Defined in equation (3.71)
J_l	Defined in equation (3.51)
J_T	Defined in equation (3.97)
k	Constant related to the cohesion of the soil, defined in equation (3.122)
k_l	Intrinsic permeability of pore liquid
k_a	Effective permeability of pore air
K	Bulk modulus
K_a	Unsaturated conductivity of pore air
K_{aa}	Defined in equation (3.70)
K_{al}	Defined in equation (3.69)
$K_{fracture}$	Saturated hydraulic conductivity of a representative fracture
K_l	Unsaturated hydraulic conductivity
K_m	Modified hydraulic conductivity due to micro/macro effects
K_{la}	Defined in equation (3.50)
K_{ll}	Defined in equation (3.48)
K_{lT}	Defined in equation (3.49)

K_{rock}	Saturated hydraulic conductivity of the rock mass
K_{sat}	Saturated hydraulic conductivity
K_{Ta}	Defined in equation (3.96)
K_{Tl}	Defined in equation (3.94)
K_{TT}	Defined in equation (3.95)
K_{va}	Defined in equation (4.12)
K_{vl}	Defined in equation (4.10)
K_{vT}	Defined in equation (4.11)
$\mathbf{K_{aa}}$	Defined in equation (4.38)
$\mathbf{K_{al}}$	Defined in equation (4.37)
$\mathbf{K_{la}}$	Defined in equation (4.21)
$\mathbf{K_{ll}}$	Defined in equation (4.19)
$\mathbf{K_{lT}}$	Defined in equation (4.20)
$\mathbf{K_{Ta}}$	Defined in equation (4.30)
$\mathbf{K_{Tl}}$	Defined in equation (4.28)
$\mathbf{K_{TT}}$	Defined in equation (4.29)
L	Latent heat of vaporisation
M	Slope of the critical state line
$\mathbf{m}$	Unit vector
n	Porosity
$\underline{\boldsymbol{n}}$	Direction cosine normal to the surface, defined in equation (4.8)
N_s, N_r	Shape functions
$N(s)$	Intercept of the normal compression line for a soil at suction s
$N(0)$	Intercept of the normal compression line for the saturated soil
$\mathbf{N}$	Matrix of shape functions
p	Net mean stress
p_{atms}	Atmospheric pressure
p_i	Initial net mean stress
p_c	Reference stress
p_s	Parameter controlling suction effect on cohesion
p_0	Preconsolidation stress at a suction s
p_0^*	Preconsolidation stress of saturated soil
P_0	Air entry value, defined in equation (7.6)

$\mathbf{P}$	Strain matrix
q	Deviatoric stress
$\mathbf{Q}$	Heat flux per unit area
Q_1	Plastic potential for LC yield surface, defined in equation (3.124)
Q_2	Plastic potential for SI yield surface, defined in equation (3.125)
r	Radial distance from centre of deposition hole
r	Parameter controlling the maximum stiffness of the soil
R_Ω	Residual error introduced due to approximation
R_{da}	Specific gas constant for dry air
R_v	Specific gas constant for water vapour
s	Suction at a temperature T
s_i	Initial suction
s_m	Matric suction
s_o	Osmotic suction
s_r	Suction at reference temperature T_r
s_t	Total suction
s_0	Critical value of suction - suction hardening parameter
S_a	Degree of saturation of pore air
S_l	Degree of saturation of pore water
t	Time
T	Temperature
T_r	Reference temperature
$\hat{T}$	Approximate value of temperature
$\hat{\underline{T}}_r$	Approximate traction, defined in equation (4.51)
$(\nabla T)_a/\nabla T$	Ratio of the microscopic temperature gradient in pore space to the macroscopic temperature gradient
$\mathbf{T}_s$	Temperature vector, defined in equation (4.13)
$\dot{\mathbf{T}}_s$	Time differential of temperature, as defined in equation (4.59)
$\mathbf{TL}_{abs}$	Matrix of absolute tolerances
$\mathbf{TL}_{rel}$	Matrix of relative tolerances
u_a	Pore-air pressure
u_{da}	Partial pressure of dry air
u_l	Pore-water pressure

u_v	Partial pressure of water vapour
$\hat{u}_a$	Approximate value of pore air pressure
$\hat{u}_l$	Approximate value of pore water pressure
u_{var}	Defined in equation (4.1)
$\hat{u}_{var}$	Defined in equation (4.1)
$\mathbf{u}$	Displacement vector
$\mathbf{u}_{as}$	Pore air pressure vector, defined in equation (4.13)
$\mathbf{u}_{ls}$	Pore water pressure vector, defined in equation (4.13)
$\mathbf{u}_s$	Displacement vector, defined in equation (4.13)
$\hat{\mathbf{u}}$	Approximate value of displacement
$\dot{\mathbf{u}}_{as}$	Time differential of pore air pressure, as defined in equation (4.59)
$\dot{\mathbf{u}}_{ls}$	Time differential of pore water pressure, as defined in equation (4.59)
$\dot{\mathbf{u}}_s$	Time differential of displacement, as defined in equation (4.59)
v	Specific volume
v_0	Initial specific volume
v_s	Specific volume due to suction changes
v_v	Mass flow factor
V_s	Volume of solids
$\mathbf{v}_a$	Velocity of air
$\mathbf{v}_l$	Velocity of liquid
$\mathbf{v}_v$	Velocity of water vapour
$\hat{\mathbf{v}}_{fn}$	Approximate velocity of free air flux normal to the boundary surface
$\hat{\mathbf{v}}_{an}$	Approximate velocity of dissolved air flux normal to the boundary surface
$\hat{\underline{\mathbf{v}}}_{ln}$	Approximate liquid velocity normal to the boundary surface
$\hat{\underline{\mathbf{v}}}_{vn}$	Approximate pressure vapour velocity normal to the boundary surface
$\hat{\underline{\mathbf{v}}}_{vd}$	Approximate diffusive vapour velocity normal to the boundary surface
w	Water content
x, y, z	Global coordinates
α	Constant used in equation (7.2)
α_q	Parameter for non-associated flow rule
α_T	Coefficient of thermal expansion
β	Parameter controlling the rate of increase of soil stiffness with suction

β_1	Material parameter defined in equations (7.5), (7.6), (8.7) and (8.8)
χ	Parameter related to the degree of saturation, defined in equation (2.1)
χ_1, χ_2	Plastic multipliers determined through plastic consistency conditions
δ	Parameter used in equation (7.1)
∂V	Incremental volume
ε	Total strain
$\boldsymbol{\varepsilon}$	Strain vector
ε^e	Elastic component of strain
ε^p	Plastic component of strain
ε_q^e	Elastic deviatoric strain
ε_q^p	Plastic deviatoric strain
ε_p^e	Elastic component of strain due to stress changes
ε_s^e	Elastic component of strain due to suction changes
ε_T^e	Elastic component of strain due to temperature changes
ε_v	Volumetric strain
ε_v^p	Total volumetric plastic strain
ε_{vp}^p	Volumetric plastic strain due to stress changes
ε_{vs}^p	Volumetric plastic strain due to suction changes
ϕ_l	Defined in equation (4.62)
γ_l	Unit weight of liquid
ϕ'	Angle of friction for saturated soils
κ	Stiffness parameter for changes in net mean stress in the elastic region
κ_s	Stiffness parameter for changes in suction in the elastic region
λ	Coefficient of thermal conductivity of saturated soil
λ_s	Stiffness parameter for changes in suction for virgin states of the soil
λ_T	Coefficient of thermal conductivity of unsaturated soil
$\lambda(0)$	Stiffness parameter for changes in net mean stress for virgin states of saturated soil
$\lambda(s)$	Stiffness parameter for changes in net mean stress for virgin states of the soil
μ_a	Absolute viscosity of air

μ_l	Absolute viscosity of pore liquid
θ	Volumetric water content
θ_a	Volumetric content of air
θ_l	Volumetric liquid content
θ_{res}	Residual water content, defined in equation (7.2)
θ_{sat}	Saturated water content, defined in equation (7.2)
θ_v	Volumetric vapour content
ξ	Surface energy at temperature T
ξ_r	Surface temperature at reference temperature T_r
ρ_0	Density of saturated soil water vapour
ρ_b	Bulk density
ρ_d	Dry density
ρ_{da}	Density of dry air
ρ_l	Density of liquid water
ρ_s	Density of solid particles
ρ_v	Density of water vapour
σ	Total stress
σ'	Effective stress
σ''	Net stress
σ_1, σ_2, σ_3	Principal stresses
σ_x, σ_y, σ_z	Normal stresses
τ_{xz}, τ_{zx}	Shear stresses
τ_v	Tortuosity factor
υ	Poisson's ratio
ϖ	Integration constant, defined in equation (4.61)
ψ	Capillary potential
Γ^e	Element boundary surface
ϑ	Defined in equation (4.62)
∇	Gradient operator
Ω	Heat content of moist soil
Ω^e	Element domain
ϕ	Variable vector
ζ	Residual force, defined in equation (4.67)

Chapter 1

Introduction

Most radioactive waste is produced by the nuclear power industry. It is estimated that over 30 countries now operate between 400 and 500 nuclear power reactors worldwide. Following the introduction of the United Nations Framework Convention on Climate Change (United Nations, 1992) and the adoption of the Kyoto Protocol in 1997 many countries have agreed to reduce their emissions of greenhouse gases and to promote more sustainable, renewable sources of energy by 2012. The use of fossil fuels to generate energy has declined and nuclear power has become a more viable alternative. Nuclear energy produces virtually no greenhouse gases, but public concern over safety, transport and disposal of radioactive wastes means that the responsible employment of nuclear power will likely remain limited. It now accounts for about 6.8 % of global energy supplies.

More recently, decommissioning of nuclear sites has become a major issue in governmental policy as facilities reach the end of their useful lives. It is estimated that by 2010 there will be almost 250 nuclear power plants awaiting decommissioning (BNFL, 2004). This presents a number of challenges to the nuclear power industry in terms of safe demolition, maintenance, and the generation of additional radioactive waste.

In the nuclear power industry radioactive fuel undergoes a cycle of extraction, preparation, use and disposal. Throughout the course of this cycle there are hazards that threaten health and property and that, in some instances, present society with enormous social and ethical questions. Handling the waste from the reactors is an important environmental issue and the method in which it is handled depends largely on the local conditions and the type of waste. The fuel is considered spent when approximately 75 % of the Uranium-235 has been fissioned. Many of the by-products of this process are extremely toxic and their storage and disposal present many difficult problems. Not only are these elements highly radioactive, but they also continue to generate heat. Both the radioactivity and the heat decline through the process of radioactive decay but this process can take thousands of years for the elements to reach safe radiation levels. The current systems in place for the

storage of radioactive waste are land-based and comprise of deep geological storage, storage at moderate depths and storage at the surface.

Radioactive waste is classified under four levels depending on the intensity of the radioactivity and the duration of the half-life. Very Low-Level Waste (VLLW) covers wastes with very low concentrations of radioactivity. It arises from a variety of sources, including hospitals and industry in general. Because VLLW contains little total radioactivity, it can be disposed of safely with domestic refuse either directly at landfill sites or indirectly after incineration. Low-Level Waste (LLW) includes metals, soils, building rubble and organic materials, which arise principally as lightly, contaminated miscellaneous scrap. Metals are mostly in the form of redundant equipment. Organic materials are mainly in the form of paper towels, clothing and laboratory equipment that have been used in areas where radioactive materials are used, such as hospitals, research establishments and industry. Intermediate-Level Waste (ILW) is waste with radioactivity levels exceeding the upper boundaries for LLW. ILW arises mainly from the reprocessing of spent fuel, and from general operations and maintenance of radioactive plant. The major components of ILW are metals and organic materials, with smaller quantities of cement, graphite, glass and ceramics. This waste is often stored in repositories on the ground surface or in blasted chambers at a moderate depth under ground. In many countries this waste is processed to reduce the volume and activity (by means of combustion) or it can be transformed into more chemically durable, environmentally safer products through a process of vitrification. High-Level Waste (HLW) is the fourth and final level and comes primarily from the nuclear power industry. It is extremely hazardous and is characterised by an extremely long half-life and high activity level. Currently, no country has a complete system in place for the permanent disposal of spent nuclear fuel and so the high-level waste is placed in intermediate storage in either water-cooled or air-cooled storage systems.

In the UK the amount of radioactive waste is very small compared with the total industrial and domestic waste produced each year and accounts for approximately 0.02 % of the total waste (BNFL, 2004). Each year the UK produces around 40 million cubic metres of industrial waste compared to 16,000 cubic metres of nuclear waste. Figures published by DEFRA/NIREX in 2001 showed that there were 1,960 m^3 of high-level waste, 75,400 m^3

of intermediate-level waste and 14,700 m^3 of low-level waste held in the UK (NIREX, 2004).

Given the dangers of accidental radioactive release into the environment, long-term disposal must meet acceptable criteria of safety. Since the lifetimes of fission products are extraordinarily long, safe disposal presents unprecedented technological and societal problems. Technologically, the method of disposal must ensure a high degree of isolation for many thousands of years, thus requiring containment materials and disposal facilities that are known to be stable for periods of this magnitude. Furthermore, the technology requires a great deal of research and development and needs to be cost effective to facilitate the disposal.

There is a broad international consensus regarding the principles for long-term disposal of spent nuclear waste, and in the majority of countries, these systems are under development. The methods are based on systems with several barriers located in isolation at great depths in geological formations. This means that the placement of wastes in rock or sedimentary formations needs to remain intact and free from any seismic or anthropogenic interference for many thousands of years. Such formations exist both on land and beneath the oceans, although identifying them does present further problems. However, attempts to develop an acceptable disposal technique have proven difficult. The continued generation of decay heat may cause unstable molten conditions in some of the disposal media, and there have been concerns that these conditions might lead to rock fractures that in turn could permit migration of radioactive nuclides into groundwater. Therefore, several countries have undertaken extensive research programmes into the feasibility of the deep geological disposal concept.

The structure and design of the disposal schemes depend on the geological conditions on site, but also on the different requirements and laws that exist in the various countries.

In Belgium, the National Radioactive Waste Agency (ONDRAF-NIRAS) is responsible for the final disposal of radioactive waste. They are interested in deep clay layers, and much of the recent research has focussed on the boom clay formation underlying the Mol research centre.

AECL (Atomic Energy of Canada Limited) is responsible for research and development on a final repository for high-level waste in Canada. Final disposal is planned to take place in

granitic rock approximately 500 metres beneath the surface. The fuel will be encapsulated in copper canisters and surrounded by bentonite clay.

Finland selected a site for its deep geological repository near the nuclear power plant in Olkiluoto in 2000. Work at the final repository is expected to start in 2020.

In Germany they are studying how salt formations can be used to store spent nuclear fuel. BfS, Bundesamt für Strahlenschutz (the Federal Office for Radiation Protection), has been given responsibility by the federal government for final disposal of radioactive waste. Final disposal is planned to take place in salt formations in Gorleben. However, doubts have been expressed about using the salt dome for final disposal and an expert group, AkEnd, has been appointed to arrive at selection criteria for finding suitable sites for a future repository. The goal is that all radioactive waste will be disposed of at one site.

SKB (Svensk Kärnbränslehantering AB) the Swedish Nuclear Fuel and Waste Management Company is responsible for the handling, transport, storage and disposal of all nuclear waste produced by the Swedish nuclear power stations. The proposed disposal concept shares many characteristics with that adopted by AECL and site investigation work is currently underway to select a suitable repository site.

In Switzerland, research conducted by NAGRA has focused on both crystalline bedrock and opalinus clay and currently two sites at Northern Aargau and Zurcher Weinland are being considered.

In the UK, they reprocess both some of their own spent nuclear fuel and some from other countries. This reduces the waste quantities but generates radioactive liquid residues that are cast in glass, encapsulated and placed in intermediate storage until such time as they can be deposited in a geological formation. Planning application for a rock characterisation facility at Sellafield was rejected in 1997 and NIREX is now developing the site specific Sellafield design into a series of generic repository designs for use at other potential sites in the UK.

In the USA they are studying a volcanic type of rock in Nevada, known as tuff and it is envisaged that the first geological repository for high-level waste will be in operation by 2010. The current plans are to locate this facility below the Yucca Mountain in an unsaturated zone.

The majority of the disposal schemes under development are designed around a multi-barrier concept (see Figure 1.1). This concept contains some or all of the following components – the radioactive waste itself, the waste container, an engineered buffer material, the natural barrier and the tunnel backfill and seals. Each component of this system provides certain functions and when coupled together it is envisaged that the multi-barrier concept will provide an effective means for the long-term disposal of high-level nuclear waste. A great deal of research and experimental work has been conducted to investigate this disposal concept and in particular the use of unsaturated clays to form the buffer barrier has become the primary focus in a number of research programmes (Chapman and McKinley, 1987). The use of swelling clays such as bentonite from the montmorillonite family have been given a great deal of attention due to its advantageous properties, these were defined by Felix et al. (1996) as – a high swelling potential and relatively low dry densities, naturally sealing any fractures that may develop in the bentonite as it dries under high temperatures; a high sorption capacity, to prevent radionuclide and chemical transfer into the groundwater; and, a low permeability to liquid and gas, thus isolating the waste canister from corrosive elements in the groundwater.

The experimental work performed to date has varied from small scale laboratory tests focussing on specific phenomena to large scale in-situ experiments intended to investigate coupled thermo/hydro/mechanical behaviour of the multi-barrier materials on a full scale under realistic conditions. These experiments not only highlight the feasibility of the proposed concepts for disposal but also provide a great deal of quality information to improve knowledge and understanding and to develop and validate computer models to predict the long-term transient behaviour of the systems.

A number of large scale in-situ experiments are currently being conducted worldwide and in particular this thesis focuses on the numerical modelling of principally, SKB's Prototype Repository Experiment and secondly, AECL's Tunnel Sealing Experiment.

The Prototype Repository Experiment is currently being performed at the Äspö Hard Rock Laboratory in Sweden. The project is an international, EC-supported activity co-ordinated by SKB with additional partners from Sweden, Finland, Spain, Germany, UK and Japan. Its principal aim is to investigate, on a full-scale, the integrated performance of engineered barriers and near-field rock of a deep repository in crystalline rock with respect to heat

evolution, mechanics, water permeation, water chemistry, gas evolution and microbial processes under natural and realistic conditions (Svemar and Pusch, 2000).

In the Tunnel Sealing Experiment two different types of bulkheads are subjected to both hydraulic and thermal gradients. One of the bulkheads is fabricated using a high performance concrete and the other is made from highly compacted bentonite. As both these experiments involve complex coupling processes there is a requirement for a highly sophisticated numerical code to simulate the potential thermo/hydro/mechanical behaviour of the materials in a large scale three-dimensional model.

The foundation of this research work is based on the fully coupled heat, moisture, air and deformation model developed by Thomas and Sansom (1995), Thomas and He (1994, 1995, 1998) and Thomas and Cleall (1999). This work has been incorporated into a finite element modelling code called COMPASS (**CO**de for **M**odelling **PA**rtially **S**aturated **S**oils), a mechanistic model where the various aspects of soil behaviour are included in an additive manner. In this way the approach adopted describes heat transfer, moisture migration, solute transport and air transfer coupled with stress/strain behaviour in the material.

The conservation of energy equation governs the flow of heat. In COMPASS this approach includes flow of heat due to conduction, convection and the latent heat of vaporisation.

The conservation of mass equation governs the flow of moisture which is considered a combination of liquid and vapour transfer. Liquid and vapour flows caused by pressure gradients are governed by Darcy's Law and vapour transfer due to diffusion is represented by a modified Philip and de Vries approach (Philip and de Vries, 1957; Ewen and Thomas, 1989).

The movement of dry air within the soil is also governed by the conservation of mass equation. In the approach the movement of dry air includes both the bulk flow of free air, which is represented by Darcy's Law, and the movement of dissolved air in the pore liquid, which is represented by Henry's Law.

The stress/strain approach adopted in the model for the behaviour of soils under load is governed by an elasto-plastic constitutive relationship based on the state surface approach and is controlled by the stress equilibrium equation.

Approximation techniques and numerical methods are required to attain accurate solutions to the above complex coupled theoretical model. A numerical solution of the formulation is achieved by the implementation of finite element techniques for spatial discretisation and finite difference techniques for temporal discretisation.

To ensure the model provides accurate, realistic predictions for a number of different materials under varying conditions comprehensive verification and validation exercises have been performed in previous work. The numerical model has then been applied to the two large scale in-situ tests described above. In the Prototype Repository Experiment comparisons between experimental and numerical results are presented and discussed. For the Tunnel Sealing Experiment the numerical analysis was conducted as part of a programme of predictions requested by AECL with only limited experimental data available, and therefore only preliminary comparisons are made.

In order to undertake these large scale analyses the modelling infrastructure of the numerical model COMPASS has been developed, via the use of data visualisation techniques, parallel computing and iterative solution techniques. In addition to this the COMPASS code has been successfully interfaced with both a pre and post-processing software package capable of generating large three-dimensional finite element models and a fully interactive three-dimensional visualisation facility, based in Cardiff University.

1.1 Study objectives

The primary objectives of this research may be summarised as follows:

1. To review the past and current status of experimental programmes and numerical studies in relation to the investigation of the multiple-barrier concepts for the disposal of high-level nuclear waste in deep geological repositories.

2. To effectively combine and integrate the numerical code COMPASS with a suitable pre and post-processing piece of software to generate large scale three-dimensional models and finite element meshes.

3. To interface COMPASS with the highly sophisticated three-dimensional visualisation suite recently installed at the Geoenvironmental Research Centre. This is to be used to visualise and interpret results from the large scale numerical analyses investigated in this study.

4. To increase the performance and efficiency of COMPASS to tackle large scale three-dimensional problems via the application of high performance computing techniques and implementation of parallel computing methods.

5. To investigate the three-dimensional thermo/hydro/mechanical behaviour of the buffer, backfill and host rock in the Prototype Repository Experiment and to compare the simulated results to the experimentally measured results.

6. To investigate the fully coupled thermo/hydro/mechanical behaviour of the highly compacted bentonite bulkhead and host rock in the Tunnel Sealing Experiment and make preliminary comparisons with experimental data.

1.2 Research background

This section summaries research work that has been conducted previously at the Geoenvironmental Research Centre at Cardiff University in relation to the scope of this study. A thorough literature review is presented in Chapter 2.

Thomas (1985) presented a two-dimensional numerical solution of a theoretical model representing heat and mass transfer in unsaturated soil. Vapour flow was modelled by incorporating the de Vries approach (de Vries, 1958) and the latent heat of vaporisation was represented using Luikov (1966). The model was further developed (Thomas, 1987; Thomas, 1988a; Thomas 1988b) to include non-linearity of material parameters and revised time stepping schemes were investigated (Thomas and Rees, 1988; Thomas and Rees, 1990).

Experimental work on heat and moisture redistribution in unsaturated medium sand surrounding a heated rod was conducted by Ewen and Thomas (1987). A range of tests involving different combinations of initial moisture contents and heat output levels were carried out. The observed behaviour from this work was later simulated via a numerical model based on the variables of moisture content and temperature (Ewen and Thomas,

1989). The theoretical formulation was based upon the Philip and de Vries approach (Philip and de Vries, 1957) but with amendments to the vapour transfer diffusivities.

Thomas and King (1991) presented a coupled theory of heat and moisture transfer based on capillary potential and temperature. The governing equations were solved using the finite element method and it was found that there was good agreement between the numerical results and the experimental results from Ewen and Thomas (1987).

The approach presented by Thomas and King (1991) was further updated to include the effects of elevated pore air pressure (Thomas and Sansom, 1995). This model was validated against a series of laboratory controlled heating tests on medium sand (Ewen and Thomas, 1989; King, 1991; Thomas and Li, 1991) and a good correlation between the experimental and numerical results was obtained. An extension of the above formulation to incorporate three-dimensional simulation and visualisation was presented by Thomas et al. (1998b).

Thomas and Rees (1990, 1993) addressed the coupling of the flow models with models for deformation behaviour through the application of a numerical model to simulate experimentally measured seasonal ground movements. This was then followed by a coupled moisture transfer and deformation model to simulate isothermal consolidation in unsaturated soil (Thomas et al., 1992). The deformation behaviour of the soil was represented by the non-linear elastic state surface approach presented by Lloret and Alonso (1985). This model was later applied in the simulation of seasonal ground movements presented by Thomas and Zhou (1995).

As part of the assessment of the performance of high-level nuclear waste disposal schemes Thomas and He (1994) incorporated an elasto-plastic constitutive relationship (Alonso et al., 1990) into the coupled thermo/hydro/mechanical model to describe the behaviour of deformable unsaturated soils. The model has more recently been developed to incorporate highly expansive soil behaviour (Thomas and Cleall, 1999). Non-reactive chemical solute and contaminant transport capabilities were also included (Thomas and Cleall, 1997).

Sloper (1997) presented a new three-dimensional numerical model to describe fully coupled heat, moisture and air transfer through unsaturated soil. The development and verification of the new finite element formulation was also presented. Particular attention was also given to the pre and post-processor visualisation of the three-dimensional

numerical results. A small test problem was used to illustrate three-dimensional coupled flow processes and highlighted the requirement for scientific visualisation. Parallel computing techniques were also investigated and allowed more computationally demanding problems to be addressed.

Mitchell (2002) presented a fully coupled thermo/hydro/mechanical model to investigate the behaviour of two large scale in-situ experiments, namely the Isothermal Experiment and the Buffer/Container Experiment. In particular, the saturation and swelling behaviour of bentonite buffers were investigated. Thomas et al. (2003a) later presented some of the research conducted into the Isothermal Experiment where the re-saturation behaviour of the buffer was investigated. To correctly capture the rates of resaturation of the bentonite buffer material the micro/macro behaviour was investigated. A new hydraulic conductivity relationship was incorporated into the numerical formulation. This yielded significant improvements in the analysis results. This area of research has formed the foundation to the work presented in this study.

Hashm (1999) developed a two-dimensional model for coupled moisture and reactive multi chemical solute transport in unsaturated soils. This work was further developed and Seetharam (2003) presented a coupled thermo/hydro/chemical/mechanical model whereby any number of chemical components could be accommodated. However, these research areas are beyond the scope of the work presented in this thesis.

1.3 Scope and limitations

The scope and limitations of the above mentioned theoretical and numerical formulations are described below.

1. Soils are recognised as exhibiting a degree of heterogeneity. However, due to a lack of experimental data, in the present model the unsaturated soil is assumed to be isotropic and homogeneous. This limitation only applies to an individual element in the numerical formulation and therefore problems containing different soil types may be used within an analysis.

2. Hysteresis effects have been observed in the moisture retention relationship between the degree of saturation and the suction. However, in this formulation the effects of hysteresis are not included.

3. The temperature range that can be modelled is between 0 °C and 100 °C, and the phenomena of freezing and boiling are excluded from the formulation. It should be noted that although some high-level nuclear waste disposal concepts are designed on maximum temperatures in excess of 100 °C, the large scale in-situ experiments investigated in this work are designed to ensure that the temperature remains below that of boiling.

4. The constitutive model representing the stress/strain behaviour is valid for slightly and moderately swelling soils. Both cyclic and monotonic loading paths may be accommodated in this relationship.

5. Due to the highly coupled and non-linear nature of the governing equations an approximate solution of the proposed model is achieved via the implementation of numerical methods. In particular, the finite element method is used to achieve spatial discretisation and the finite difference method is used to achieve temporal discretisation.

1.4 Thesis overview

This thesis consists of eight further chapters and a summary of the contents of each chapter is presented below.

Chapter 2 presents a focussed review of recent developments in the theoretical modelling of coupled heat, moisture, air and deformation behaviour in an unsaturated soil. Furthermore, a review of small scale laboratory experiments and large scale in-situ experiments associated with high-level nuclear waste repository development and design is presented. The numerical modelling work conducted as part of this work is also detailed. Finally, a brief summary is presented on the solution methods and high performance computing techniques that are available for analysing large finite element problems.

Chapter 3 presents the theoretical formulation of the governing differential equations for the thermal, hydraulic and mechanical behaviour of unsaturated soils. The governing

equations are expressed in terms of four primary variables; pore water pressure (u_l), pore air pressure (u_a), temperature (T) and displacement ($\mathbf{u}$), and the associated derivations and assumptions are described.

Chapter 4 presents the numerical formulation for the solution of the governing differential equations presented in Chapter 3. A finite element method is implemented to spatially discretise the equations, and a backwards difference mid-interval time-stepping algorithm is used to achieve temporal discretisation. Also presented is a description of the software, solution methods and three-dimensional visualisation facilities used in this investigation.

Chapter 5 presents a detailed review of SKB's Prototype Repository Project. The chapter firstly concentrates on the development and current role of SKB as the Swedish agency in charge of the handling, transport, storage and disposal of the nuclear waste. The Äspö Hard Rock Laboratory is examined in detail and its main objectives and current experimental programmes are highlighted. The chapter then presents the Prototype Repository Project and discusses the experimental set-up, the characterisation of the rock mass and the instrumentation installed in the experiment.

Chapter 6 presents the preliminary experimental results from the Prototype Repository Experiment. At the time of writing the experiment is still in its early stages and therefore only the results from the first 710 days are discussed. The key results from Section I and II of the experiment are presented and cover temperature, relative humidity and total stress measurements in the buffer, backfill and host rock.

Chapter 7 presents the fully coupled thermo/hydro/mechanical model that has been used to simulate SKB's Prototype Repository Experiment. Firstly, the material parameters are defined for the relevant material types. A detailed description of the finite element meshes adopted for this analysis is then presented. The results from the numerical investigations are then presented and compared against corresponding experimental results. The findings from the simulation work are then discussed, with the key conclusions presented.

Chapter 8 presents the coupled thermo/hydro/mechanical model that has been used to simulate AECL's Tunnel Sealing Experiment. The material parameters are defined for the relevant material types and this is followed by a description of the finite element meshes adopted for the analyses. The results from the predictions are then presented and discussed

in detail and preliminary comparisons are made with the experimental behaviour. The main conclusions from this numerical study are then presented.

Finally, in Chapter 9 the overall conclusions from this work are presented and discussed. Suggestions for future research into this area are highlighted.

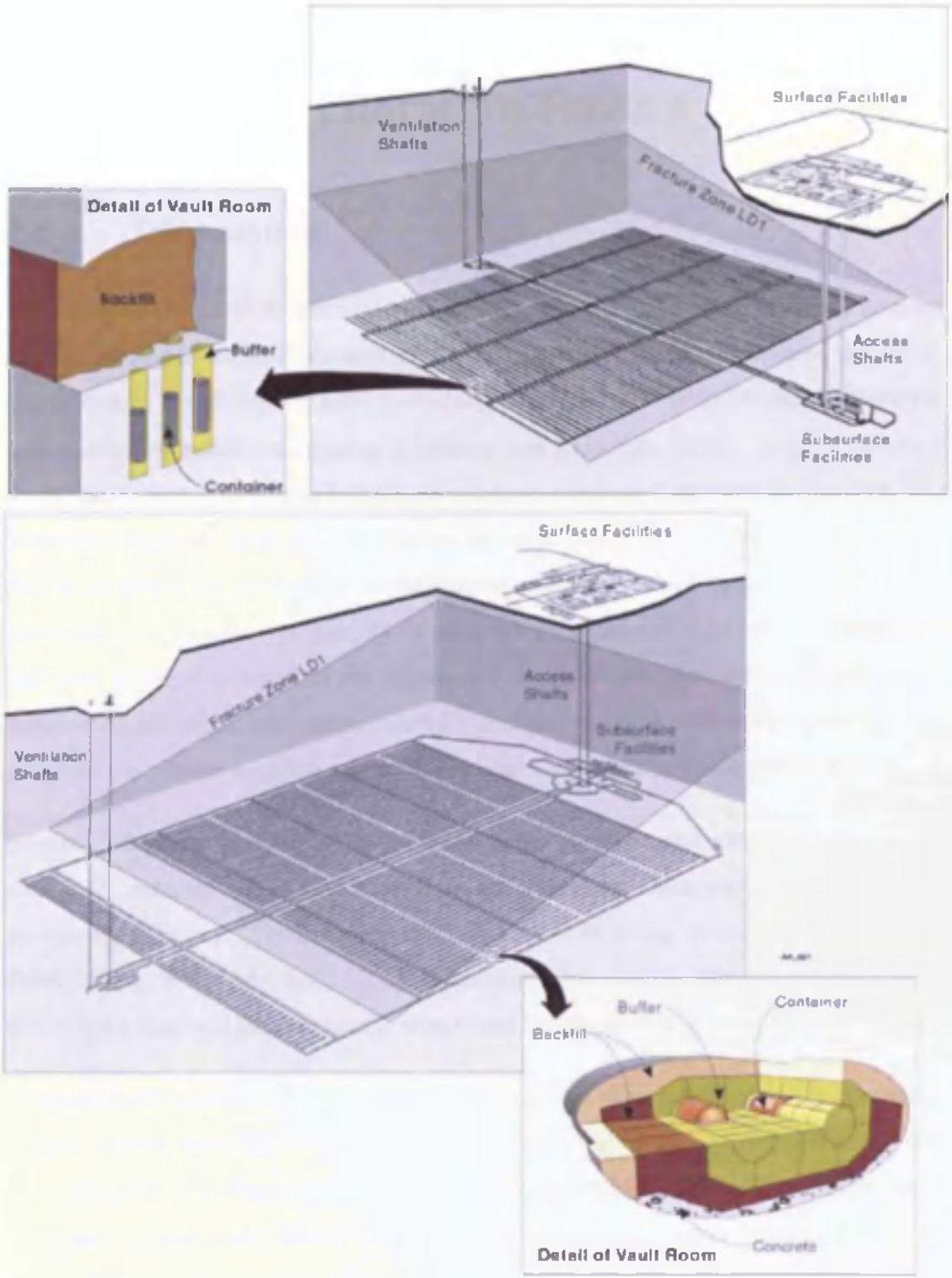

Figure 1.1 Vertical (upper diagram) and horizontal (lower diagram) disposal concepts for the disposal of high-level nuclear waste

Chapter 2

Literature Review

2.1 Introduction

The study of flow and deformation behaviour of partially saturated soils has been of great interest to engineers and researchers for many years. Since unsaturated soil is a three-phase system consisting of solid particles, liquid and gas its behaviour is more complex than that of saturated soil phases (Fredlund and Rahardjo, 1993). It is the interaction of these phases that govern this behaviour and have dominated research in this area. In recent years the study of unsaturated soils has gathered further momentum and global attention due to its proposed application in the current concepts for the long-term disposal of high-level radioactive waste. A variety of research programmes have been performed and are currently being conducted to investigate the thermo/hydro/mechanical behaviour of these engineered materials both experimentally and theoretically. Therefore, the intent of this chapter is to present a review of the recent literature covering these subjects.

Section 2.2 presents a review of coupled heat, moisture and air transfer in unsaturated soils. A number of excellent reviews on this flow behaviour have been presented previously (Thomas, 1980; Ewen, 1987; Rees, 1990; King, 1991; Sansom, 1995; Cleall, 1998; Wang, 2000; Mitchell, 2002). Therefore, this section offers a concise summary of this subject area and focuses on the significant developments in coupled flow behaviour.

In Section 2.3 a review of the deformation behaviour of unsaturated soil is presented. This subject matter has again been reviewed in detail by Cleall (1998), Wang (2000) and Mitchell (2002) and hence this section concentrates principally on both elastic constitutive relationships and elasto-plastic constitutive relationships. Further attention is also given to recent developments in constitutive modelling.

Section 2.4 presents a review of the theoretical and numerical formulations for coupled transient heat, moisture and deformation processes in unsaturated soils. Coupled flow and deformation models have been given a great deal of attention in recent years and therefore

the intention of this section is to summarise the earlier work and to augment it with a review of more current developments.

Section 2.5 presents a detailed investigation of laboratory experiments based on the concept for the disposal of high-level nuclear waste. In this section both recent small scale laboratory bench top experiments and large scale mock-up experiments are discussed.

In Section 2.6 a review of large scale in-situ experiments associated with high-level nuclear waste repository development and design is presented. This section describes both the experiments carried out as part of a benchmarking exercise and also other large scale in-situ experiments designed to increase knowledge about the complex thermo/hydro/mechanical processes occurring at a realistic scale. The numerical modelling work conducted as part of this work is also detailed.

In Section 2.7 a review of the available solution methods for performing finite element analyses is presented. This section highlights the development of these methods and the available preconditioning to improve the efficiency of the analyses. Owen (2000) has comprehensively reviewed this work and hence only a short summary is presented here.

Section 2.8 presents a review of the advances in high performance computing and the development of techniques such as parallel computing, which have enabled large scale three dimensional analyses to be performed in this work. Again, a full review of this work can be found in Owen (2000).

Finally the overall conclusions of this literature review are given in Section 2.9.

2.2 Coupled heat, moisture and air flow in unsaturated soil

This section presents a chronological review of the development of theoretical and numerical formulations representing fully coupled heat, moisture and air flow in unsaturated soil. A number of extensive reviews on this work have been presented in previous studies (Thomas, 1980; Ewen, 1987; Rees, 1990; King, 1991; Sansom, 1995; Cleall, 1998; Wang, 2000; Mitchell, 2002) and therefore the following section presents a summary of the key developments in this area for the sake of completeness and relevance.

A one-dimensional mathematical model using three partial differential equations to describe heat, moisture and air flow was developed by Dakshanamurthy and Fredlund (1981). As a simplification the model did not consider the coupling between heat and moisture transfer and it was assumed that fluid permeability was constant. The model was implemented to solve four example problems involving flow in unsaturated soils under hydraulic and temperature gradients. It was found that the model performed reasonably well in capturing the observed behaviour. This work was followed by Couvillion and Hartley (1986) who presented a model to investigate the movement of thermally induced drying fronts in an unsaturated sandy soil. A similar approach was adopted in the formulation, however the liquid component of moisture flow used the Philip and de Vries (1957) approach to relate moisture flux to temperature and moisture content gradients. An explicit finite difference technique was applied to solve the governing equations but resulted in numerical difficulties. Therefore, the heat transfer equation was simplified and the air phase was removed in order to provide a solution.

In the same year Geraminegrad and Saxena (1986a) presented a coupled thermo-elastic model for heat, moisture and air flow in partially saturated media. Again the Philip and de Vries (1957) model was employed for heat and moisture flow. The transfer of air dissolved within the pore liquid was considered in the gas continuity equation, and volume changes in the soil due to pore pressure changes were also included. A finite element formulation was proposed but again the solution encountered numerical difficulties. To alleviate the problem the researchers removed the air phase and applied the revised model to a series of examples obtained from the literature.

Pollock (1986) developed three coupled non-linear partial differential equations based on the Whitaker approach (Whitaker, 1977). A numerical solution was achieved in terms of

temperature, degree of liquid saturation and total gas pressure by a finite difference technique with Newton-Raphson linearisation. The model was used to simulate a one-dimensional transport process in a large scale hypothetical nuclear waste repository over a period of one thousand years.

Connell and Bell (1993) developed a numerical model to predict the climatic influences on liquid and vapour transport processes in waste dumps. In contrast to the established approach, thermodynamic equilibrium between liquid and vapour phases was not assumed in this formulation. Liquid flow was described by Richards' equation (Richards, 1931), which neglects the influence of thermal and air pressure effects on liquid flow. Vapour flow was assumed to comprise of viscous vapour flux and diffusive vapour flux. Darcy's Law defined the former while the latter was described using the dusty gas model (Thorstenson and Pollock, 1989). The governing equations were solved using a moving node finite element method. A numerical simulation of isothermal infiltration in Yolo light clay was presented and it was found that the results showed good agreement with those obtained by alternative models.

Thomas and Sansom (1995) developed a theoretical formulation to represent coupled heat, moisture and air transfer in unsaturated soil. In the formulation the liquid phase was considered to be water containing dissolved air, and the air phase was considered to be a binary mixture of dry air and water vapour. Three fully coupled governing differential equations were developed. Liquid flow was represented by Darcy's Law, whilst the flow of water vapour was represented by implementing the modified Philip and de Vries (1957) approach, after Ewen and Thomas (1989). In addition, the effects of vapour flow due to bulk flow of air were included. The governing equation for dry air flow included the bulk flow of dry air and the flow of air dissolved in the liquid. Thermal effects on the dry air flow were also incorporated into the formulation. The governing equation for heat flow covered heat transfer by conduction, convection and latent heat of vaporisation. The three coupled equations were solved spatially using the finite element method, and temporally by a finite difference time-stepping scheme. The model was used to simulate coupled heat, moisture and air transfer in a highly compacted unsaturated sand. The results showed a good correlation with results derived from an independent model presented by Pollock (1986).

Experimental and numerical investigations on the movement of moisture in highly compacted bentonite under temperature gradients were presented by Kanno et al. (1996). Based on the assumption that the vapour flow area increased linearly as volumetric air content increased, it was observed that there was a good correlation between the numerical and experimental results.

Thomas and Ferguson (1999) proposed a fully coupled heat and mass transfer theoretical model to describe the migration of gas through a clay liner in a municipal landfill site. Darcy's Law and Fick's Law represented liquid and energy flows respectively. The migration of liquid, heat, air and contaminant gas were considered independently with system variables of capillary potentials, temperature, pore air pressure and molar concentration of the contaminant gas. Good correlation was observed between the numerical results and the analytical solution and the research showed the importance of the effect of temperature on the transport of contaminated gas.

2.2.1 Conclusions

In this section developments in the theoretical and numerical formulations for coupled heat, moisture and air flow in unsaturated soil over the last three decades have been presented. These models use governing differential equations to describe the heat, moisture and air flow based on established flow laws. In more recent years these thermo/hydraulic formulations have become fully coupled with deformation models and the focus of the research has been in developing thermo/hydro/mechanical formulations to represent behaviour in both two and three-dimensional problems. These developments will be addressed in the following sections.

2.3 Deformation behaviour in unsaturated soil

This section reviews the development of theories to describe the deformation behaviour of unsaturated soils and the representation of this behaviour with constitutive models. There are a range of extensive reviews available on this subject (Alonso et al., 1987; Fredlund and Rahardjo, 1993; Delage and Graham, 1996; Wheeler and Karube, 1996; Sultan et al., 2002) and therefore this section is divided into two parts. Section 2.3.1 provides a

focussed summary of the development of elastic constitutive relationships and Section 2.3.2 presents a review of elasto-plastic constitutive relationships.

2.3.1 Elastic constitutive relationships

The development of constitutive relationships for unsaturated soils led from the effective stress theories adopted for saturated soils. Biot (1941) investigated three-dimensional consolidation of an elastic linear isotropic soil. An effective stress state variable was used to describe the deformation behaviour. This was defined as the difference in total stress and pore air pressure (σ - u_a) and pore water pressure, u_l.

Bishop (1959) presented one of the first theoretical models to explain the deformation behaviour of unsaturated soil based on the effective stress concept as;

$$\sigma' = (\sigma - u_a) + \chi(u_a - u_l) \qquad (2.1)$$

where, χ is a parameter related to the degree of saturation and varies between zero for a dry soil and one for a saturated soil. This equation extended Terzaghi's classical concept that "all measurable effects of a change in stress...are exclusively due to changes in the effective stress" (Terzaghi, 1936).

In response to this approach the effective stress concept was investigated by a number of researchers (Jennings and Burland, 1962; Bishop and Blight, 1963; Aitchison, 1965; Burland, 1965). It was concluded that the proposed effective stress law, while appearing to explain shear strength behaviour, could not provide an adequate relationship between volume change and effective stress for most soils. Coleman (1962) and Bishop and Blight (1963) suggested the use of two stress state variables instead. These variables were net stress ($\sigma - u_a$) and matric suction ($u_a - u_l$).

Following a series of oedometer and triaxial tests, Matyas and Radhakrishna (1968) proposed the use of state variables and state surfaces to relate changes in the degree of saturation, S_l and the void ratio, e to the two independent stress parameters, ($\sigma - u_a$) and ($u_a - u_l$). It was discovered that the state surfaces were unique for monotonic loading sequences and increases in the degree of saturation. These findings were later reinforced by Barden et al. (1969).

Fredlund and Morgenstern (1977) conducted a series of null tests and established that the stress state variables, $(\sigma - u_a)$ and $(u_a - u_l)$, adequately described a stress system for unsaturated soil. A third stress state variable, $(\sigma - u_l)$ could also be defined and it was proposed that any two of the stress state variables could be used to form a suitable stress system for unsaturated soil.

Fredlund (1979) proposed two mathematical expressions defining the state surfaces for void ratio, e and gravimetric water content, w as;

$$e = e_0 - C_t \ln(\sigma - u_a) - C_m \ln(u_a - u_l) \tag{2.2}$$

$$w = w_0 - D_t \ln(\sigma - u_a) - D_m \ln(u_a - u_l) \tag{2.3}$$

where, C_t and C_m represent compressive indices with respect to net stress and suction, and D_t and D_m are coefficients of water content changes with respect to net stress and suction. These expressions only include wetting induced swelling and wetting induced collapse if the compressive indices are defined as stress dependent.

Lloret and Alonso (1980) developed a one-dimensional consolidation model that included state surfaces for void ratio and degree of saturation. They were based on a two-dimensional spline interpolation of experimental data from Matyas and Radhakrishna (1968). Following this work Lloret and Alonso (1985) performed a series of confined and isotropic compression tests under controlled air and water pressures on both a kaolin and a pinolen clayey sand. On the basis of this work a number of linear and non-linear mathematical expressions to describe the state surfaces for void ratio and degree of saturation were proposed. For a limited range of total external stress, the most suitable expression for the state surface of void ratio was given as;

$$e = a + b(\sigma - u_a) + c \ln(u_a - u_l) + d \ln(\sigma - u_a)(u_a - u_l) \tag{2.4}$$

For a large range of total external stress variation the most suitable expression for state surface of void ratio was given as,

$$e = a + b \ln(\sigma - u_a) + c \ln(u_a - u_l) + d \ln(\sigma - u_a)(u_a - u_l) \tag{2.5}$$

For the state surface of degree of saturation excellent results were obtained with the following expressions;

$$S_l = a - Th\left[b(u_a - u_l)\right]\left[c + d(\sigma - u_a)\right] \quad (2.6)$$

$$S_l = a - \left\{1 - \exp\left[-b(u_a - u_l)\right]\right\}\left[c + d(\sigma - u_a)\right] \quad (2.7)$$

Where a, b, c and d are constants in each of the four expressions above.

State surface based elastic models have many uses but only allow modelling of wetting induced swelling and wetting induced collapse in unsaturated soils provided the loading or wetting process is monotonic. They are further limited since state surfaces can only represent elastic deformation behaviour and they do not include the influence of deviatoric stress on volumetric deformation.

2.3.2 Elasto-plastic constitutive relationships

The limitations of the elastic constitutive relationships detailed above have given rise to research and development into elasto-plastic constitutive relationships for unsaturated soils (Alonso et al., 1990; Gens and Alonso, 1992; Kohgo et al., 1993a; Wheeler and Sivakumar, 1995; Bonelli and Poulain, 1995). These relationships differentiate between plastic and elastic strains and also provide a framework in which the deformation behaviour of unsaturated soils can be better represented.

Alonso et al. (1990) presented the Barcelona Basic Model (BBM) describing the stress-strain behaviour of partially saturated soils. It was formulated in the framework of hardening elasto-plasticity and extended the modified Cam-Clay model by considering two independent sets of stress variables: the net stress and the suction. The model had the capacity to represent three important features of soil behaviour, namely,

1. The stiffness changes of the soil induced by suction changes.

2. The wetting collapse behaviour of the soil, corresponding to irrecoverable volumetric strains.

3. The level of net stress was directly related to the quantity of collapse.

The model defined two yield surfaces in net mean stress (p), deviatoric stress (q), and suction (s) space as defined by Coleman (1962). A three-dimensional view of these yield surfaces is shown in Figure 2.1. Within these yield surfaces elastic behaviour was

assumed. When the stress state reached the yield surfaces plastic straining occurred. For isotropic stress states with $q = 0$, the yield surfaces were defined by two yield curves, namely, the loading-collapse curve (LC) and suction-increase curve (SI). The LC and SI yield curves in (p, q), and (p, s) space are shown graphically in Figures 2.2(a) and 2.2(b) respectively. A constitutive equation for specific volume was proposed by Alonso et al. (1990) where the stiffness parameter for stress changes within the plastic region, $\lambda(s)$, was defined as being a function of suction. Furthermore, an expression for $\lambda(s)$ was presented which related the increase of soil stiffness with increasing suction.

A number of experimental investigations have been conducted (Josa, 1988; Wheeler and Sivakumar, 1995; Cui and Delage, 1996) which provide reliable evidence over the existence of the LC yield curve. The results of which showed that the shape of the LC yield curve demonstrated the same trends presented by Alonso et al. (1990). Furthermore, the mathematical representation of the LC curve has been developed. Josa et al. (1992) proposed an expression that gave a maximum possible collapse on wetting, and Wheeler and Sivakumar (1995) proposed an expression based on results from a series of suction-controlled triaxial tests on compacted kaolin.

The experimental evidence over the existence of the SI yield curve is less convincing. The model presented by Alonso et al. (1990) defined a yield curve that represented the development of irreversible strains when a previously unattained level of suction was reached. This model was based upon the experimental results presented by Yong et al. (1971) and Josa et al. (1987) which showed that during a drying wetting cycle irreversible plastic shrinkage strains were produced. Hence, due to a lack of further evidence Alonso et al. (1990) assumed that the suction at yield is independent of the stress, and the SI yield curve took the form of a straight line parallel to the p axis.

Alonso et al. (1995) presented the coupled flow-deformation analysis of an in-situ isothermal wetting experiment. Two constitutive models were employed in the simulation; a state surface approach and an elasto-plastic relationship. When the numerical results were compared against experimental records an excellent correlation was observed. It was highlighted that the elasto-plastic model required additional material parameters compared to the state surface model and that they were more difficult to establish. Furthermore, it was shown that the numerical results were highly dependent on some of the key

parameters, particularly the hardening parameter, and that these were difficult to measure experimentally.

Gens and Alonso (1992) established an elasto-plastic framework for modelling unsaturated expansive clays. Some of the basic concepts from this work were adopted by Cui et al. (2002) with the addition of a critical swelling curve (CSC). This curve accounted for the effects of the hydraulic-mechanical coupling on the volume change behaviour of heavily compacted swelling clay, considered for the possible use as an engineering barrier in the deep geological disposal of radioactive waste. The non-linear model required only six material parameters and provided satisfactory predictions for both hydration tests and mechanical compression tests. However, the model was limited in that it only considered the volume change behaviour of isotropically compacted clays under isotropic stress, and oedometric compacted clays under oedometric stress.

Sultan et al. (2002) extended an earlier elasto-plastic model by Hueckel and Baldi (1990) to include additional plastic mechanisms to take into account the over-consolidation ratio (OCR) during thermal expansion or shrinkage behaviour. It was proposed that a thermal yield curve (TY) should be introduced to take account of thermally induced volume changes under both normal and high OCR's.

The above models employ net stress, deviatoric stress and suction as stress state variables. However, a number of other models have been suggested which use alternative stress state variables (Kohgo et al., 1993a, 1993b; Jommi and di Prisco, 1994; Kato et al., 1995; Bolzon et al., 1996). These models attempt to simplify the elasto-plastic formulations by adopting alternative combinations of more complex stress state variables. A review of these models has been presented elsewhere (Wheeler and Karube, 1996; Gens, 1995).

Efforts have been made to model the mechanical behaviour of expansive clays using dual porosity models. Alonso et al. (1999) presented a two level formulation to model the behaviour of expansive clays. The behaviour of the macrostructure followed the model developed for unsaturated soils by Alonso et al. (1990) and the behaviour of the microstructure was adapted from the work of Gens and Alonso (1992) in order to include the possibility of the micropores being partially saturated. The mechanical coupling between both levels of structure was defined through a drying function and a wetting function. These were based on experimental evidence and expressed the change in

macrostructural void ratio due to a change in microstructural void ratio and are dependent on the level of compaction of the macrostructure. The model was able to represent the dependency of strain on stress-suction paths, the accumulation of expansion strain during suction cycles at low confining stress, the accumulation of compression strain during suction cycles at high confining stress, strain fatigue during drying-wetting cycles, macropore invasion by expanded microstructure and development of macroporosity during strong drying. Comparison with experimental tests performed in a suction-controlled oedometer apparatus showed that the model was able to capture the trends and data qualitatively.

Gallipoli et al. (2003a) presented an improved relationship for the variation of degree of saturation in an unsaturated soil, which incorporated the influence of changes in void ratio. This was combined with an elasto-plastic stress-strain model to represent irreversible changes of degree of saturation caused by shearing. Experimental data from tests performed by Sivakumar (1993) and Zakaria (1995) were used to demonstrate the success of the proposed new expression for degree of saturation and excellent agreement was reached in the results for the full range of stress paths. It was noted that this new relationship for degree of saturation was limited in that it did not take into account any influence of hydraulic hysteresis during wetting and drying cycles.

Wheeler et al. (2003) presented a new elasto-plastic framework for unsaturated soils that did involve coupling hydraulic hysteresis and mechanical behaviour. The stress variables employed were Bishop's stress tensor and modified suction (suction multiplied by porosity). Within the framework, plastic changes of degree of saturation influence the stress-strain behaviour and plastic volumetric strains influence the water retention behaviour. They developed a specific constitutive model for isotropic stress states so that simulation results could be compared at a qualitative level with experimental results. Not only did the model have the capability to capture the basic forms of unsaturated soil behaviour but also was able to simulate forms of mechanical behaviour observed in experimental tests that are not represented by existing constitutive models. These include proper transitions between saturated and unsaturated response, irreversible compression during the drying stages of wetting-drying cycles, and the influence of a wetting-drying cycle on subsequent behaviour during isotropic loading. The model also provided a realistic representation of the variation of degree of saturation including the influence of

both hydraulic hysteresis and plastic volumetric strains. However it was acknowledged that further research was needed to refine some of the mathematical expressions within the constitutive model especially in the way in which the water retention behaviour was modelled.

Gallipoli et al. (2003b) presented an elasto-plastic model that takes explicitly into account the mechanisms with which suction affects mechanical behaviour as well as their dependence on degree of saturation. An innovative constitutive framework for unsaturated soil was proposed that was able to explain the various mechanical features of the material by using physical descriptions of the different effects of suction on soil straining. The proposed model was formulated in terms of two constitutive variables related to these suction mechanisms. These were the average skeleton stress, which includes the average fluid pressure acting on the soil pores and an additional scalar constitutive variable related to the magnitude of the bonding effect exerted by meniscus water at the inter-particle contacts. Based on experimental evidence it was assumed that, during the elasto-plastic loading of a soil element, the ratio of void ratio, e, under unsaturated conditions to void ratio, e_s, under saturated conditions is a unique function of the bonding variable. This single yield curve assumption was successfully validated against several sets of published experimental data for different materials. This assumption was incorporated into a full elasto-plastic stress-strain model and its performance was demonstrated by the comparison between predicted and laboratory test results for a wide variety of different stress paths. This showed that the model was able to correctly capture the most important features of the mechanical behaviour of unsaturated soils even though it was formulated in terms of a single yield curve. It was also observed that another advantage of this approach was that a reduced number of laboratory tests were necessary for calibrating the proposed model and for material parameter determination.

2.3.3 Conclusions

This section reviewed the recent developments of theories to describe the deformation behaviour of unsaturated soils and highlighted that a good understanding of the principal processes has been achieved. Furthermore, a number of elastic and elasto-plastic constitutive models have been presented to describe several fundamental features of the mechanical behaviour of unsaturated soils. More recently, attempts have been made to

incorporate the effects of suction, degree of saturation and hydraulic hysteresis on mechanical behaviour of unsaturated soils with varying levels of success.

2.4 Coupled flow and deformation behaviour in unsaturated soils

This section presents a review of the literature concerning theoretical models which couple the flow effects of heat, mass and air on deformation behaviour of unsaturated soils. Thorough reviews of this work are available (Cleall, 1998; Wang 2000; Mitchell, 2002) and the intention of this section is to provide a focussed review of the previous work combined with a review of the most recent publications.

Barden (1965) proposed a consolidation model for unsaturated clay including four governing equations for pore air pressure, pore water pressure, unsaturated fluid conductivity and porosity. The flow equations were based on Darcy's Law and the unsaturated fluid conductivity was related to the degree of saturation. The deformation behaviour was described by a constitutive equation based on the effective stress approach after Bishop (1960). An analysis of a one-dimensional consolidation problem was conducted by applying a finite difference solution to the governing equations.

A further one-dimensional consolidation model for unsaturated clay was presented by Fredlund and Hasan (1979). They employed a modified version of Terzaghi's theory, (Terzaghi, 1943) to represent the vertical compression, which reverted back to its previous form under saturated conditions. The pore water and pore air flow were described using two mass continuity equations. The model was used to simulate a simple one-dimensional consolidation problem with both loading and boundary conditions applied.

Lloret and Alonso (1980) proposed a coupled one-dimensional model for water, air and deformation in an unsaturated soil. Again the pore water and pore air flow were based on Darcy's Law and described using two mass continuity equations. Dissolved air was included in the formulation but water vapour transfer was not included. The deformation behaviour was based upon the state surface approach as presented by Matyas and Radhakrishna (1968) whereby the stress state variables employed were net stress and suction. A numerical solution was achieved via the finite element method for spatial discretisation and a finite difference scheme for temporal discretisation. The model was

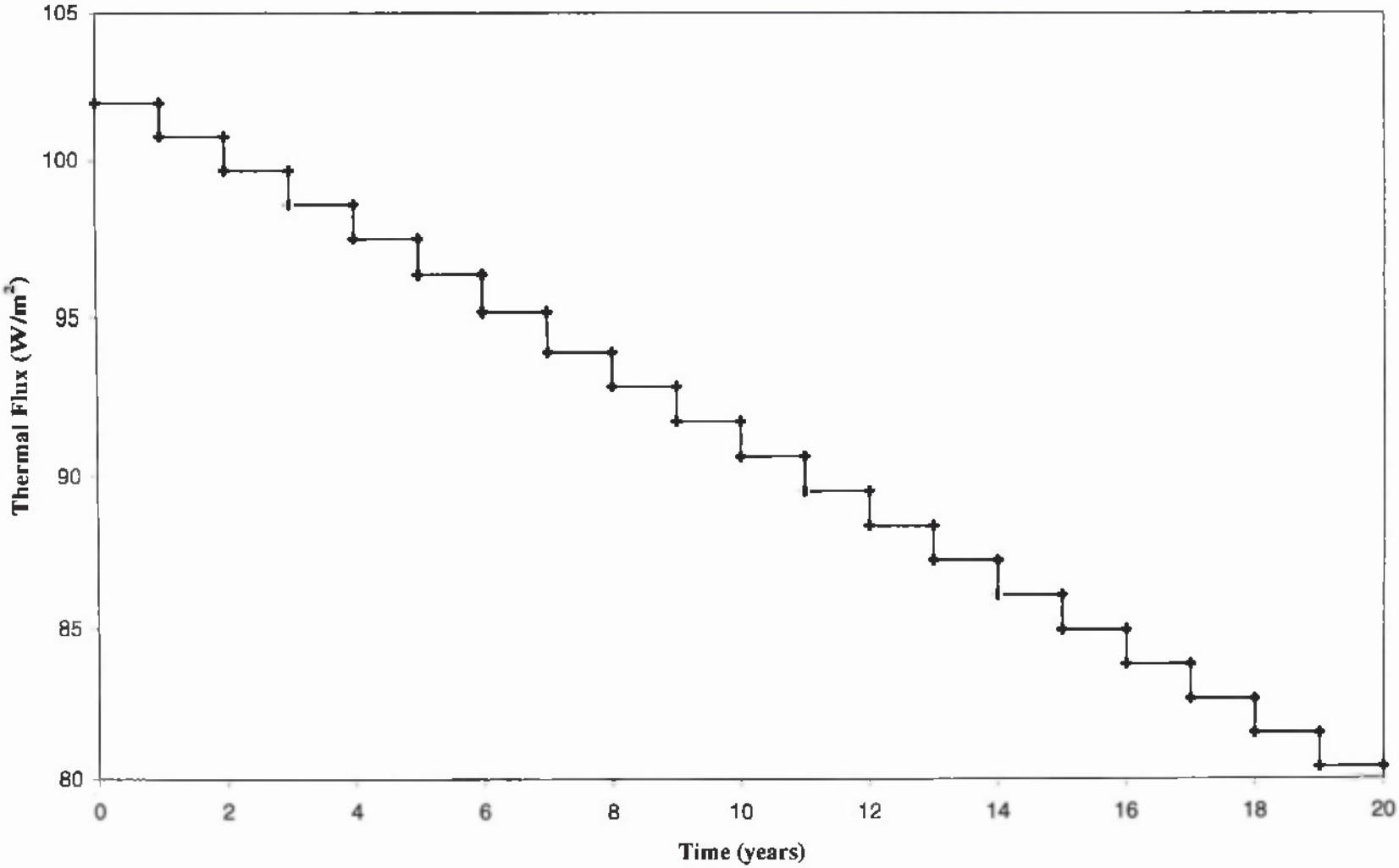

Figure 7.16 Thermal flux boundary condition applied to the surface of each of the canisters

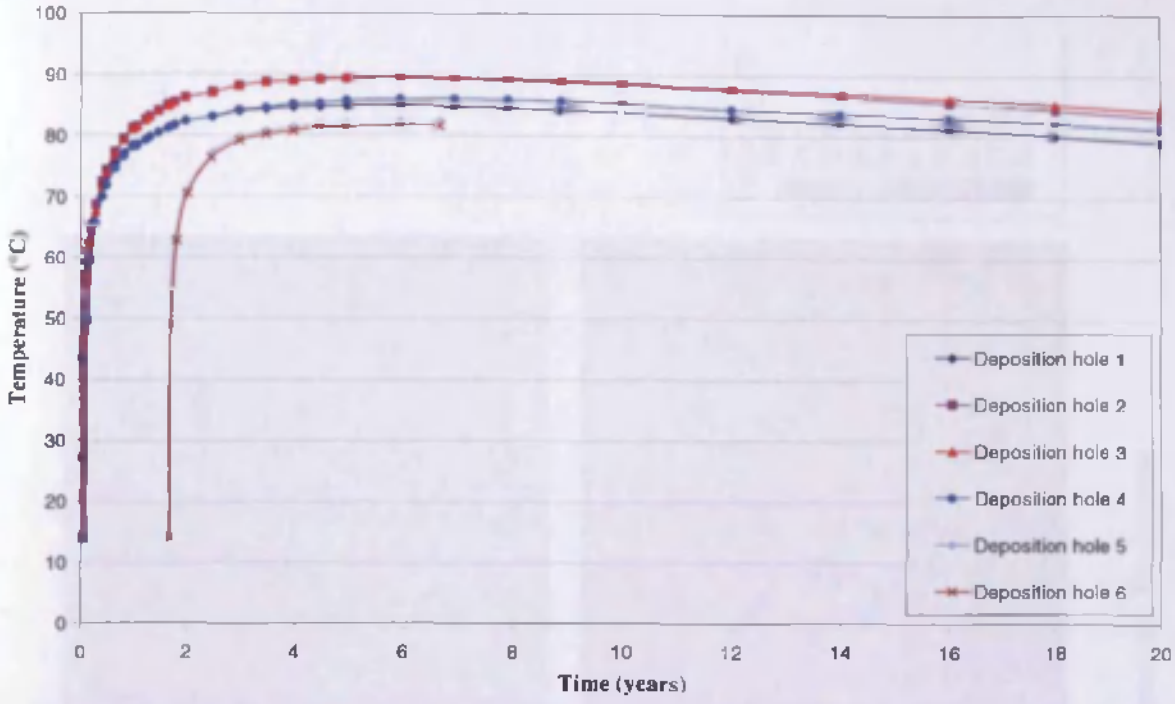

Figure 7.17 Simulated maximum surface temperature of the canisters in each of the deposition holes over the duration of the experiment

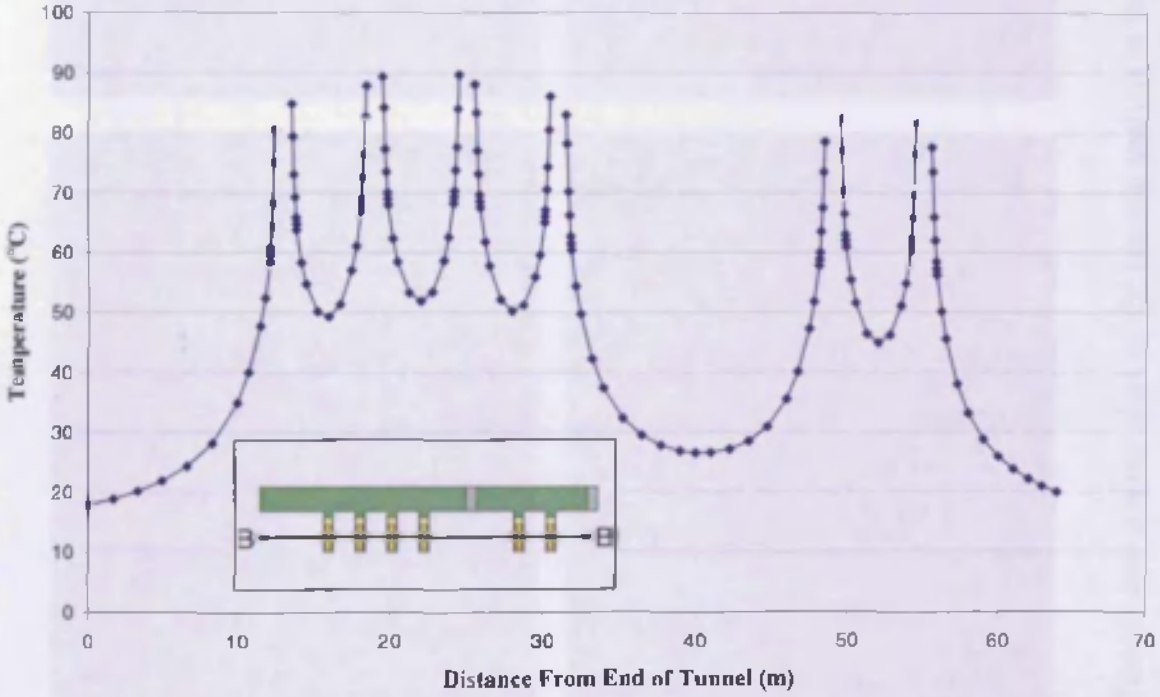

Figure 7.18 Temperature profile at mid-height of the deposition holes (section B-B) after 6 years

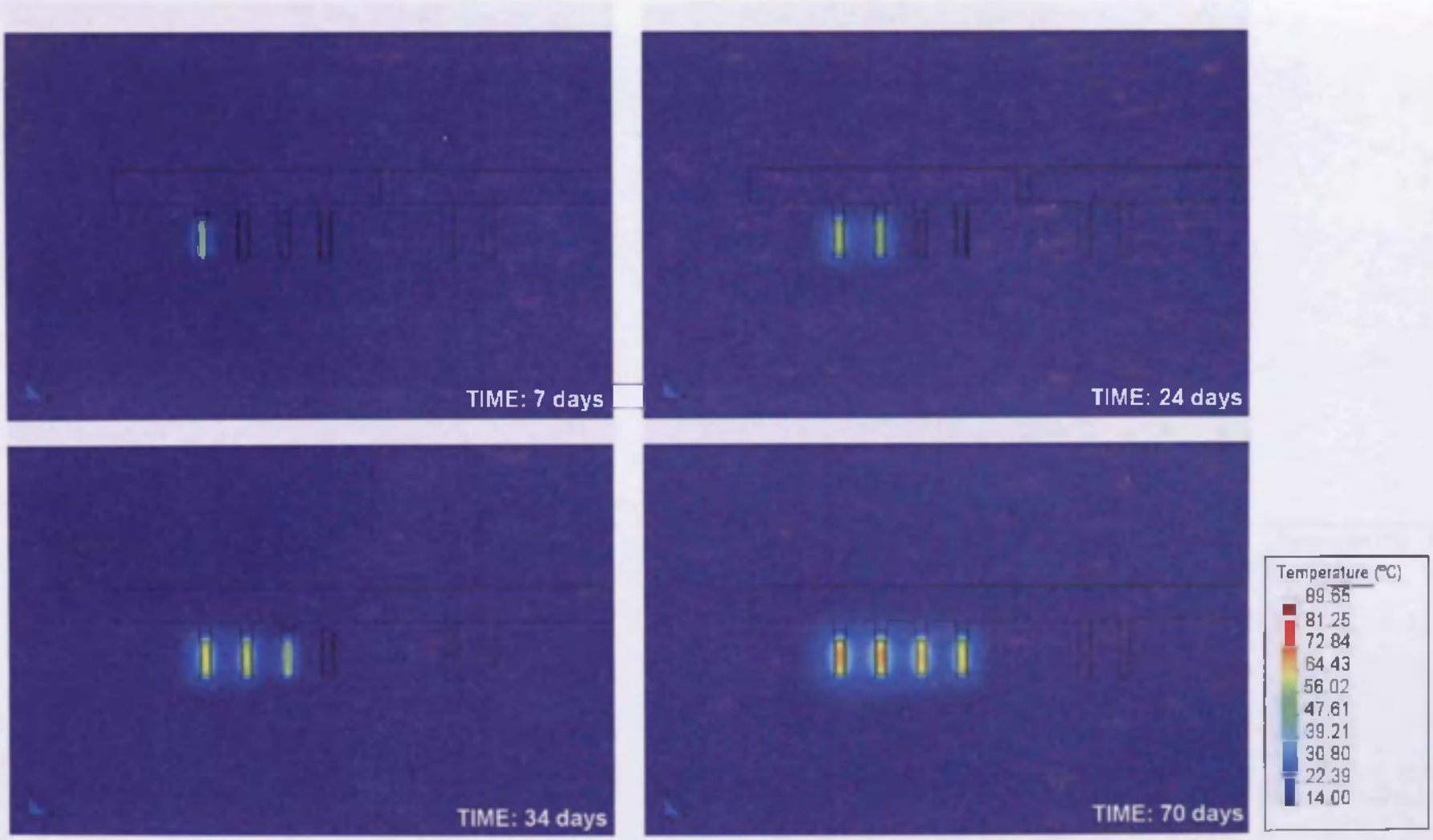

Figure 7.19 Temperature contour plots for the thermal analysis of the Prototype Repository Experiment

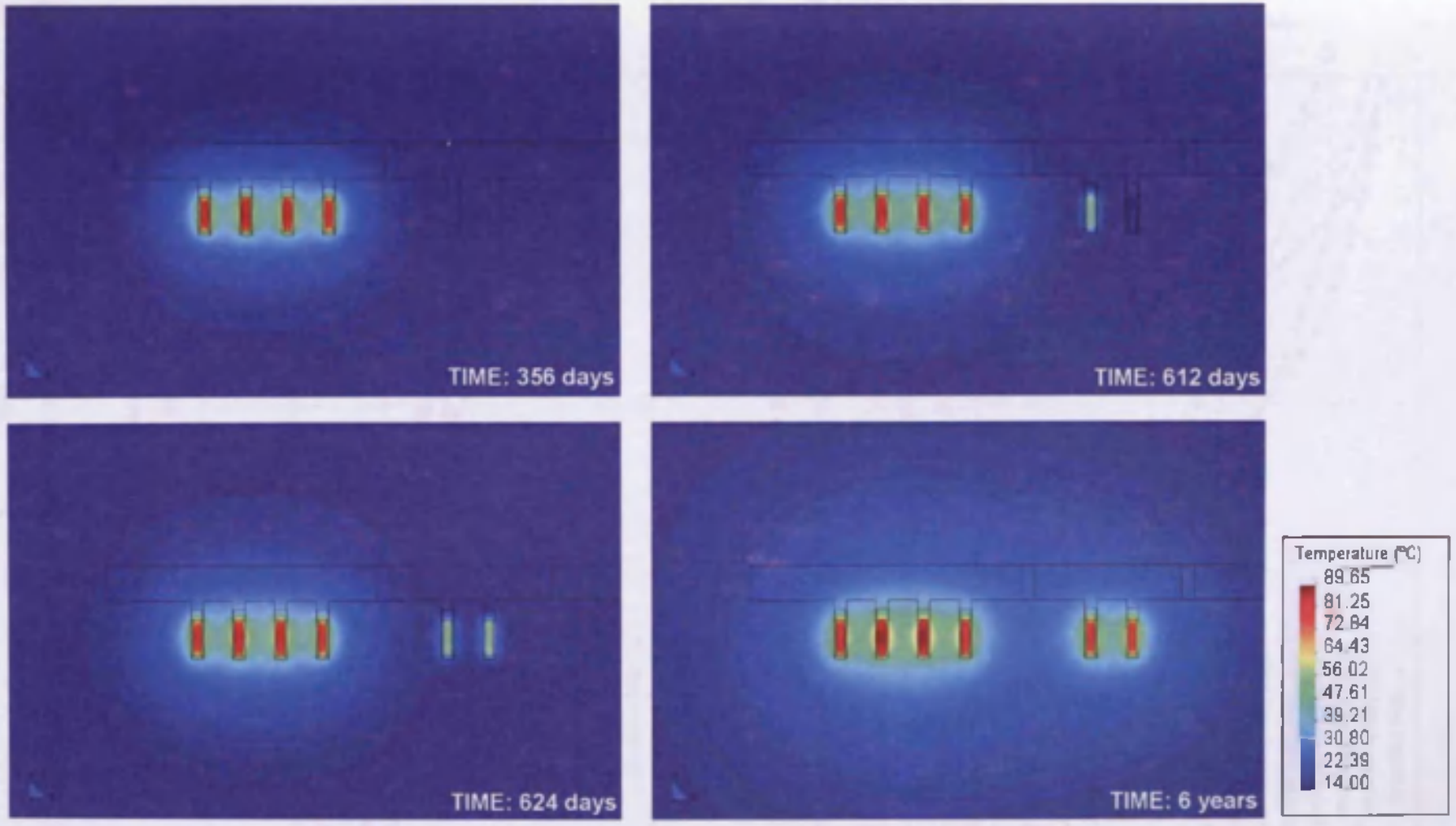

Figure 7.19 (cont.) Temperature contour plots for the thermal analysis of the Prototype Repository Experiment

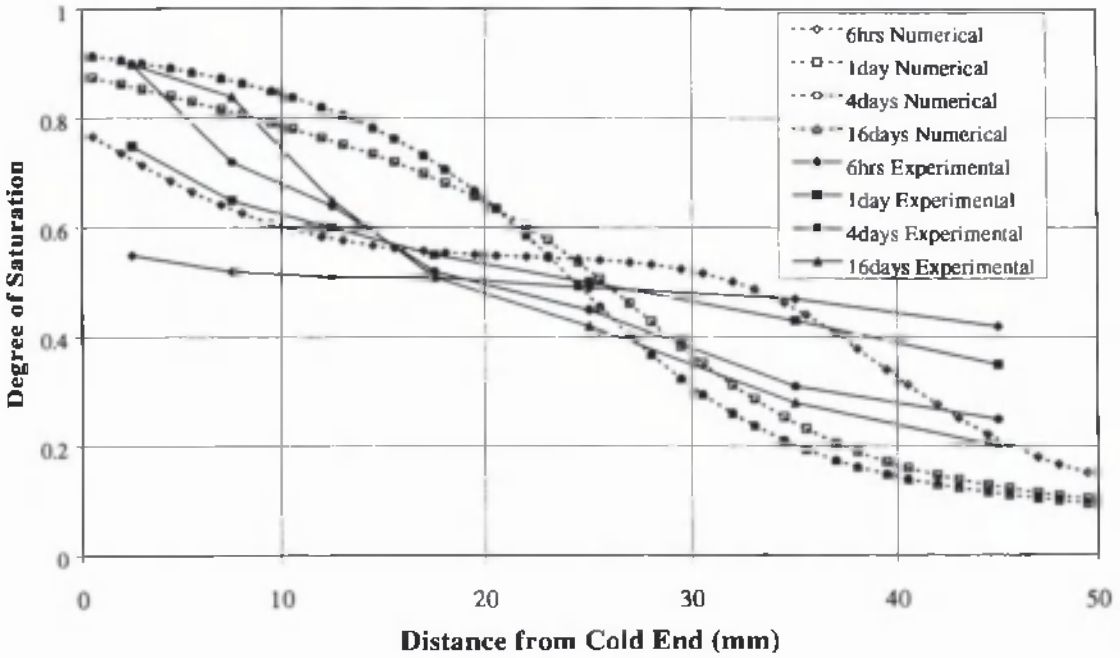

Figure 7.20 (a) Experimental (after Börgesson et al, 2001) and numerical results using the original Philip and de Vries flow law

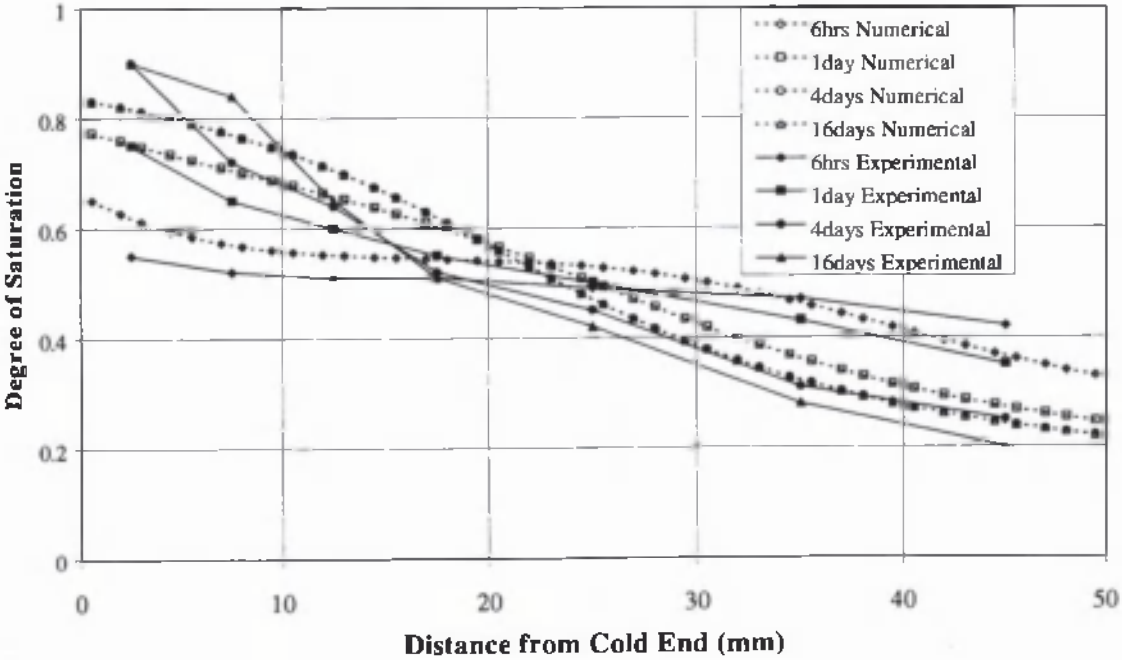

Figure 7.20 (b) Experimental (after Börgesson et al, 2001) and numerical results using the calibrated flow law

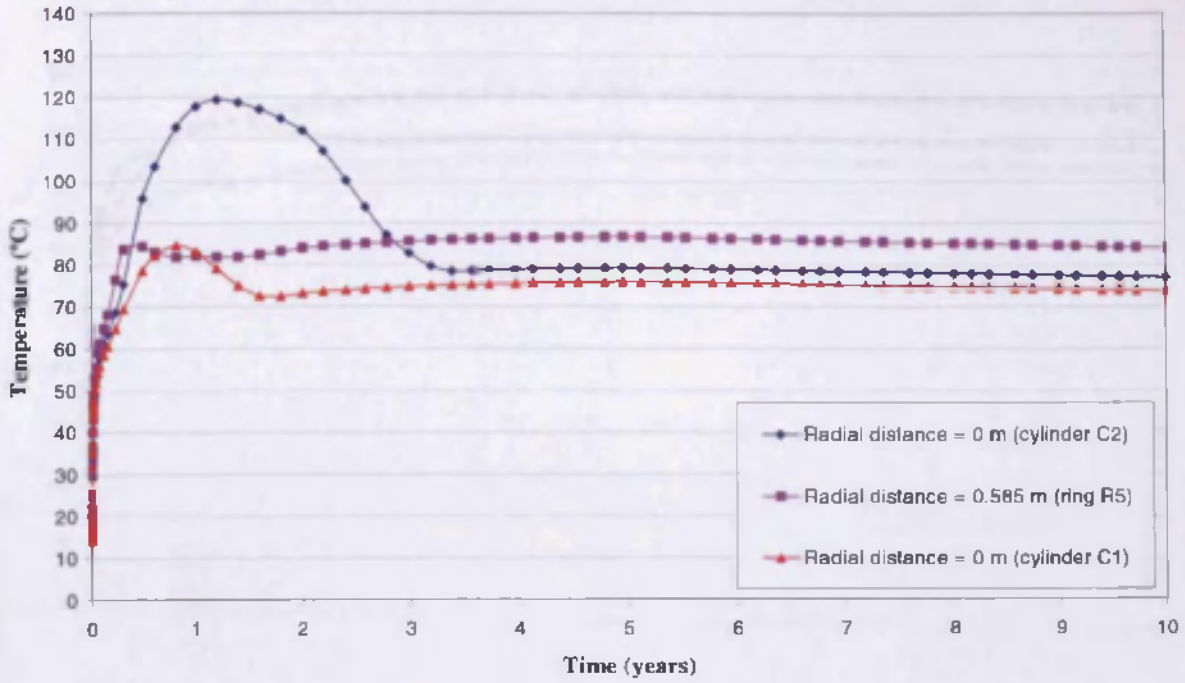

Figure 7.21 (a) Temperature at different positions in the buffer using the original Philip and de Vries flow law

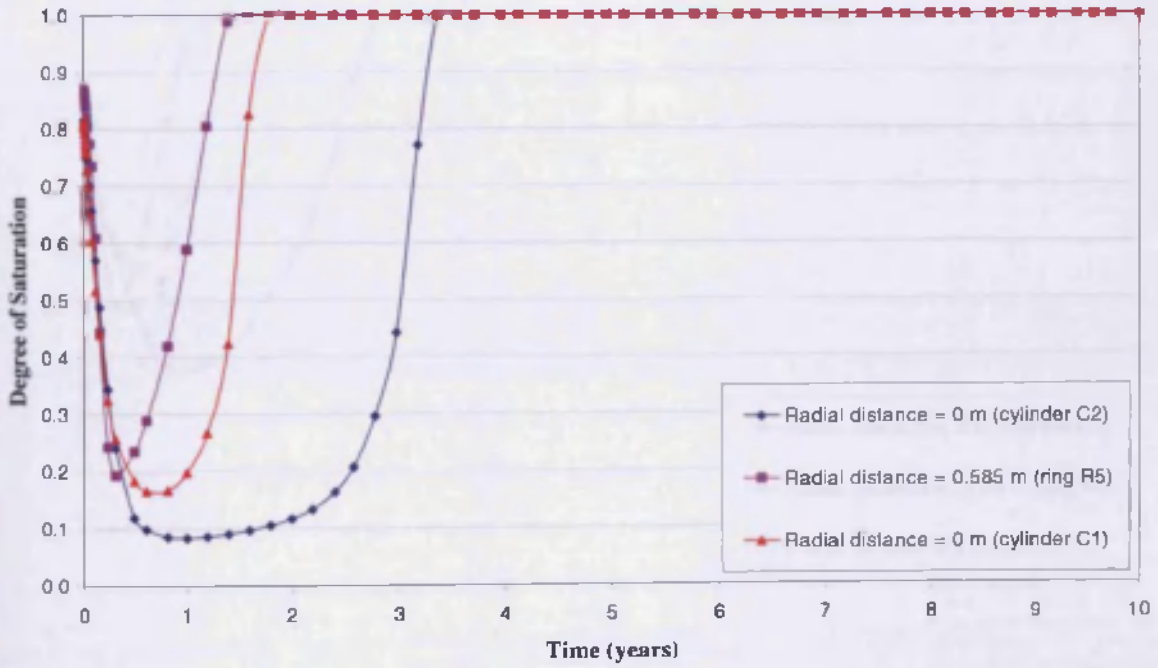

Figure 7.21 (b) Degree of Saturation at different positions in the buffer using the original Philip and de Vries flow law

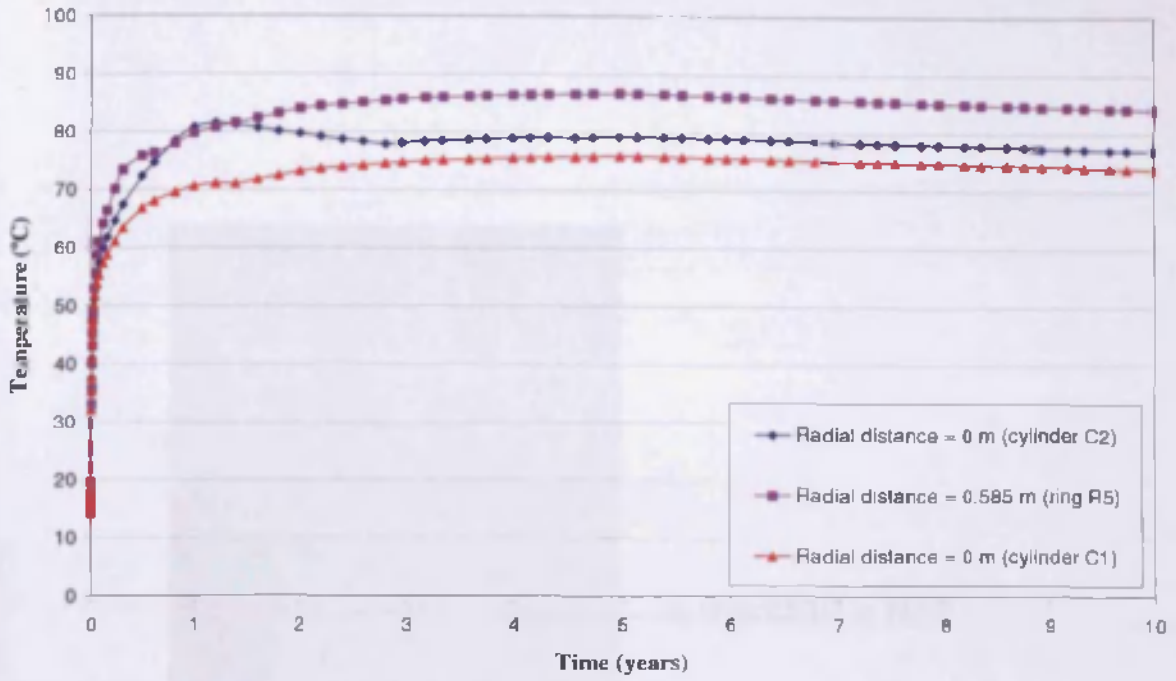

Figure 7.22 (a) Temperature at different positions in the buffer using the calibrated flow law

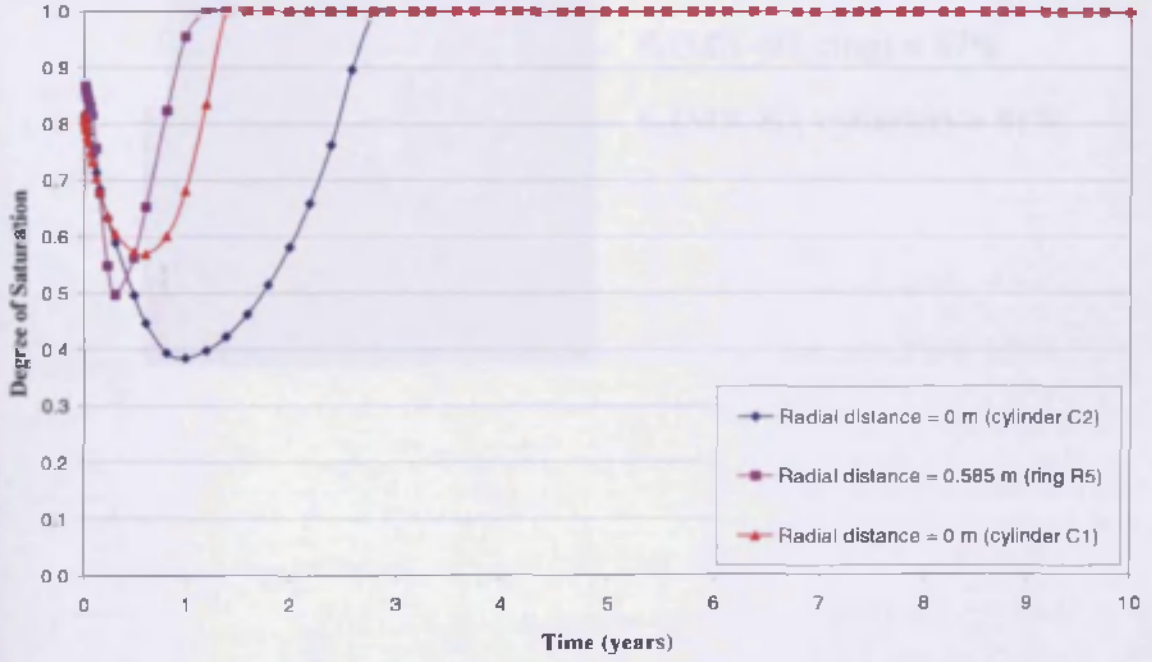

Figure 7.22 (b) Degree of Saturation at different positions in the buffer using the calibrated flow law

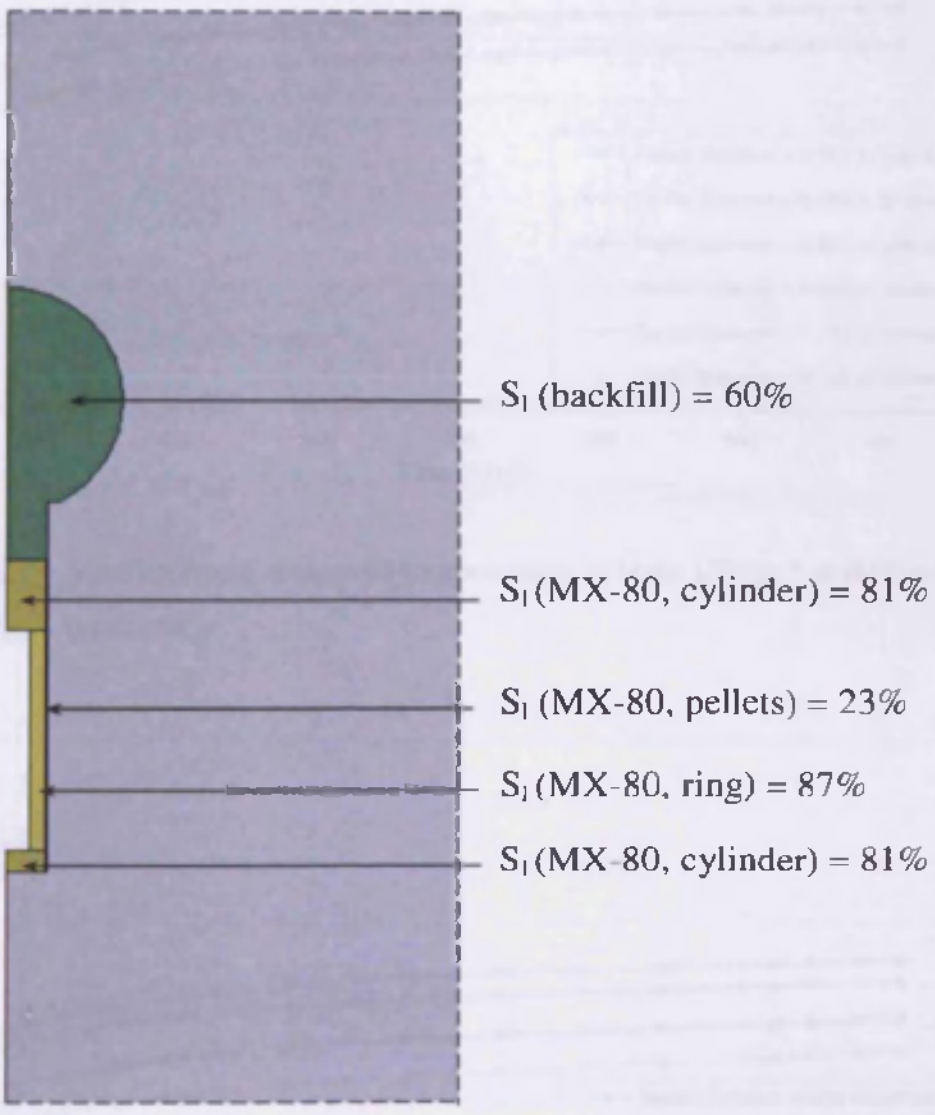

Figure 7.23 Initial degree of saturation used for the materials in the TH analysis

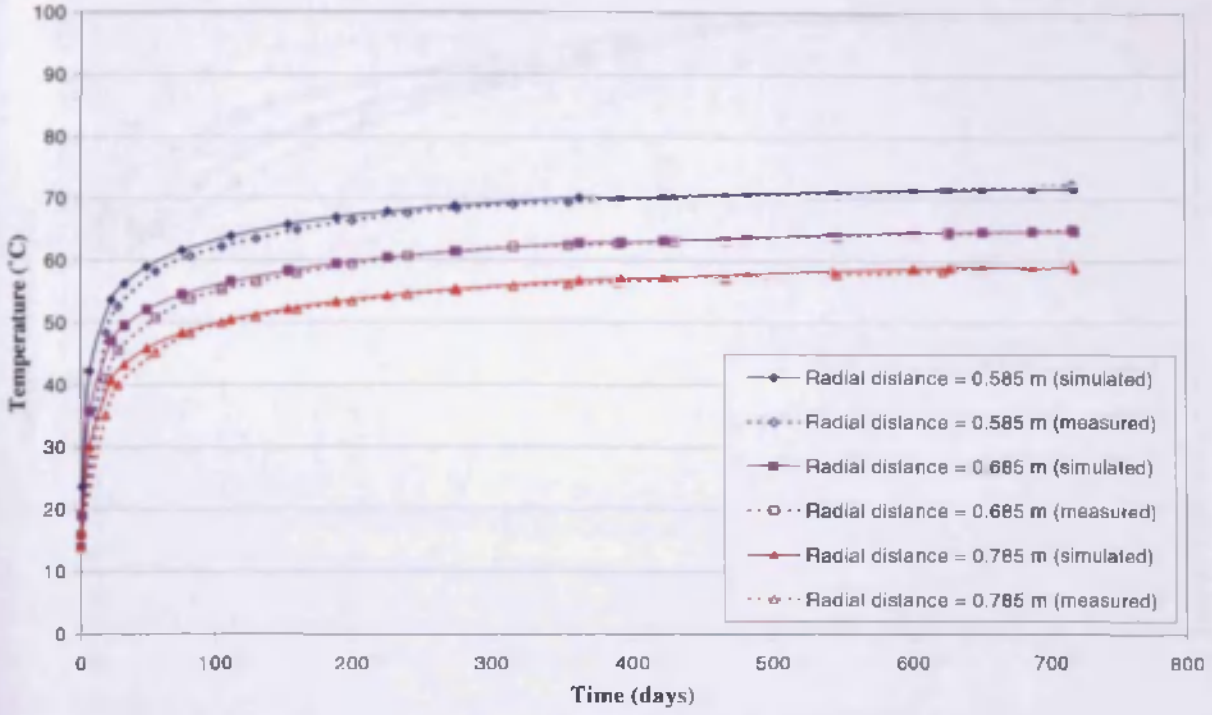

Figure 7.24 (a) Simulated and measured temperatures in Hole 1/Ring 5 at different positions

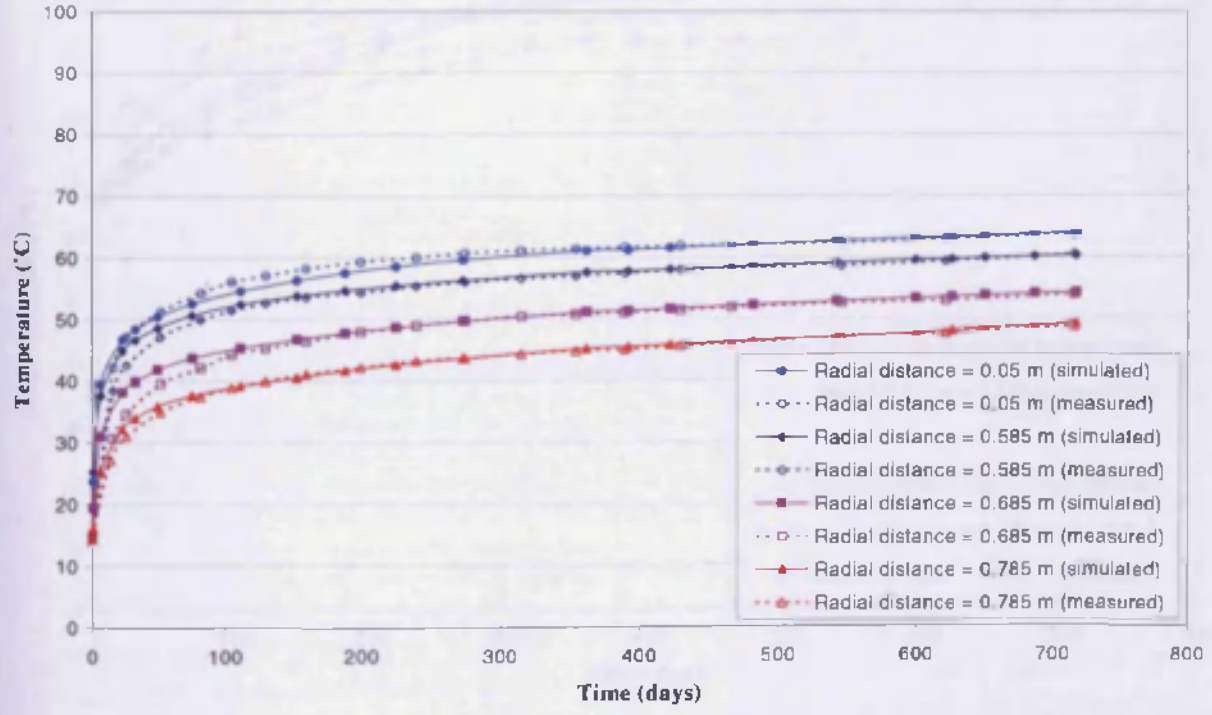

Figure 7.24 (b) Simulated and measured temperatures in Hole 1/Cylinder 1 at different positions

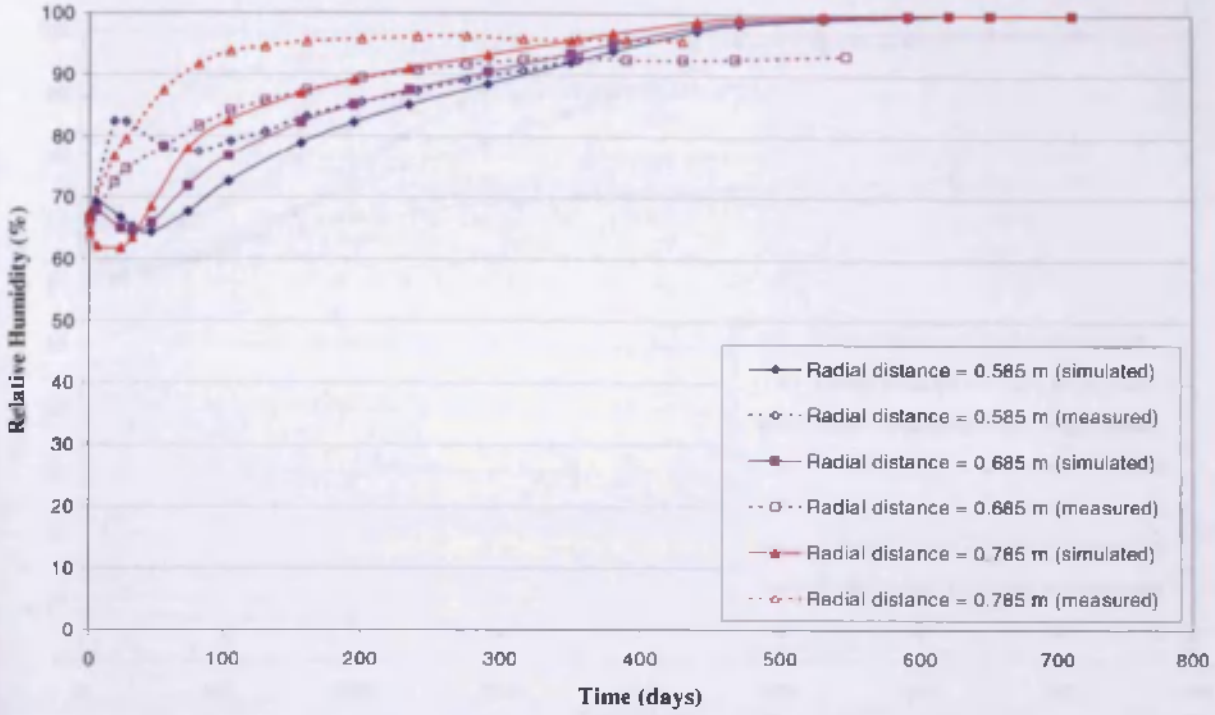

Figure 7.25 (a) Simulated and measured relative humidity in Hole 1/Ring 5 at different positions

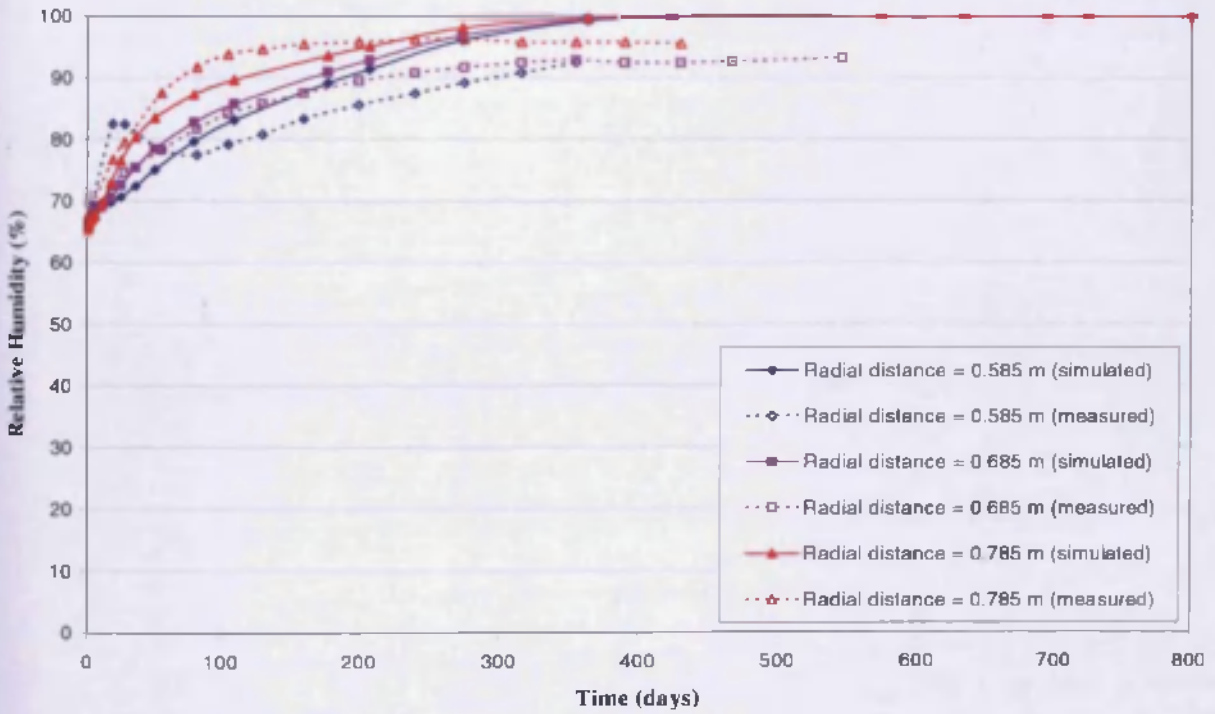

Figure 7.25 (b) Simulated and measured relative humidity in Hole 1/Ring 5 at different positions with the pellet region replaced with buffer

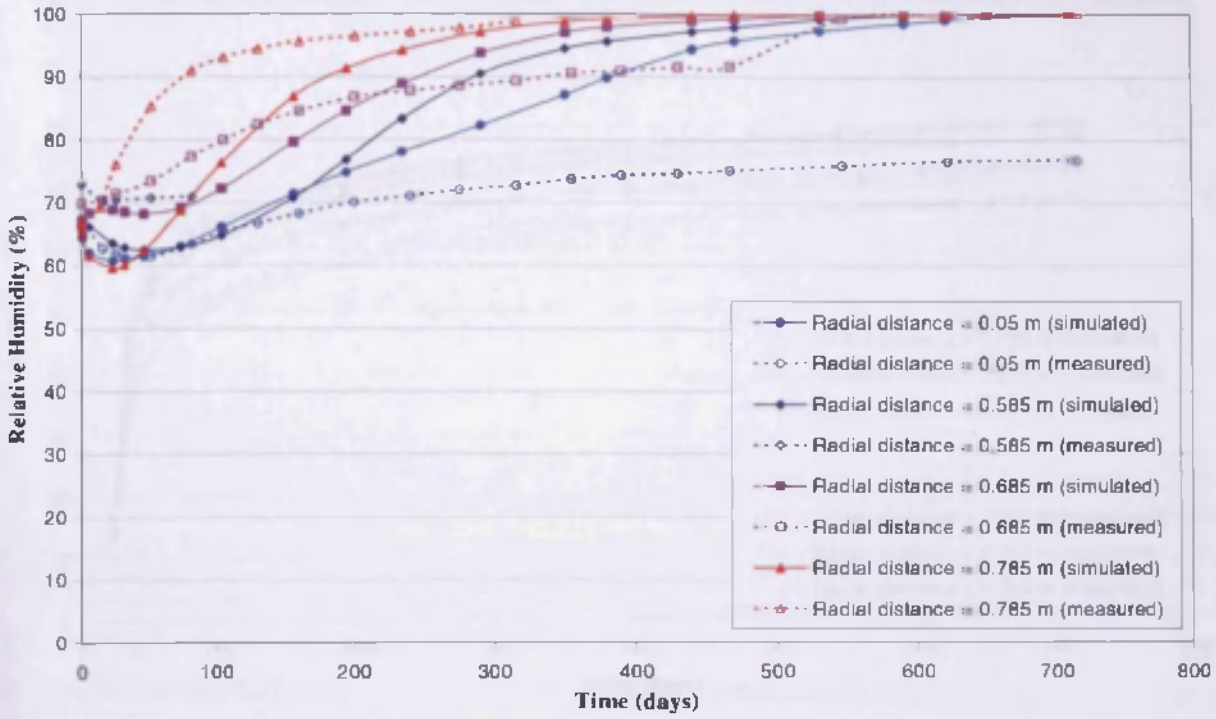

Figure 7.25 (c) Simulated and measured relative humidity in Hole 1/Cylinder 1 at different positions

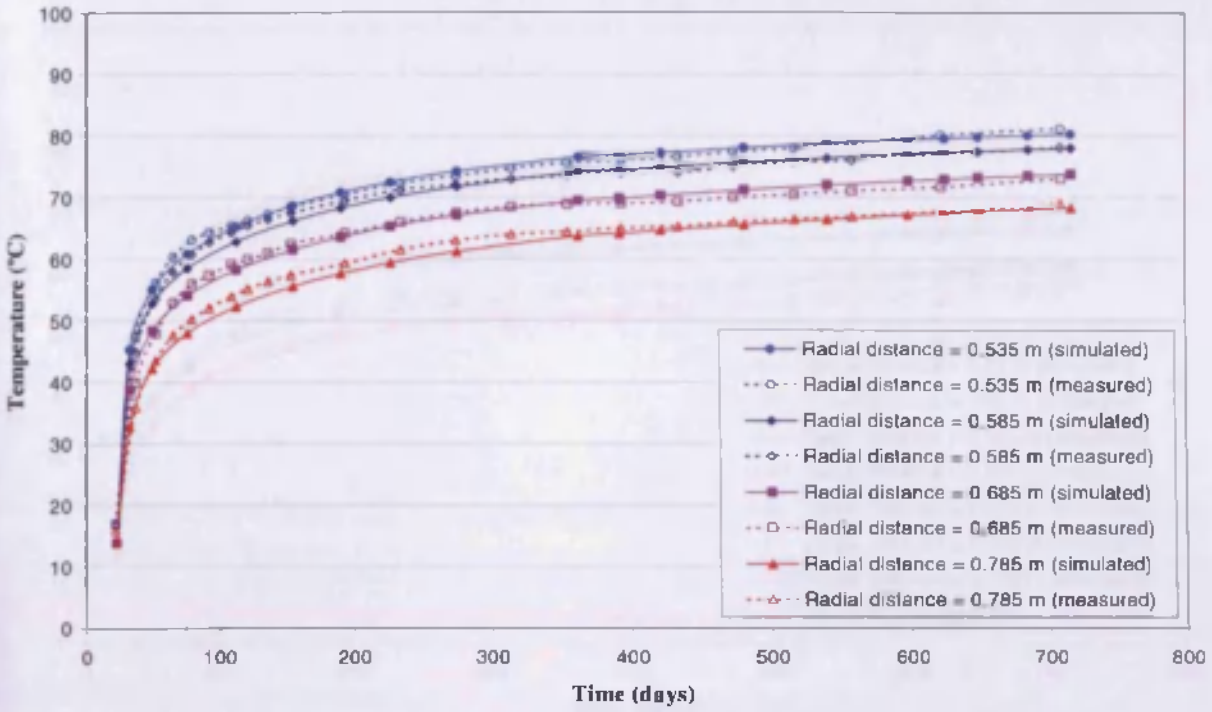

Figure 7.26 (a) Simulated and measured temperatures in Hole 3/Ring 5 at different positions

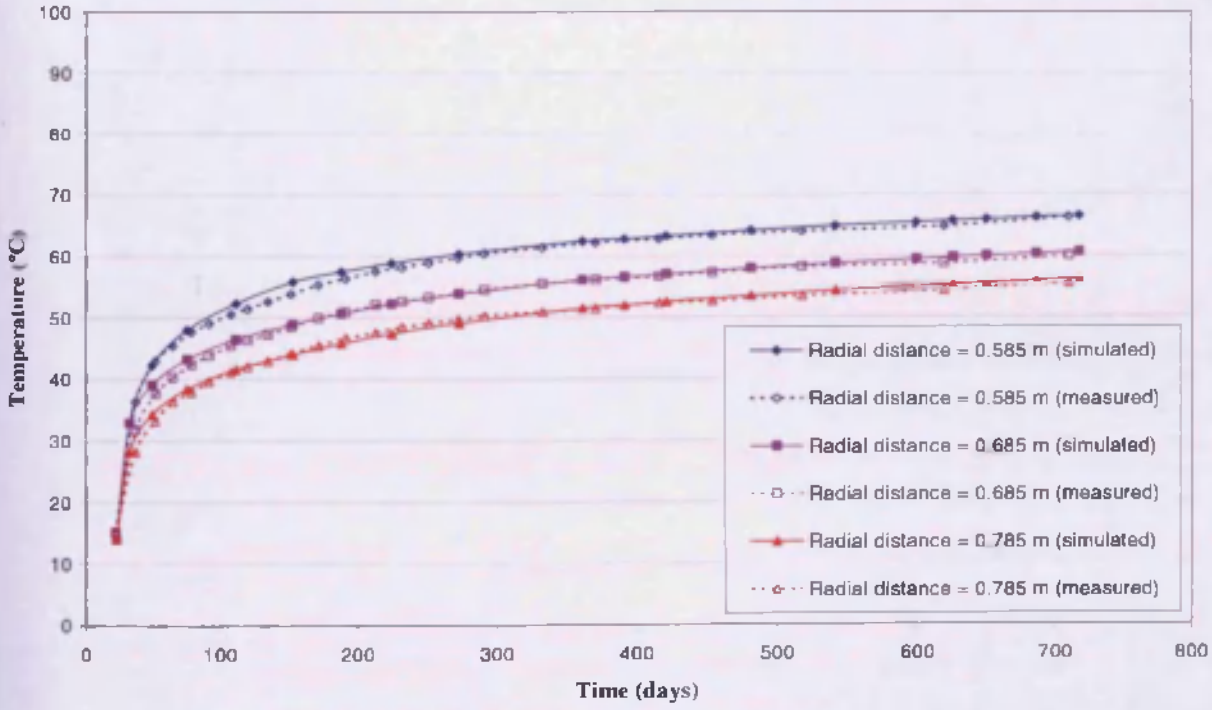

Figure 7.26 (b) Simulated and measured temperatures in Hole 3/Cylinder 1 at different positions

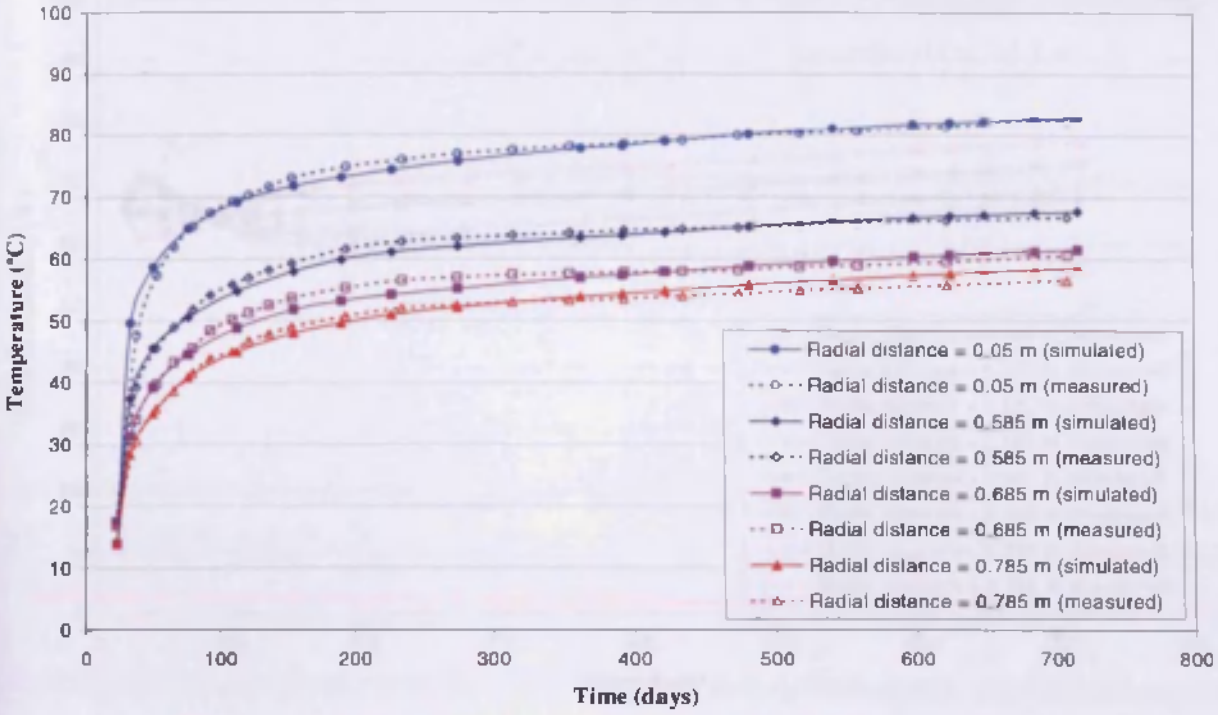

Figure 7.26 (c) Simulated and measured temperatures in Hole 3/Cylinder 2 at different positions

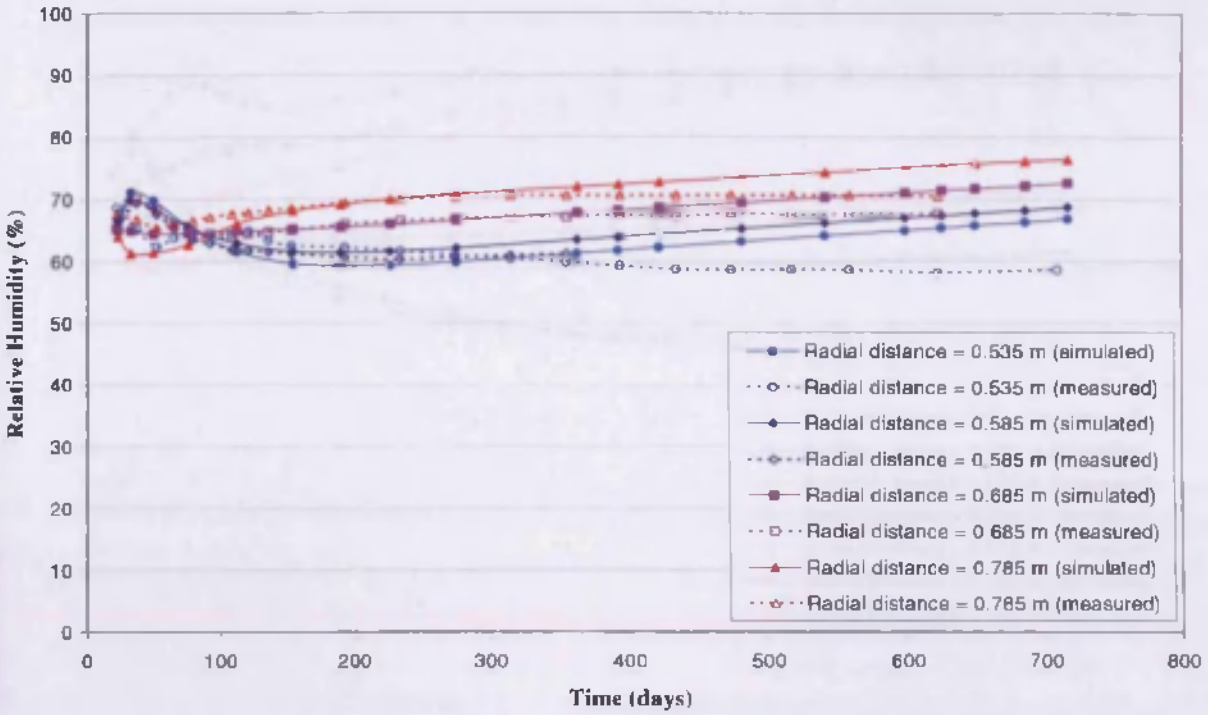

Figure 7.27 (a) Simulated and measured relative humidity in Hole 3/Ring 5 at different positions

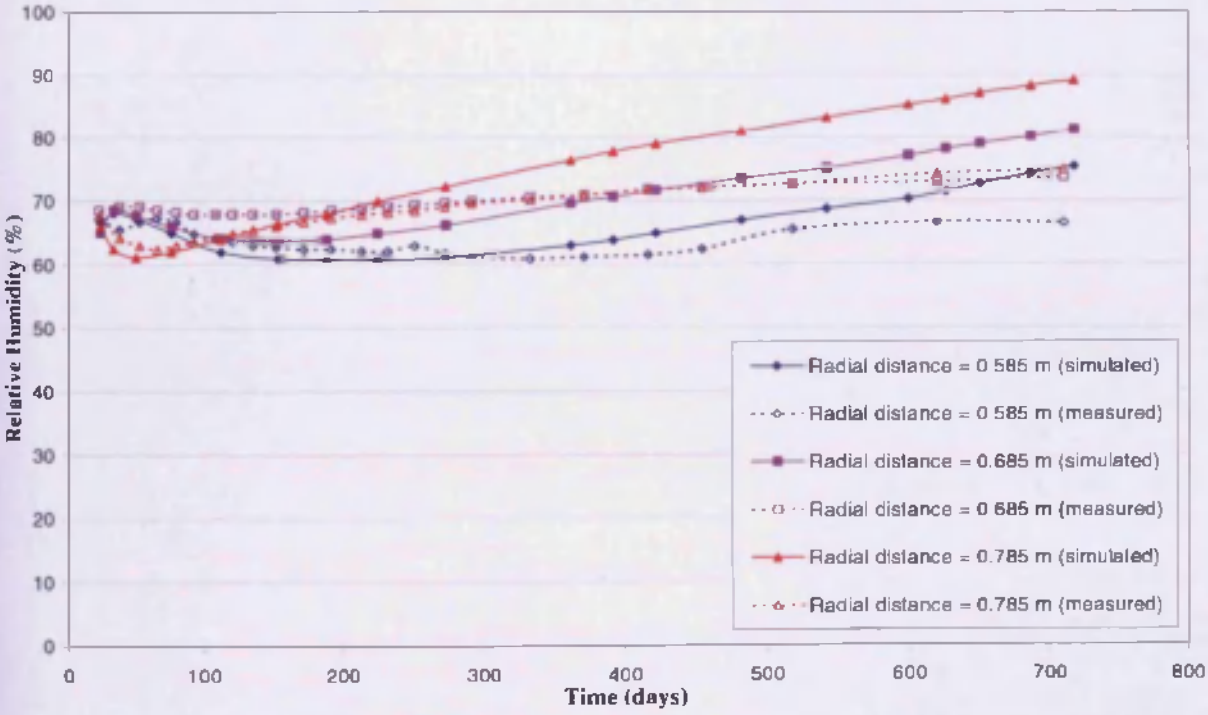

Figure 7.27 (b) Simulated and measured relative humidity in Hole 3/Cylinder 1 at different positions

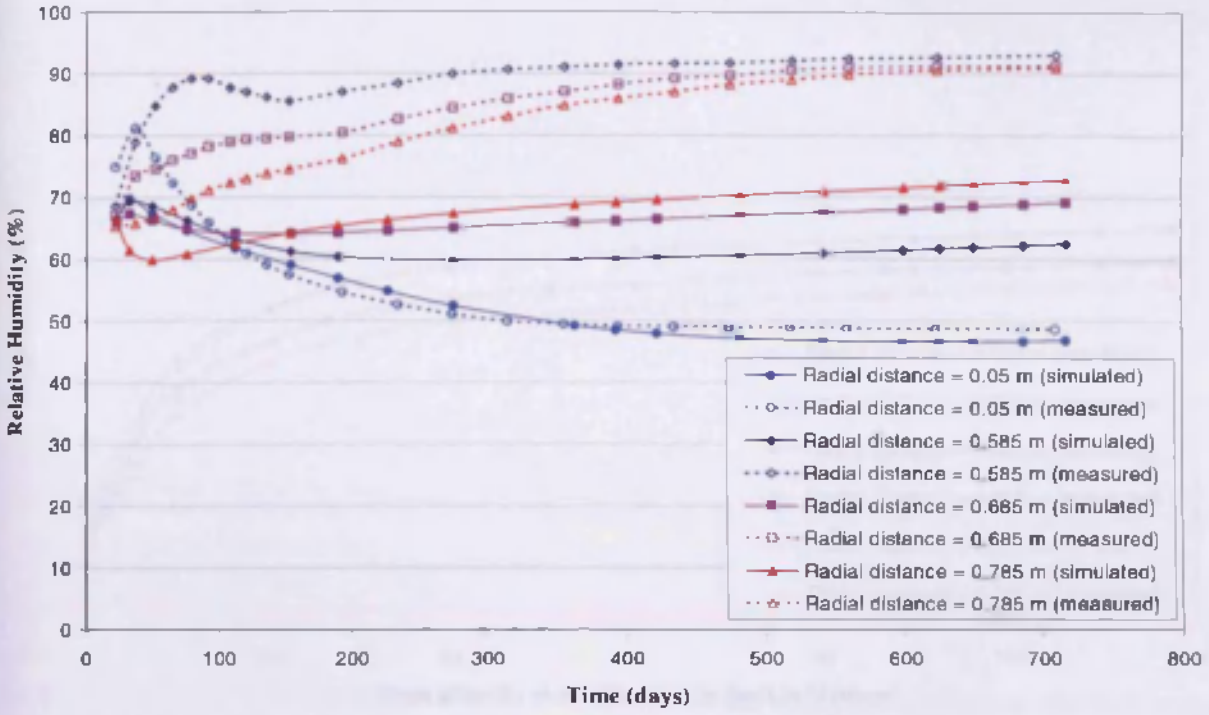

Figure 7.27 (c) Simulated and measured relative humidity in Hole 3/Cylinder 2 at different positions

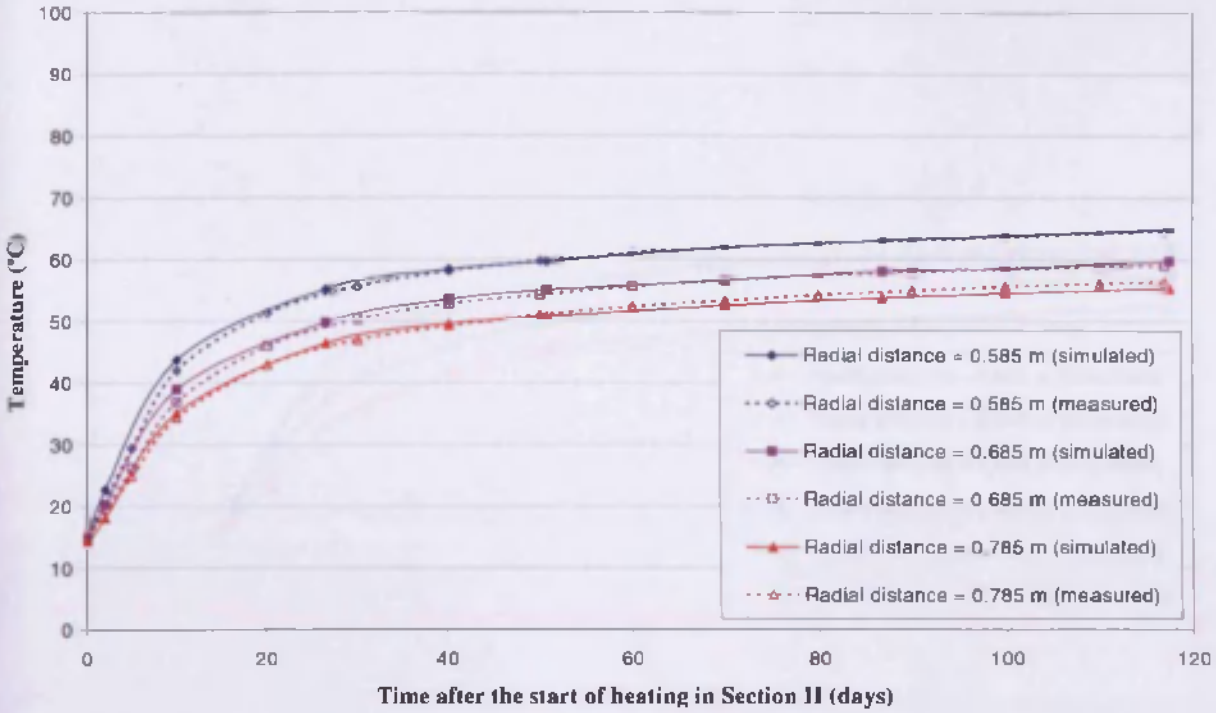

Figure 7.28 (a) Simulated and measured temperatures in Hole 5/Ring 5 at different positions

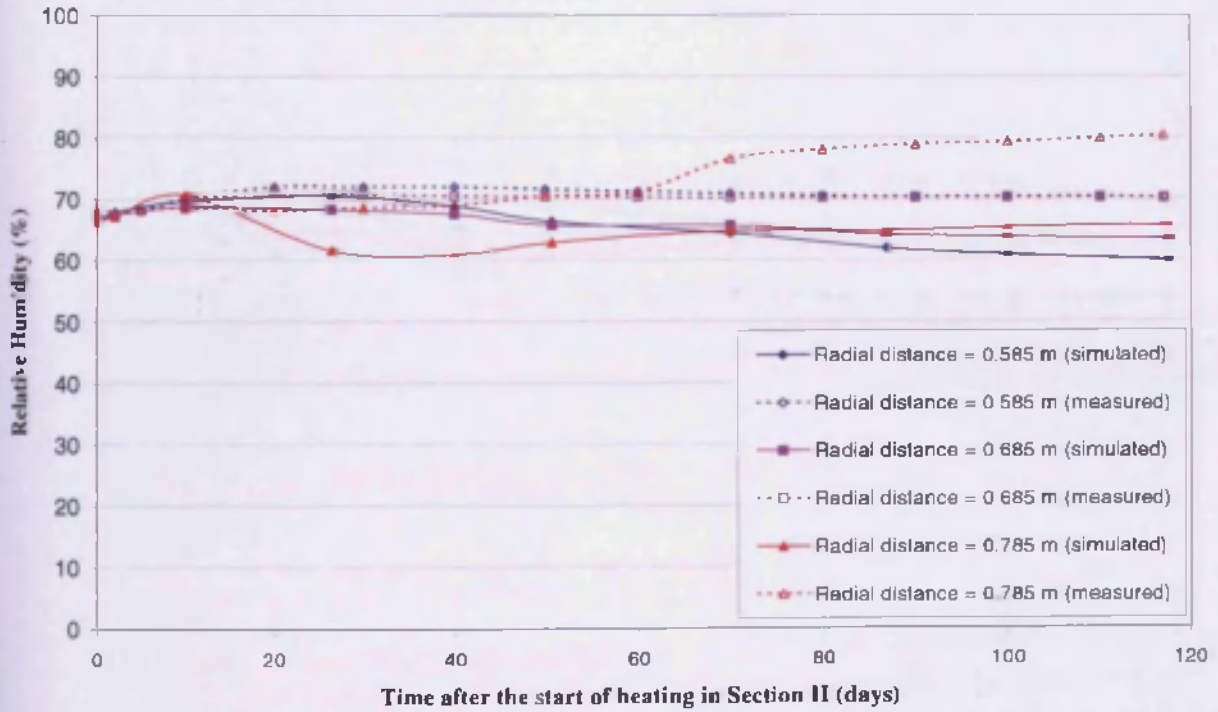

Figure 7.28 (b) Simulated and measured relative humidity in Hole 5/Ring 5 at different positions

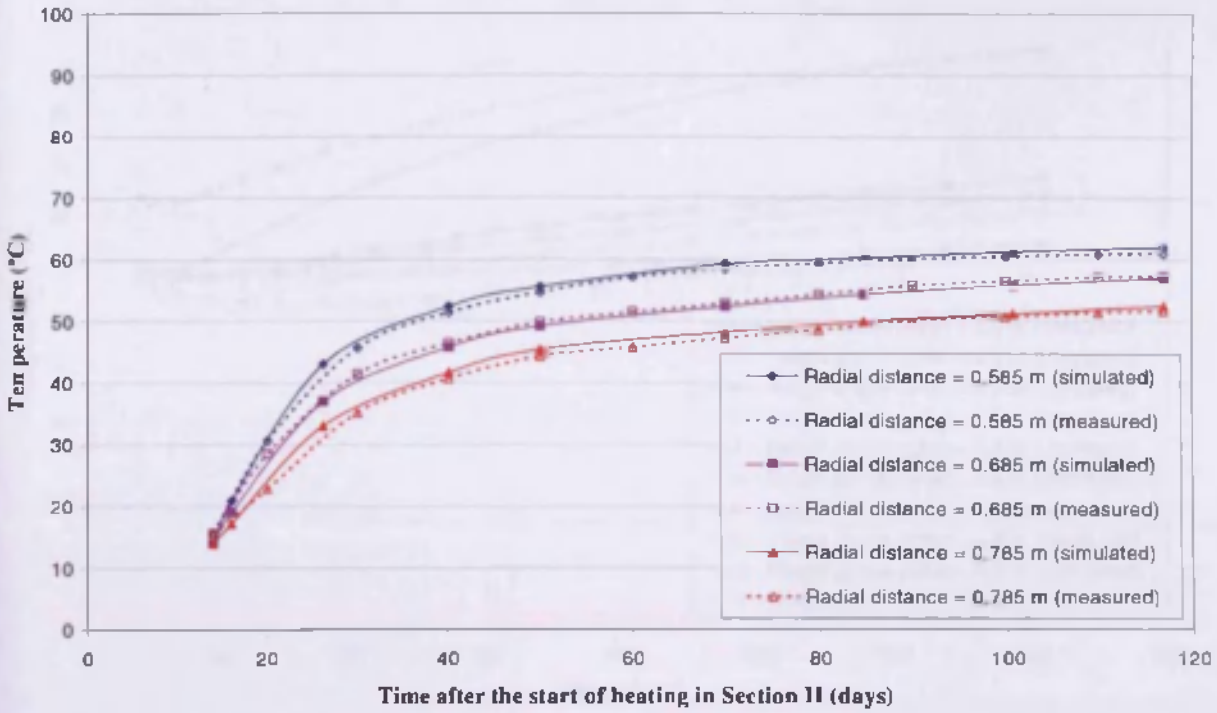

Figure 7.29 (a) Simulated and measured temperatures in Hole 6/Ring 5 at different positions

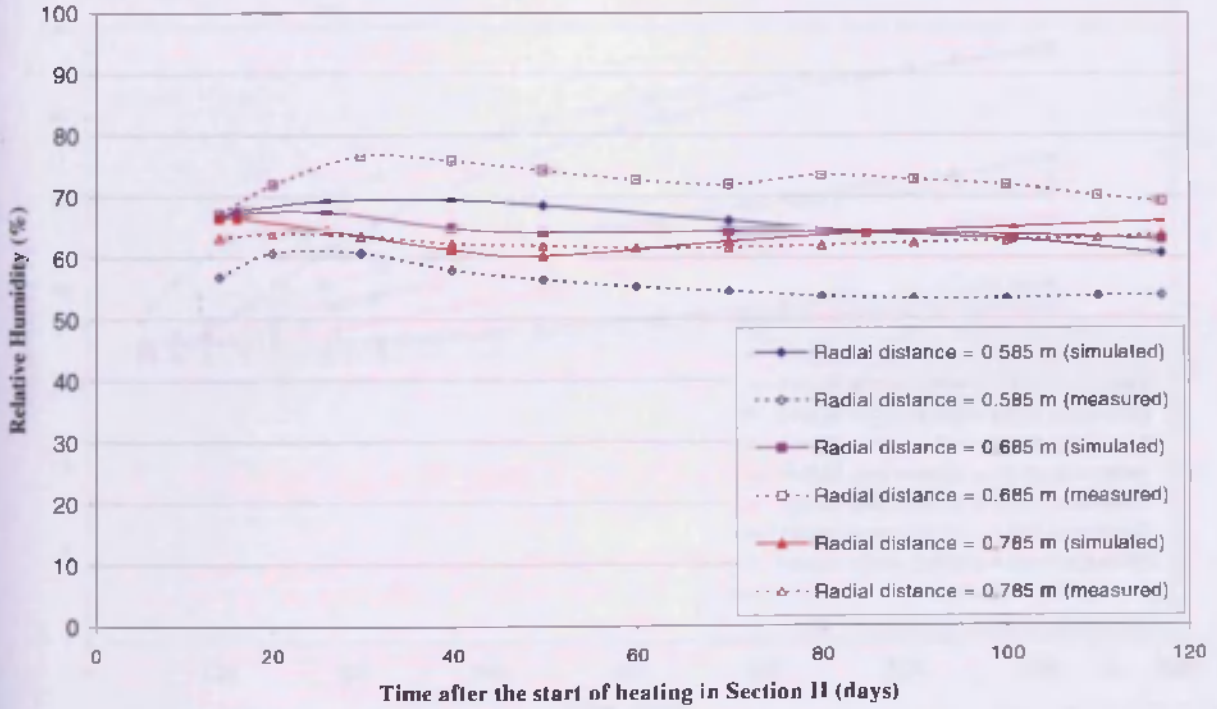

Figure 7.29 (b) Simulated and measured relative humidity in Hole 6/Ring 5 at different positions

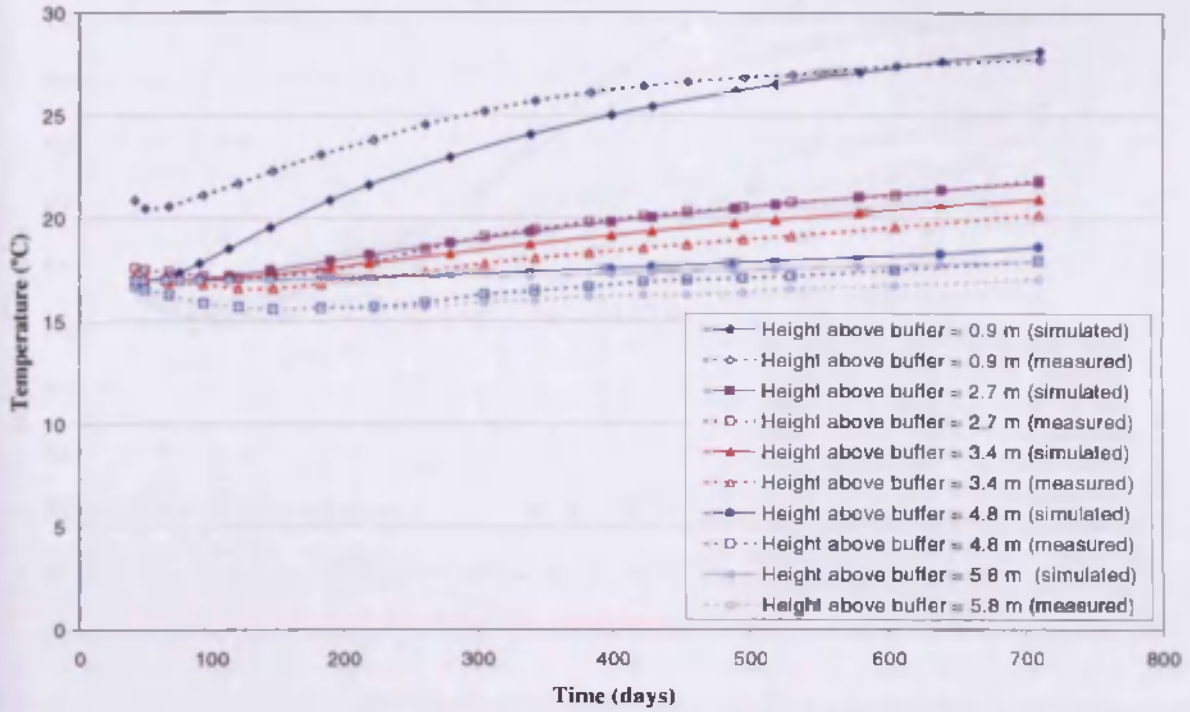

Figure 7.30 (a) Simulated and measured temperatures in the backfill directly above Hole 1 at different heights above the top of the buffer

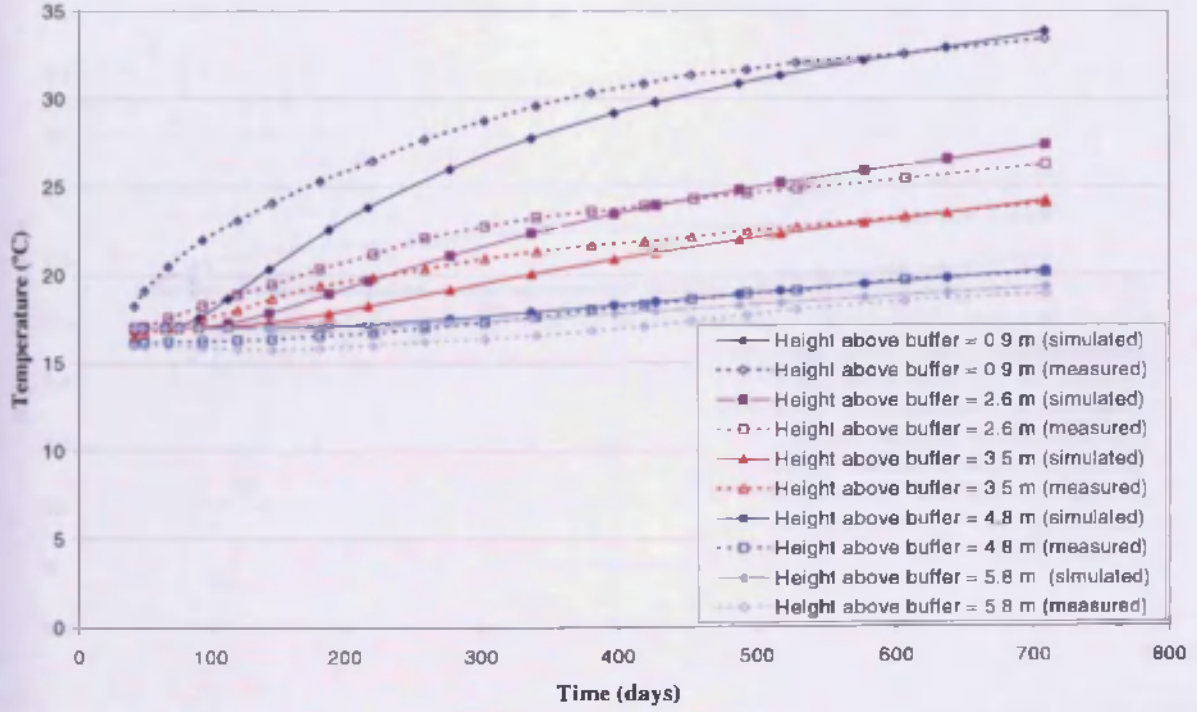

Figure 7.30 (b) Simulated and measured temperatures in the backfill directly above Hole 3 at different heights above the top of the buffer

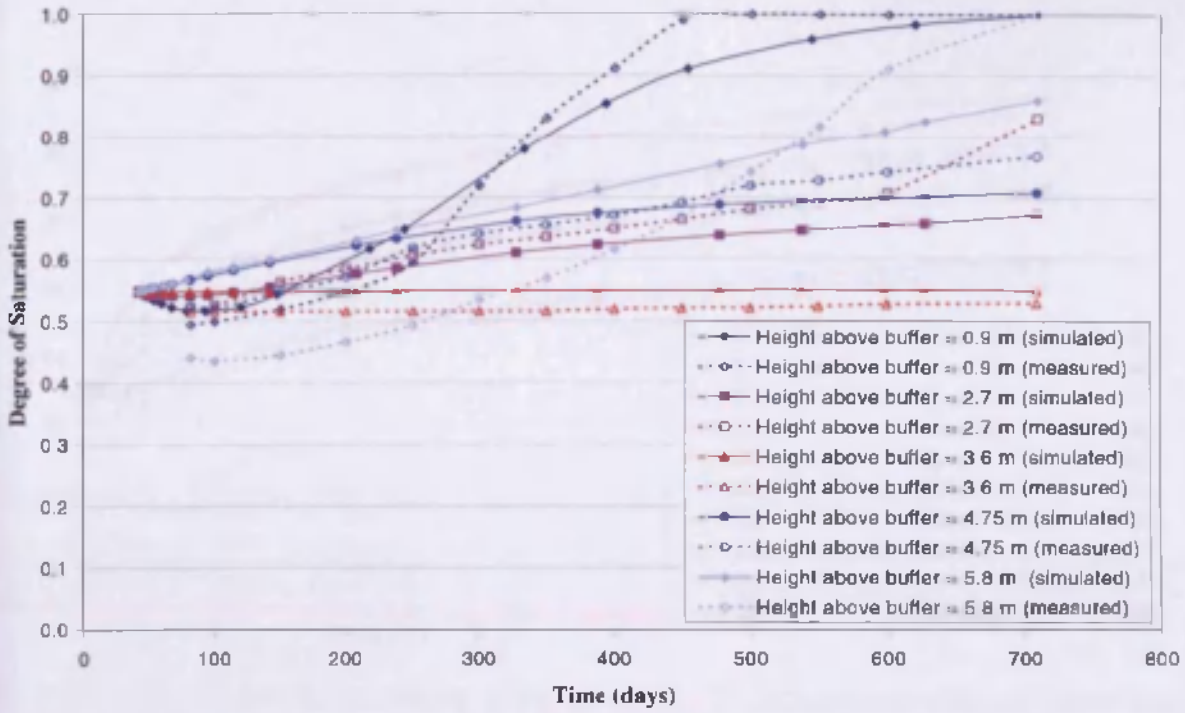

Figure 7.31 (a) Simulated and measured degree of saturation in the backfill directly above Hole 1 at different heights above the top of the buffer

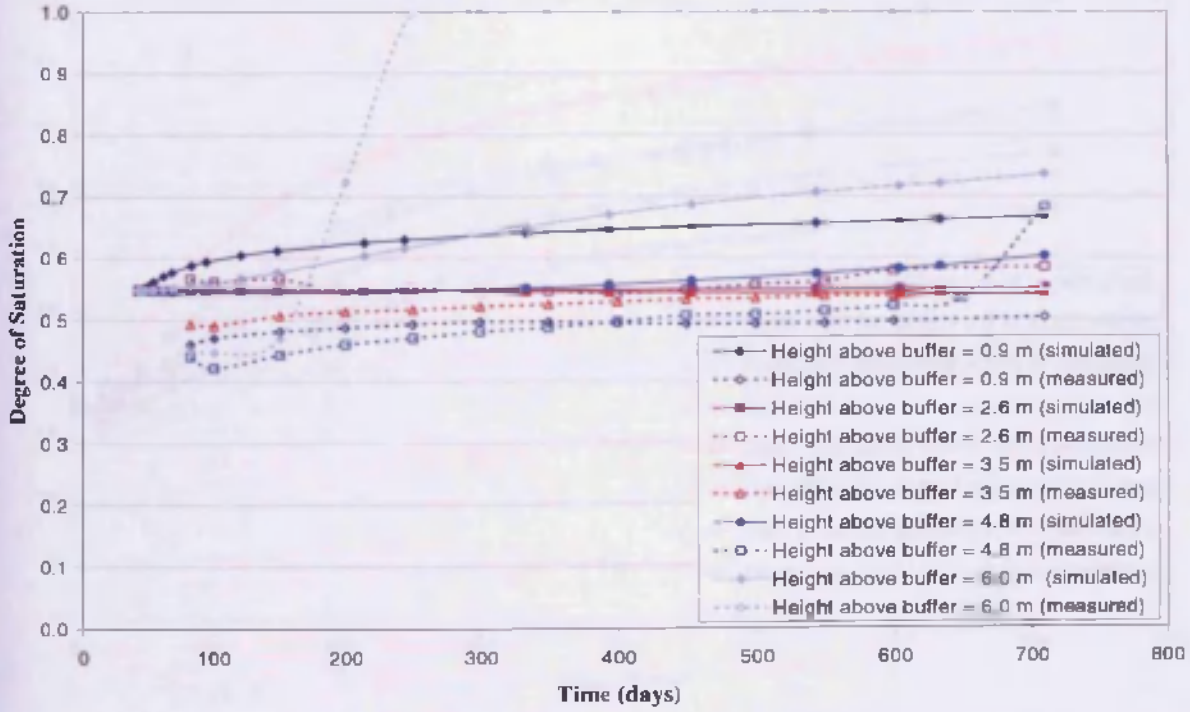

Figure 7.31 (b) Simulated and measured degree of saturation in the backfill directly above Hole 3 at different heights above the top of the buffer

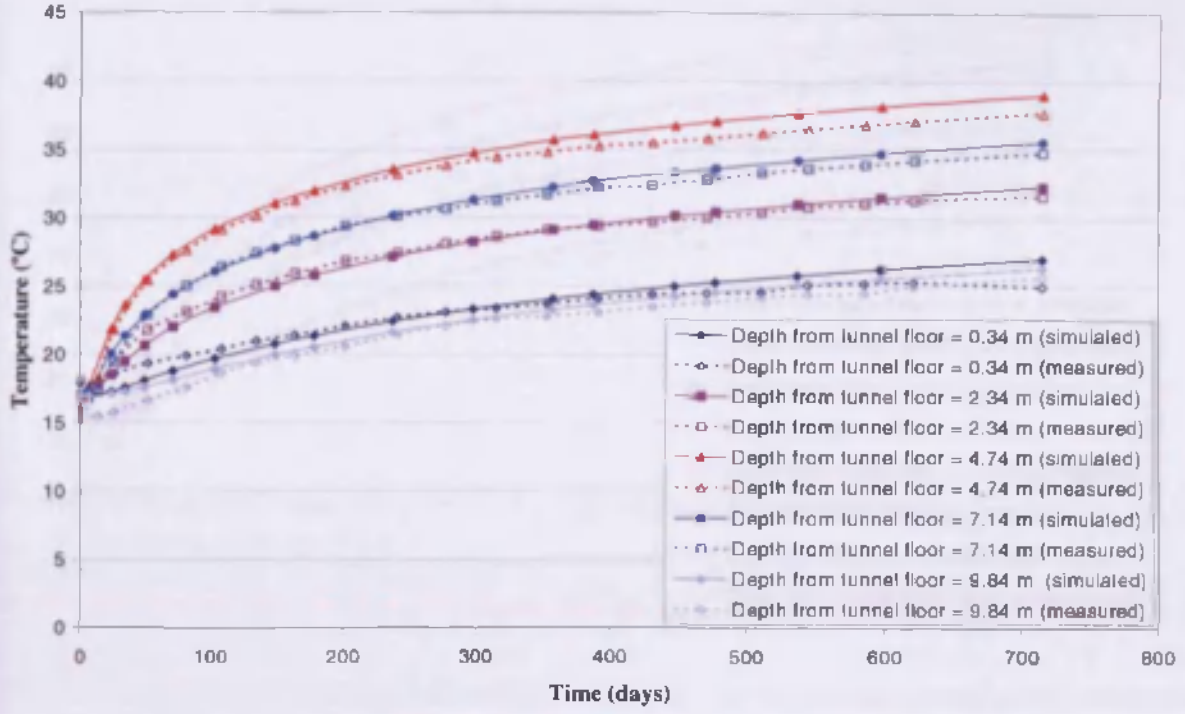

Figure 7.32 (a) Simulated and measured temperatures in the rock at a radius of 2 m from Hole 1 at different depths

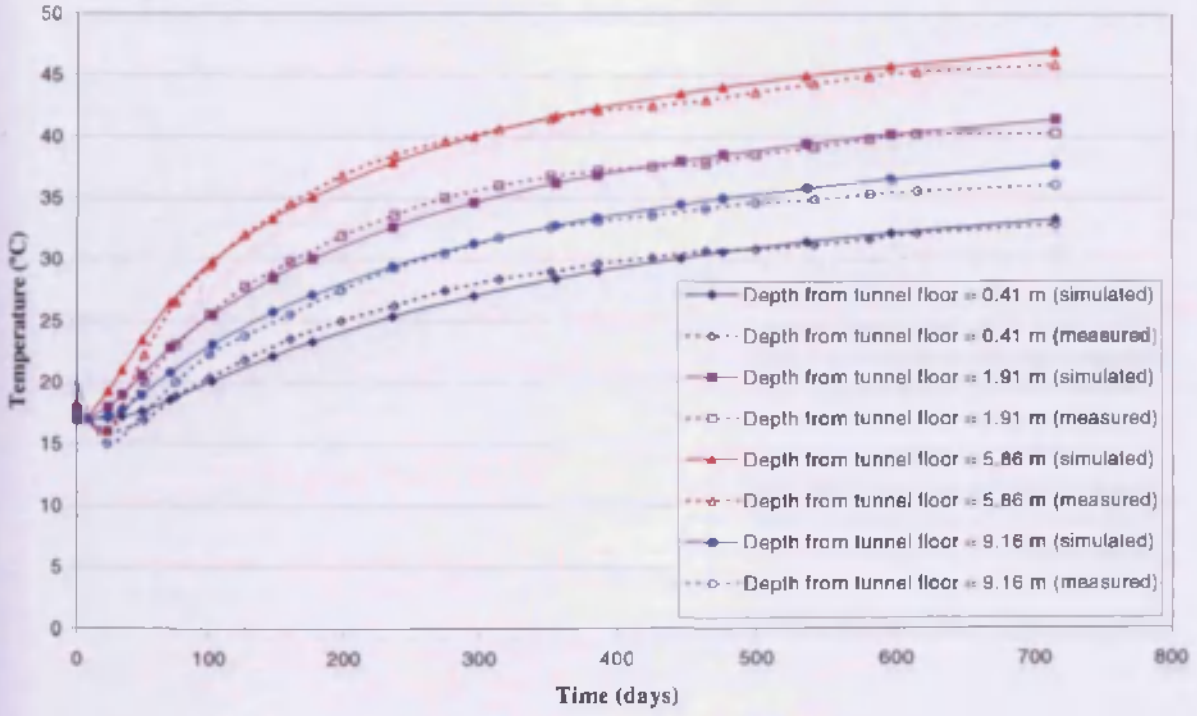

Figure 7.32 (b) Simulated and measured temperatures in the rock at a radius of 2.5 m from Hole 2 at different depths

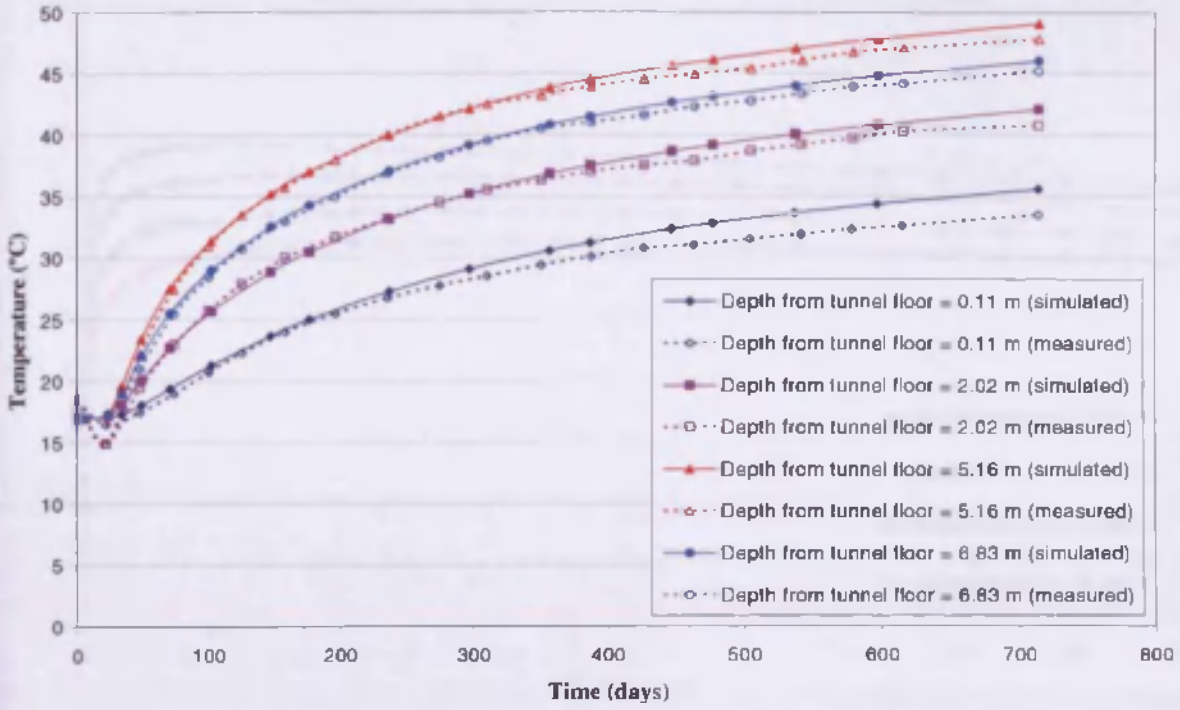

Figure 7.32 (c) Simulated and measured temperatures in the rock at a radius of 2 m from Hole 3 at different depths

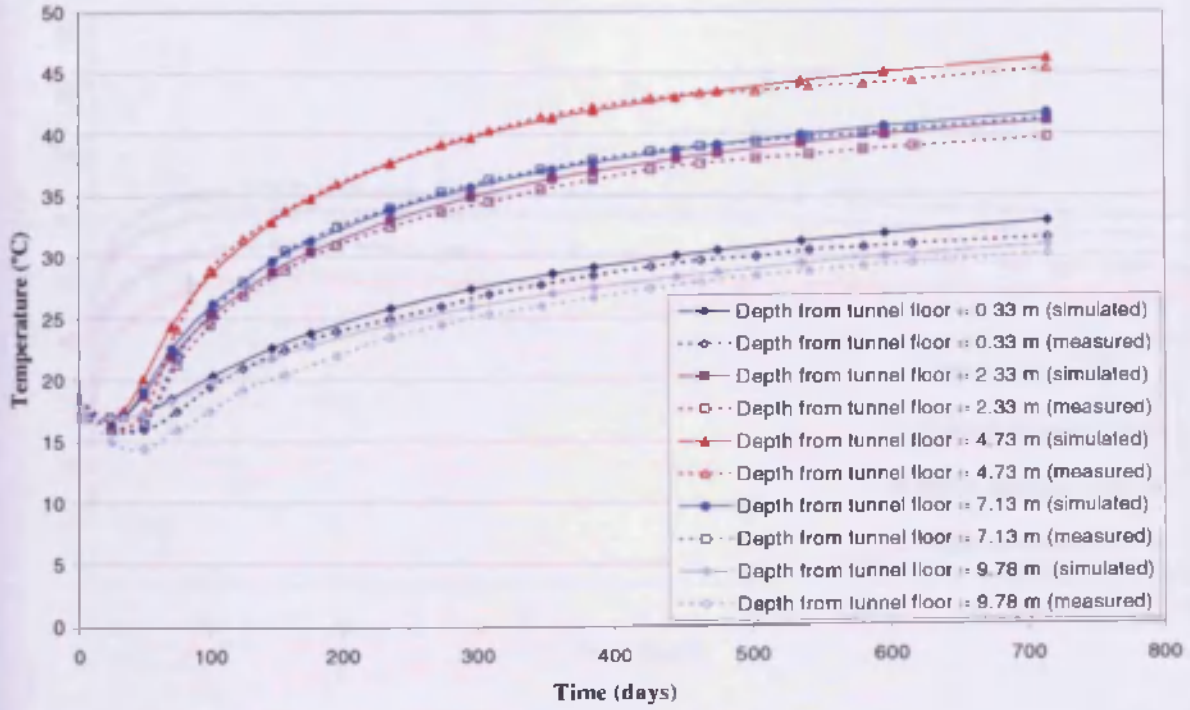

Figure 7.32 (d) Simulated and measured temperatures in the rock at a radius of 2 m from Hole 4 at different depths

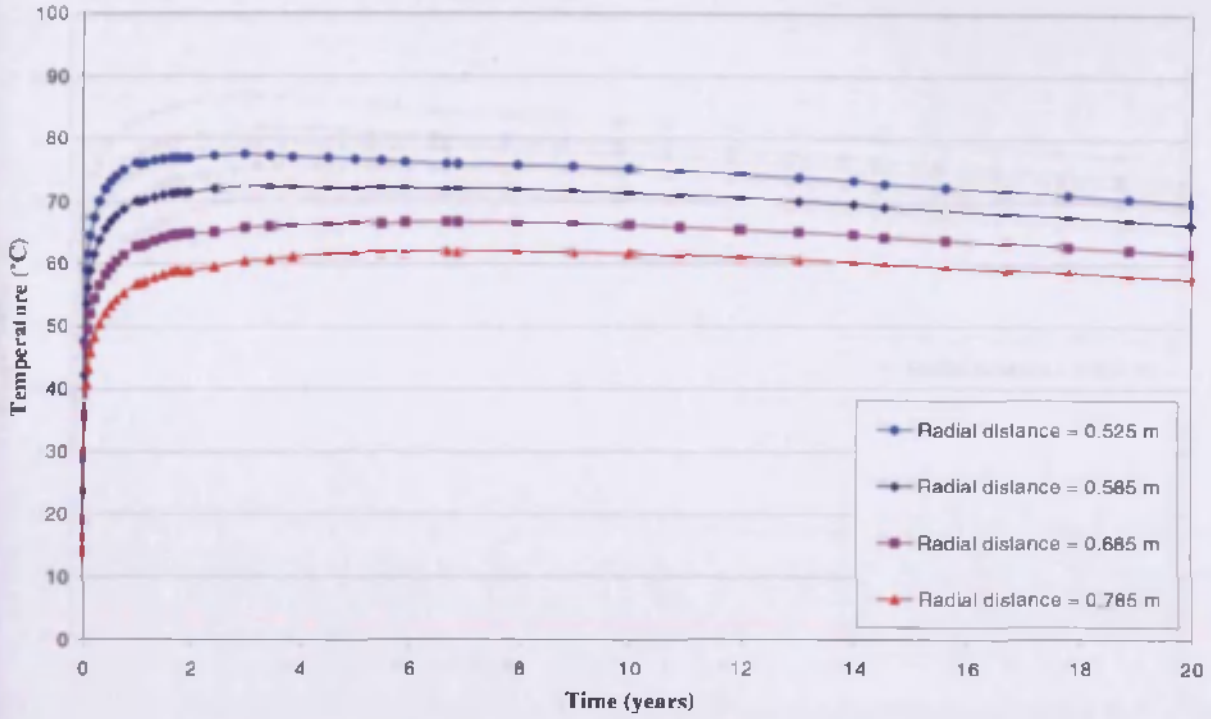

Figure 7.33 (a) Simulated temperatures in Hole 1/Ring 5 over 20 years

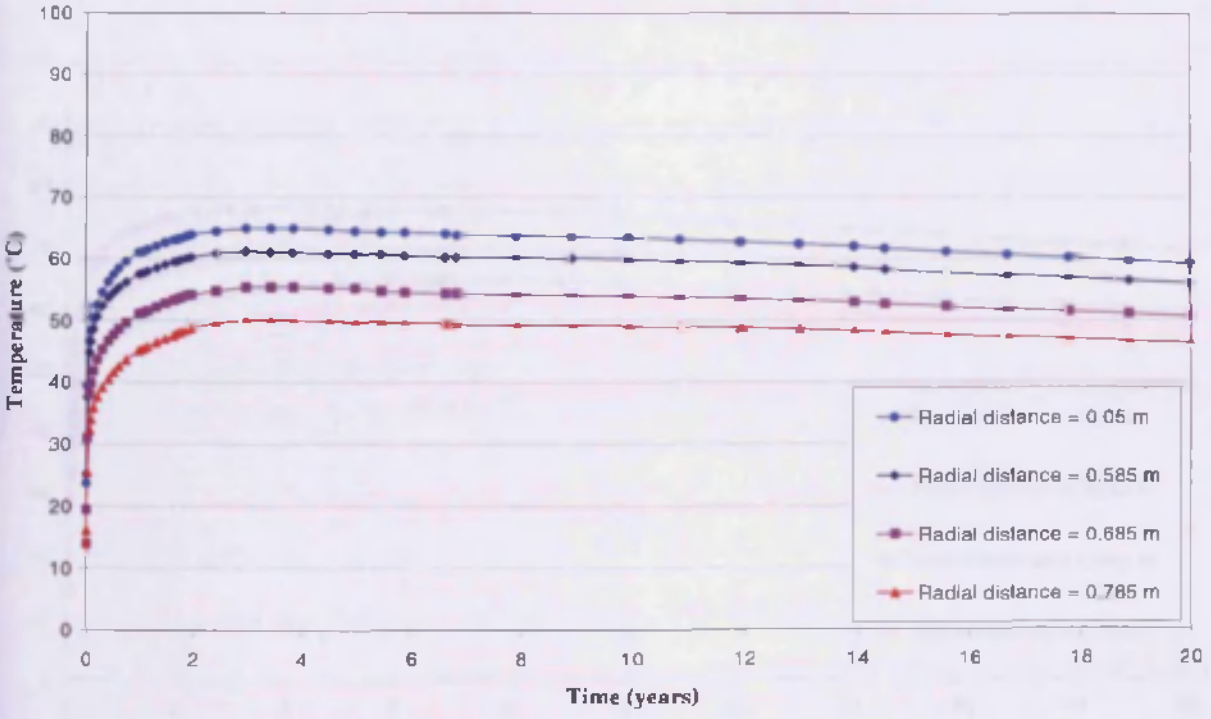

Figure 7.33 (b) Simulated temperatures in Hole 1/Cylinder 1 over 20 years

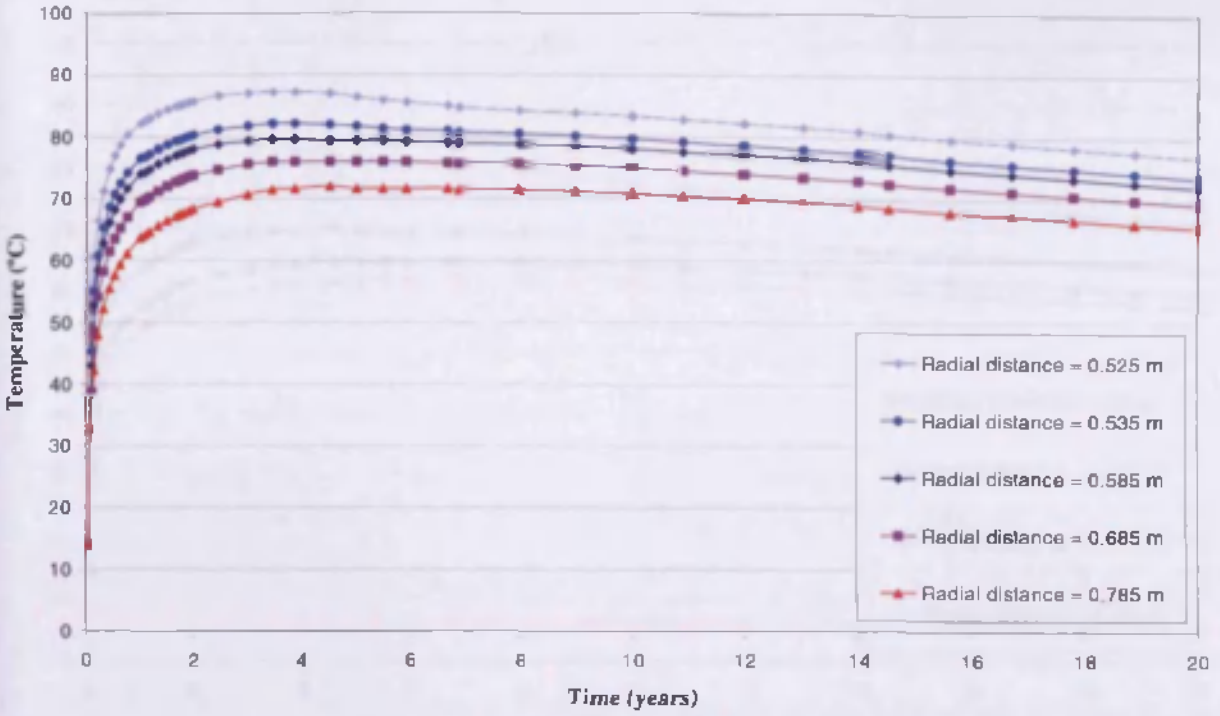

Figure 7.33 (c) Simulated temperatures in Hole 3/Ring 5 over 20 years

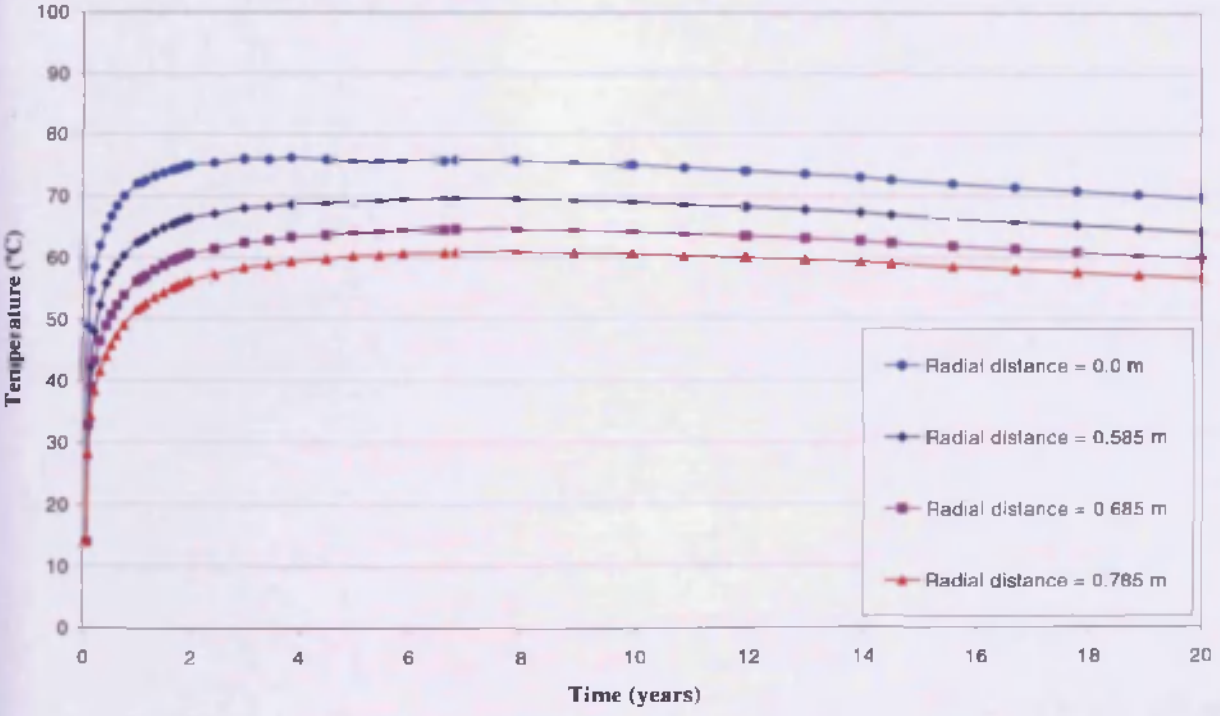

Figure 7.33 (d) Simulated temperatures in Hole 3/Cylinder 1 over 20 years

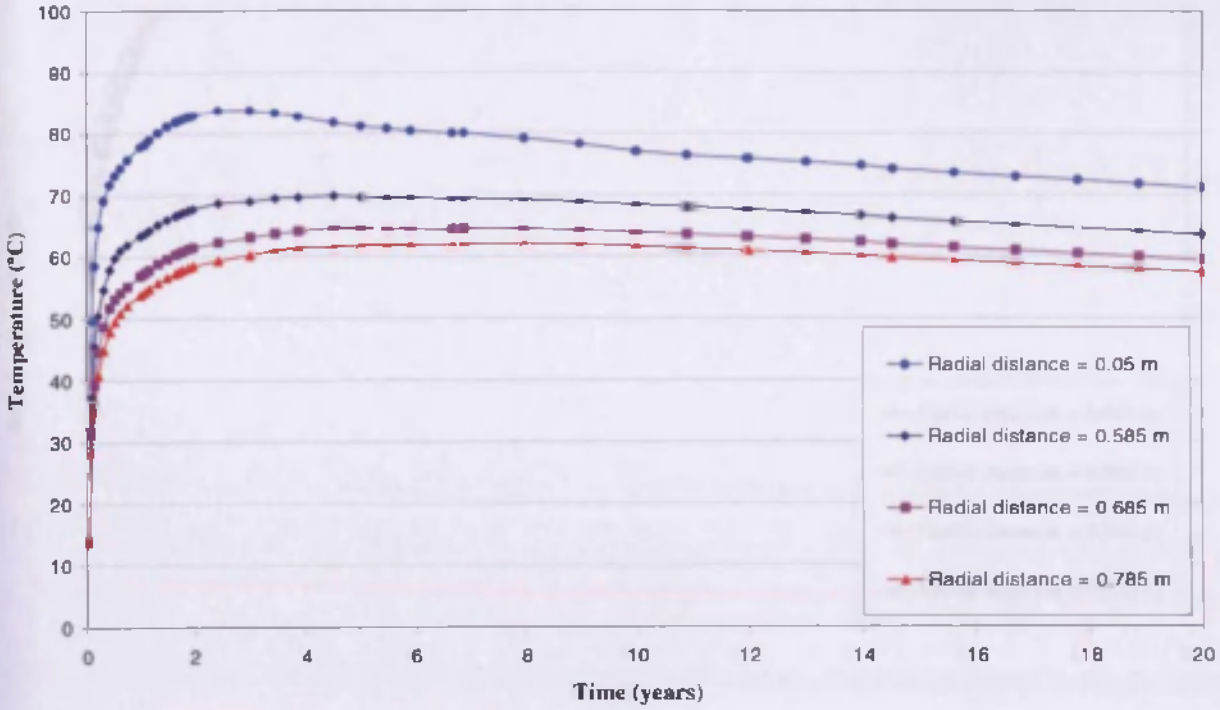

Figure 7.33 (e) Simulated temperatures in Hole 3/Cylinder 2 over 20 years

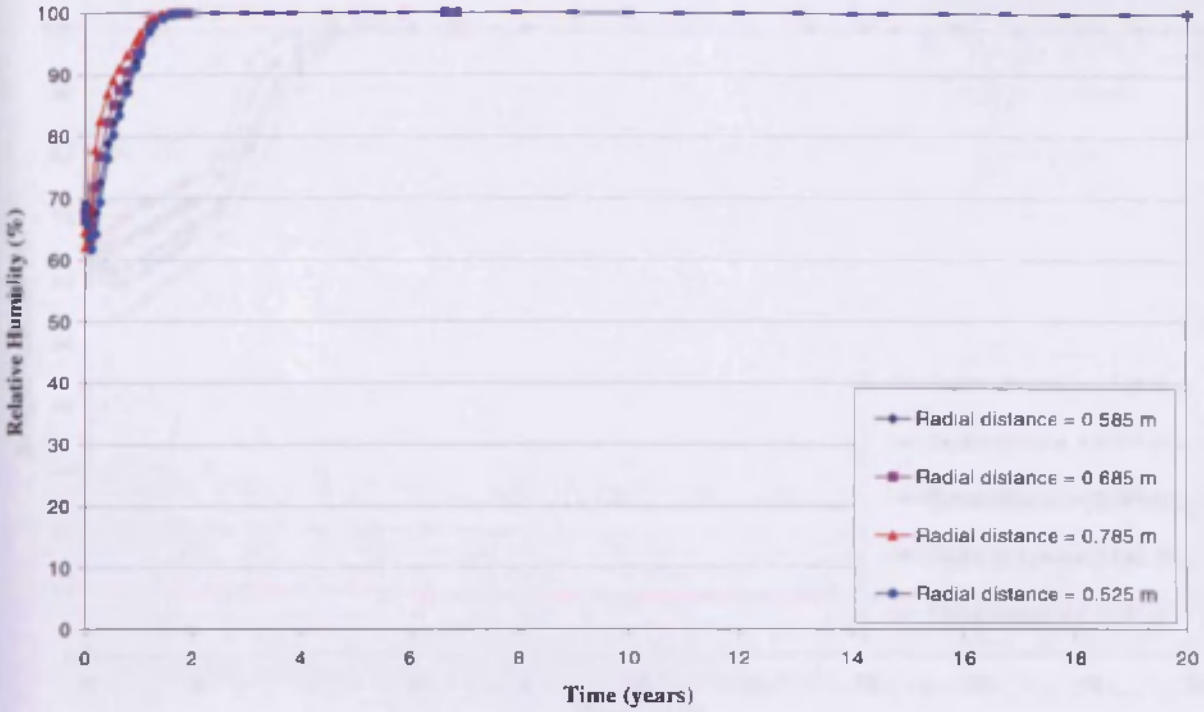

Figure 7.34 (a) Simulated relative humidity in Hole 1/Ring 5 over 20 years

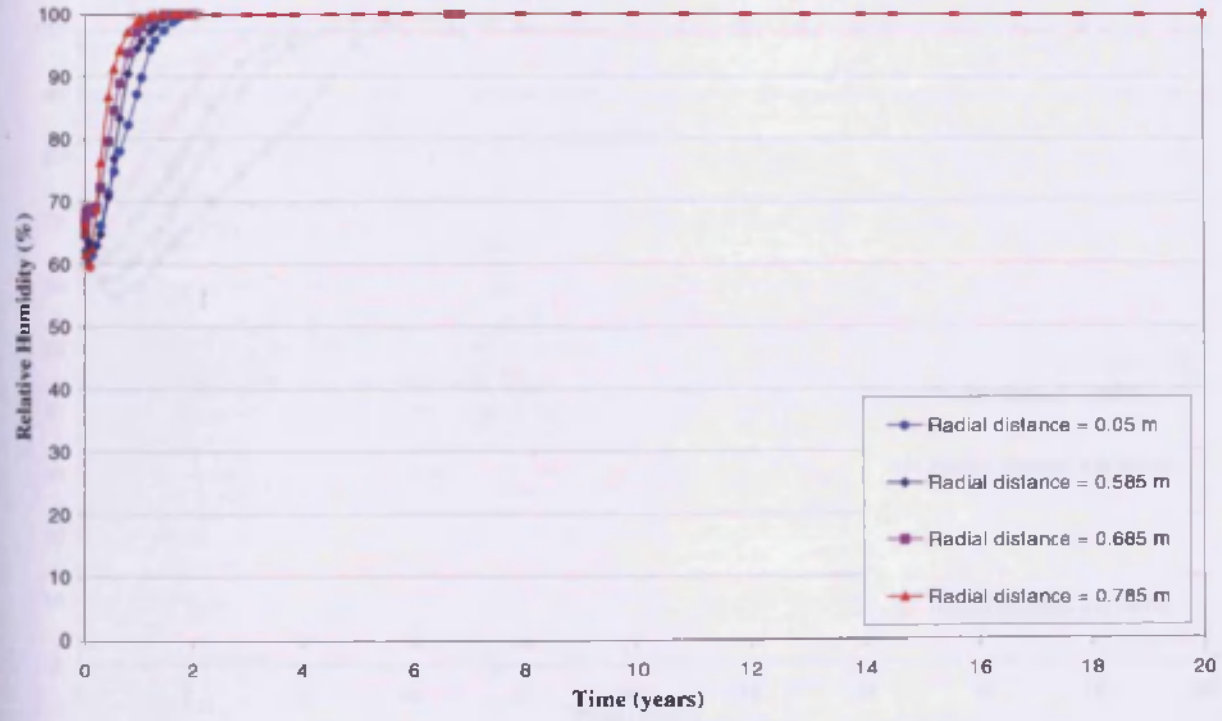

Figure 7.34 (b) Simulated relative humidity in Hole 3/Cylinder 1 over 20 years

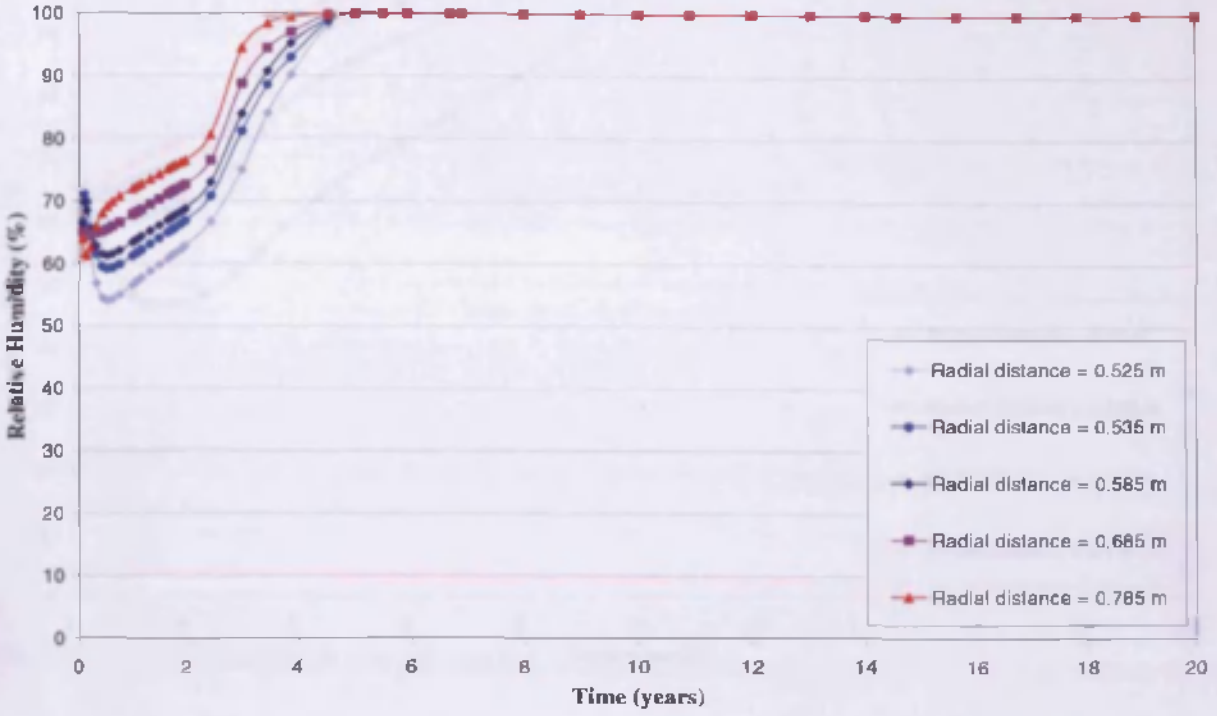

Figure 7.34 (c) Simulated relative humidity in Hole 3/Ring 5 over 20 years

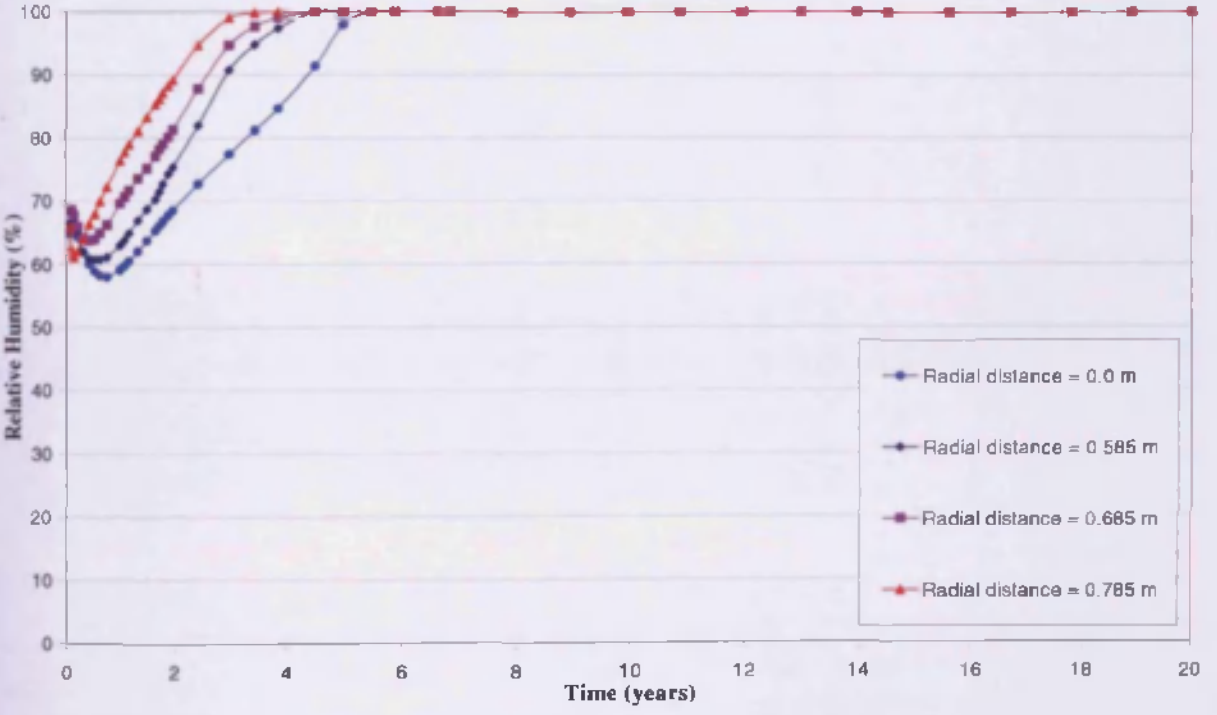

Figure 7.34 (d) Simulated relative humidity in Hole 3/Cylinder 1 over 20 years

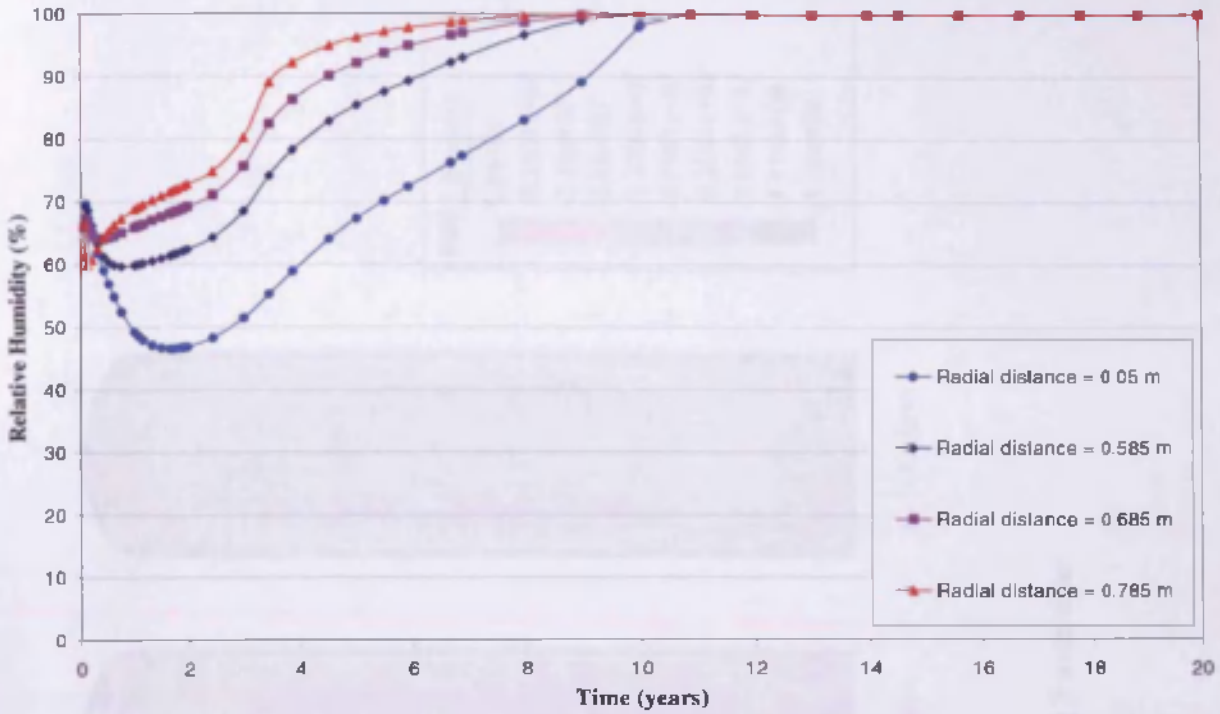

Figure 7.34 (e) Simulated relative humidity in Hole 3/Cylinder 2 over 20 years

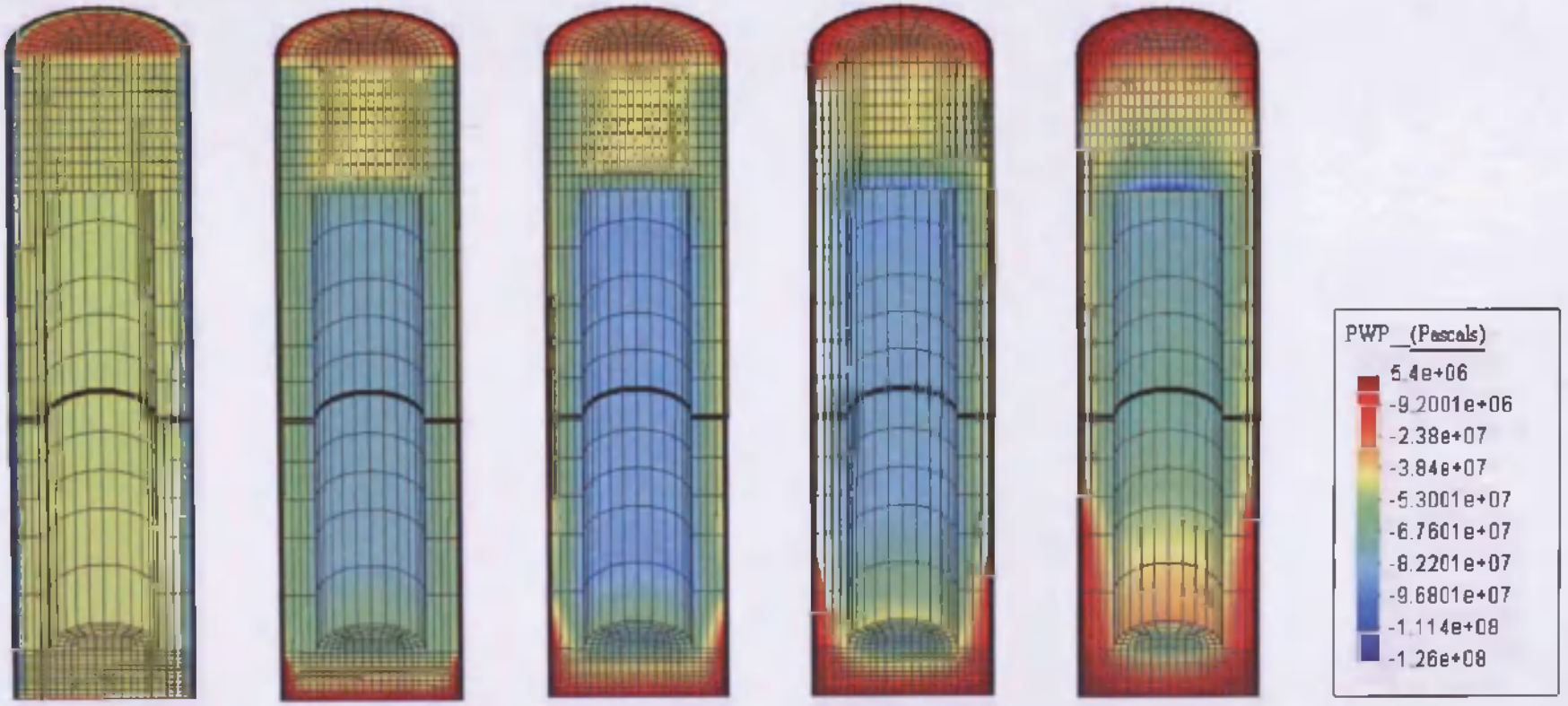

a) 1 day b) 100 days c) 200 days d) 365 days e) 600 days

Figure 7.35 Pore water pressure contour plots in the buffer in deposition hole 3 over time

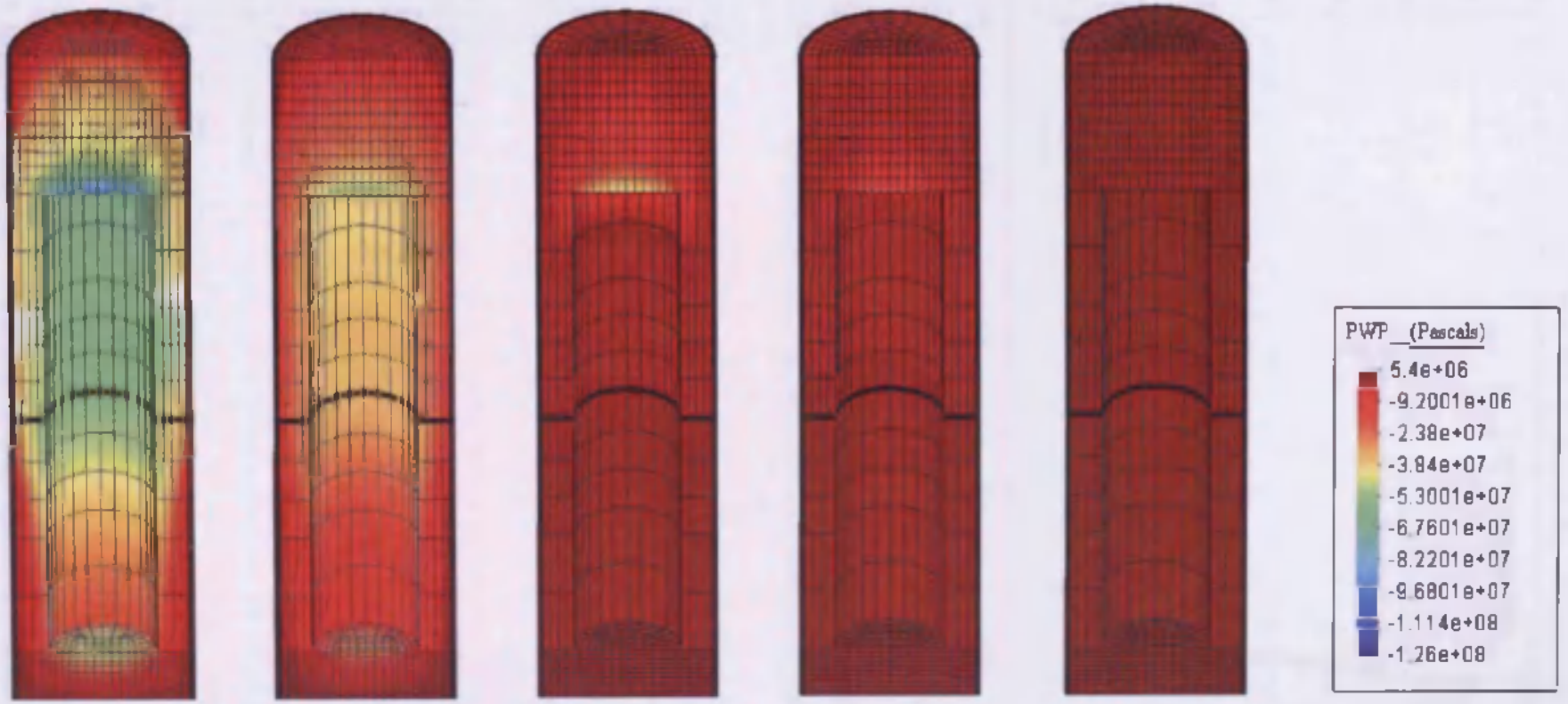

f) 3 years g) 5 years h) 7 years i) 9 years j) 11 years

Figure 7.35 (cont.) Pore water pressure contour plots in the buffer in deposition hole 3 over time

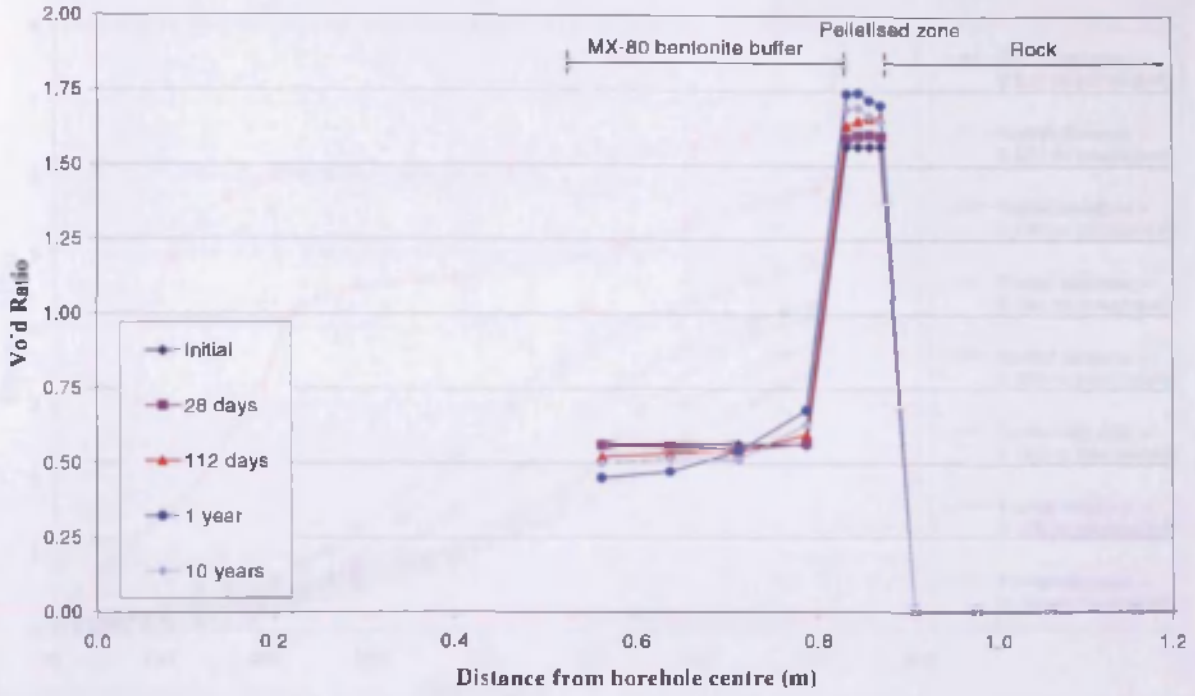

Figure 7.36 (a) Variation of void ratio through the buffer and pellets using original mechanical material parameters for the pelletised region

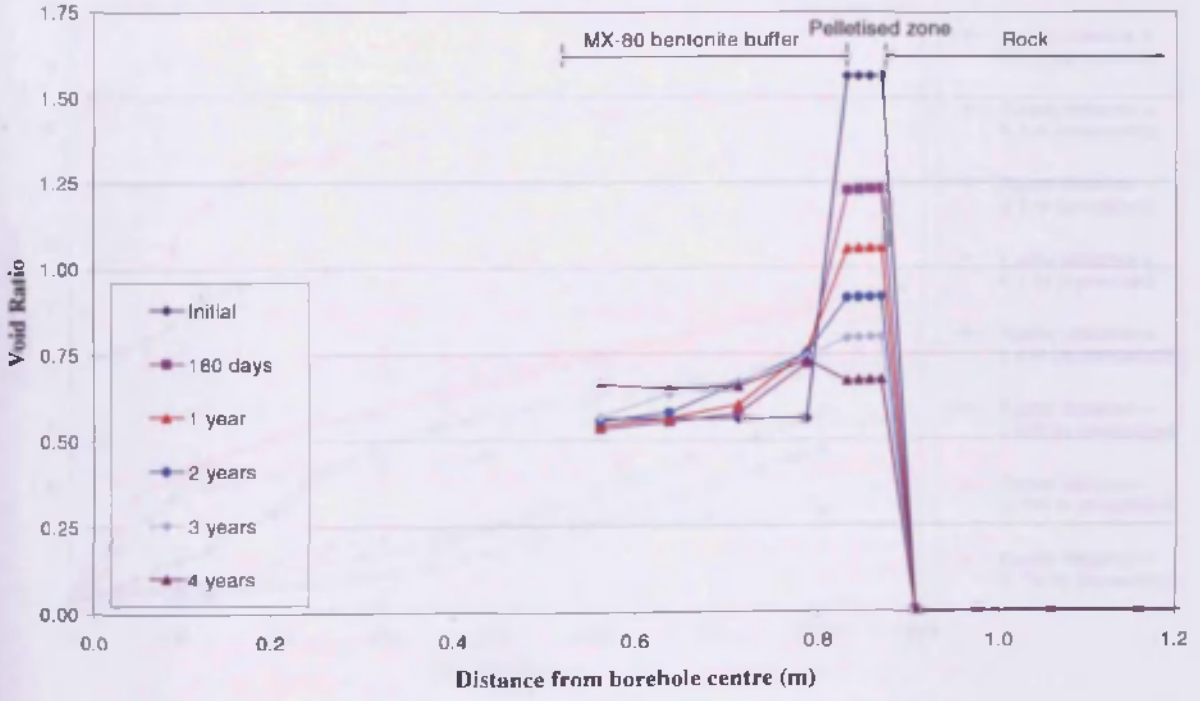

Figure 7.36 (b) Variation of void ratio through the buffer and pellets using modified mechanical material parameters for the pelletised region

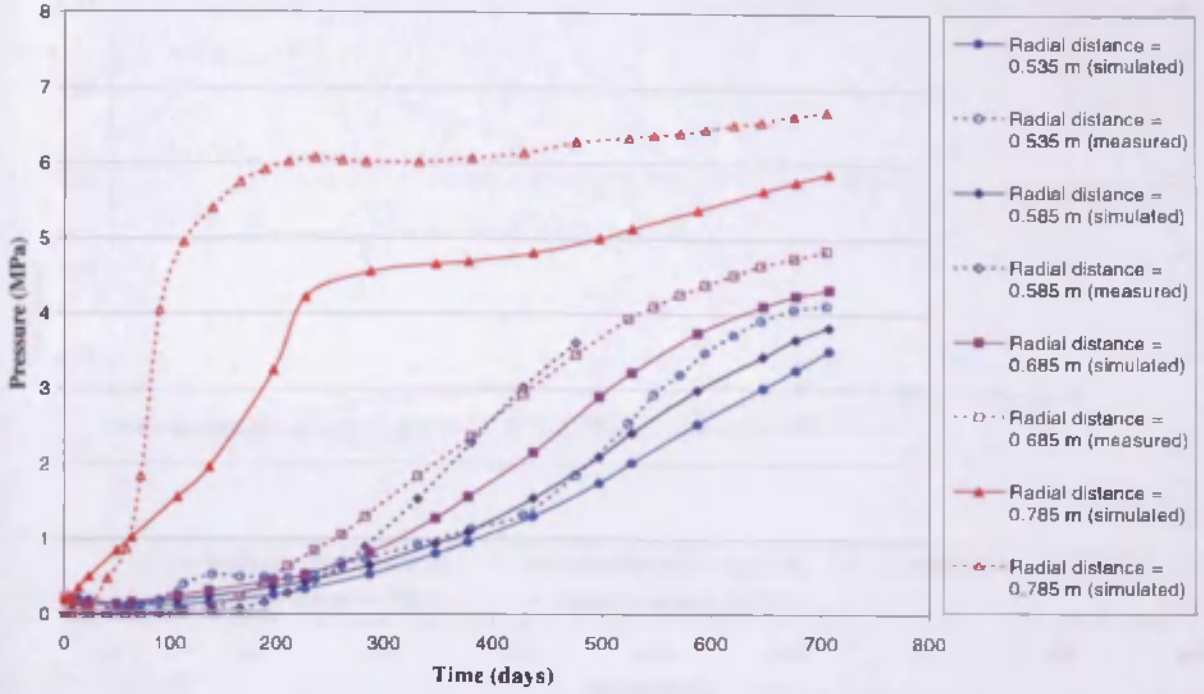

Figure 7.37 (a) Simulated and measured total pressure in Hole 1/Ring 5 at different positions

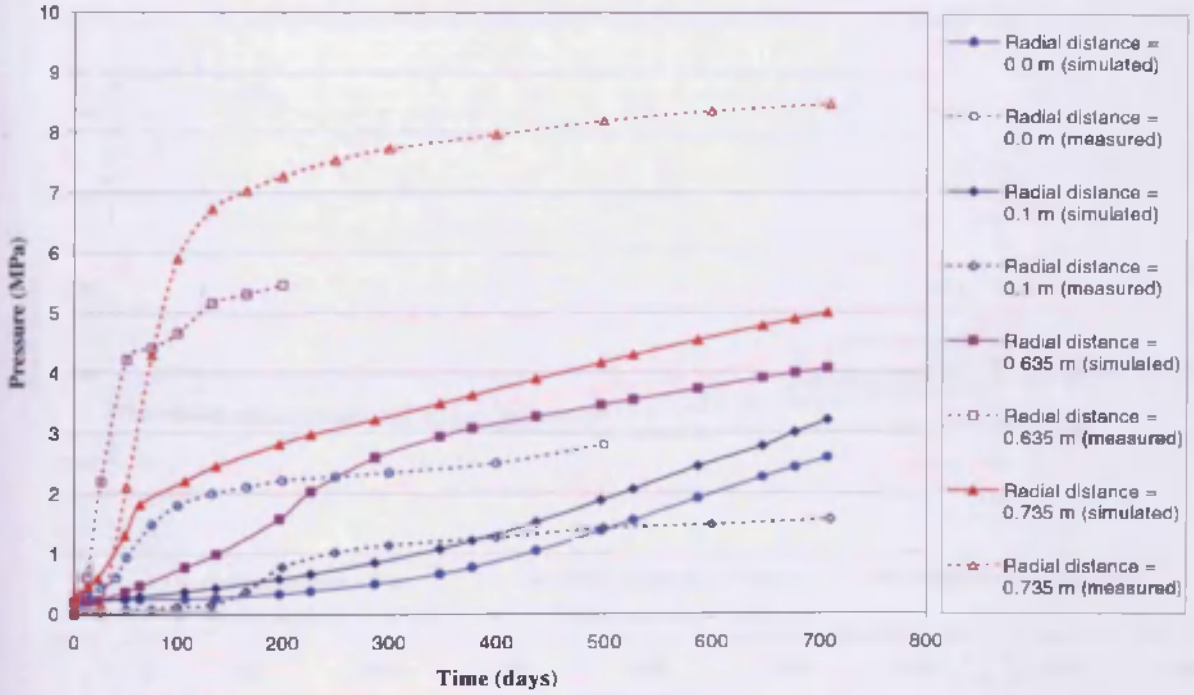

Figure 7.37 (b) Simulated and measured total pressure in Hole 1/Cylinder 1 at different positions

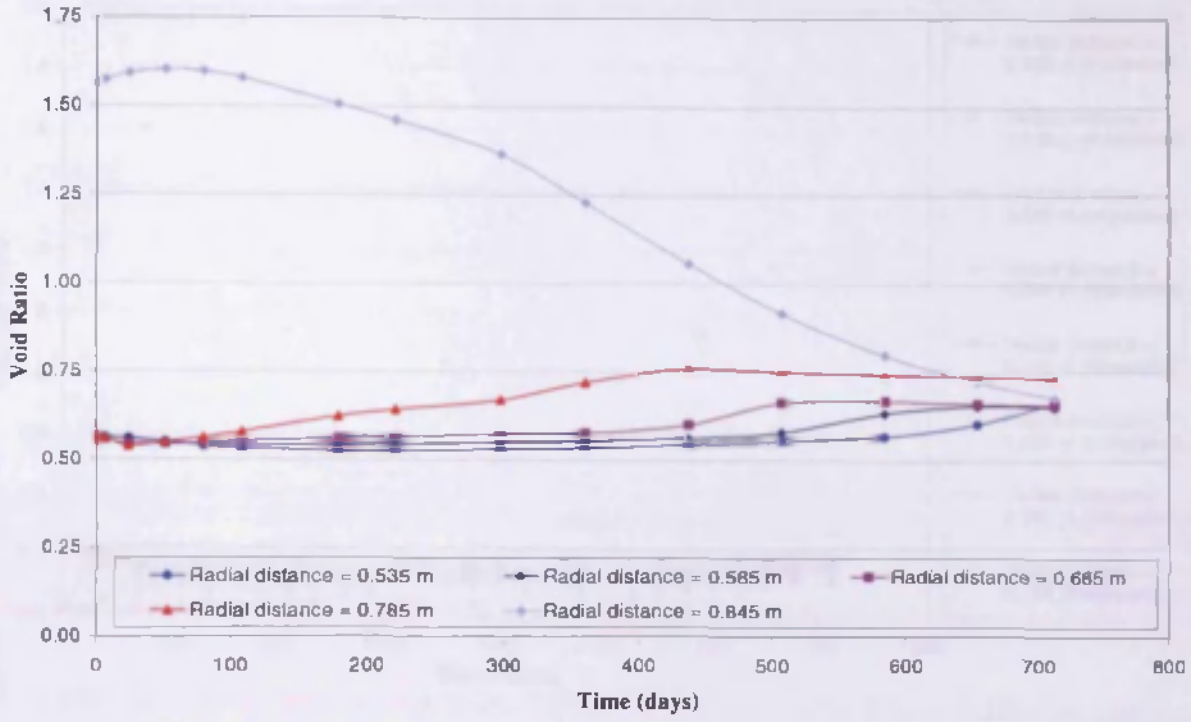

Figure 7.38 (a) Variation of void ratio in the buffer and pelletised region in Hole 1/Ring 5 at different positions

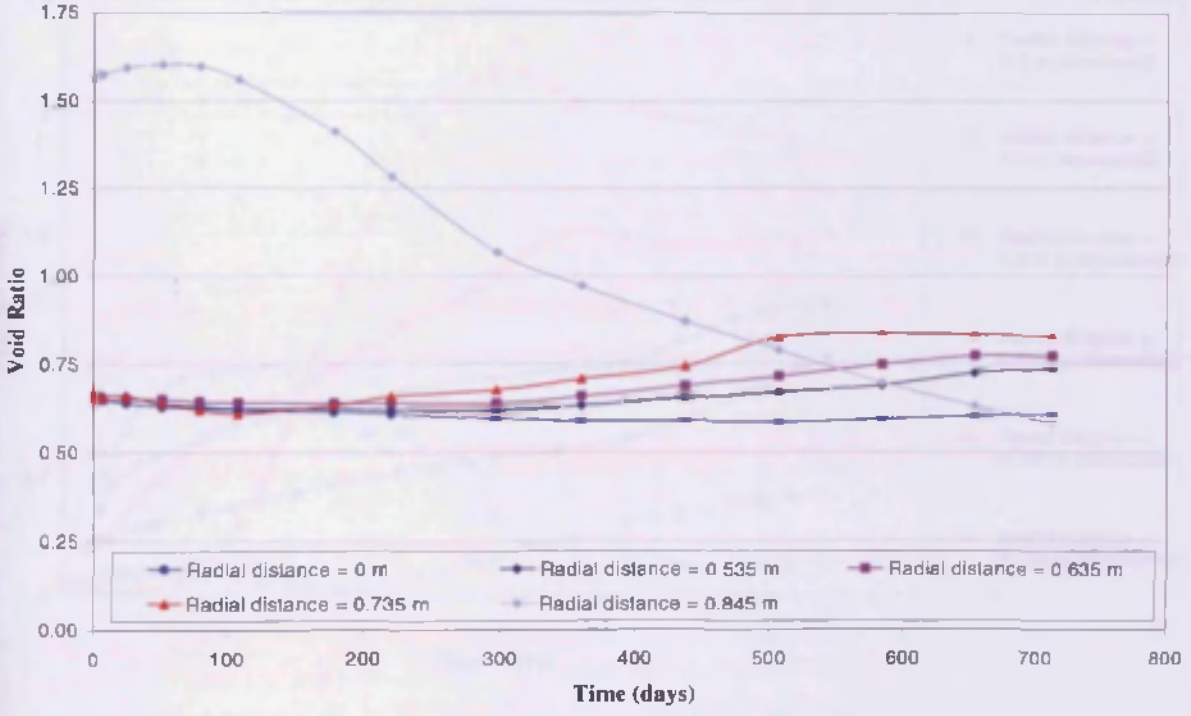

Figure 7.38 (b) Variation of void ratio in the buffer and pelletised region in Hole 1/Cylinder 1 at different positions

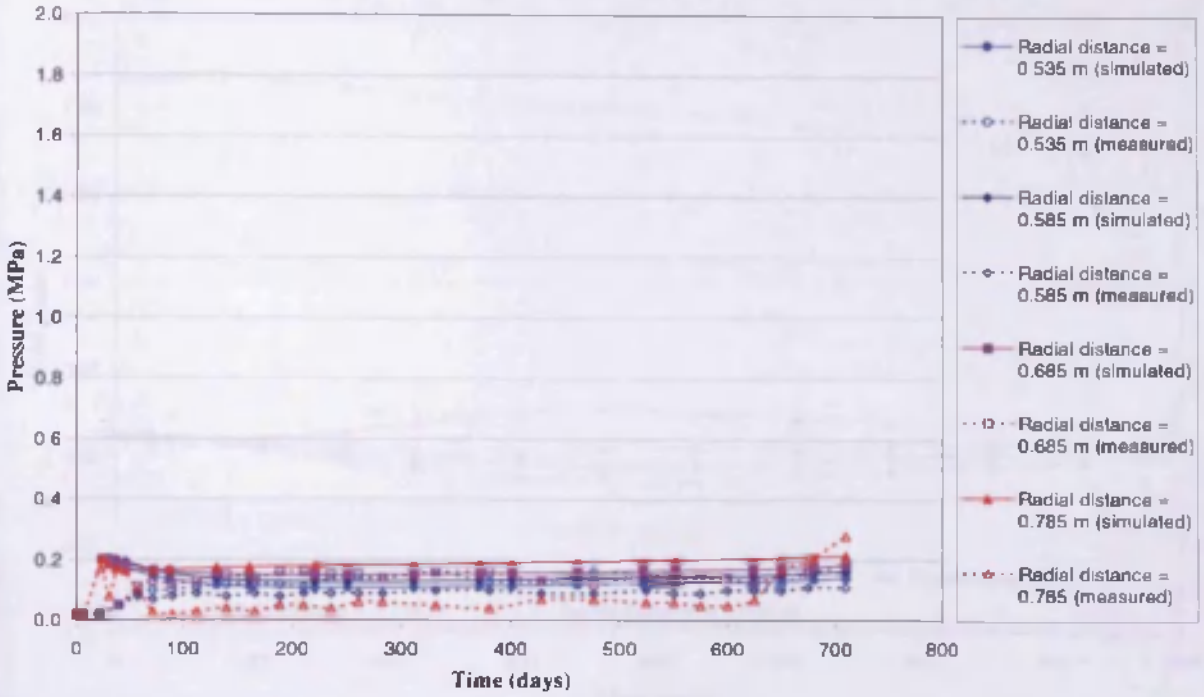

Figure 7.39 (a) Simulated and measured total pressure in Hole 3/Ring 5 at different positions

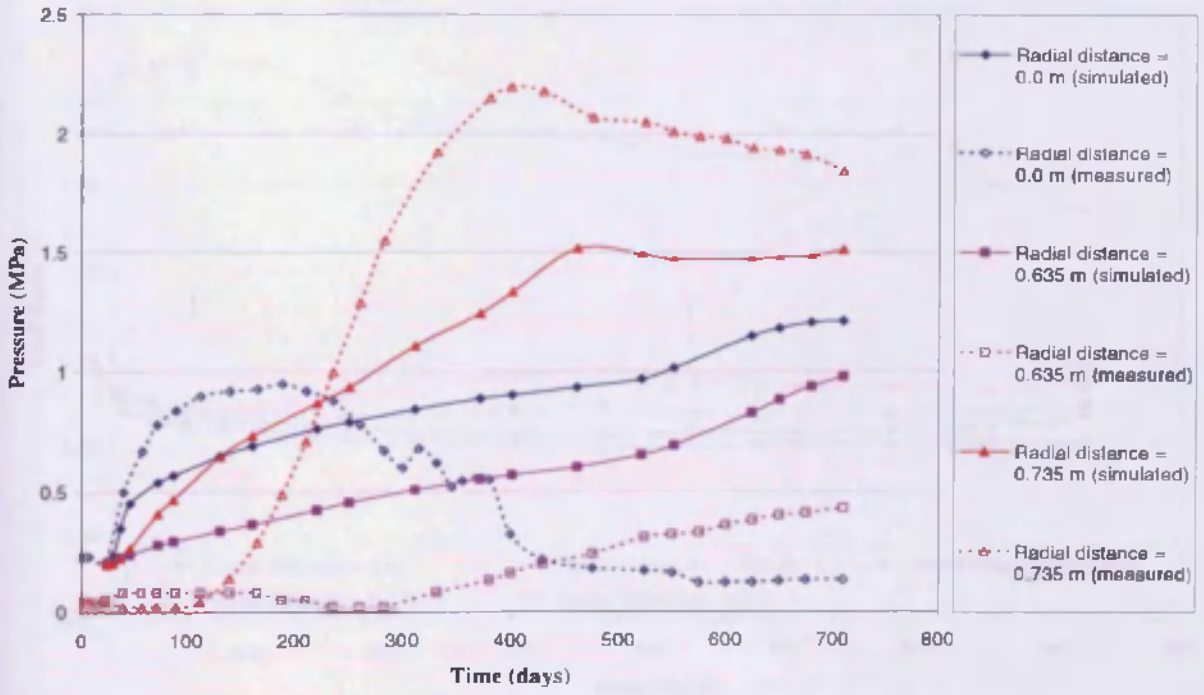

Figure 7.39 (b) Simulated and measured total pressure in Hole 3/Cylinder 1 at different positions

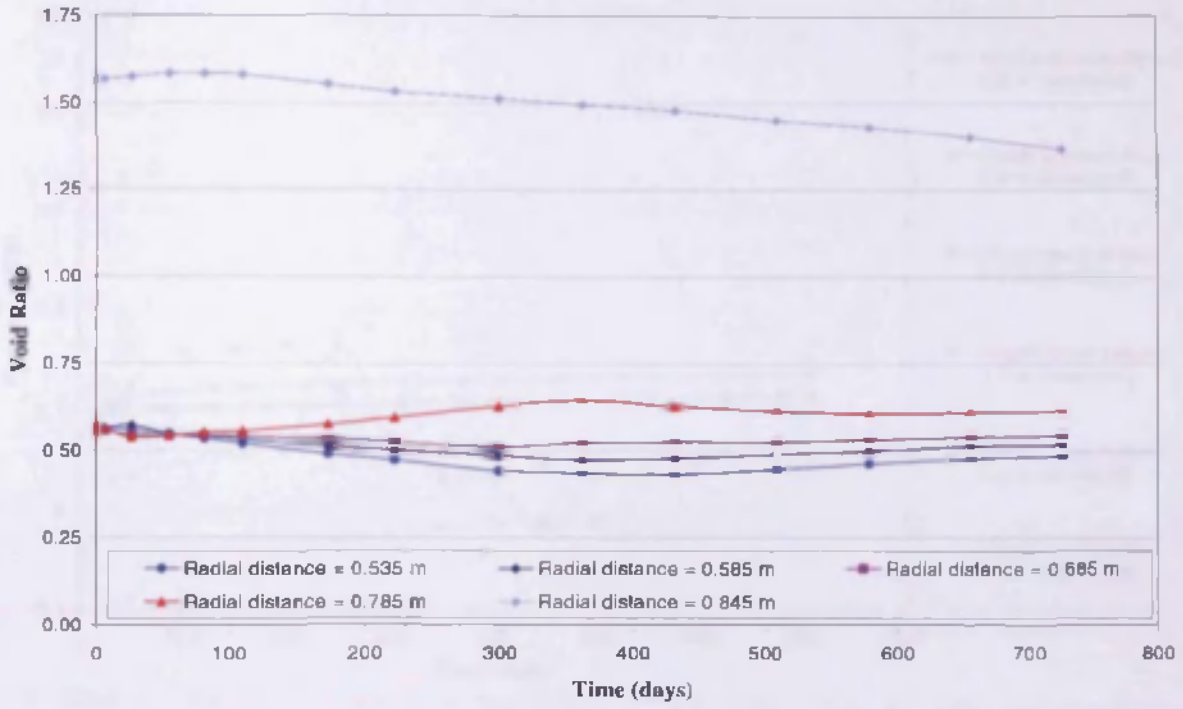

Figure 7.40 (a) Variation of void ratio in the buffer and pelletised region in Hole 3/Ring 5 at different positions

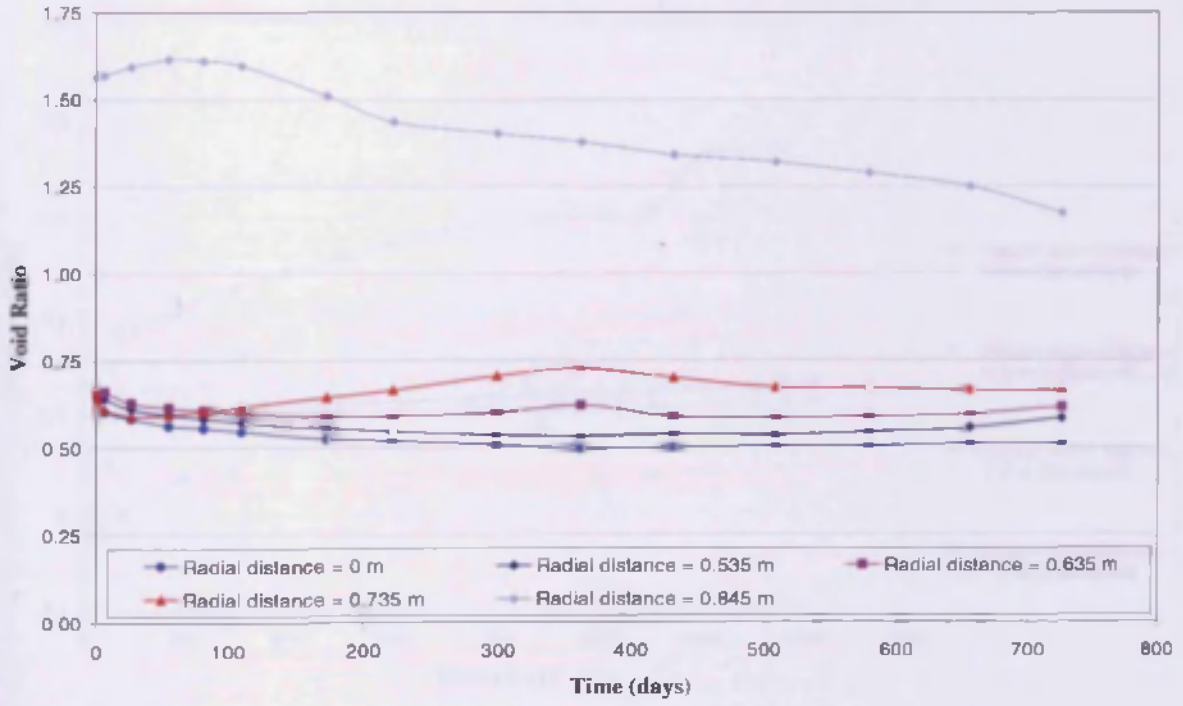

Figure 7.40 (b) Variation of void ratio in the buffer and pelletised region in Hole 3/Cylinder 1 at different positions

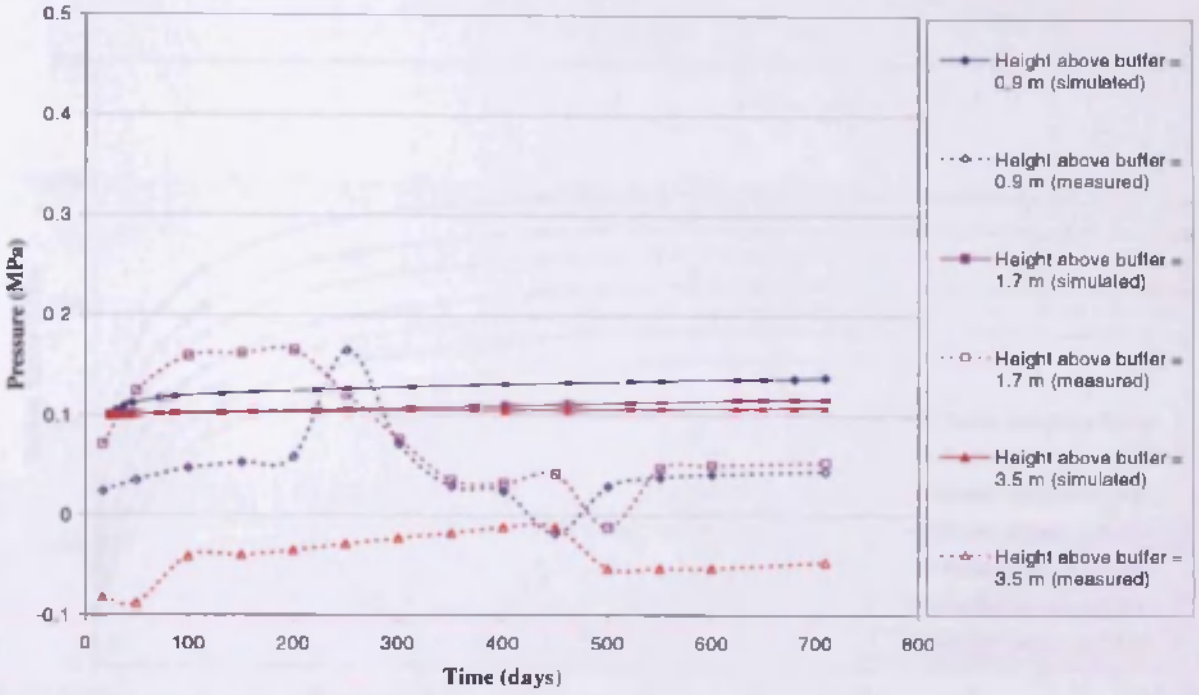

Figure 7.41 (a) Simulated and measured total pressure in the backfill directly above Hole 1 at different heights above the top of the buffer

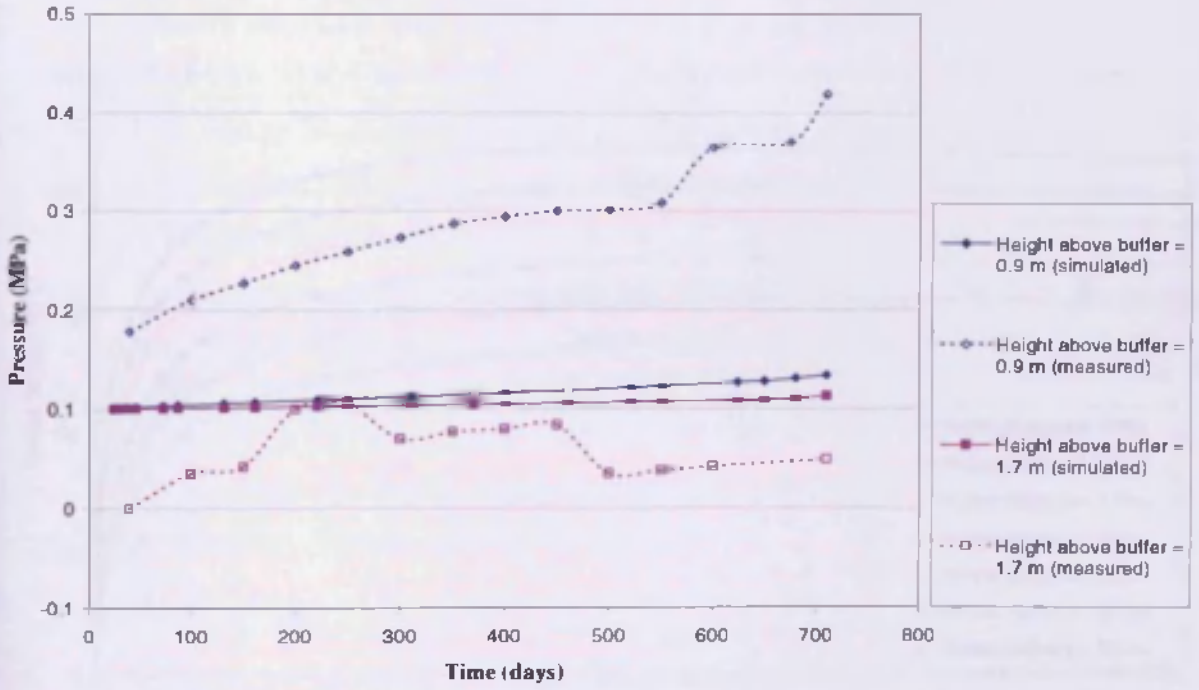

Figure 7.41 (b) Simulated and measured total pressure in the backfill directly above Hole 3 at different heights above the top of the buffer

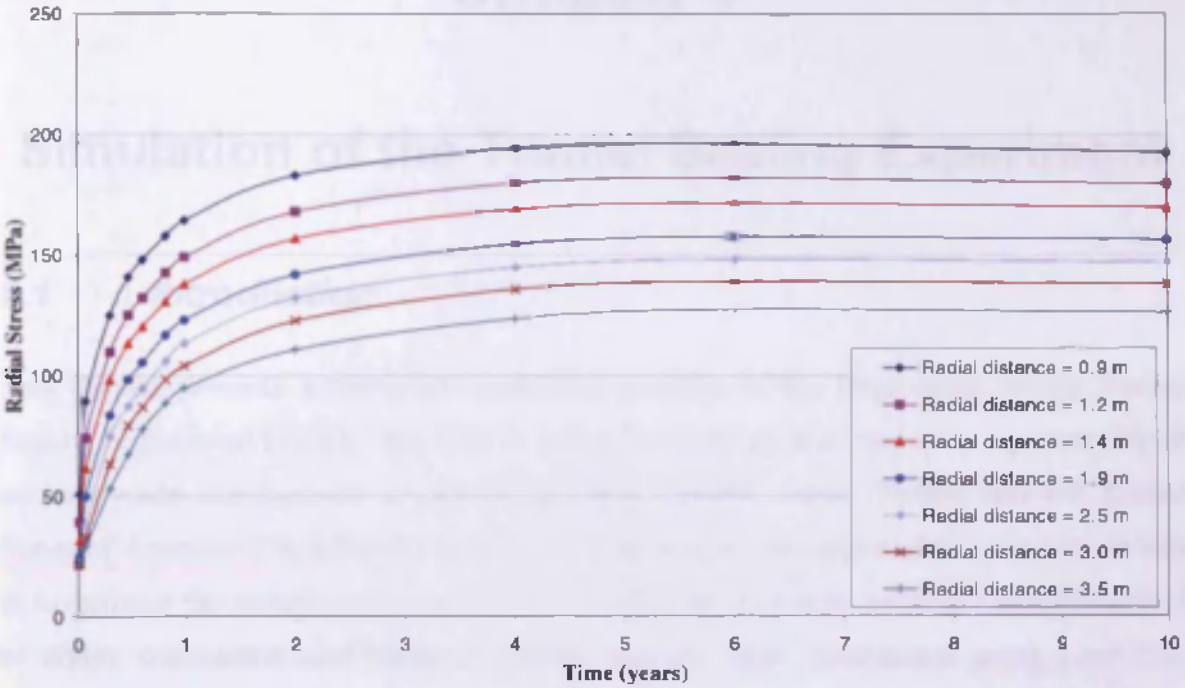

Figure 7.42 (a) Development of radial stress in the rock near to deposition hole 1

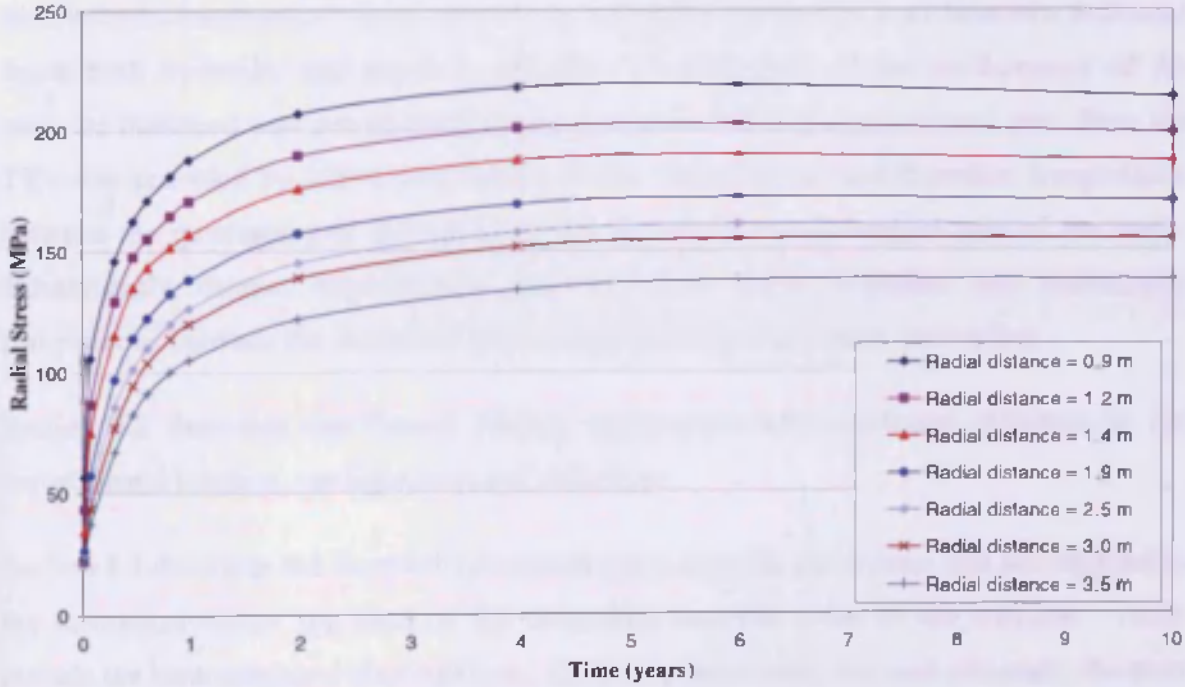

Figure 7.42 (b) Development of radial stress in the rock near to deposition hole 3

Chapter 8

Simulation of the Tunnel Sealing Experiment

8.1 Introduction

This chapter presents a numerical modelling analysis of the large scale, in-situ Tunnel Sealing Experiment (TSX). The TSX is an international project funded by a partnership of nuclear waste management organisations from Canada, Japan, France and the United States of America (Chandler et al., 2002a). The primary objective of the experiment was to investigate the overall performance of two different bulkhead materials, one comprised of highly compacted sand-bentonite blocks and the other constructed using Low-Heat High-Performance concrete (Chandler et al., 2002b).

A fully coupled mechanistic thermal-hydraulic-mechanical model is presented in this chapter. The modelling work was performed in collaboration with Atomic Energy of Canada Limited (AECL) and constituted a series of predictions concerning the thermo/hydro/mechanical behaviour of only the highly compacted sand-bentonite bulkhead under both hydraulic and thermal gradients. Investigation of the performance of the concrete bulkhead was not attempted in this study. Limited experimental data from the TSX was provided by AECL at the time of the investigation, and therefore comparisons between the measured and simulated results did not form an integral part of the study. Subsequently, further experimental data has been made available and preliminary comparisons between the numerical and measured results have been undertaken.

Section 8.2 describes the Tunnel Sealing Experiment with particular reference to the experimental location, configuration and objectives.

Section 8.3 describes the thermo/hydro/mechanical material parameters that are required in the theoretical model for each of the individual material types in the analysis. These include the bentonite/sand clay bulkhead, the host granite rock, the sand materials, the steel plate and the reinforced concrete ring.

Sections 8.4, 8.5 and 8.6 present the work undertaken for the simulation of Pre-Phase I, Phase I and Phase II respectively. These include a description of the initial and boundary conditions employed, details of the simulation numerics and a presentation of all the results produced for the range of coupled analyses performed.

In Section 8.7 preliminary comparisons of the simulated and experimental behaviour are made. This focuses principally on the hydraulic and thermal behaviour of the clay bulkhead and the associated deformation behaviour.

Finally, in Section 8.8 the overall conclusions from the simulation work are presented.

8.2 The Tunnel Sealing Experiment

The Tunnel Sealing Experiment is being performed at Atomic Energy of Canada Limited's (AECL) Underground Research Laboratory (URL) by an international partnership representing Japan, France, the United States and Canada. The TSX is located at the 420 m level of the URL in the granite rock of the Precambrian Canadian Shield and can be seen in Figure 8.1. The experiment involved the construction of two full scale tunnel seals at either end of a single excavated tunnel. One of the bulkheads was an assembly of pre-compacted sand-bentonite blocks and the second was fabricated using a single cast of Low-Heat High-Performance concrete. A permeable sand fill was installed in the chamber between the two bulkheads. The experimental configuration is shown in Figure 8.2.

The experiment is divided into a number of phases. In the first phase the bulkheads were constructed and the sand-filled chamber was incrementally pressurised with water at ambient temperature over a period of time up to 4 MPa pore water pressure, following the pressure profile shown in Figure 8.3. This allowed the performance of each of the bulkheads under hydraulic flows to be monitored and evaluated. In the second phase, currently in progress, heated water is circulated through the sand-filled chamber. This phase has been conducted in two Stages. In Stage 1 the water was heated to a target temperature of 50 °C and maintained for a year. In Stage 2, which is currently in progress, the temperature has been increased to 85 °C and is expected to be maintained for a further year. This will allow the performance of the bulkheads and host rock to be evaluated based on the influence of elevated temperatures in the sand chamber.

The Tunnel Sealing Experiment has been designed and constructed to characterise the sealing potential of well-constructed, full scale bulkheads under representative hydraulic and thermal conditions. The primary objective of the experiment as defined by Chandler et al. (2002b) is "to assess the applicability of technologies for construction of practicable concrete and bentonite bulkheads; to evaluate the performance of each bulkhead; and to identify and document the parameters that affect that performance". In this context, performance was defined as the ability of the bulkheads to restrict the flow of water in the axial direction of the tunnel. However, Chandler et al. (2002b) did recognise that the most important characteristic of a seal in the role of waste isolation is its ability to limit the transport of radionuclides.

8.3 *Material parameters*

The theoretical model, as defined in Chapter 3, used for the simulation of the Tunnel Sealing Experiment requires a detailed set of thermo/hydraulic/mechanical material parameters to define the behaviour of each of the individual materials present in the analysis. Five primary materials are used in this analysis. These are: 1) the bentonite/sand blocks that make up the clay bulkhead, 2) sand materials, 3) the steel plate, 4) the reinforced concrete ring, and 5) the host granite rock. As part of the collaborative effort AECL provided a comprehensive list of experimentally derived material parameters to be used in the simulation work. However, it has been necessary to assume certain parameters and relationships from similar materials when they were not available. Similar materials have been investigated in earlier modelling work for the Isothermal Test and Buffer/Container Experiment by Mitchell (2002) and therefore material parameters employed in that study have also been adopted here where no other information was available.

8.3.1 Bentonite/sand clay bulkhead

The clay bulkhead is composed of highly compacted bentonite/sand blocks. The bentonite, known as Kunigel V1 bentonite, was provided by the Japan Nuclear Cycle Development Institute (JNC) as part of the international collaboration. The use of bentonite as a seal is considered in most international radioactive waste disposal programs, however, the methods of placement and composition do differ from concept to concept. Dixon and Gray (1985) performed a series of tests which showed that the addition of an inert material, such as sand, to the bentonite mixture would not greatly affect the important sealing characteristics such as saturated permeability and swelling pressure, whilst increasing the thermal conductivity and decreasing cost. AECL have adopted this principal in their past experimental work whereby a 50:50 bentonite/sand buffer material was used in both the Isothermal Test and the Buffer/Container Experiment. In Japan, a great deal of work has been conducted using clay-based sealing materials composed of 70% Kunigel V1 bentonite and 30% sand. This material composition was used in the large scale experiment at the Big-Bentonite (BIG-BEN) facility (Fujita et al., 1996) and in the in-situ experiment in the Kamaishi mine (Chijimatsu et al., 1999). The same composition of 70% Kunigel V1 bentonite and 30% graded silica sand was used in the TSX and was installed with a bulk

density of 1900 kg/m^3. In the following sections the material parameters adopted for the clay bulkhead are detailed. Some of the relationships have needed to be assumed from parameters adopted for the 50:50 bentonite/sand buffer material used in AECL's Buffer/Container Experiment (Mitchell, 2002) and as such are only representative.

8.3.1.1 Hydraulic and thermal material parameters

The bentonite/sand bulkhead was installed in the TSX with an initial moisture content of 14 %. Guo and Chandler (2002) defined the effective porosity of the material as 0.315. Hence the void ratio, e can be calculated as 0.46. With reference to equation (7.4) the initial degree of saturation of the material can be determined;

S_l (initial) = 0.822

The hydraulic conductivity curve was determined using the approach proposed by Green and Corey (1971) using a measured saturated hydraulic conductivity of 1 x 10^{-12} m/s, (Guo and Chandler, 2002). The form of the variation with degree of saturation is shown in Figure 8.4. This relationship is applied in the finite element code COMPASS as a series of data points with linear interpolation being used between the discrete values. As part of the modelling exercise it was considered necessary to investigate the interaction of the microstructure and the macrostructure on the saturation rates of the clay bulkhead. Following the work of Thomas et al. (2003a) the approach described in Section 3.2.1.1 and equation (3.22) was employed as a first approximation. This assumed that as the clay bulkhead saturated 94% of the water would be adsorbed in the micropore and become unavailable for further flow (Pusch, 1998). The swelling of the micropore thus tends to "choke" the flow of water and reduce the effective hydraulic conductivity of the clay bulkhead. This relationship is also shown in Figure 8.4.

The water retention curve relationship for this material is based upon the approach presented by Mitchell (2002). This approach followed the work of Wan et al. (1995a) who measured the relationship between moisture content and total suction for an unsaturated 50:50 bentonite/sand buffer material, and fitted a curve to the data. Therefore, for the clay bulkhead used in this work the initial porosity has been used to determine the relationship between the total suction and degree of saturation. Wan's approach, has been

supplemented to include suction values less than 2.59 MPa. The equations defining the water retention curve are given below and the relationship is shown in Figure 8.5;

when, $s < 2.59 \times 10^6$ Pa

$$S_l = 1 + 2.26 \times 10^{-5} (1 - \exp (2.8 \times 10^{-6} s)) \quad (8.1)$$

when, 2.59×10^6 Pa $< s < 17 \times 10^6$ Pa

$$S_l = \frac{\log_{10}(s) - 8.23}{-1.98} \quad (8.2)$$

when, $s > 17 \times 10^6$ Pa

$$S_l = \frac{\log_{10}(s) - 8.74}{-2.97} \quad (8.3)$$

Hence, from Figure 8.5 and equation (8.2) for the clay bulkhead, with an initial $S_l = 0.822$ %, the initial suction, $s_i = 4$ MPa.

The thermal conductivity relationship is based on experimental measurements presented by Wan et al. (1995b). In order to implement this relationship into the COMPASS model linear interpolation has been performed between the values. This is expressed below;

when, $S_l < 0.2$

$$\lambda = 0.7 \text{ W/m/K} \quad (8.4)$$

when, $0.2 < S_l < 0.8$

$$\lambda = 1.667 S_l + 0.366 \text{ W/m/K} \quad (8.5)$$

when, $0.8 < S_l$

$$\lambda = 1.7 \text{ W/m/K} \quad (8.6)$$

The thermal conductivity relationship plotted against degree of saturation is shown in Figure 8.6.

The heat capacity of the clay bulkhead material was defined by Guo and Chandler (2002) as 1400 J/kg/K when the moisture content, w = 14 %. Hence the specific heat capacity of the solids has been calculated to be;

C_{ps} = 850 J/kg/K

8.3.1.2 *Mechanical material parameters*

Very little information was available concerning the mechanical material parameters of the clay bulkhead and so the material parameters required have been based on a literature review of experimental work carried out for the 50:50 bentonite/sand buffer from AECL's Buffer/Container Experiment (Mitchell, 2002). These parameters are summarised in Table 8.1 below.

Table 8.1 Mechanical material parameters adopted for the clay bulkhead

Parameter	Symbol	Value
Stiffness parameter for changes in net mean stress for virgin states of the soil at saturation	$\lambda(0)$	0.0597
Parameter defining the maximum soil stiffness	r	0.65
Parameter controlling the rate of increase of soil stiffness with suction	β	5×10^{-7} Pa^{-1}
Elastic stiffness parameter for changes in net mean stress	κ	0.0125
Reference stress	p_c	1.8×10^{5} Pa
Stiffness parameter for changes in suction in the elastic region	κ_s	0.0111
Stiffness parameter for changes in suction for virgin states of the soil (Volckaert et al., 1996)	λ_s	0.111
Suction hardening parameter	s_0	4 MPa
The slope of the critical state line (Saadat et al., 1992; Graham et al., 1989; Lingnau et al., 1994)	M	0.526
Shear modulus (Graham et al., 1997)	G	10 MPa
Coefficient of thermal expansion (AECL, 2002)	α_T	2.3×10^{-4} /K

8.3.2 Granite rock

AECL's underground research laboratory is situated in the Lac du Bonnet granite batholith, 120 km ENE of Winnipeg, Canada. The Tunnel Sealing Experiment is located on the 420 m level. At this level the rock is generally homogenous grey granite which is essentially unfractured. The rock has an effective porosity of 0.003 and a bulk density of 2650 kg/m^3 (Guo and Chandler, 2002). A literature review of the granite material parameters revealed that there was little information available on several of the key properties and relationships needed for the water uptake modelling, hence some assumptions were required.

8.3.2.1 Hydraulic and thermal material parameters

The material data that was provided by AECL (2002) for the granite did not cover the principal hydraulic relationships and so the approach taken by Thomas et al. (2003a) has been adopted here. This approach is similar to the one used for the Äspö granite detailed in Chapter 7, Section 7.2.5 with the relevant parameters from AECL implemented.

Following the approach adopted by Gens et al., (1998), which was presented in Section 7.2.5.2 and shown in equation (7.5) the hydraulic conductivity for the granite rock was taken as, when, $S_l \leq 1$;

$$K_l = K_{sat} . S_l^{1/2} (1 - (1 - S_l^{1/\beta_l})^{\beta_l})^2 \qquad (8.7)$$

Guo and Chandler (2002) defined the saturated hydraulic conductivity for the granite, K_{sat} as 10^{-12} m/s. The material parameter, β_l is again taken as 0.33, after Gens et al. (1998). The hydraulic conductivity relationship for the granite can be seen in Figure 8.7.

From Section 7.2.5.2 and equation (7.6) the relationship between degree of saturation and suction for the granite was defined by Gens et al. (1998) as;

$$S_l = \left[\left(1 + \left(\frac{s}{P_0} \right)^{1/(1-\beta_l)} \right) \right]^{-\beta_l} \qquad (8.8)$$

where, S_l is the degree of saturation, s is the suction, P_0 is the air entry value, and β_l is a material parameter, taken as 0.33 for granite after Gens et al. (1998). Using equation (7.7)

the saturated hydraulic conductivity corresponds to an intrinsic permeability of 10^{-19} m^2. Therefore, using the approach presented by Davies (1991), as discussed in Section 7.2.5.2 and Figure 7.8, a threshold pressure of 1.75 MPa was selected and substituted into equation (8.8). The corresponding water retention curve is shown in Figure 8.8.

The thermal conductivity for the granite was taken as a constant value of 3.5 W/m/K after Guo and Chandler (2002). The specific heat capacity for the rock, C_{ps}, was given in Guo and Chandler (2002) as;

C_{ps} = 1015 J/kg/K

8.3.2.2 *Mechanical material parameters*

For the granite rock it was assumed that only elastic deformation would occur within the bounds of the analysis. Therefore only the material parameters defining the elastic behaviour of the rock are given below, these were provided by AECL (2002) as;

Uniaxial compressive strength = 167 MPa

Young's Modulus, E = 57.59 GPa

Poisson's ratio, υ = 0.207

Coefficient of thermal expansion, $\alpha_T = 7 \times 10^{-6}$ /K

Given that Young's modulus can be expressed in terms of the bulk modulus, K, and shear modulus, G, by the following expression;

$$E = \frac{9KG}{3K + G} \tag{8.9}$$

And Poisson's ratio may be expressed as;

$$\upsilon = \frac{3K - 2G}{6K + 2G} \tag{8.10}$$

The following values are found for the shear modulus and the bulk modulus respectively, G = 23.86 GPa, and K = 32.74 GPa.

It was assumed that there would be little deformation caused by changes in suction within the rock, and so κ_s, the elastic stiffness parameter for changes in suction of the soil was set to a negligible value.

8.3.3 Sand materials

Two different sand materials were used in the Tunnel Sealing Experiment. The first was placed in the chamber between the clay bulkhead and concrete bulkhead and the second formed part of the restraint system and was installed between the downstream face of the clay bulkhead and the steel plate. It was decided from an early stage in the simulation that since the sand in the chamber only effectively acted as a source of water and heat it could be removed from the analyses and replaced by a series of representative boundary conditions. This also had the added advantage of reducing the complexity of the domain and allowed savings to be made in terms of computational run-times. The sand used to fill the space between the clay bulkhead and steel plate has a dry density of 2000 kg/m^3 and an initial effective porosity of 0.24 (AECL, 2002).

8.3.3.1 Hydraulic and thermal material parameters

In order to represent the hydraulic relationships of the sand fill it was necessary to adopt the approach taken by Mitchell (2002) for the sand in the Buffer/Container Experiment. Mitchell (2002) compared the particle size distribution for the sand used in AECL's Buffer/Container Experiment with a Garside Grade medium sand and found that the materials were of a similar consistency. Therefore, some of the material parameters and relationships for Garside Grade medium sand have been employed in this work, (Ewen and Thomas, 1987; Ewen and Thomas, 1989).

The saturated hydraulic conductivity of the sand fill was the same as the sand used in the chamber and was defined by Guo and Chandler (2002) as 6.25×10^{-5} m/s. Hence, the hydraulic conductivity relationship, expressed in terms of degree of saturation, has been defined as;

$$K_l = 8.37\times10^{-12}\exp\left[28.01(S_l)-12.235(S_l)^2\right] \text{ m/s} \qquad (8.11)$$

This relationship is shown graphically in Figure 8.9.

The water retention curve has been modelled using the following set of equations;

when, $0 \leq nS_l \leq 0.2$

$$nS_l = \left(\frac{s}{\rho_l 0.002} - 1205 \right)^{\frac{-1}{1.75}} \tag{8.12}$$

when, $0.2 \leq nS_l \leq n$

$$nS_l = n - \frac{\left(\frac{s}{\rho_l g} \right)^{\frac{1}{0.0226249}}}{1.101416 \times 10^{-26}} \tag{8.13}$$

This relationship is shown graphically in Figure 8.10.

The thermal conductivity of the sand fill was provided by AECL (2002) as 0.5 W/m/K and the thermal capacity of the material is assumed to be the same as the chamber sand, that is, 820 J/kg/K (Guo and Chandler, 2002).

8.3.3.2 *Mechanical material parameters*

The sand fill is modelled using a linear elastic constitutive model. Therefore, only the material parameters defining the elastic behaviour of the sand fill are given below (AECL, 2002);

Young's Modulus, $E = 600$ MPa

Poisson's ratio, $\upsilon = 0.3$

Coefficient of thermal expansion, $\alpha_T = 1.9 \times 10^{-5}$ /K

Using equations (8.9) and (8.10) the shear modulus was calculated to be, $G = 230.77$ MPa.

It was expected that there would be very little deformation caused by changes in suction within the sand, and so κ_s, the elastic stiffness parameter for changes in suction of the soil was set to a negligible value.

8.3.4 Steel plate

On the downstream end of the clay bulkhead the resistance to bentonite expansion is provided by a rigid steel restraint system. The restraint system was designed to resist the combined loading of 4 MPa of hydraulic pressure from within the tunnel and 1MPa of swelling pressure from the clay bulkhead. The restraint system is an elongated hemispherical steel plate with a minimum plate thickness of 25 mm and a maximum thickness of 50 mm. The steel plate was designed to transfer the load outward onto a high-strength concrete ring beam (Chandler et al., 2002b). The steel plate supports and restrains the sand fill and the clay bulkhead. The steel has a bulk density of 7800 kg/m^3 and an effective porosity of zero (AECL, 2002).

8.3.4.1 Hydraulic and thermal material parameters

To reflect the effectively impermeable nature of the steel plate the hydraulic conductivity was set to an extremely low value.

The thermal conductivity of the steel was provided by AECL (2002) as 56 W/m/K and the thermal capacity of the steel plate was defined as 465 J/kg/K.

8.3.4.2 Mechanical material parameters

Due to a lack of available mechanical material parameters for the steel plate it was necessary to model it using a linear elastic constitutive model. Therefore, only the material parameters defining the elastic behaviour of the steel plate are given below (AECL, 2002);

Young's Modulus, $E = 200$ GPa

Poisson's ratio, $\upsilon = 0.29$

Coefficient of thermal expansion, $\alpha_T = 14.8 \times 10^{-6}$/K

Using equations (8.9) and (8.10) the shear modulus was calculated to be, $G = 77.52$ GPa.

8.3.5 Reinforced concrete ring

The steel plate is supported by a reinforced concrete ring, which is keyed into the surrounding granite. The purpose of the concrete bearing ring is to transfer load from the steel plate onto the rock. A high strength concrete was specified for the ring beam with a minimum concrete strength of 60 MPa achieved within 90 days of placement (Chandler et al., 2002b). The concrete has a bulk density of 2430 kg/m^3 and an effective porosity of 0.1 (AECL, 2002).

8.3.5.1 Hydraulic and thermal material parameters

As a first assumption the concrete is modelled using the same hydraulic conductivity relationship as that described in equation (8.7) for the host granite. However, the saturated hydraulic conductivity for the concrete has been defined as 3.0×10^{-14} m/s (Guo and Chandler, 2002). As there was no information available regarding the water retention curve of the concrete it has been assumed to follow the same form as that employed for the granite. It is acknowledged that this is an assumption only, but since the concrete ring is only a small element to the simulation it can be considered to have a negligible effect on the flow and mechanical behaviour of the clay bulkhead.

The thermal conductivity of the reinforced concrete ring has been defined as 1.8 W/m/K and the thermal capacity of the concrete has been defined as 900 J/kg/K (AECL, 2002).

8.3.5.2 Mechanical material parameters

The reinforced concrete ring is modelled using a linear elastic constitutive model. Therefore, only the material parameters defining the elastic behaviour of the reinforced concrete ring are given below (AECL, 2002):

Young's Modulus, $E = 36$ GPa

Poisson's ratio, $\upsilon = 0.3$

Coefficient of thermal expansion, $\alpha_T = 1 \times 10^{-5}$/K

Using equations (8.9) and (8.10) the shear modulus was calculated to be, $G = 13.85$ GPa.

It was expected that there would be very little deformation caused by changes in suction within the concrete ring, and so κ_s, the elastic stiffness parameter for changes in suction of the concrete was set to a negligible value.

8.3.6 Conclusions

Material parameters necessary to model the Tunnel Sealing Experiment have been described. Where possible the parameters have been attained from results of laboratory or in-situ testing of the materials presented in the literature. However the set of parameters available from this experiment was not comprehensive, and where necessary approximations have been made.

8.4 Simulation Pre-Phase I

The numerical code COMPASS, was used to simulate the hydraulic response of the granite in the Tunnel Sealing Experiment prior to the construction of the clay bulkhead and sand chamber. Both a three-dimensional and a two-dimensional axisymmetric finite element analysis have been performed. This procedure was undertaken to compare and contrast the results from a more complex three-dimensional domain with those from a simpler two-dimensional domain. Based on these results a suitable model could then be adopted for the subsequent work. The mesh and time stepping schemes used in these numerical models were checked for spatial and temporal convergence respectively.

8.4.1 Hydraulic simulation of granite prior to Phase I

8.4.1.1 Initial and boundary conditions

The boundary conditions along the edges of the far-field rock were restrained and the pore water pressure was set to a hydrostatic value. In the three-dimensional analysis this varied with depth from 3.82 MPa at the top of the domain to 4.18 MPa along the bottom of the domain. The variation of the pore water pressure at the boundaries of the domain can be seen in Figure 8.11. In the two-dimensional axisymmetrical analysis an average value of 4 MPa was used. A zero flux boundary condition was prescribed on the central surface of the section, which represents the axis of symmetry in the system. The internal rock surface of the tunnel was set at zero pore water pressure, effectively representing air at 100 % humidity and atmospheric pressure. This approach has been adopted in earlier modelling exercises (Mitchell, 2002) and it is acknowledged that this boundary condition is only representative and hence the assumption is only made as a first approximation. The initial conditions of the analysis were set at hydrostatic pressure values.

8.4.1.2 Simulation numerics

Both a three-dimensional tunnel mesh and two-dimensional axisymmetric mesh were implemented in this analysis, whereby only the rock was modelled without the clay bulkhead, sand chamber, sand filler, steel plate or concrete ring installed. In the three-dimensional analysis a vertical plane of symmetry was identified and only half of the

domain was modelled. Therefore the overall size of the mesh could be reduced by a factor of 2 and thus composed of 11,968 nodes and 9,952 elements. The three-dimensional domain and mesh can be seen in the Figures 7.12. In the two-dimensional axisymmetrical analysis a mesh composed of 2,144 nodes and 2,034 elements was used (refer to Figure 8.13). Following the investigation summarised in Chapter 4, Section 4.5 the hydraulic analyses of the rock mass were performed using a Preconditioned Conjugate Gradient (PCG) solver combined with a Jacobi preconditioner. The analyses were run in parallel on 4 processors on the SUN HPC system. The time step for these analyses started at 100 seconds and was allowed to increase to a maximum of 30 days in response to the rate of numerical convergence, via the algorithm described in Chapter 4, Section 4.3. These analyses were run for 510 days, corresponding to the time that the tunnel had been left open following the tunnel and key excavation prior to the commencement of Phase I (Guo and Chandler, 2002). The hydraulic material parameters of the rock are described in Section 8.3.2.1

8.4.1.3 Simulation results

Figure 8.14 shows pore water pressures versus radial distance from the tunnel centre over time. The results for both the three-dimensional tunnel mesh analysis (section A-A, see Figure 8.12) and the two-dimensional axisymmetrical analysis (section A1-A1, see Figure 8.13) are shown. It can be seen that there is very little variation between the two sets of results. The influence of the tunnel is clear with a draw down of pore water pressure from the far field hydrostatic values to zero head at the rock surface. It also shows that the system reaches steady-state pore water pressure conditions relatively quickly, since the 24 day profile closely matches the final steady-state profile at 510 days. Figure 8.15 (a – d) shows pore water pressure contour plots for differing times within the analysis for the three-dimensional analysis. These plots again illustrate how rapidly the system reaches steady-state pore water pressure conditions. Since the comparison between the three-dimensional tunnel analysis and the two-dimensional axisymmetrical analysis of this phase showed negligible difference in the results, the two-dimensional axisymmetrical approach was adopted in this numerical investigation from this point onwards. Employing the two-dimensional axisymmetrical analysis for later, more complex coupled analyses was also advantageous because the computational run-times were significantly reduced and this allowed a range of different analyses to be performed in the required time frame.

8.4.1.4 Conclusions

In the hydraulic simulation of the rock mass pre-Phase I the system reaches steady-state pore water pressures conditions over a relatively quick duration of 24 days. It is also evident that the construction of the open tunnel precipitates a draw down effect of pore water pressure within the rock mass.

8.5 Simulation of Phase I

Phase I of the Tunnel Sealing Experiment commenced immediately after the construction of both the clay and concrete bulkheads and placement of the sand in the chamber between these two bulkheads. This proceeded with the sand chamber being incrementally pressurised with water to a pore water pressure of 4 MPa over a period of 3.5 years, following the pressure profile shown in Figure 8.3 (Guo et al, 2002). This allowed the performance of each of the bulkheads under hydraulic flows to be monitored and evaluated.

In order to perform the numerical simulation of Phase I two distinct analyses have been undertaken: 1) a hydraulic analysis of the clay bulkhead, and 2) a hydraulic-mechanical analysis of the clay bulkhead. The first analysis was performed to investigate how quickly the clay bulkhead saturated under an applied hydraulic gradient. The latter analysis was undertaken to investigate the influence of the coupled effects of the mechanical behaviour on the saturation rates of the clay bulkhead.

8.5.1 Hydraulic simulation of Phase I

For this hydraulic simulation (H) only half of the Tunnel Sealing Experiment has been analysed using a two-dimensional axisymmetrical domain. This consisted of half of the clay bulkhead and the associated sand fill, steel plate, concrete ring, rock and open tunnel. The concrete bulkhead has not been simulated in this work. The geometry of the model is shown in Figure 8.16.

8.5.1.1 Initial and boundary conditions

The initial pore water pressure conditions in the rock were taken from the end of the pre-Phase 1 simulation of the hydraulic regime described in Section 8.4.1.3. The boundary conditions along the edges of the far-field rock were again restrained and the pore water pressure was set to an average hydrostatic pressure of 4MPa as detailed in Section 8.4.1.1. A zero flux boundary condition was prescribed on the lower horizontal boundary of the domain shown in Figure 8.16 because this represented an axis of symmetry in the Tunnel Sealing Experiment. The open internal rock surface of the tunnel downstream of the clay

bulkhead was set at zero porewater pressure, effectively representing air at 100 % humidity and atmospheric pressure. Time dependent pore water pressure boundary conditions have been implemented to model the hydraulic behaviour of the sand chamber along the sand/clay bulkhead and sand/rock interfaces. These adopt the pore water pressure profile shown in Figure 8.3. The clay bulkhead is installed with an initial suction of 4 MPa as detailed in Section 8.3.1.1. A zero flux boundary condition was applied on the surface of the steel plate to prevent the transfer of moisture through this material.

An investigation has been carried out to study the influence of the sand fill on the resaturation rate of the clay bulkhead. In the first simulation, *Analysis_H_1*, the sand was initially installed saturated with a pore water pressure of 0 Pa. Hence, the hydraulic pore water pressure on the downstream surface of the clay bulkhead was initially 0 Pa. A second analysis was then performed, *Analysis_H_2*, which reduced the artificial supply of moisture from the sand to the clay bulkhead and this was achieved by installing the sand in a very dry state with an initial suction value of 4 MPa. This corresponded to an initial degree of saturation of approximately zero. In the third simulation, *Analysis_H_3*, the sand was prevented from supplying water to the clay bulkhead. This was achieved by making the sand highly impermeable to the flow of water, which was supplied by the host rock along the sand/rock boundary. These analyses were then repeated with the micro/macro interaction effects taken into account. In these cases the modified hydraulic conductivity relationship defined in Section 8.3.1.1 and Figure 8.4 was employed for the clay bulkhead which assumed 94 % of the moisture was adsorbed by the micropore.

8.5.1.2 Simulation numerics

As summarised in Chapter 4, Section 4.5 a comprehensive investigation into the available non-symmetrical iterative solvers found that the Bi-Conjugate Gradient stabilised (Bi-CG-STAB) solver combined with the ILU-Crout preconditioner performed with the greatest stability and accuracy when compared to direct solver (LU) analyses. The hydraulic analyses were run in parallel on 4 processors on the SUN HPC system. A two-dimensional axisymmetric mesh was implemented for this analysis. The two-dimensional analysis used a mesh composed of 2,568 nodes and 2,454 elements. This domain is shown in Figure 8.17. The time-step for these analyses started at 100 seconds and was allowed to increase to a maximum of 30 days in response to the rate of numerical convergence, via the

algorithm described in Chapter 4, Section 4.3. The hydraulic material parameters for the clay bulkhead, sand, steel plate and concrete ring are described in Section 8.3. These analyses were run for 3.5 years corresponding to the experimental duration of Phase I. In order to make predictions concerning the total time taken for the clay bulkhead to become fully saturated, it was necessary to continue some of the analyses beyond the 3.5 years. This is discussed later.

8.5.1.3 Simulation results

The simulation results are presented below for the range of analyses that were conducted for the hydraulic analysis of Phase I.

8.5.1.3.1 *Analysis_H_1*

Figure 8.18 (a – h) shows the pore water pressure contour plots in the clay bulkhead for *Analysis_H_1* during Phase I of the Tunnel Sealing Experiment using the two-dimensional axisymmetrical modal detailed above. The initial conditions in the bulkhead can be seen in Figure 8.18 (a). The clay bulkhead has an initial pore water pressure of –4 MPa and along the interface with the sand fill and rock the pore water pressure is 0 MPa. After 7 days (Figure 8.18 (b)) the region of the clay bulkhead closest to the boundary with the sand chamber is beginning to saturate as water is supplied. On the downstream face of the bulkhead saturation is also taking place as the clay draws the water out of the saturated sand fill material. As a consequence of this strong hydraulic gradient the sand fill material becomes unsaturated. The area of the bulkhead close to the rock does not saturate at the same rate due to the rock having a very low hydraulic conductivity and porosity. Figure 8.18 (c) shows the pore water pressure plot after 1 year. From Figure 8.3 it can be observed that after 1 year the sand chamber/clay bulkhead interface has reached a positive pore water pressure of 750 kPa and as a result the clay bulkhead adjacent to this region is saturating at a much faster rate compared to the other boundaries. This effect is further magnified in the plot for 2 years (Figure 8.18 (d)) as the sand chamber approaches a pore water pressure of 2 MPa and hence becomes the main supplier of water into the clay bulkhead. By 2.6 years (Figure 8.18 (e)) the clay bulkhead is beginning to fully saturate along all boundaries with only the core of the clay remaining in an unsaturated state. The unsaturated core gradually saturates as more water is supplied into the clay bulkhead

(Figure 8.18 (f)). This is characterised by suction values in the order of 2.8 MPa which correspond to a degree of saturation of 95 %. As Figure 8.18 (g) illustrates, after 3 years the clay has become fully saturated in all regions. By the end of Phase I, the pore water pressure in the clay bulkhead is increasing (Figure 8.18 (h)) and beginning to reach the hydrostatic pore water pressures present in the surrounding granite rock. However, the sand fill region on the downstream face of the bulkhead is still unsaturated and only slowly reaching saturation by the end of Phase I.

The hydraulic conditions within the clay bulkhead are illustrated in Figure 8.19, which shows the pore water pressure through the centre of the clay throughout Phase I. Figure 8.20 shows the variation of degree of saturation through the centre of the clay bulkhead throughout Phase I. Again it can be observed how the core of the clay bulkhead becomes fully saturated by the third year of the simulation.

Figure 8.21 shows the pore water pressure versus radial distance along section B-B in the rock. It can be observed that throughout Phase I the pressures in the rock increase in response to the pressure build up in the sand chamber.

When the micro/macro effects were taken into consideration by applying the modified hydraulic conductivity relationship for the clay bulkhead significant differences were apparent in the saturation rates. Figures 8.22 (a – d) show the pore water pressure contour plots in the clay bulkhead through Phase I. It can be seen that by the end of Phase I (3.5 years) the clay bulkhead has remained largely unsaturated except along its boundaries with the sand chamber and rock. As these boundaries began to saturate the hydraulic conductivity reduced and thus "choked" the flow of water into the clay bulkhead, simulating the potential effects of 94 % of moisture being adsorbed in the micropores and becoming unavailable for further flow. It was decided that this simulation should be continued indefinitely, employing the same hydraulic boundary conditions, until the clay bulkhead had reached fully saturated conditions. Hence, the prediction showed that this was achieved after 24.6 years, over eight times slower than the original analysis without the micro/macro effects.

8.5.1.3.2 *Analysis_H_2*

In this analysis the initial conditions in the sand fill were virtually dry and this had a significant effect on the saturation rate of the clay bulkhead. With reference to Figures 8.23 and 8.24 it can be seen how the downstream face of the clay bulkhead shows a reduction in the level of saturation that takes place when compared to the results in *Analysis_H_1*. It can be seen that by the end of the 3.5 years the core of the clay bulkhead remained largely unsaturated with only a small increase in degree of saturation of 2 % from the initial conditions. Continuation of this analysis found that the clay bulkhead reached fully saturated conditions after 4.3 years, taking approximately 475 days longer to saturate than the bulkhead in *Analysis_H_1*. When the micro/macro interaction in the clay was taken into consideration it was found that the clay bulkhead did not reach fully saturated conditions until after 28.5 years. This again illustrated how this phenomenon can have a potentially significant effect on saturation rates for swelling buffer materials.

8.5.1.3.3 *Analysis_H_3*

The results from *Analysis_H_3* can be seen in Figures 8.25 and 8.26. In this analysis the sand was made highly impermeable so that it did not provide any water to the downstream face of the clay bulkhead. From the results it can be seen that since the inflow of water is from one direction only the clay bulkhead saturates at a slower rate than the early analyses. At the end of the analysis the saturated front has moved into the bulkhead by around 1.5 m. Continuing this analysis yielded full bulkhead saturation after 5.9 years. Again taking the micro/macro interaction into account proved significant in delaying the total time taken for full saturation to 40 years.

8.5.1.4 Conclusions

For the hydraulic simulation of Phase I a series of investigations have been carried out. The effect of the initial and boundary conditions on the downstream face of the clay bulkhead have been considered. In the first analysis the sand fill was installed initially saturated and provided a source of water. It was observed that after 3 years the clay bulkhead had resaturated in all regions and was beginning to reach the surrounding hydrostatic pore water pressures inherent in the adjacent granite rock. In the second analysis the sand was installed dry and this delayed the total time taken for the clay

bulkhead to reach saturation by 1.3 years. In the third investigation the sand was made highly impermeable and as a result the clay took 5.9 years to reach fully saturated conditions. These analyses were then repeated and the micro/macro behaviour of the clay bulkhead was taken into account by using a modified hydraulic conductivity relationship that assumed that 94 % of the available moisture was adsorbed in the micropores of the clay. This yielded significant results in terms of saturation rates and delayed the total time taken to reach full saturation by up to a factor of 8. It should be noted that Phase I only lasted 3.5 years and therefore saturation times beyond this are hypothetical. A summary of these results is presented in Table 8.2 below.

Table 8.2 *Total saturation times for clay bulkhead*

	Original hydraulic conductivity relationship	Modified hydraulic conductivity relationship assuming 94 % of moisture adsorbed in the micropores
Analysis_H_1	3 years	24.6 years
Analysis_H_2	4.3 years	28.5 years
Analysis_H_3	5.9 years	40 years

8.5.2 Hydraulic-Mechanical simulation of Phase I

The hydraulic-mechanical (H-M) simulation of Phase I of the Tunnel Sealing Experiment uses the same geometry and domain adopted for the hydraulic simulation detailed in Section 8.5.1. However, for this analysis the hydraulic flow field has been fully coupled with the mechanical response of the system.

8.5.2.1 Initial and boundary conditions

All of the initial hydraulic conditions are the same as those detailed in Section 8.5.1.1. Similarly, all of the hydraulic boundary conditions are the same as those adopted for the hydraulic analysis of Phase I. The initial stress in the clay bulkhead was assumed from similar work based on similar materials (Graham et al., 1997) and was thus approximated to a value of 200 kPa. The centre-line of the domain has been restrained in the x direction.

Along the sand chamber/clay bulkhead interface a uniformly distributed load has been applied. This corresponds to the time dependent variation of the pore water pressure being developed in the sand chamber. Hence, the sand chamber/clay bulkhead boundary is free to move and to consolidate under the applied load. The steel plate and the sand in front of it are free to deform while the concrete ring is modelled as a rigid undeformable material. Again, an investigation of the initial hydraulic conditions in the sand fill was conducted with three analyses performed following the same format as those analyses detailed in Section 8.5.1. In *Analysis_H-M_1* the sand was installed saturated, in *Analysis_H-M_2* the sand was installed dry, and in *Analysis_H-M_3* the sand was made highly impermeable to prevent moisture flow into the clay bulkhead.

8.5.2.2 Simulation numerics

As summarised in Chapter 4, Section 4.5 a direct LU solver method was implemented to perform the two-dimensional axisymmetrical coupled hydraulic-mechanical (H-M) analyses accurately because the iterative solvers were found to be unstable for this type of analysis. The analysis was run in serial on the SUN HPC system. The coupled hydraulic-mechanical analysis was conducted using the two-dimensional axisymmetrical mesh detailed in Section 8.5.1.2 and Figure 8.17. The time-step for this analysis started at 100 seconds and was allowed to increase to a maximum of 7 days in response to the rate of numerical convergence, via the algorithm described in Chapter 4, Section 4.3. The mechanical material parameters for the clay bulkhead, sand, steel plate, concrete ring and granite rock are described in Section 8.3. This analysis was run for 3.5 years corresponding to the experimental duration of Phase I.

8.5.2.3 Simulation results

The simulation results are presented below for the range of analyses that were conducted for the hydraulic-mechanical analysis of Phase I.

8.5.2.3.1 *Analysis_H-M_1*

With reference to Figure 8.27 the hydraulic performance of the clay bulkhead for the H-M analysis of Phase I can be observed. Whilst similar to the behaviour observed in Section

8.5.1.3.1 and Figure 8.20 for the H-only analysis, the clay bulkhead is predicted to reach saturation at a slightly faster rate. The H-M analysis predicts that the core of the clay bulkhead has reached a degree of saturation of 99.9 % at 2.8 years. When compared to Figure 8.20 for the same time in the H-only analysis the core of the clay bulkhead has reached a degree of saturation of 95.8 %. However, in both analyses the clay bulkhead is predicted to be fully saturated throughout by the end of Phase I (i.e. 3.5 years).

This faster rate of saturation is due to the coupling effect of the mechanical behaviour of the clay. Figure 8.28 shows the void ratio profile along the centre line of the clay bulkhead. As the bulkhead begins to saturate, it swells and the void ratio increases. This pattern of behaviour can be seen after 1 year where the clay in contact with the sand chamber has swelled to a void ratio of 0.475. It can also be observed that swelling takes place on the downstream face of the bulkhead as water is drawn out of the sand fill material. This swelling process at the outer edges of the clay results in the centre of the bulkhead consolidating, and this is characterised by a void ratio of 0.453. This behaviour can also be seen after 2 years and results in a further reduction in the void ratio of the material, hence the volume of voids reduces and less water influx is required to saturate the core of the bulkhead. As a consequence the core begins to saturate at a faster rate than that found in the H-only analysis. It should also be observed that after 2 years the clay in contact with the sand chamber begins to consolidate. This is a result of the increase in applied load overcoming the swelling characteristics of the bulkhead. After 3 years the centre of the clay bulkhead is approaching complete saturation and as a result the centre starts to swell and the void ratio increases to 0.456. By the end of Phase I the clay bulkhead has fully saturated and very little swelling or compression is observed. This is characterised by the void ratio reaching near steady-state conditions. It is acknowledged that another consequence of the void ratio decreasing would be to reduce the hydraulic conductivity of the material. In other words the flow of water into the material would be restricted and this would effect the rate of resaturation. This process is not taken into account in the presented model and is recognised as a limitation in the simulation.

Figure 8.29 shows the displacement of nodal surface positions on the steel plate at the downstream face of the clay bulkhead during the H-M analysis of Phase I. The figure shows the variation of displacement from the centre of the steel plate to the edge of the plate that intersects with the concrete ring. It can be seen that the steel plate moves in

response to the applied load imposed by the build up of pore water pressure in the sand chamber. By the end of Phase I the centre of the steel plate is predicted to have moved by 5.8 mm. The displacement in the steel plate incrementally reduces across its surface to zero at the concrete ring intersection.

8.5.2.3.2 *Analysis_H-M_2*

The hydraulic response of the clay bulkhead in this analysis is given in Figure 8.30 and shows a similar pattern to that observed in *Analysis_H_2* detailed in Section 8.5.1.3.2. However, again it can be seen that due to the coupling of the mechanical behaviour the clay saturates at a slightly faster rate. By the end of the analysis the core region of the bulkhead is still unsaturated and the degree of saturation had increased by 6 % from the initial conditions. Continuing this analysis showed that the bulkhead took 4.1 years to reach fully saturated conditions.

The void ratio profile along the centre-line of the clay bulkhead can be seen in Figure 8.31. It can be seen that in the first 2 years of the analysis the void ratio profile shows similar trends to those discussed in Section 8.5.2.3.1 for *Analysis_H-M_1* above. There is initial swelling in the clay on the upstream face as it begins to saturate and compression in the core of the bulkhead. By 3 years it can be seen that the core of the bulkhead, which is still largely unsaturated, has consolidated to a minimum void ratio of 0.446. By the end of the simulation the swelling front has moved further into the core of the bulkhead and as a consequence the void ratio at 1.9 m has reduced to 0.445. It should also be noted that the clay on the downstream end next to the sand fill is now beginning to swell after initial compression.

The displacement of the steel plate for this analysis can be seen in Figure 8.32. When compared to the displacements simulated in *Analysis_H-M_1* (Figure 8.28) it can be seen that the trends are similar. The displacements follow the pressure profile shown in Figure 8.3, that is, as the pore water pressure in the sand chamber increased in steps the displacement in the steel plate responded. However, by the end of Phase I the clay bulkhead has still not fully saturated and as a result the clay does not swell to the same degree as that observed in the previous analysis. The consequence of this is that the maximum displacement of the steel plate centre has reduced to 4.2 mm.

8.5.2.3.3 *Analysis_H-M_3*

In this analysis the sand fill on the downstream face of the clay bulkhead was prevented from supplying water to the clay and as a result by the end of Phase I the clay is still unsaturated from 1.5 to 2.6 m along the centre-line. This can be seen in Figure 8.33 and shows a similar pattern to that observed in *Analysis_H_3* and Figure 8.26. Continuing this analysis found that the clay bulkhead became fully saturated after 5.7 years.

The void ratio profile shown in Figure 8.34 shows very similar trends to that observed in Figure 8.31 for *Analysis_H-M_2*. The patterns of swelling and compression are the same and by the end of the simulation the region of the clay from 1.5 to 2.6 m has been compressed to a minimum void ratio of 0.445. However, as this region is still highly unsaturated the void ratio is not increasing at the same rate as that observed in Figure 8.31.

Since the downstream region of the clay bulkhead remains unsaturated by the end of the simulation this has a significant effect on the displacement of the steel plate. From Figure 8.35 it can be seen that the maximum displacement at the steel plate centre has reduced to 3.8 mm, a 34% reduction from the simulated behaviour in *Analysis_H-M_1*.

8.5.2.4 Conclusions

In the hydraulic-mechanical simulation of Phase I a series of investigations were performed which investigated the initial and boundary conditions of the downstream face of the clay bulkhead by adopting the same approach as that detailed in the hydraulic analysis. In the first analysis it was found that the rate of resaturation of the clay bulkhead was slightly accelerated compared to the hydraulic only analysis since the clay became fully saturated just after 2.8 years. This was due to the localised swelling of the clay along the sand chamber/clay bulkhead interface and subsequent shrinkage of the core. Hence less water was needed to fully saturate the core. It was found that the steel plate deformed incrementally throughout Phase I in response to the applied pore water pressure load generated by the sand chamber, with a maximum displacement of 5.8 mm being predicted at the centre of the steel plate. In the second simulation, it was found that the clay bulkhead took 4.1 years to reach full saturation, which again was slightly faster than the simulated behaviour from the corresponding hydraulic analysis. By the end of Phase I the clay bulkhead was still unsaturated in some regions as a result of less swelling taking place

compared to the previous analysis, therefore the maximum displacement of the steel plate was reduced to 4.2 mm. In the final analysis, where water was effectively supplied from only the upstream face of the clay bulkhead, the time taken to reach fully saturated conditions was delayed to 5.7 years. As a result the total displacement of the steel plate was further reduced at the end of Phase I to 3.8 mm.

A preliminary investigation of the experimental results from Phase I is presented in Section 8.7. This shows that at the start of the hydration phase water flowed around the edge of the clay bulkhead and quickly saturated the sand fill on the downstream face. As a result of this process the sand fill was then able to supply water to the downstream face of the clay bulkhead and by the end of Phase I the bulkhead had resaturated. When compared to the hydraulic and hydraulic-mechanical analyses that were performed in this study for the simulation of Phase I it can be seen that *Analysis_H_1* and *Analysis_H-M_1* best represent the experimental behaviour in the TSX. Therefore, the final results from these analyses have been employed as initial conditions for the simulations of Phase II presented in the next section.

8.6 Simulation of Phase II

Phase II of the Tunnel Sealing Experiment began immediately after Phase I had been completed. The objective of Phase II is to evaluate the performance of both the clay and concrete bulkheads and the host rock in response to elevated temperatures (Guo and Chandler, 2002). The heating is achieved by circulating heated water through headers installed in the sand-filled chamber. For the first year of Phase II the water in the inlet header will be fixed at 50 °C. This will be increased to 85 °C for the second year of Phase II.

In order to perform the numerical simulation of Phase II four distinct analyses have been undertaken: 1) a thermal analysis of the system 2) a hydraulic analysis of the system 3) a thermal-hydraulic analysis of the system, and 4) a thermal-hydraulic-mechanical analysis of the system.

8.6.1 Thermal simulation of Phase II

The thermal simulation (T) of Phase II of the Tunnel Sealing Experiment uses the same two-dimensional axisymmetrical geometry and domain adopted for the hydraulic simulation of Phase I detailed in Section 8.5.1. The primary objective of this analysis is to monitor the thermal response of the clay bulkhead under the applied thermal conditions. It also offers a comparison to the temperature results obtained in the thermal-hydraulic (T-H) analysis detailed later in Section 8.6.3.

8.6.1.1 Initial and boundary conditions

The initial temperature throughout the domain and for all materials was set at 14.5 °C (AECL, 2002). The far-field rock boundaries have adiabatic conditions prescribed to them by fixing the thermal flux to zero. Following initial thermal analyses it was found that this assumption was reasonable since the temperature rise did not approach the rock boundary by the end of the Phase II. A zero thermal flux boundary condition was also prescribed on the central surface of the section, which represents the axes of symmetry in the system. As a simplifying assumption the thermal advection processes in the, relatively permeable, sand chamber have been assumed to lead to a uniform temperature distribution in this

region. Therefore the temperature along the sand/clay bulkhead and sand/rock interfaces was initially set at 14.5 °C and then linearly increased to 50 °C over a 2 day period. The 2 day period is an approximation only and represented the assumed time it would take for the sand chamber to reach the target temperature of 50 °C since the temperature increase would not be instantaneous. This temperature was then kept constant during the first year of the analysis. The temperature was then increased over a period of 2 days to a constant 85 °C for the second year of the analysis. The surface of the rock along the open tunnel was fixed at 14.5 °C to allow the heat to flow into the tunnel.

8.6.1.2 Simulation numerics

As summarised in Chapter 4, Section 4.5 the thermal analysis of the Tunnel Sealing Experiment was performed using a Preconditioned Conjugate Gradient (PCG) solver combined with a Jacobi preconditioner. The analysis was run in parallel on 4 processors on the SUN HPC system. The thermal analysis was conducted using the two-dimensional axisymmetrical mesh detailed in Section 8.5.1.2 and Figure 8.17. The time-step for this analysis started at 100 seconds and was allowed to increase to a maximum of 30 days in response to the rate of numerical convergence, via the algorithm described in Chapter 4, Section 4.3. The thermal material parameters for the clay bulkhead, sand, steel plate, concrete ring and granite rock are described in Section 8.3. This analysis was run for 2 years corresponding to the experimental duration of Phase II.

8.6.1.3 Simulation results

Figure 8.36 (a) shows the temperature contour plot in the Tunnel Sealing Experiment after the first year of Phase II. The maximum temperature along the sand chamber boundary is 50 °C and the heat is slowly being conducted through the clay bulkhead and host granite rock. Figure 8.36 (b) shows a contour plot of the final temperature distribution in the Tunnel Sealing Experiment at the end of Phase II. In Figure 8.37 a plot of temperature through the centre of the clay bulkhead is shown over time. It can be seen that after 365 days the temperature on the downstream face of the clay bulkhead has reached 28.9 °C. By the end of Phase II this value has risen to 44.8 °C but has not reached steady-state conditions as there is still an increase in temperature in the bulkhead.

8.6.1.4 Conclusions

In the thermal simulation of Phase II the thermal response of the clay bulkhead to the elevated temperatures imposed by the heated water in the sand chamber was demonstrated. The temperature profile in the clay bulkhead had not reached stead-state conditions and was still rising on the dowstream face. This analysis helps to illustrate how the flow of heat through an engineered clay bulkhead is a relatively slow process and is an important characteristic of buffer materials in relation to disposal of heat-producing, high-level radioactive waste.

8.6.2 Hydraulic simulation of Phase II

The hydraulic simulation (H) of Phase II of the Tunnel Sealing Experiment uses the same two-dimensional axisymmetrical geometry and domain adopted for the hydraulic simulation of Phase I detailed in Section 8.5.1.2 and Figure 8.17. Following the preliminary investigation of the experimental results from Phase I, discussed in Section 8.5.2.4, this analysis continues from the end of *Analysis_H_1*, with the clay bulkhead being fully saturated at the start of Phase II. Therefore, any further pore water pressure re-distribution within the clay bulkhead as the system approaches steady-state conditions is investigated. It also allows a comparison to the non-isothermal hydraulic results presented in the thermal-hydraulic (T-H) analysis detailed in Section 8.6.3. It should also be noted that the sand fill region on the downstream face of the clay bulkhead was still slightly unsaturated at the end of Phase I and was starting to resaturate as further water was provided by the adjacent rock.

8.6.2.1 Initial and boundary conditions

The initial hydraulic pore water pressures in the system are taken from the final results for 3.5 years from the simulation, *Analysis_H_1*, detailed in Section 8.5.1.3.1. The same fixed hydrostatic pressures are applied along the far-field rock boundaries as detailed in Section 8.4.1.1 and Figure 8.11. Along the sand chamber/clay bulkhead interface and the sand chamber/rock interface the pore water pressures are fixed at a constant 4 MPa. The hydraulic boundary conditions applied at the downstream face of the experiment are the same as those adopted for *Analysis_H_1*.

8.6.2.2 Simulation numerics

As in the hydraulic analysis of Phase 1 a combination of solver (Bi-CG-STAB) and preconditioner (ILU-Crout) has been adopted for the hydraulic analysis of Phase II. The analysis was run in parallel on 4 processors on the SUN HPC system. The hydraulic analysis was conducted using the two-dimensional axisymmetrical mesh detailed in Section 8.5.1.2 and Figure 8.17. The time-step for this analysis started at 100 seconds and was allowed to increase to a maximum of 30 days in response to the rate of numerical convergence, via the algorithm described in Chapter 4, Section 4.3. The hydraulic material parameters for the clay bulkhead, sand, steel plate, concrete ring and granite rock are described in Section 8.3. This analysis was run for 2 years corresponding to the experimental duration of Phase II.

8.6.2.3 Simulation results

The hydraulic (H) analysis of Phase II shows that by the end of the analysis the pore water pressure is building up in the clay bulkhead. The clay bulkhead is fully saturated by the end of Phase I and by the end of Phase II the pore water pressure on the downstream face is slowly approaching 4 MPa. As can be observed in Figure 8.38, the pore water pressure on the downstream face of the clay bulkhead has risen to 2.9 MPa by the end of the analysis.

8.6.2.4 Conclusions

In the hydraulic simulation of Phase II it was found that by the end of the analysis the pore water pressures in the clay bulkhead had not reached steady-state conditions. This was apparent since the pore water pressure in the clay bulkhead were not in equilibrium with the hydrostatic pressure in the surrounding rock. This is a slow process since there is little build up of pore water pressure in the sand fill region on the downstream face of the clay bulkhead. However, after 2 years the sand fill material has become fully saturated and as a result the pore water pressure in the clay bulkhead along this boundary has risen to 2.9 MPa.

8.6.3 Thermal-Hydraulic simulation of Phase II

The thermal-hydraulic (T-H) simulation of Phase II of the Tunnel Sealing Experiment uses the same two-dimensional axisymmetrical geometry and domain adopted for the hydraulic simulation of Phase I detailed in Section 8.5.1.2 and Figure 8.17. However, for these sets of analyses the hydraulic flow field has been fully coupled with the thermal response of the system. In addition to this the variation of the hydraulic conductivity with temperature has been incorporated into the simulation for the clay bulkhead. This is due to the reduction in viscosity of water at elevated temperatures which results in an increase in the hydraulic conductivity for the material. For the T-H analysis of Phase II it was also necessary to investigate the thermal expansion of water since the clay bulkhead was fully saturated by the end of Phase I. Hence for this simulation, 2 analyses were performed; one with the thermal expansion of water taken into account and one without.

8.6.3.1 Initial and boundary conditions

The initial hydraulic pore water pressures in the system are taken from the final results for 3.5 years from the hydraulic simulation of Phase I detailed in Section 8.5.1.3.1, *Analysis_H_1*, and hence assumes that the clay bulkhead was saturated at the start of Phase II. The same fixed hydrostatic pressures are applied along the far-field rock boundaries as detailed in Section 8.5.1.1 and Figure 8.11. Along the sand chamber/clay bulkhead interface and the sand chamber/rock interface the pore water pressures are fixed at a constant 4 MPa. A zero flux boundary condition was applied on the surface of the steel plate to prevent the transfer of moisture through this material. The initial temperature throughout the domain and for all materials was set to 14.5 °C. The far-field rock boundaries had adiabatic conditions prescribed to them by fixing the flux to zero. A zero temperature flux boundary condition was also prescribed on the central surface of the section, which represents the axes of symmetry in the system. The temperature along the sand chamber/clay bulkhead and sand chamber/rock interfaces was fixed at 50 °C for the first year of the analysis and then increased up to 85 °C for the second year of the analysis.

8.6.3.2 Simulation numerics

It was found that the same combination of solver (Bi-CG-STAB) and preconditioner (ILU-Crout) adopted for the hydraulic analysis of Phase I performed with the greatest stability

for the thermal-hydraulic analyses. The analyses were run in parallel on 4 processors on the SUN HPC system. The coupled thermal-hydraulic analyses were conducted using the two-dimensional axisymmetrical mesh detailed in Section 8.5.1.2 and Figure 8.17. The time-step for these analyses started at 100 seconds and was allowed to increase to a maximum of 30 days in response to the rate of numerical convergence, via the algorithm described in Chapter 4, Section 4.3. The thermal-hydraulic material parameters for the clay bulkhead, sand, steel plate, concrete ring and granite rock are described in Section 8.3. These analyses were run for 2 years corresponding to the experimental duration of Phase II.

8.6.3.3 Simulation results

8.6.3.3.1 Thermal expansion of water not considered

Figure 8.39 shows the temperature profile through the centre line of the clay bulkhead for the T-H analysis of Phase II. The temperature distribution compares closely with the results simulated in the Thermal only analysis described in Section 8.6.1.3. It can be seen that after 365 days the temperature on the downstream face of the clay bulkhead has reached 29.3 °C. By the end of Phase II this value has risen to 45.1 °C.

Figure 8.40 shows the pore water pressure profile through the centre line of the clay bulkhead during Phase II of the Tunnel Sealing Experiment. For the first 560 days the pressure profile through the clay is only gradually increasing as the sand fill at the downstream face of the clay slowly resaturates. Eventually, by 650 days the filler sand has fully resaturated. This resaturation is the result of the boundary conditions applied to the downstream face of the system, as discussed in Section 8.5.1.1. The pore water pressure in the clay increases towards steady-state values of 4 MPa, this is clearly evident by the end of Phase II where the pore water pressure on the downstream face of the clay has reached a value of 3.1 MPa.

8.6.3.3.2 Thermal expansion of water considered

When the thermal expansion of water is taken into consideration for the saturated clay bulkhead the temperature distribution compares closely with the results simulated in the

thermal only analysis described in Section 8.6.1.3. However, there are some distinct differences observed in the pore water pressures in the clay bulkhead compared to those detailed in Figure 8.39.

Figure 8.41 shows the pore water pressure profile through the centre line of the clay bulkhead during Phase II with the thermal expansion of water taken into account. It can be seen that initially there is a substantial increase in pore water pressure near the sand chamber/clay bulkhead interface. The pore water pressure reaches a maximum value of 6.85 MPa after 3 days into Phase II. This behaviour is due to the pore water in this fully saturated material being heated and trying to expand, and since the system is fully restrained, and in the short-term effectively undrained, this results in an increase of pore water pressure. This increase in pressure gradually reduces through the clay and after 1 year the peak has completely dissipated. This redistribution of pore water pressure in the clay bulkhead occurs as the system approaches steady-state conditions and equilibrium with the hydrostatic conditions in the surrounding rock. As discussed in Section 8.6.3.3.1 due to the applied boundary conditions the sand fill on the downstream face of the clay becomes saturated. The pore water pressure throughout the clay bulkhead then begins to approach steady-state values and by the end of Phase II the pore water pressure on the downstream face of the clay has reached a value of 3.3 MPa.

8.6.3.4 Conclusions

In the thermal-hydraulic simulation of Phase II it was found that the thermal expansion of water for the saturated clay made a significant difference to the pore water pressure profiles through the clay bulkhead. Without the thermal expansion of water considered the pore water pressure profile gradually approached the steady-state conditions of 4 MPa. With the thermal expansion of water considered there was initially a significant build up of pore water pressure in the clay bulkhead with a peak of 6.85 MPa in the region near the sand chamber/clay bulkhead interface. This was due to the thermal expansion of pore water in the saturated voids due to the thermal gradients. By the end of Phase II the pore pressures had redistributed and were approaching steady-state conditions throughout the bulkhead. These analyses help to illustrate the importance of coupled thermal-hydraulic processes on fully saturated clay materials. The thermal expansion of the pore water in an engineered buffer material generates large pressures, which in an operational disposal

facility would need to be taken into consideration in the design of the multiple barrier system.

8.6.4 Thermal-Hydraulic-Mechanical simulation of Phase II

The thermal-hydraulic-mechanical (T-H-M) simulation of Phase II of the Tunnel Sealing Experiment uses the same geometry and domains adopted for the hydraulic simulation of Phase I detailed in Section 8.5.1.2 and Figure 8.17. However, for these sets of analyses both the thermal and hydraulic flow fields have been fully coupled with the mechanical response of the system.

8.6.4.1 Initial and boundary conditions

The initial hydraulic pore water pressures in the system are taken from the final results for 3.5 years from the hydraulic-mechanical (H-M) simulation of Phase I detailed in Section 8.5.2.3.1, *Analysis_H-M_1*, and hence assumes that the clay bulkhead was saturated at the start of Phase II. The initial stresses throughout the system are also taken from the final results for 3.5 years from the H-M simulation of Phase I detailed in Section 8.5.2.3.1. All initial conditions and boundary conditions for the temperature regime in the analysis are identical to those detailed in Section 8.6.1.1. The concrete ring is again restrained both in the vertical and horizontal direction thus preventing any deformation. All other materials are allowed to deform.

8.6.4.2 Simulation numerics

As summarised in Chapter 4, Section 4.5, in order to perform the fully coupled thermal-hydraulic-mechanical analysis accurately a direct LU solver was implemented because the iterative solvers were found to be unstable for this type of analysis. The analyses were run in serial on the SUN HPC system. The coupled thermal-hydraulic-mechanical analyses were conducted using the two-dimensional axisymmetrical mesh detailed in Section 8.5.1.2 and Figure 8.17. The time-step for these analyses started at 100 seconds and was allowed to increase to a maximum of 7 days in response to the rate of numerical convergence, via the algorithm described in Chapter 4, Section 4.3. The mechanical material parameters for the clay bulkhead, sand, steel plate, concrete ring and granite rock

are described in Section 8.3. The analysis was also performed with the thermal expansion of water taken into consideration. This analysis was run for 2 years corresponding to the experimental duration of Phase II.

8.6.4.3 Simulation results

Figure 8.42 shows the temperature profile through the centre line of the clay bulkhead for the T-H-M analysis of Phase II. The temperature distribution compares closely to the results simulated in the T-only analysis and the T-H analyses described in Sections 8.6.1.3 and 8.6.3.3 respectively. It can be seen that after 365 days the temperature on the downstream face of the clay bulkhead has reached 29 °C. By the end of Phase II this value has risen to 45 °C. This illustrates how the thermal distribution in Phase II is unaffected by the introduction of a coupled mechanical analysis.

Figure 8.43 shows the pore water pressure profile through the centre line of the clay bulkhead for the T-H-M analysis of Phase II with the thermal expansion of water taken into consideration. When compared to the results obtained for the T-H analysis with the thermal expansion of water considered, as detailed in Section 8.6.3.3.2, there are some obvious differences. Primarily, there is no immediate increase in pore water pressure at the sand chamber/clay bulkhead interface but rather a decrease in pressure, as observed at 30 days. By the end of the first year the pore water pressures in the clay have recovered and are starting to approach steady-state. This behaviour can be attributed to the coupling of the thermal field and thermal expansion of the clay. At the start of the first year of Phase II the temperature in the sand chamber is raised from 14.5 °C to 50 °C. This steep temperature gradient has an immediate and significant effect on the expansion of the clay bulkhead. This can be seen in Figure 8.44, which shows the void ratio along the centre line of the clay bulkhead throughout Phase II. At 30 days the void ratio along this interface has risen from 0.463 to 0.478. This increase in pore volume leads to a reduction in the pore water pressure, as shown in Figure 8.43.

At the start of the second year the temperature in the sand chamber is raised a further 35 °C and again the clay bulkhead is seen to expand in response to this thermal gradient. At 390 days the void ratio has risen to 0.497 and the pore water pressure consequently decreases. By the end of Phase II the clay bulkhead has expanded to a void ratio of 0.5. The pore water pressure profile through the clay has fully recovered and the sand fill has resaturated

completely. The pore water pressure on the downstream face of the clay has reached a value of 3.11 MPa.

Figure 8.45 shows the displacement of nodal surface positions on the steel plate at the downstream face of the clay bulkhead during the H-M analysis of Phase I and the T-H-M analysis of Phase II. The figure shows the variation of displacement from the centre of the steel plate to the edge of the plate that intersects with the concrete ring. The results up to the end of Phase I (3.5 years) were discussed in Section 8.5.2.3.1. It can be seen that throughout Phase II there is additional movement of the steel plate in response to the thermal gradients and the subsequent thermal expansion of the clay bulkhead. This can be seen in two distinct patterns corresponding to the increase in temperature to 50 °C in the first year and 85 °C in the second year. At the end of the first year the steel plate has moved a maximum of 6.7 mm and by the end of Phase II the centre of the steel plate is predicted to have moved by 8 mm. The displacement in the steel plate incrementally reduces across its surface to zero at the concrete ring intersection.

8.6.4.4 Conclusions

In the thermal-hydraulic-mechanical simulation of Phase II it was found that the thermal expansion of the clay bulkhead had a notable effect on the pore water pressure distribution. As the temperature was increased the void ratio of the clay increased and the pore water pressure consequently reduced. This was apparent both at the start of the first year and second year of Phase II. This expansion was also evident on the surface of the steel plate whereby the centre had deformed 8 mm by the end of Phase II.

8.7 *Preliminary comparison of the experimental behaviour with the simulated behaviour*

The main objective of the modelling exercise for the Tunnel Sealing Experiment was to investigate the behaviour of the clay bulkhead during Phase I and II via a series of predictions. At the time of the investigation limited experimental data from the TSX was available for comparison. Subsequently, AECL have provided further information regarding the experimental performance of the clay bulkhead and therefore the following section presents a preliminary comparison of the behaviour.

8.7.1 Hydraulic behaviour during Phase I

Towards the end of Phase I of the TSX moisture sensors indicated that the clay bulkhead had largely achieved saturation and piezometers had begun to register positive pressures within the entire clay bulkhead (AECL, 2001). Only a small region near the core of the bulkhead appeared to be unsaturated. It was noted however that at, or near saturation, most of the moisture sensors went out-of-range, failed and/or flooded, resulting in loss of readings and in some cases water leakage through the cabling (AECL, 2001). Figure 8.46 shows the suction profiles within the clay bulkhead after approximately 3 years. It can be seen that both the upstream and downstream faces of the bulkhead have fully resaturated and that there is only a small unsaturated zone localised in the core of the bulkhead.

The transient behaviour of the hydraulic regime in the clay bulkhead is illustrated in Figure 8.47 (adopted from suction profiles in Chandler et al., 2002b). This shows the degree of saturation profile along the centre of the clay bulkhead (section C-C) over time. This experimental behaviour can be compared to the simulated hydraulic behaviour discussed in Section 8.5. Experimentally, it can be seen that the initial hydraulic conditions within the bulkhead were not homogenous compared to the conditions adopted for the analyses. This was potentially due to the installation procedure and the difficulty in achieving a completely homogenous material. As water was pumped into the sand chamber it can be seen that the bulkhead began to resaturate from the upstream face. However, part of the core of the bulkhead was seen to resaturate faster than the upstream face. This proved problematic during the experiment as seepage took place through preferential pathways in and around the bulkhead as the sand chamber was pressurised incrementally. As a result,

after approximately 1 year water had entered the system from the downstream end. This resulted in dual-directional saturation of the bulkhead. This type of hydraulic recharge was analysed in *Analysis_H_1* and *Analysis_H-M_1*. Reference to Figures 8.20 and 8.27 shows that the simulated hydraulic response of the system during Phase I represented the experimental behaviour reasonably well as a result of adopting this approach. Whilst the model did not represent the complex seepage effects it should be noted that the overall hydraulic patterns were captured with the bulkhead approaching complete saturation by 3 years.

8.7.2 Mechanical behaviour during Phase I

During the experiment, displacements in the clay bulkhead and in the steel plate were monitored using a combination of instruments. These included linear potentiometers installed in the upstream face of the clay bulkhead, a sonic probe array to measure internal movement within the bulkhead and LDT's and LVDT's mounted on instrumentation conduits to measure the movement of the steel plate (AECL, 2001). It was found that by the end of Phase I the linear potentiometers were all out of range, having exceeded their travel capacity or mechanically failed.

Figure 8.48 shows the displacement of the steel plate during Phase I as measured by the LDT's mounted across its surface. It can be seen that during the first 160 days when the pressure in the sand chamber was increased to 750 kPa there is a large movement recorded in all sensors, with a maximum displacement of 10 mm in CLDT1 at the top of the tunnel. At mid-height of the steel plate a displacement of 6.3 mm is measured. At 550 days the pressure is further increased to 2 MPa in the sand chamber and an immediate response is seen in the movement of the plate. At mid-height the displacement is seen to increase by an increment of approximately 2.3 mm. Towards the end of Phase I the pressure is further increased to 4 MPa and again additional movement can be observed in the steel plate, with an incremental increase of approximately 2.5 mm in the centre of the plate. By the end of Phase I a total displacement of 12.5 mm has been measured at mid-height of the plate.

This measured behaviour can be compared to the simulated behaviour from *Analysis_H-M_1* as illustrated in Figure 8.29. Preliminary comparisons show that the initial large displacements measured in the experiment are not captured by the model. A maximum displacement of 0.7 mm is simulated in the centre of the plate after 160 days as

the hydraulic pressure is increased to 750 kPa throughout the system. It is unclear why such large displacements were initially measured in the experiment, especially for such a relatively small increase in pressure. It is unlikely to be a result of just the hydraulic response since much smaller movements are recorded later when the pressure is increased to 2 MPa and then 4 MPa. Potentially, it could be a result of highly sensitive sensors identifying displacements following installation of the bulkhead as the system equilibrates with the host rock. This could also explain why greater displacements were measured at the top of the tunnel since noticeable warping was observed in the vertical plane of the tunnel following tunnel excavation.

Further comparisons of the results do show however that the incremental displacement of the plate after the pressure increased to 2 MPa and 4 MPa was reasonably well captured by the model. This can be seen at the centre of the plate where incremental displacements of 1.1 mm and 2.8 mm were simulated. When compared to the corresponding measured values there is a difference of 1.2 mm and 0.3 mm respectively. This gives confidence in the ability of the model to represent the complex mechanical behaviour of the TSX to a reasonable level of accuracy.

8.7.3 Thermal behaviour during Phase II

Limited experimental information was available concerning the thermal behaviour of the clay bulkhead during Phase II of the TSX. However, some transient experimental data was presented by Guo et al. (2003) for the first 180 days of the heating of the bulkhead and therefore some preliminary comparisons are made here.

Figure 8.49 shows the simulated and measured temperatures in the clay bulkhead at different axial distances from the upstream face. The simulated results are taken from the coupled thermal-hydraulic analysis discussed in Section 8.6.3.3.1, where the thermal expansion of the pore water is not considered. It can be seen from Figure 8.49 that there is a relatively weak correlation between the simulated and measured results. In the simulation results the temperature throughout the bulkhead increases at a faster rate resulting in higher overall temperatures. At an axial distance of 0.2 m the maximum increase in temperature is simulated to be 4.6 °C/day compared to a measured increase of approximately 0.5 °C/day. At approximately 180 days the simulated temperature is 46.4 °C and the corresponding experimental value is 40.1 °C; giving a percentage difference of

13.5 %. At greater axial distances from the upstream face of the clay bulkhead similar patterns are observed. At an axial distance of 1.4 m a maximum difference of 20.5 % can be observed between the simulated and measured values after 180 days.

The principal reason for these differences is due to the adoption of the thermal boundary condition prescribed on the upstream face of the clay bulkhead in the analysis. This boundary condition assumes that there is an almost immediate thermal response in the bulkhead when the heating phase begins. In reality however, heated water is circulated through the sand chamber first and the upstream face of the clay bulkhead is seen to heat up at a much more gradual rate. This delay in the thermal response of the bulkhead also means that temperatures are lower when compared to the simulated behaviour. At the time of the numerical investigation this simplified approach was adopted based on the limited data available and therefore this preliminary comparison highlights the importance of using accurate boundary conditions when modelling complex large scale in-situ experiments.

8.7.4 Conclusions

The outcome from these preliminary comparisons shows that the model is able to capture reasonable trends in the thermal, hydraulic and mechanical behaviour of the TSX. The rates of resaturation of the clay bulkhead in Phase I were well captured in some of the analyses where wetting occurred both on the upstream and downstream faces of the bulkhead. Whilst the initial deformation behaviour of the steel plate was not captured quantitatively by the model, subsequent incremental displacements were simulated more accurately. Finally, the simulated thermal response in the clay bulkhead showed that the simplified thermal boundary condition did not fully represent the actual in-situ conditions. However, there was still a reasonable agreement in the results by 180 days of heating. To conclude, this exercise has highlighted the importance of comparing predicted and observed behaviour at each stage in the modelling process. The comparisons are encouraging and illustrate that the model is able to simulate the thermo/hydro/mechanical behaviour of the Tunnel Sealing Experiment.

8.8 Conclusions

In conclusion a fully coupled mechanistic thermal-hydraulic-mechanical model has been applied to the simulation of the behaviour of AECL's Tunnel Sealing Experiment. Primarily two-dimensional axisymmetrical analyses have been performed with a small range of three-dimensional hydraulic analyses performed for the granite prior to the commencement of Phase I. A comprehensive range of analyses have been undertaken to investigate the performance of the Tunnel Sealing Experiment during Phase I and Phase II. A number of conclusions can be drawn from these analyses and are discussed below.

For this particular simulation exercise it was found that it was more beneficial both in terms of complexity and simulation runtimes to employ a smaller two-dimensional axisymmetrical model as opposed to a more complex three-dimensional model. The symmetrical nature of the Tunnel Sealing Experiment was advantageous to this type of analysis and as a result a larger range of investigations could be performed in the allotted time frame. A comparison between the hydraulic results for both two-dimensional axisymmetrical and three-dimensional analyses showed them to be very similar and gave confidence in using the two-dimensional approach for all subsequent simulations. However, it is acknowledged that this approach does have inherent simplifications and that certain assumptions were made in the simulations.

A range of hydraulic and hydraulic-mechanical simulations were performed for Phase I of the TSX. It was apparent from the results that the initial conditions on the downstream face of the clay bulkhead had a large influence over the rates of resaturation in the bulkhead. When the sand fill was installed saturated this provided an additional source of water to the bulkhead and resaturation occurred at a faster rate than in the analyses where the sand fill was installed unsaturated. This was significant because it was found from the actual experiment that wetting occurred on the downstream face of the bulkhead. This was due to problems with the clay bulkhead construction where pathways through and around the bulkhead were not sealed properly and allowed water to seep through and collect at the downstream face. Hence, this illustrated the importance of applying the correct initial and boundary conditions when performing the numerical analyses.

Research into the dual porosity of clay materials has been gathering steady momentum in recent years and the investigation of the micro/macro behaviour of the clay bulkhead

yielded significant results. This process was implemented via a first approximation whereby a modified hydraulic conductivity relationship was used which assumed that 94 % of available moisture was adsorbed in the micropores of the clay. It was seen that when the micro/macro effects were taken into account the rate of resaturation in the bulkhead was significantly delayed, by up to a factor of 8. This is an important result as it illustrates how a conventional flow model could potentially under-predict saturation times for buffer materials if the complex structure of the material is not taken into consideration. Therefore greater research into these processes is required.

It was found from the hydraulic-mechanical simulations of Phase I that the coupled effect of the mechanical behaviour had a small influence over the hydraulic behaviour in the clay bulkhead. The variation in the void ratio as a result of swelling and consolidation was small but illustrated the process by which water flowed through the bulkhead, saturating and swelling each subsequent region. This swelling process was reflected on the downstream end of the experiment where the movement in the steel plate was simulated. Again, the initial conditions in the sand fill were significant, as the displacements were greater in the saturated case. The level and degree of swelling is an important consideration in the design of multiple barrier systems where excessive displacements are undesirable. Therefore, this series of analyses show the need to accurately establish initial conditions in the proximity of highly-swelling materials.

In Phase II of the TSX the thermal response of the system was investigated. Both coupled and non-coupled analyses were performed. When the thermal analysis results were compared to the thermal-hydraulic results there was very little difference in the thermal regime in the clay bulkhead by the end of Phase II. Since the clay bulkhead was saturated at the start of this Phase it was necessary to investigate the effect of the thermal expansion of the pore water. It was found that this made a significant difference to the pore water pressure profiles through the clay bulkhead with a large increase in pore water pressure clearly evident at the start of the simulation. Therefore, this phenomenon is of importance and should be taken into consideration in the design of multiple barrier systems to accommodate large pore pressures.

The thermal expansion of the clay bulkhead was investigated in the coupled thermal-hydraulic-mechanical simulation and it was found that this did effect both the pore water pressure and void ratio. As the temperature was increased the void ratio of the clay

increased and the pore water pressure consequently reduced. The thermal expansion in the clay also gave rise to additional movement in the steel plate. This combined with swelling could have a significant effect on restraint systems and could lead to large pressures developing.

A short investigation was conducted after the numerical modelling programme to make preliminary comparisons between the simulated and measured results. Limited data was available and therefore only the hydraulic and mechanical behaviour of Phase I and the thermal behaviour of Phase II were considered. It was shown that the model did capture the hydraulic behaviour of the bulkhead reasonably well and simulated the movement of the steel plate in a qualitative sense. The model was less successful in simulating the thermal behaviour of the bulkhead due to the adoption of a simplified thermal boundary condition. However, the results were encouraging and illustrated that the model was able to simulate the behaviour of the Tunnel Sealing Experiment reasonably well.

The Tunnel Sealing Experiment represents a valuable investigation into the parameters or design elements that potentially affect seal performance. The most important outcome from the experiment is that functional full scale repository seals can be constructed using currently available technology. There is a need to monitor the performance of these repository seals over time and numerical modelling plays an integral role in providing short and long-term predictions of their potential behaviour in response to thermal and hydraulic gradients. This information can then be accommodated into future designs to improve construction and performance and give confidence in the ability of repository seals to fulfil their role in a deep geological repository for the safe disposal of high-level nuclear waste.

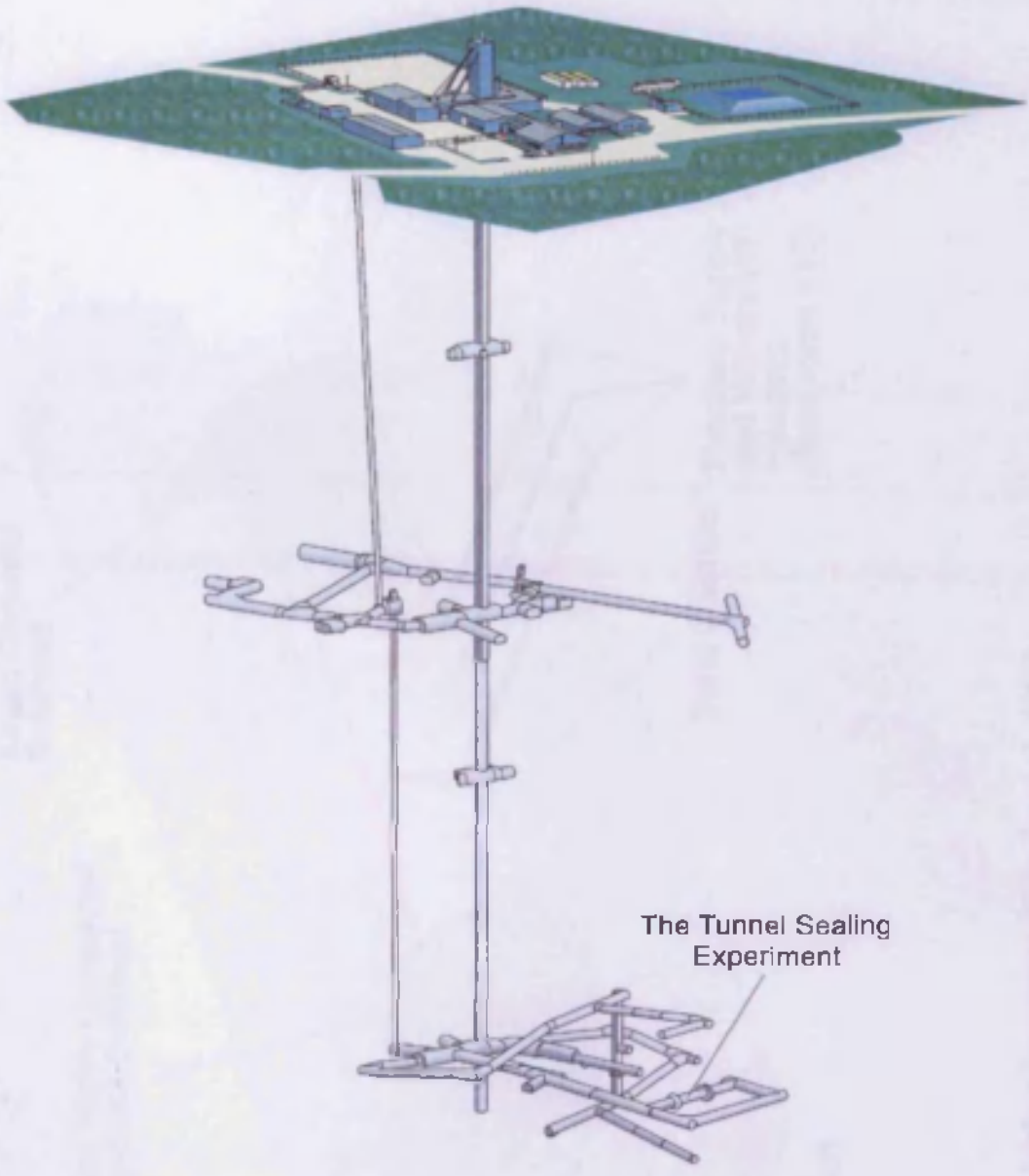

Figure 8.1 *The Underground Research Laboratory and location of the Tunnel Sealing Experiment* (Chandler et al., 2002b)

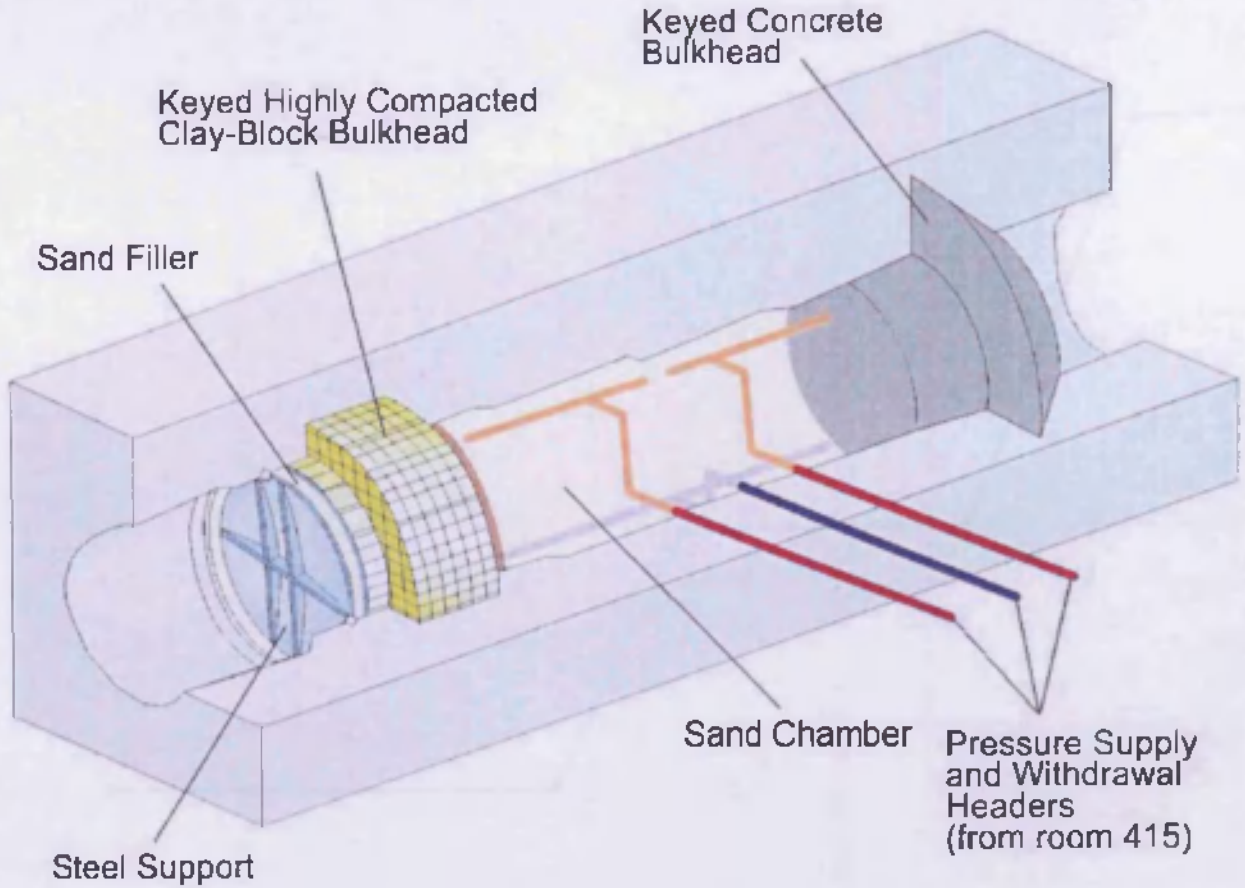

Figure 8.2 Layout of the Tunnel Sealing Experiment (Chandler et al., 2002b)

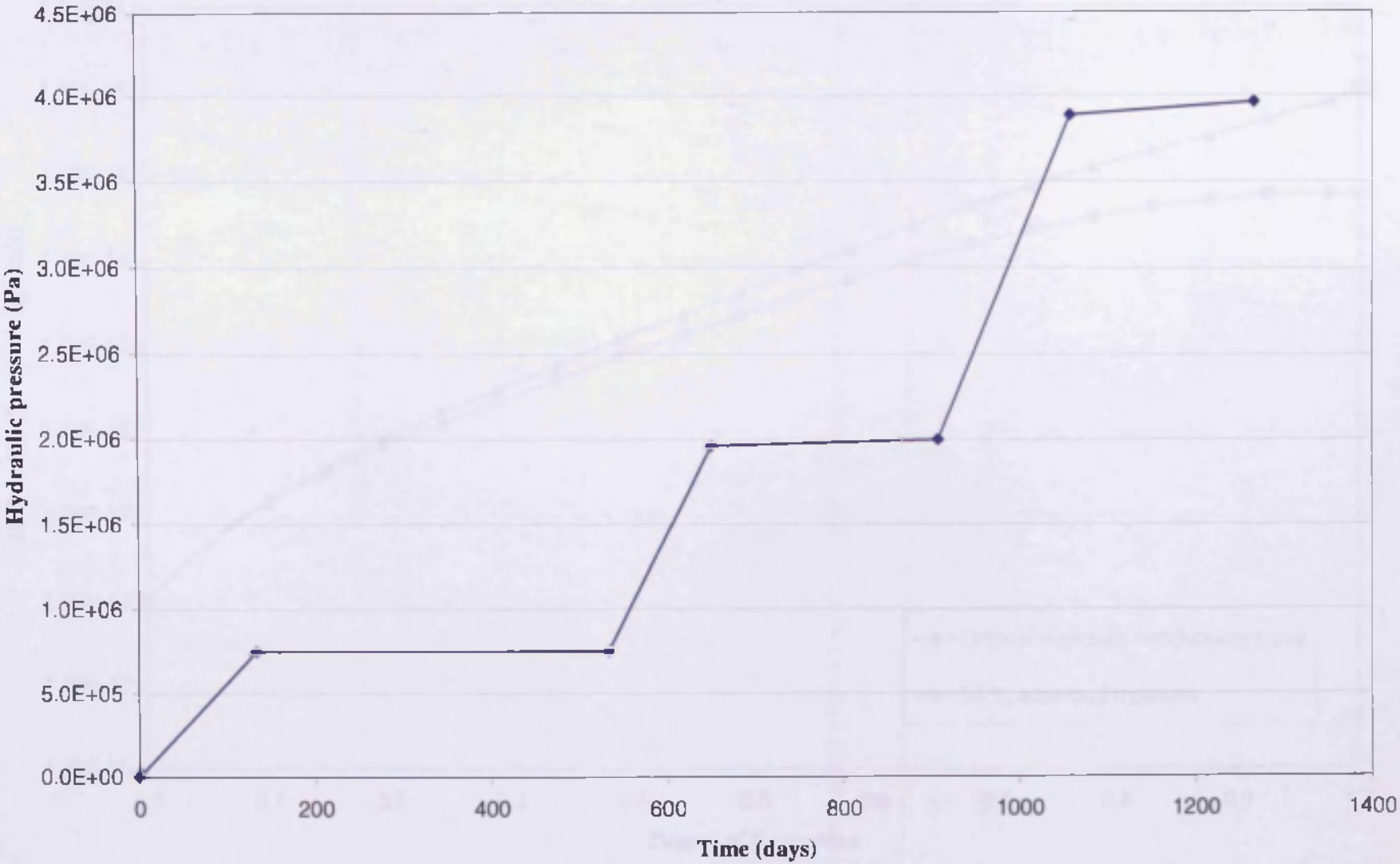

Figure 8.3 Pore Water Pressure profile in the sand chamber versus time

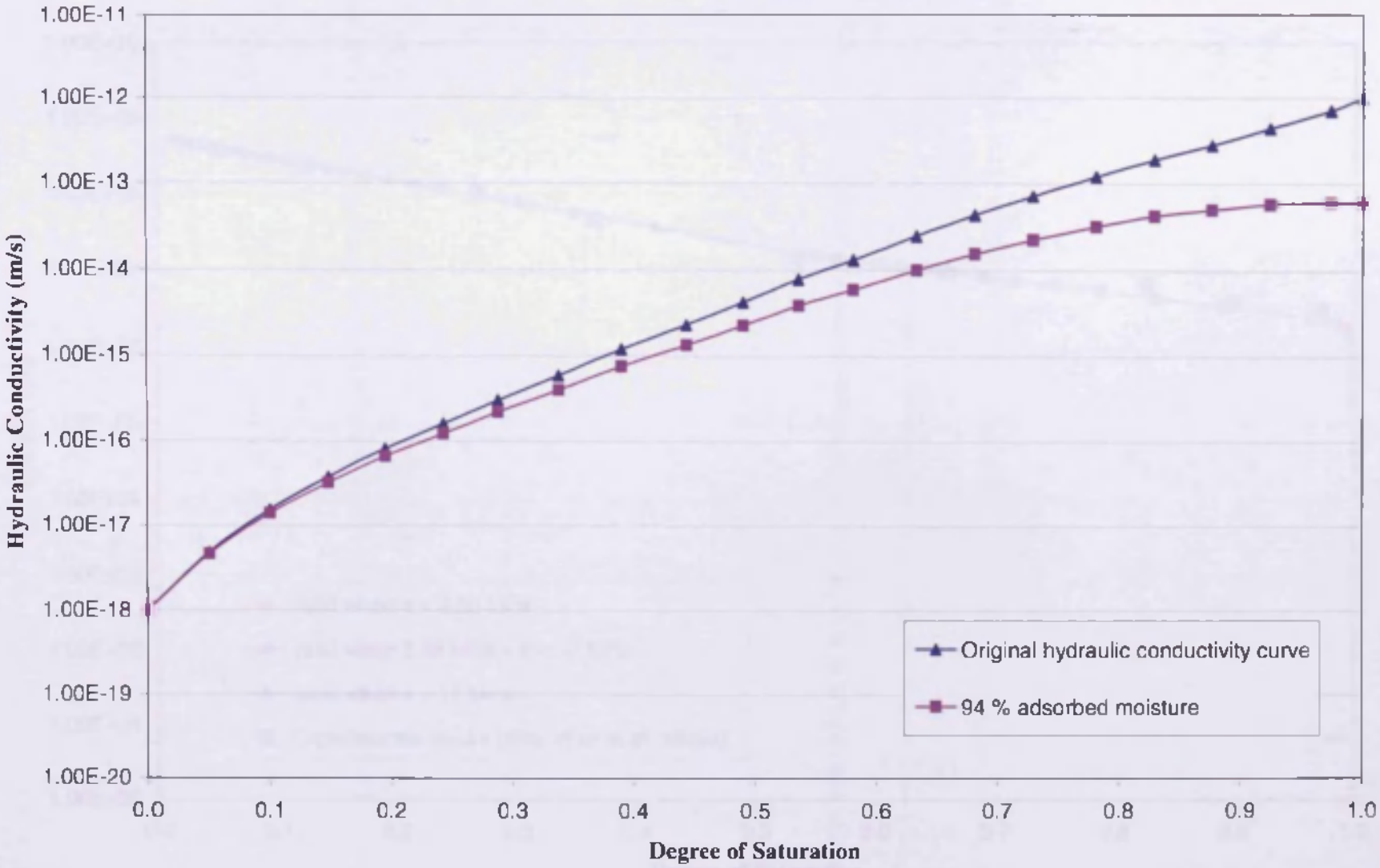

Figure 8.4 Hydraulic conductivity relationship for the clay bulkhead used in the Tunnel Sealing Experiment

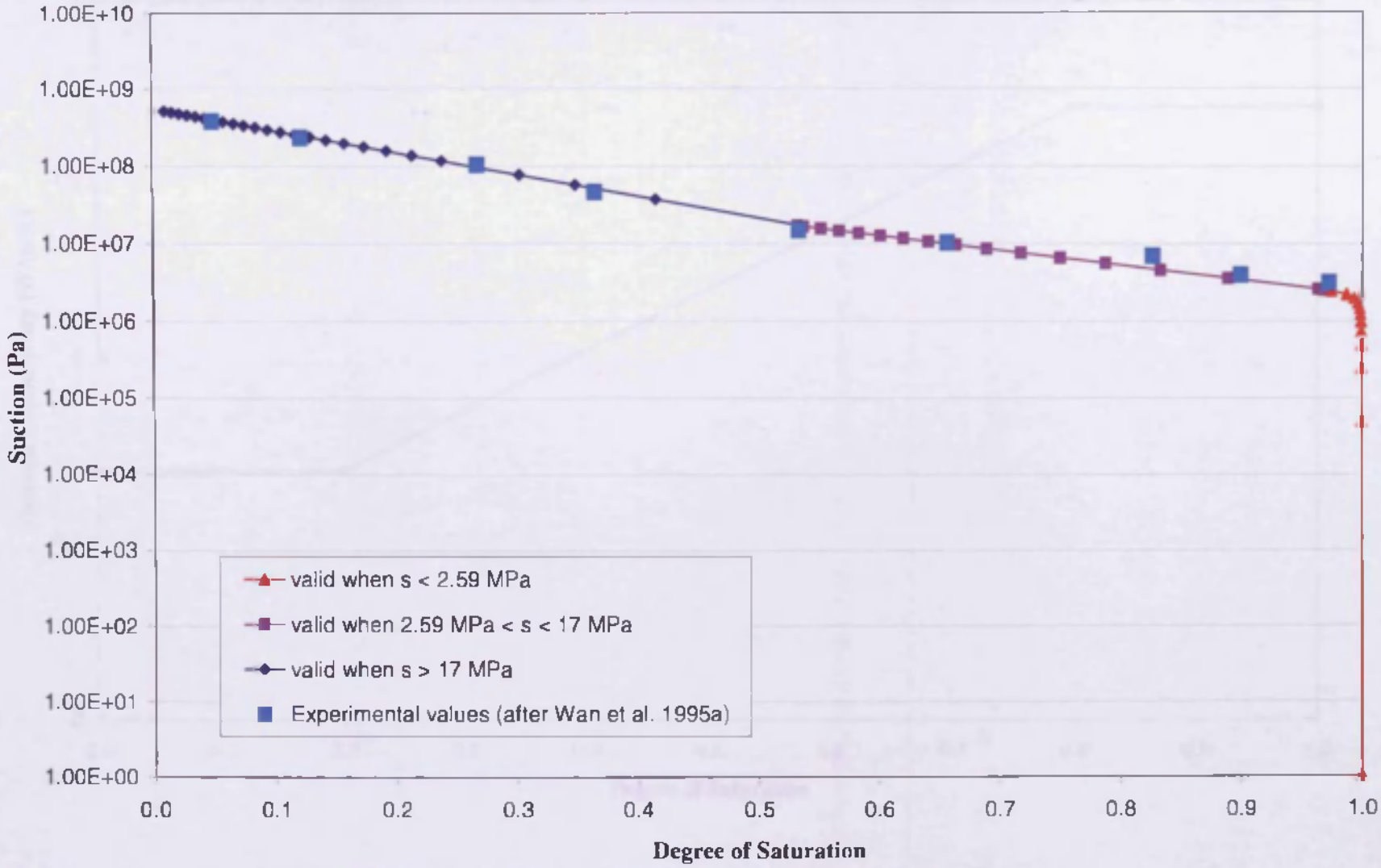

Figure 8.5 Water retention curve for the clay bulkhead used in the Tunnel Sealing Experiment

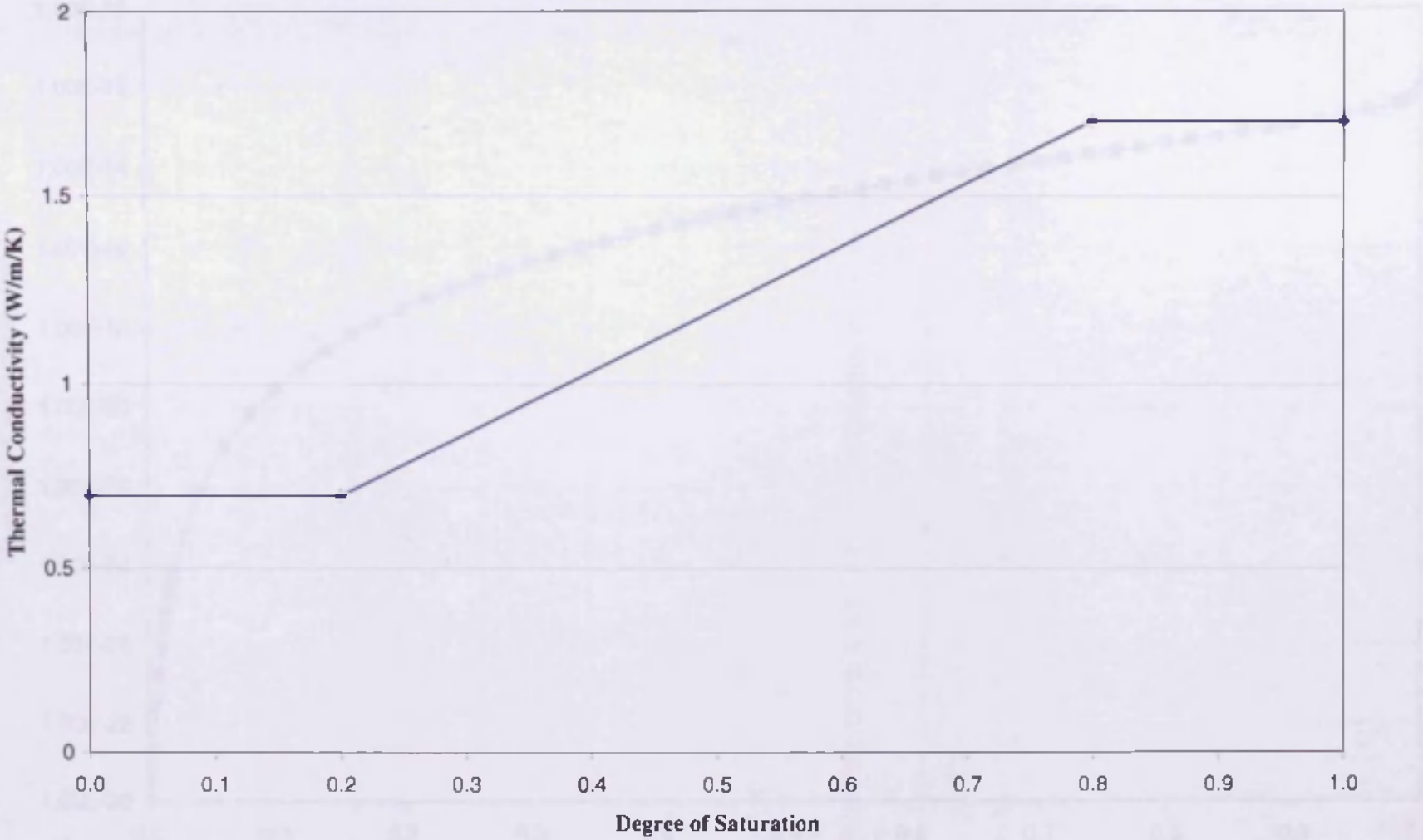

Figure 8.6 Thermal conductivity relationship for the clay bulkhead used in the Tunnel Sealing Experiment

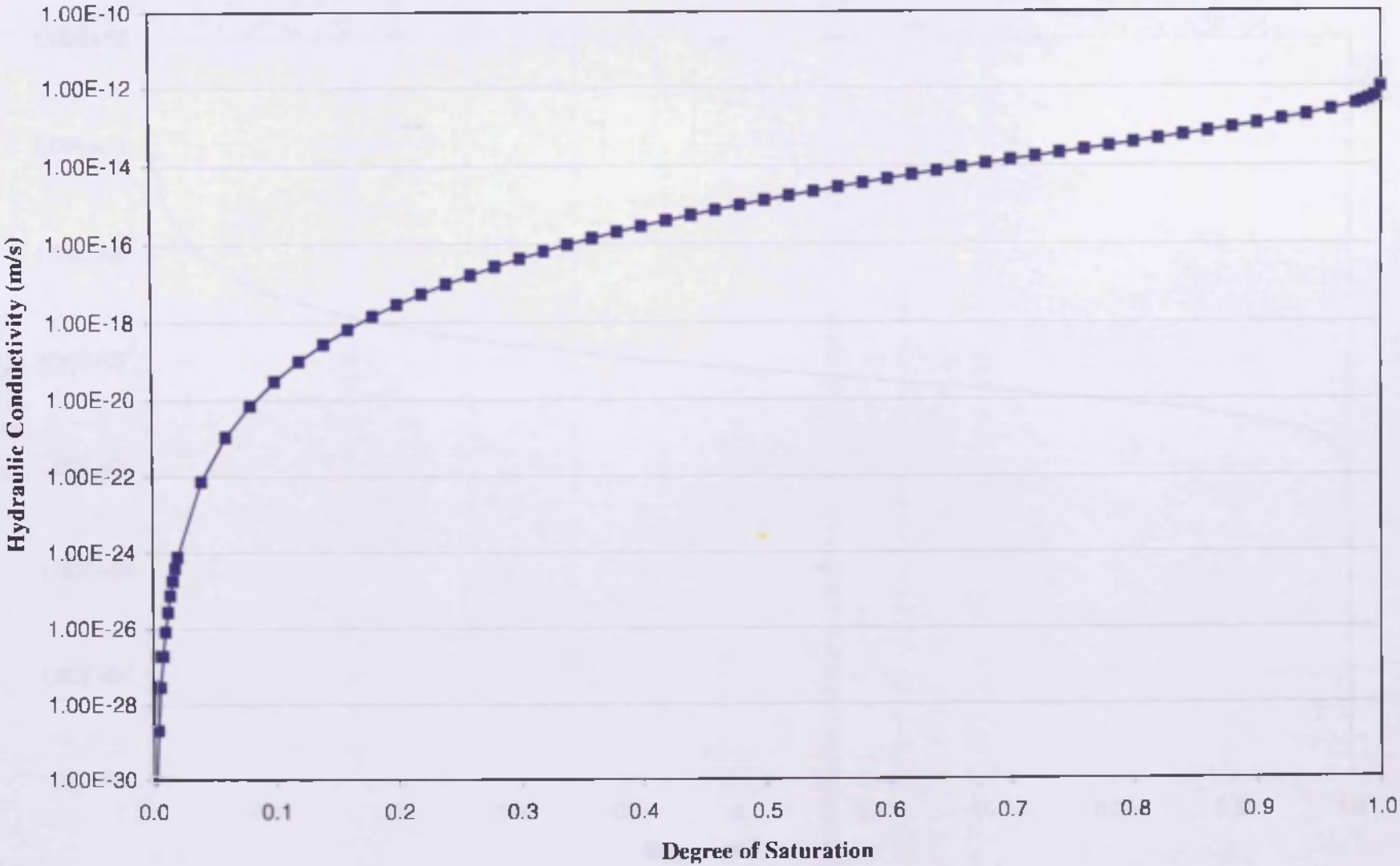

Figure 8.7 Hydraulic conductivity relationship for the granite rock used in the Tunnel Sealing Experiment

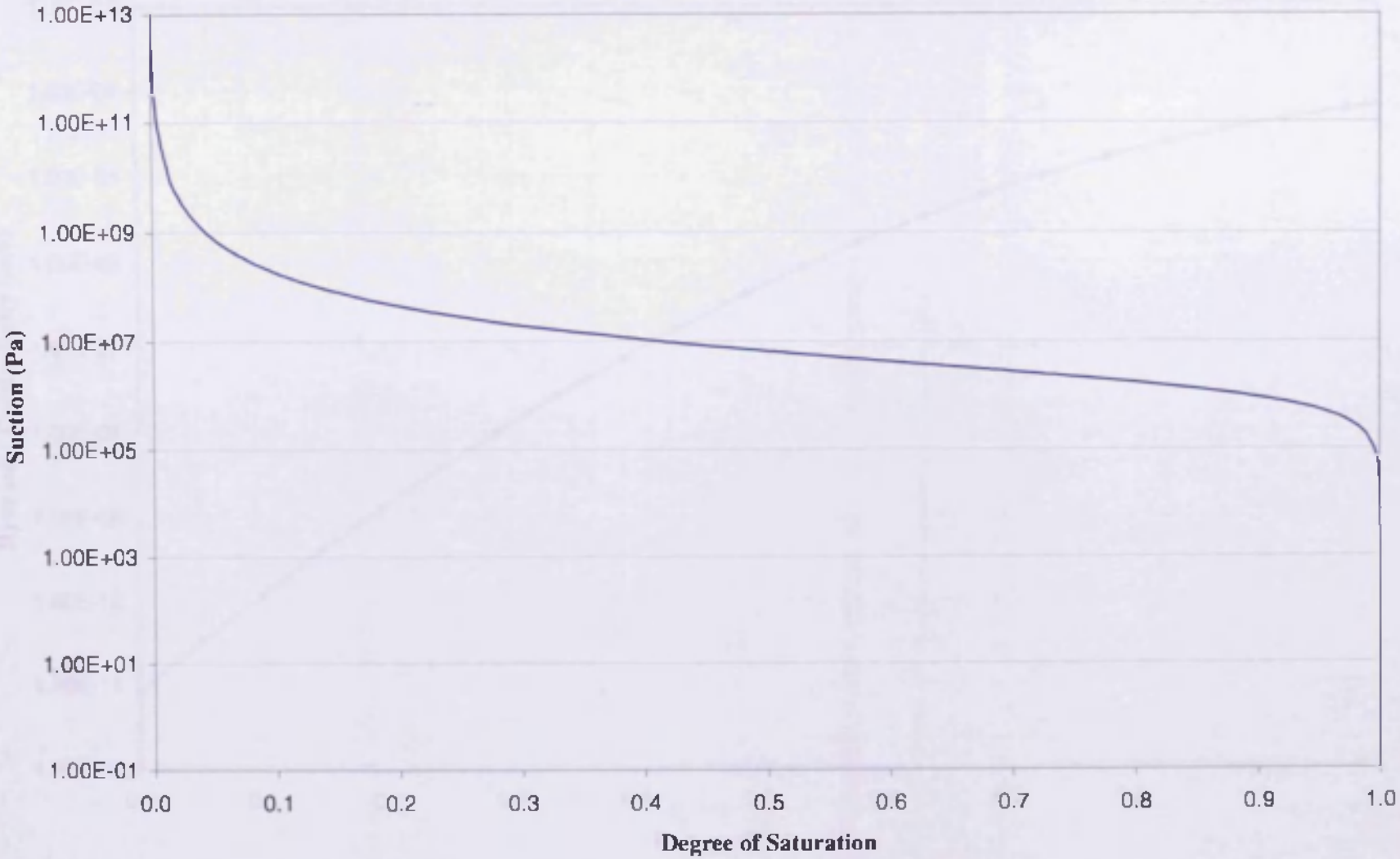

Figure 8.8 Water retention curve for the granite rock used in the Tunnel Sealing Experiment

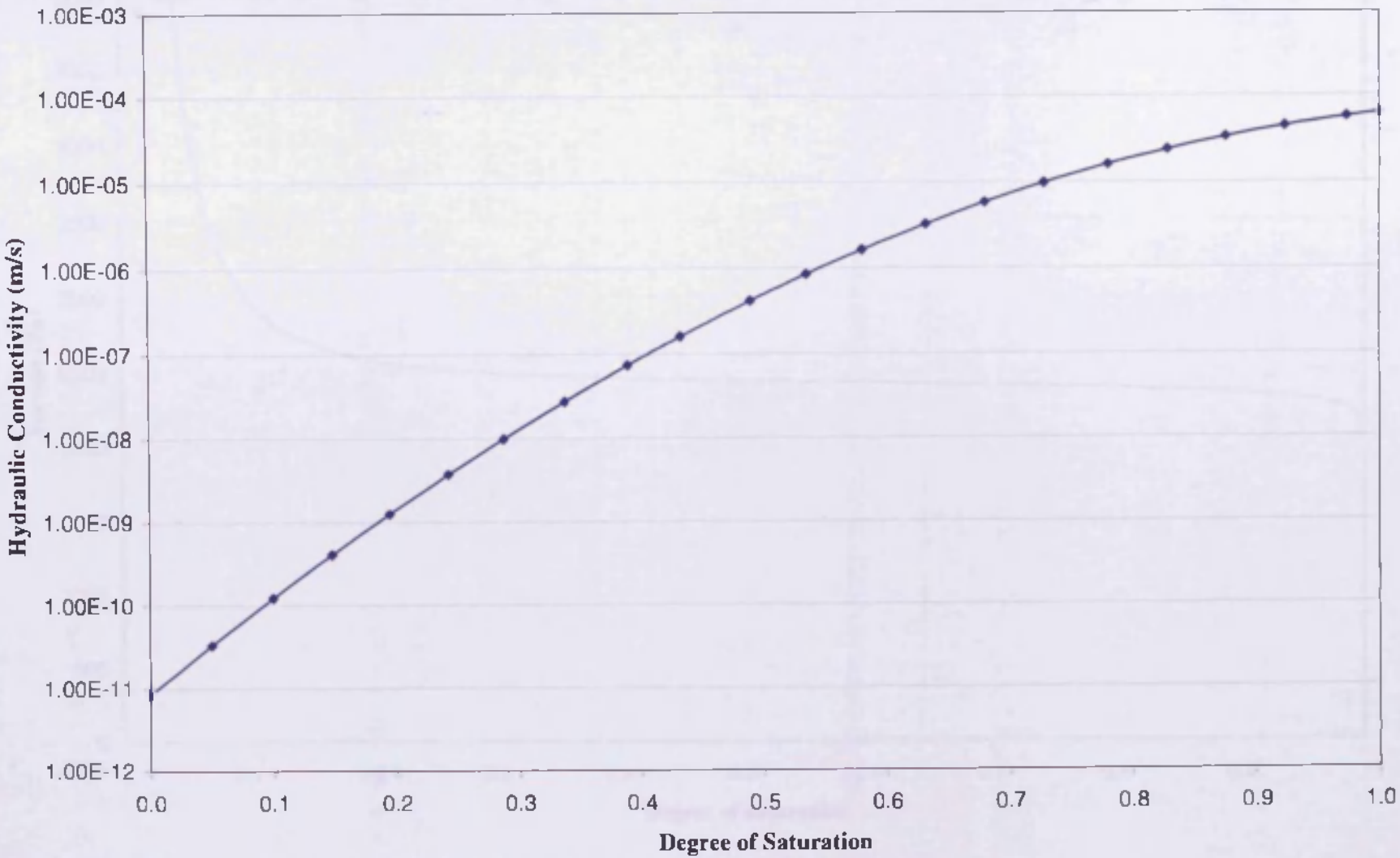

Figure 8.9 Hydraulic conductivity relationship for the sand fill used in the Tunnel Sealing Experiment

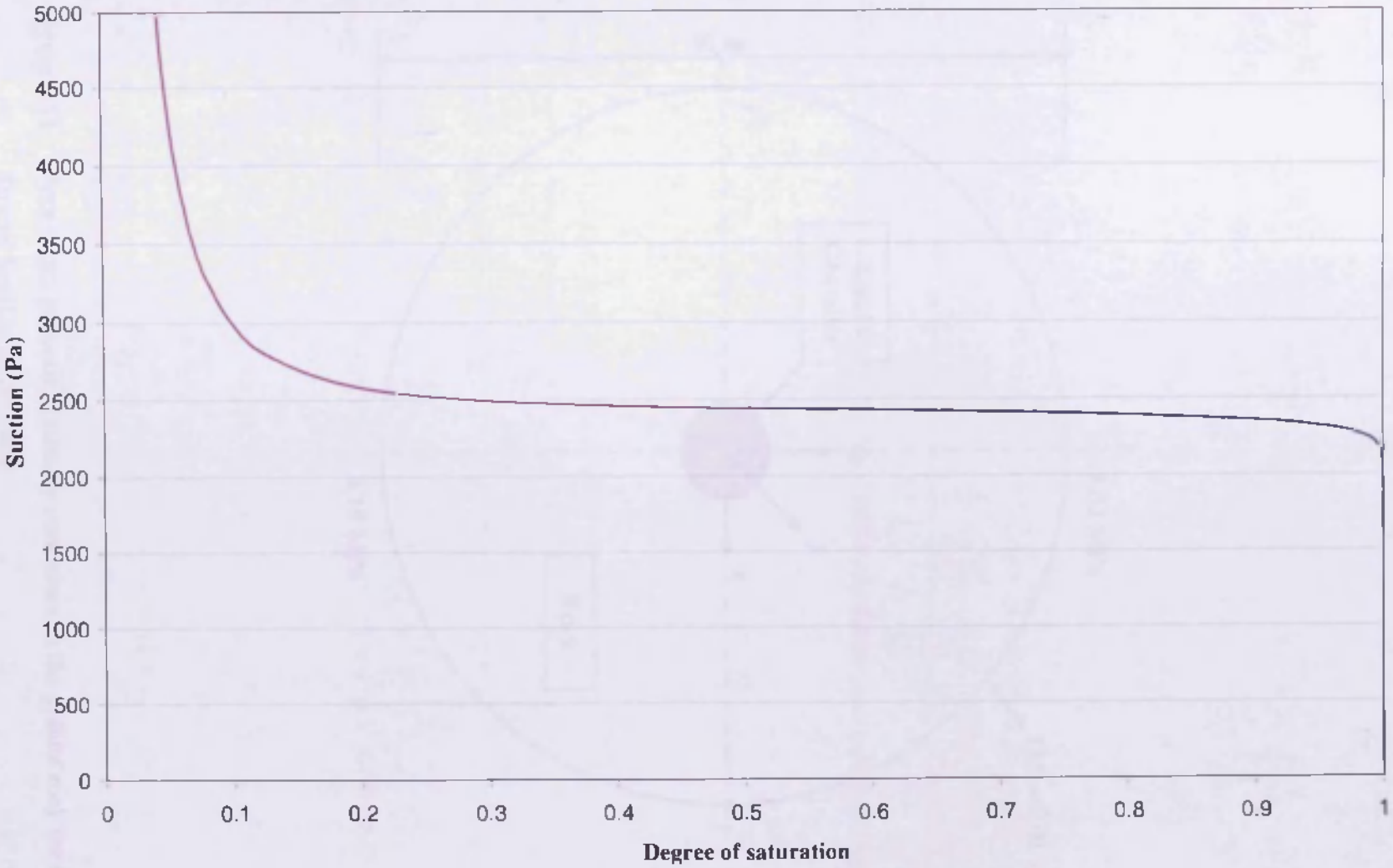

Figure 8.10 Water retention curve for the chamber sand used in the Tunnel Sealing Experiment

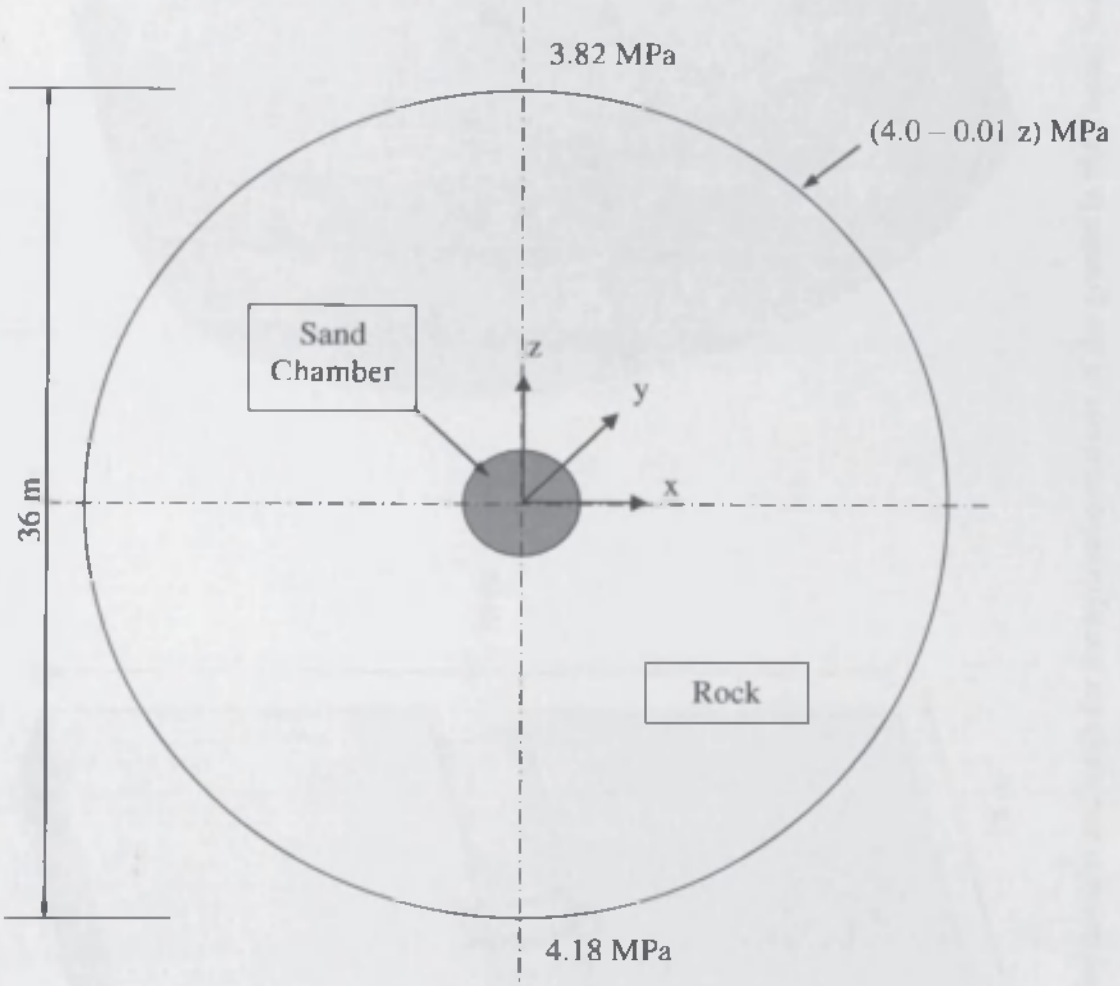

Figure 8.11 Pore water pressure boundary conditions in the granite rock for the Tunnel Sealing Experiment

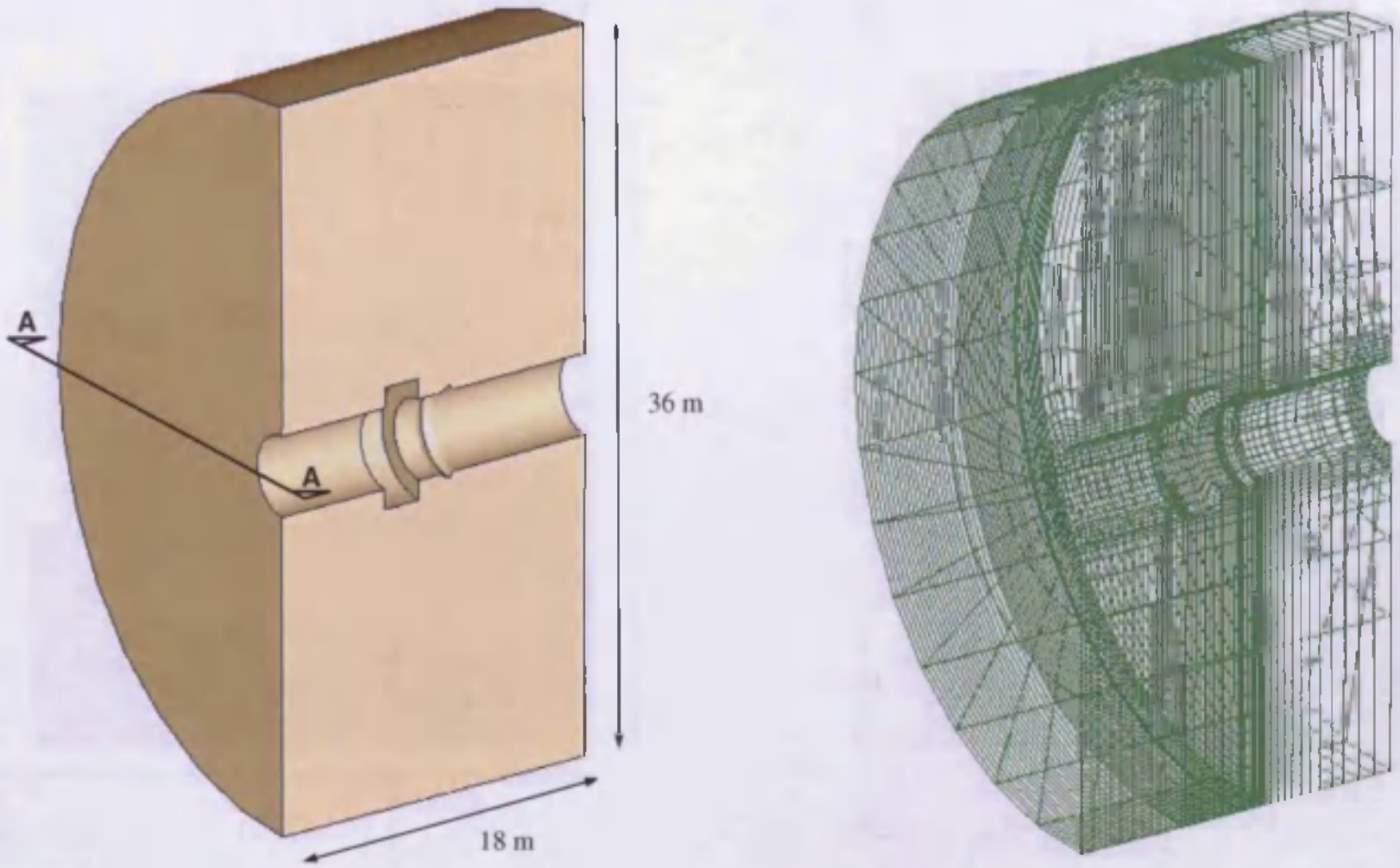

Figure 8.12 Full three-dimensional domain and mesh for the hydraulic analysis of the granite in the Tunnel Sealing Experiment

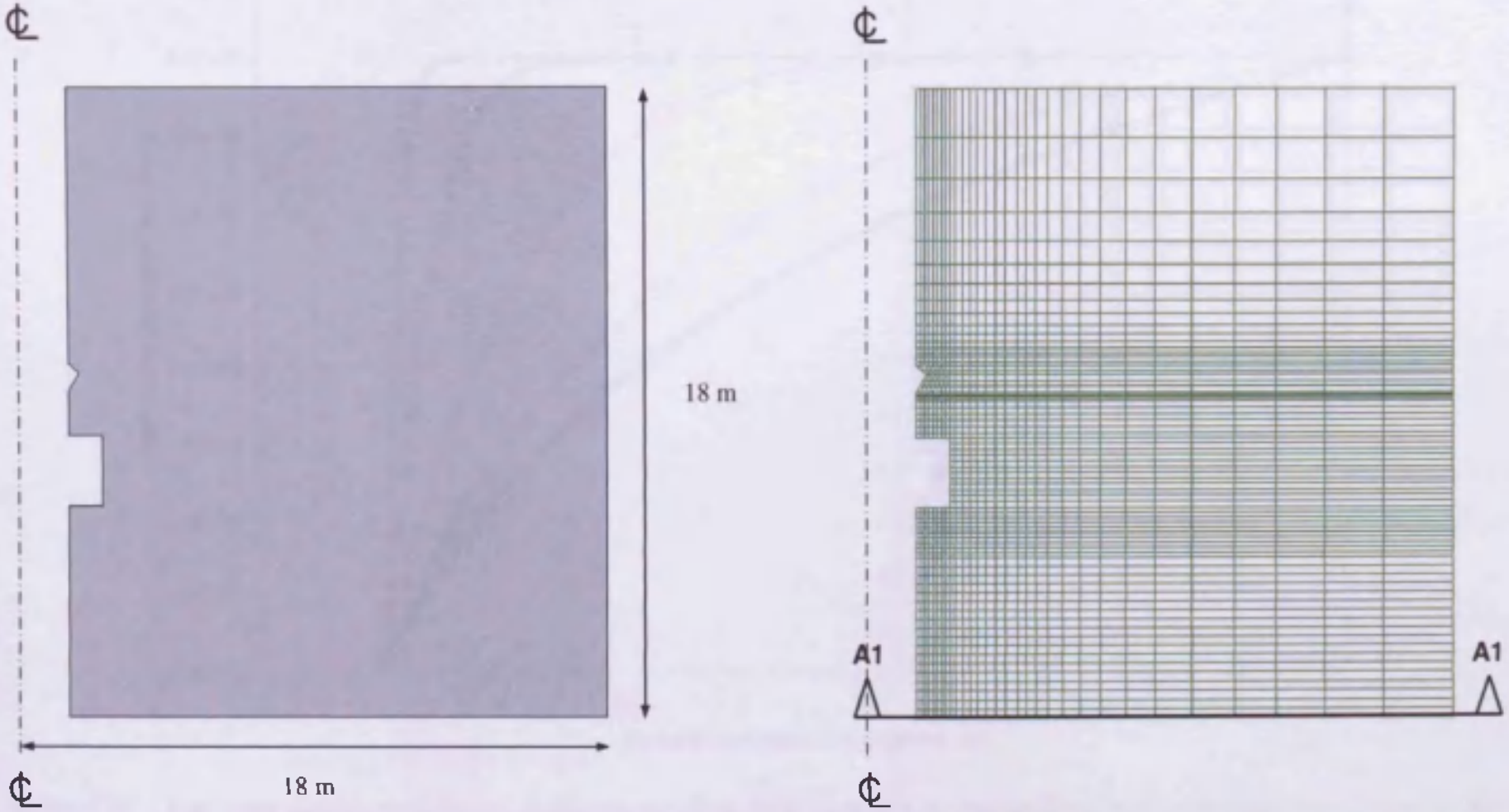

Figure 8.13 Two-dimensional axisymmetrical domain and mesh for the hydraulic analysis of the granite in the Tunnel Sealing Experiment

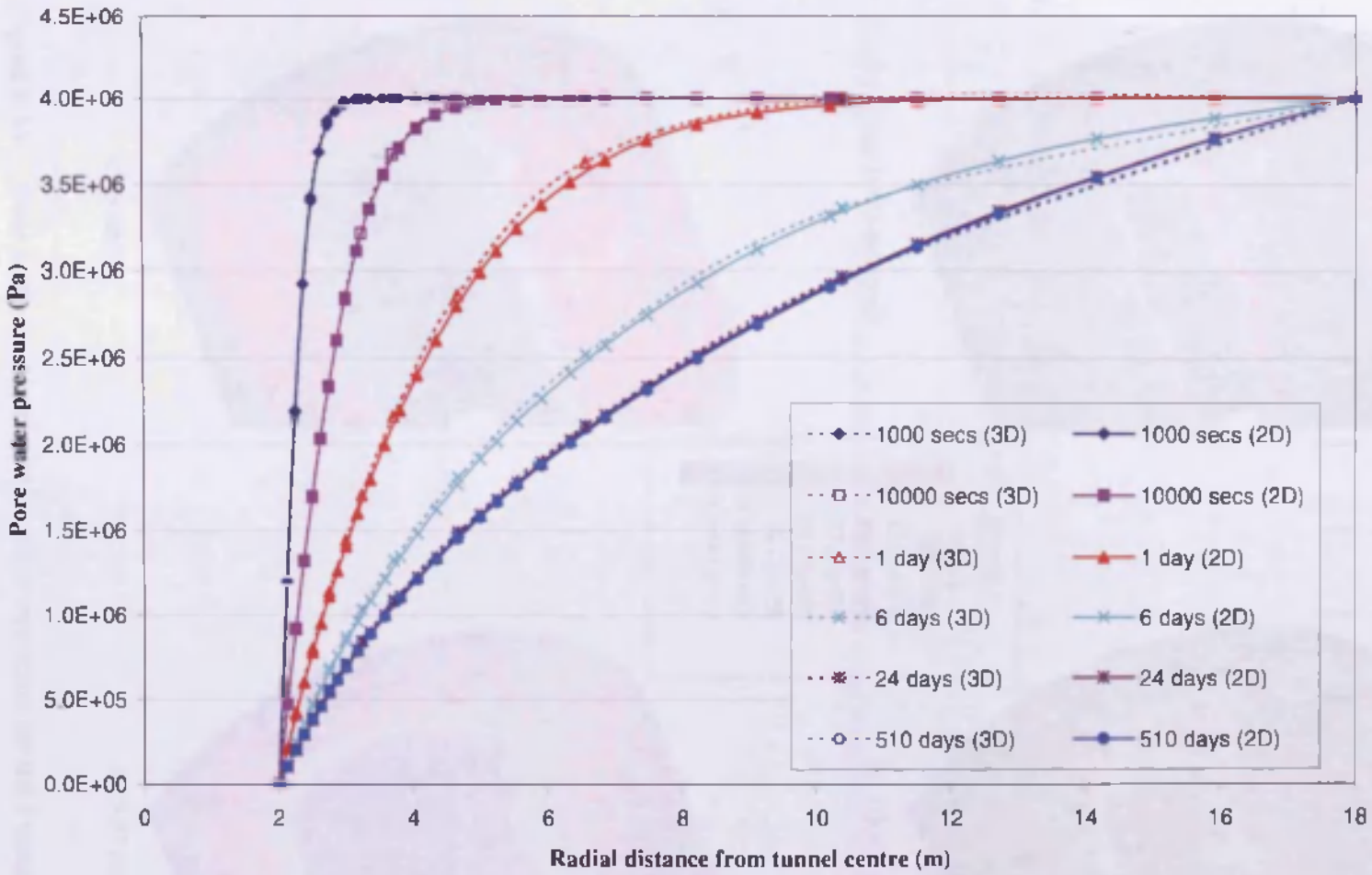

Figure 8.14 Pore water pressure versus radial distance for the 3D analysis (section A-A) and the 2D axisymmetrical analysis (section A1-A1) in the rock for the Tunnel Sealing Experiment prior to Phase 1

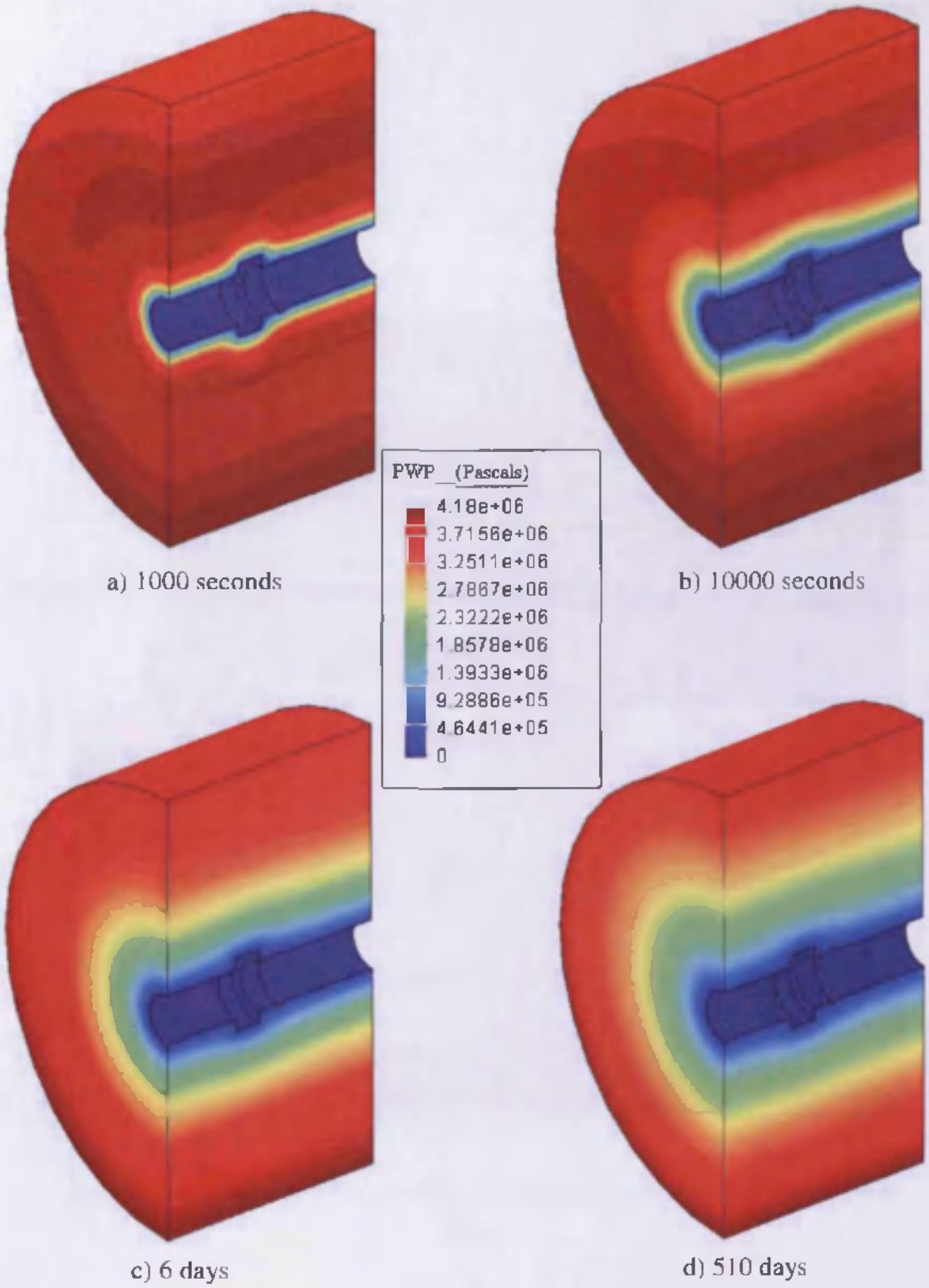

Figure 8.15 Pore water pressure contour plots over time for the Tunnel Sealing Experiment prior to Phase I

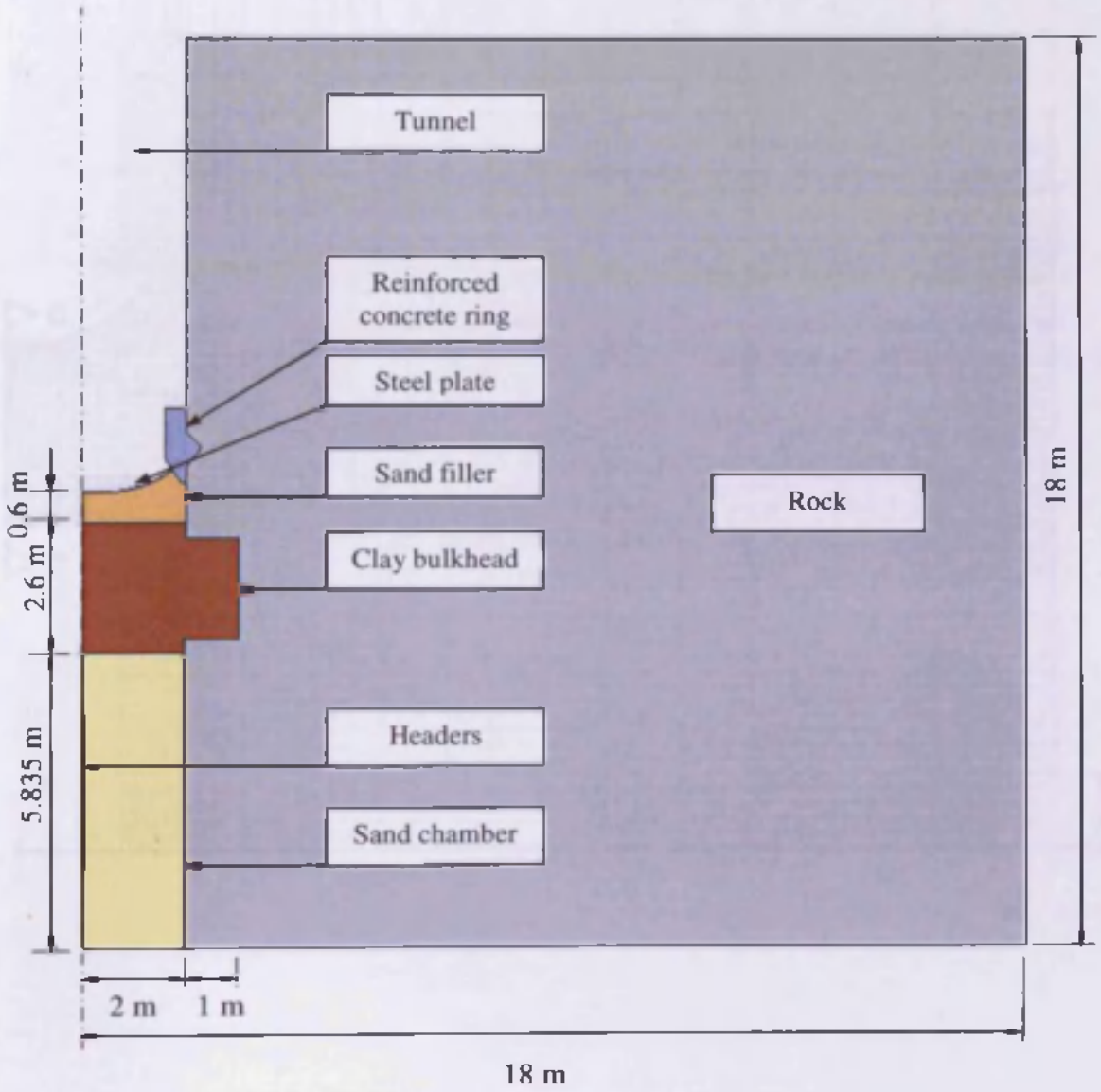

Figure 8.16 The geometry of the Tunnel Sealing Experiment for Phases I and II

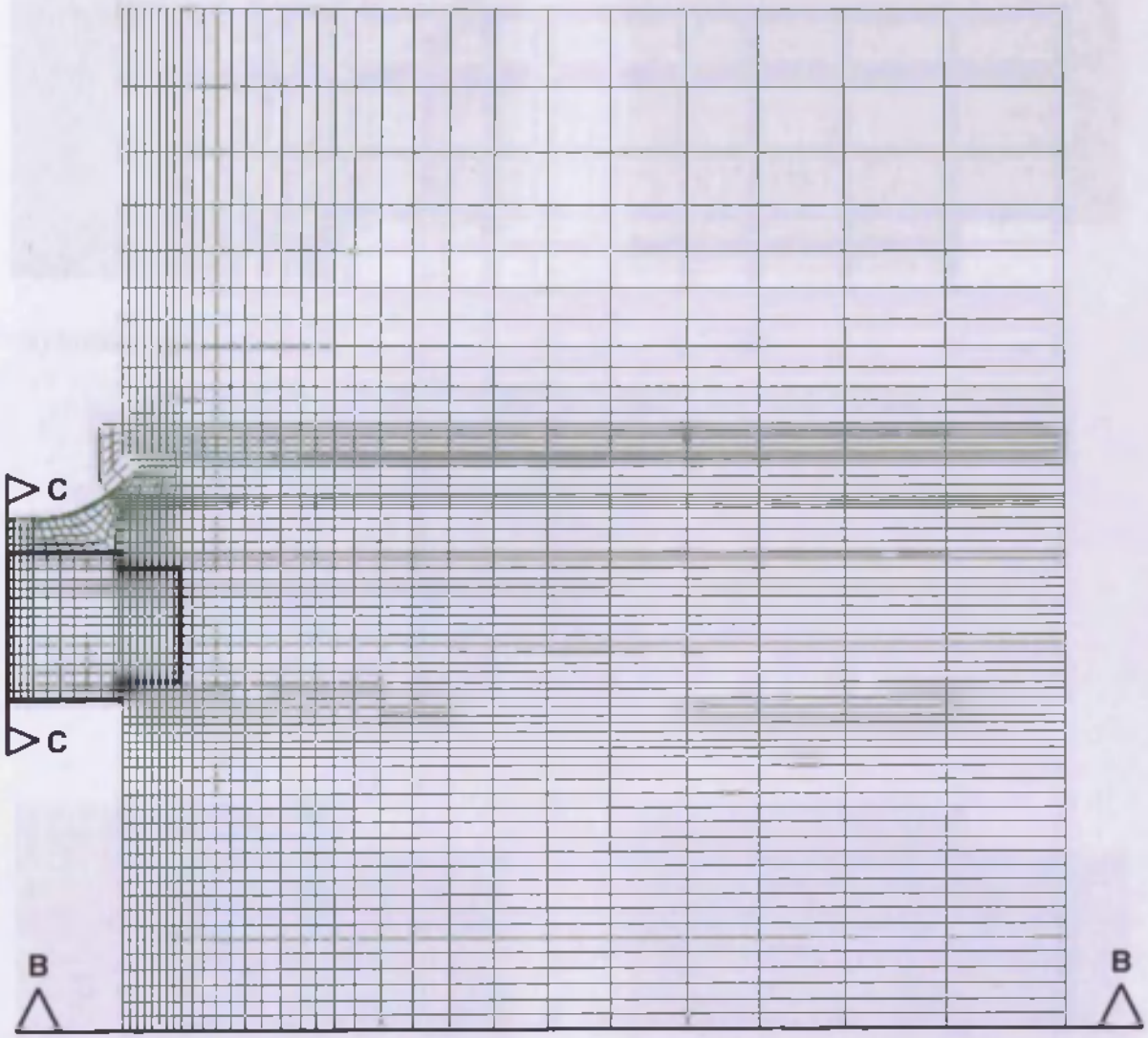

Figure 8.17 Two dimensional axisymmetrical mesh used for the hydraulic analysis of Phase I in the Tunnel Sealing Experiment

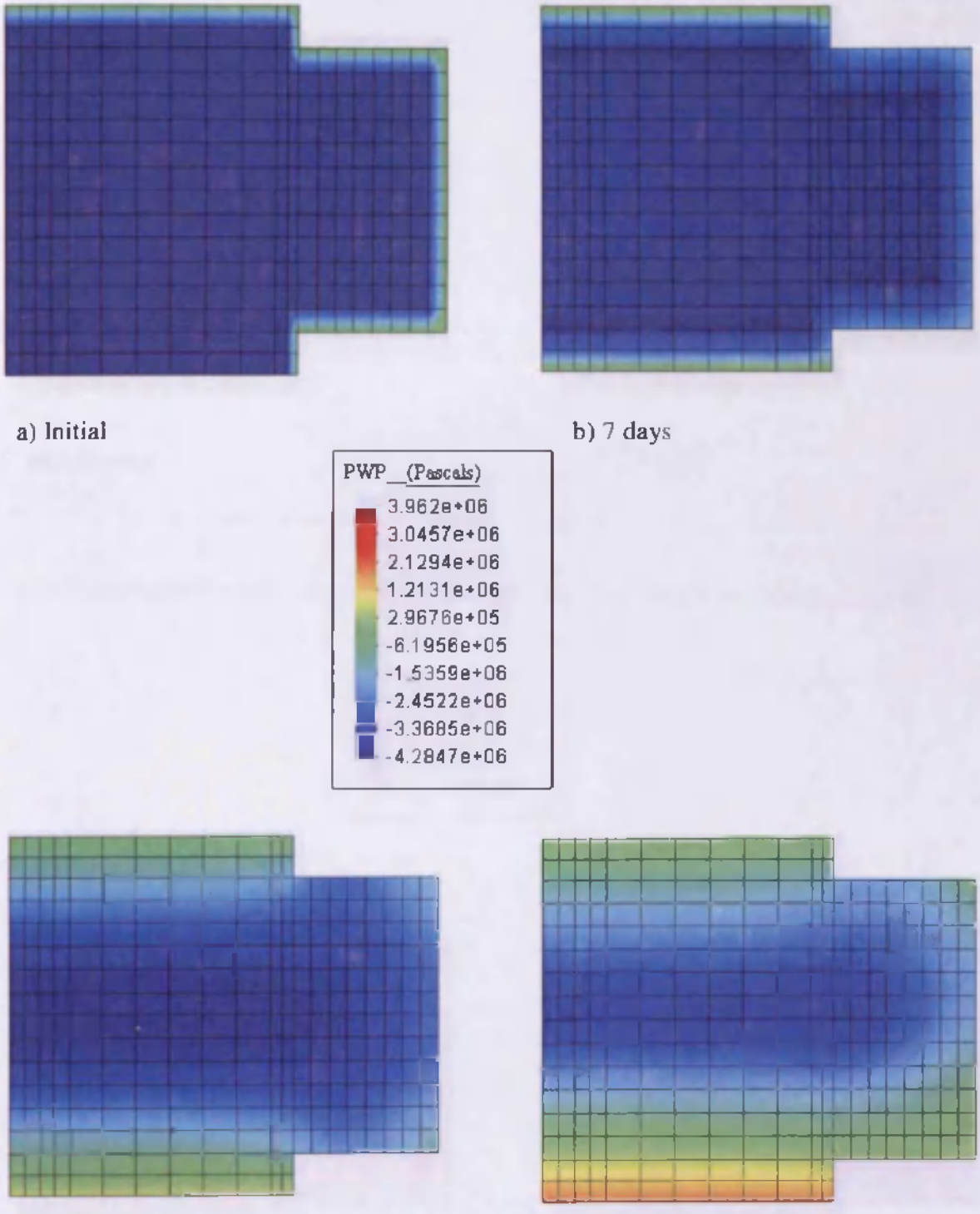

Figure 8.18 Pore water pressure contour plots in the clay bulkhead during Phase 1 from *Analysis_H_1*

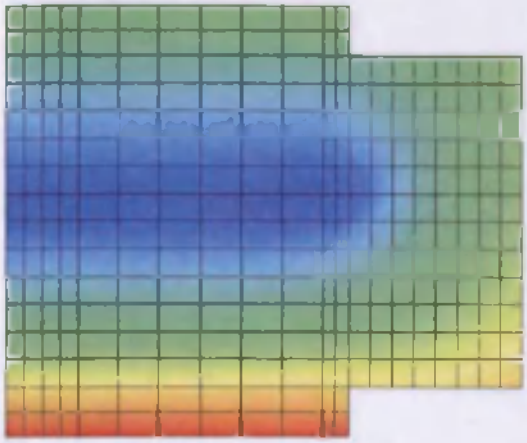

e) 2.6 years

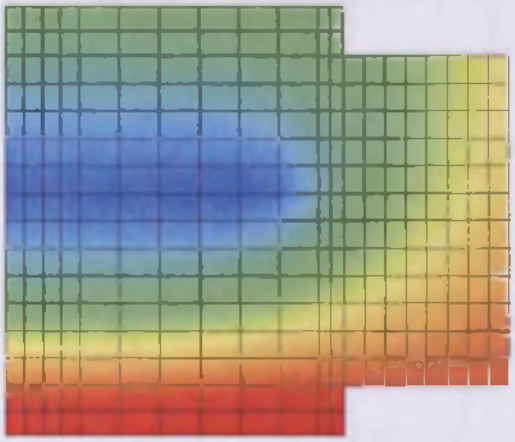

f) 2.8 years

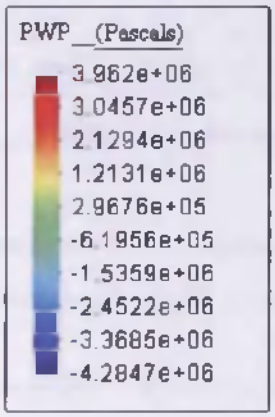

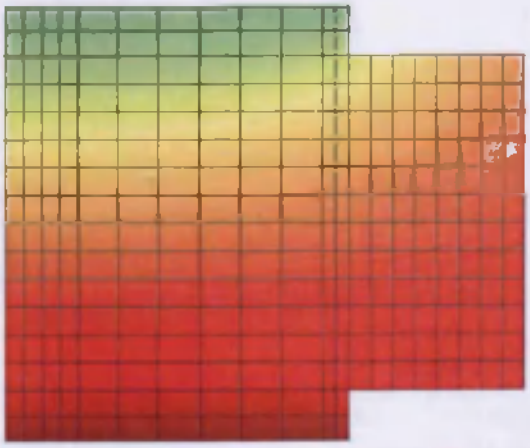

g) 3 years

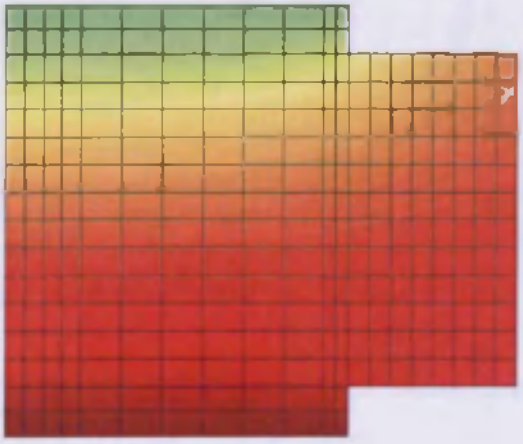

h) 3.5 years

Figure 8.18 (cont.) Pore water pressure contour plots in the clay bulkhead during Phase I from *Analysis_H_1*

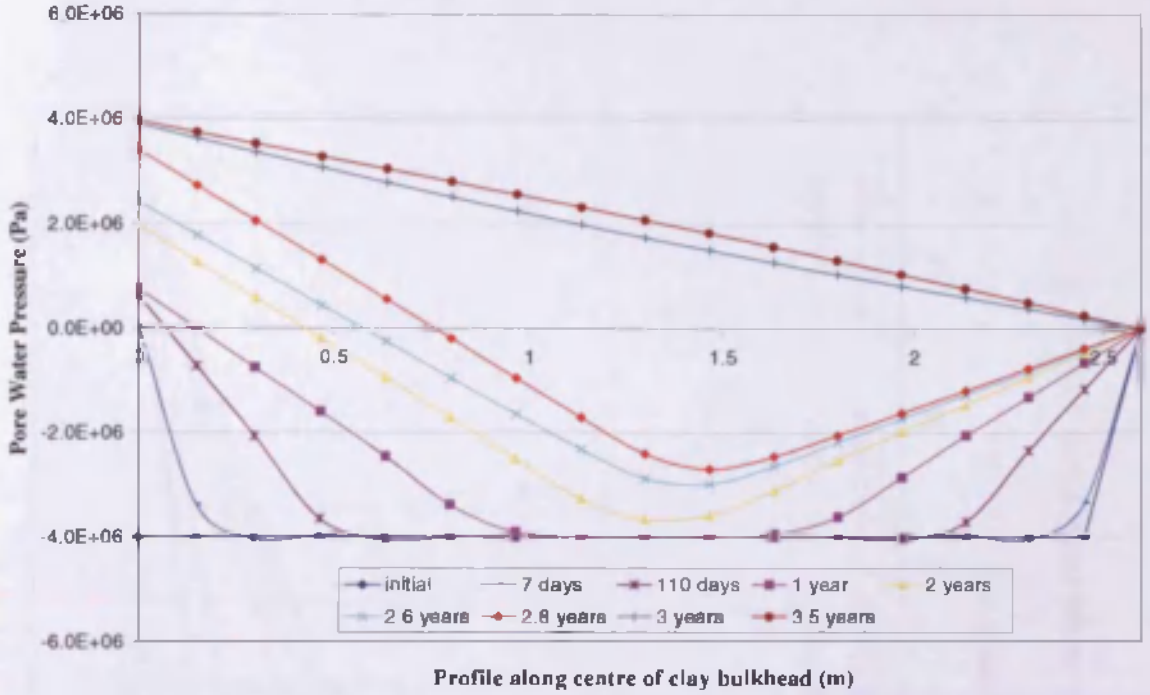

Figure 8.19 Pore Water Pressure profile along the centre line of the clay bulkhead during Phase I from *Analysis_H_1* (section C-C)

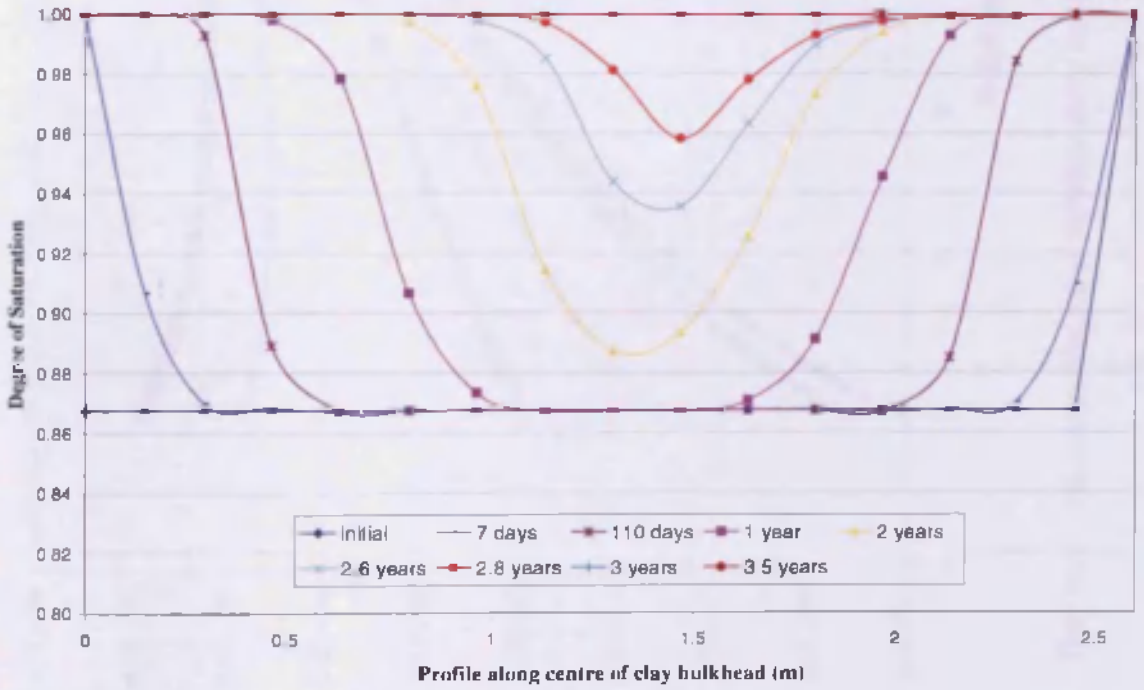

Figure 8.20 Degree of Saturation profile along the centre line of the clay bulkhead during Phase I from *Analysis_H_1* (section C-C)

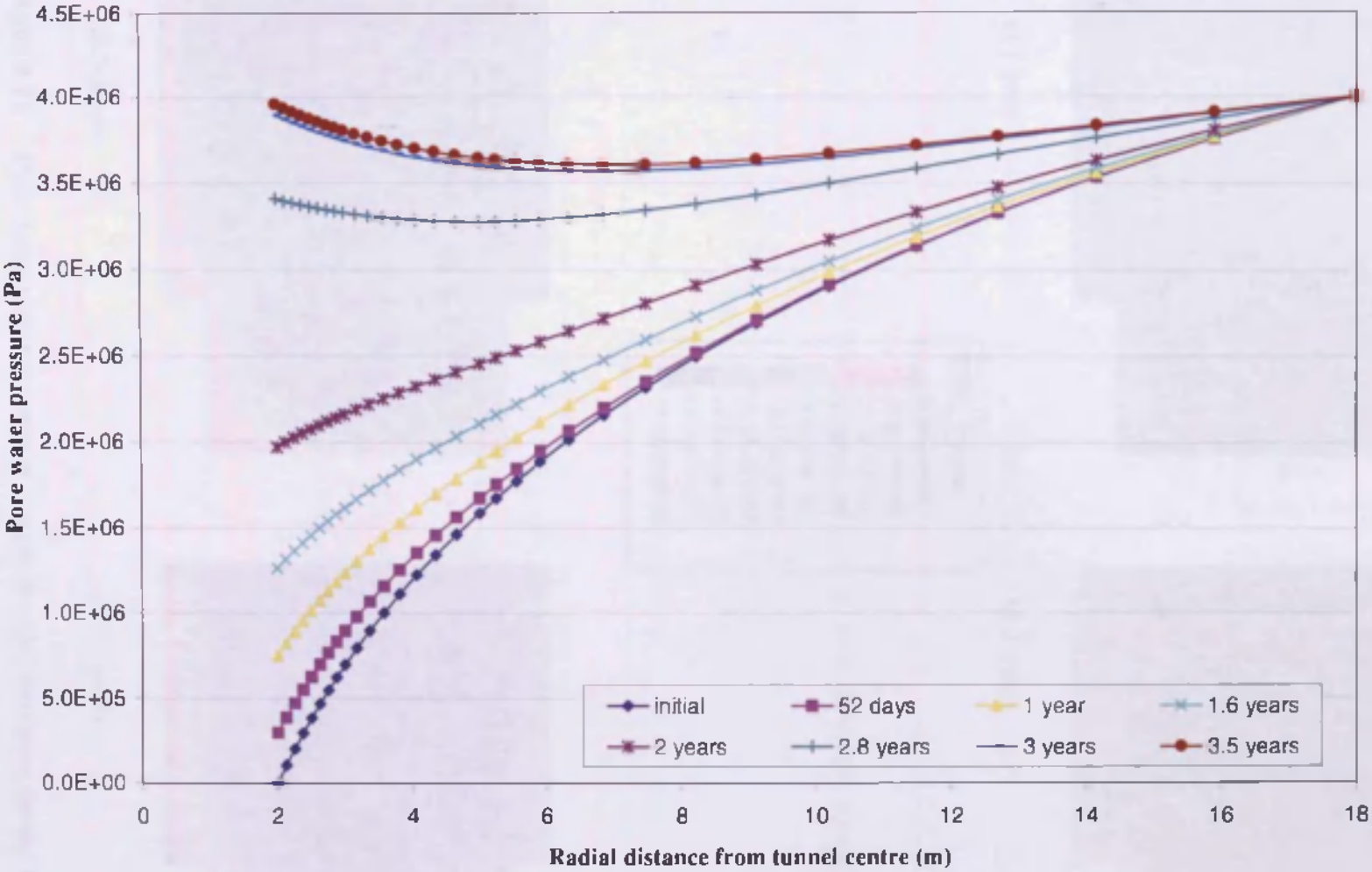

Figure 8.21 Pore water pressure versus radial distance along section B-B in the rock during Phase 1 from *Analysis_H_1*

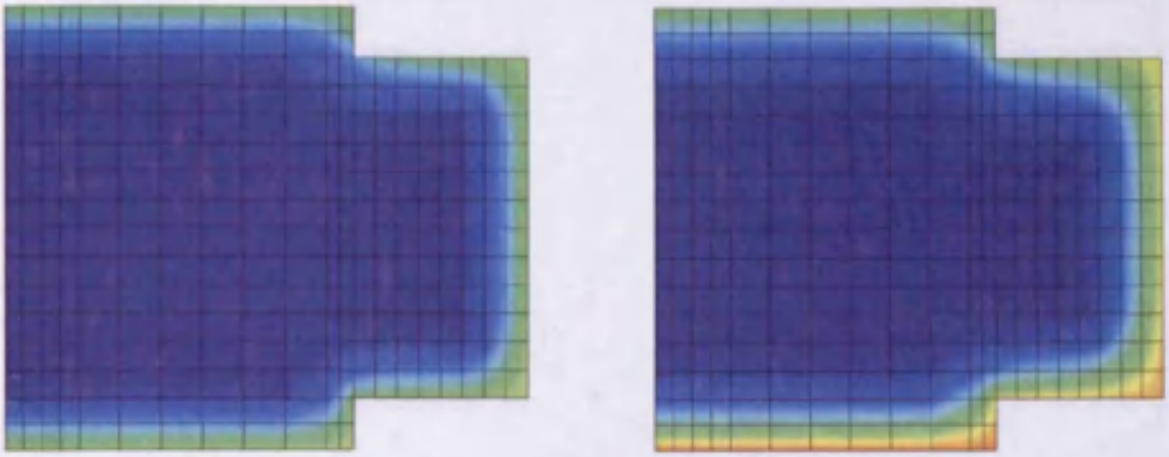

a) 1 year

b) 2 years

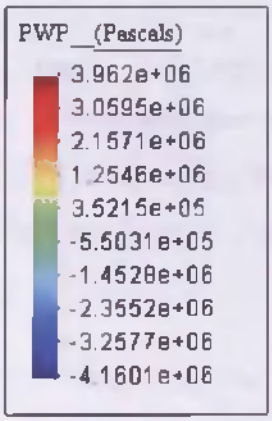

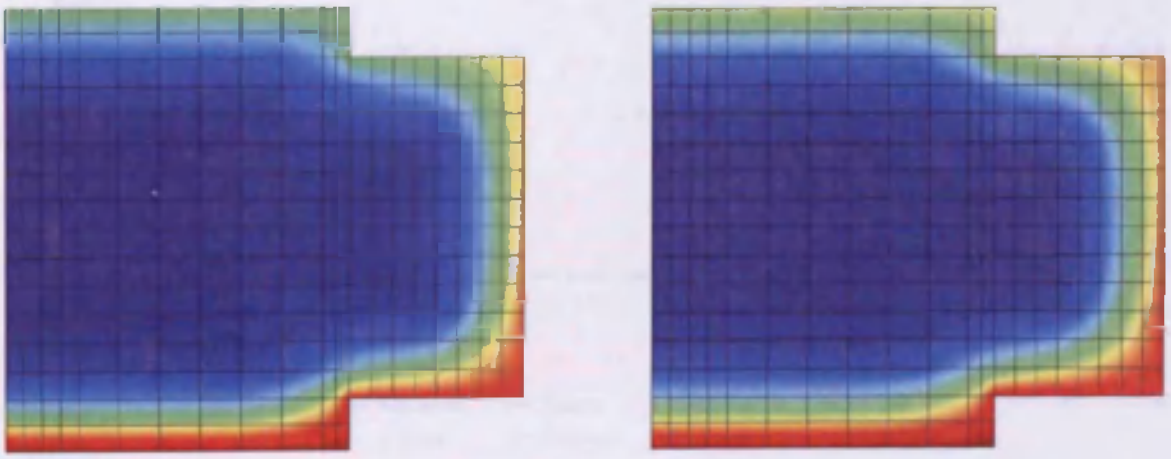

c) 3 years

d) 3.5 years

Figure 8.22 Pore water pressure contour plots in the clay bulkhead during Phase I from *Analysis_H_1* with the micro/macro interaction considered

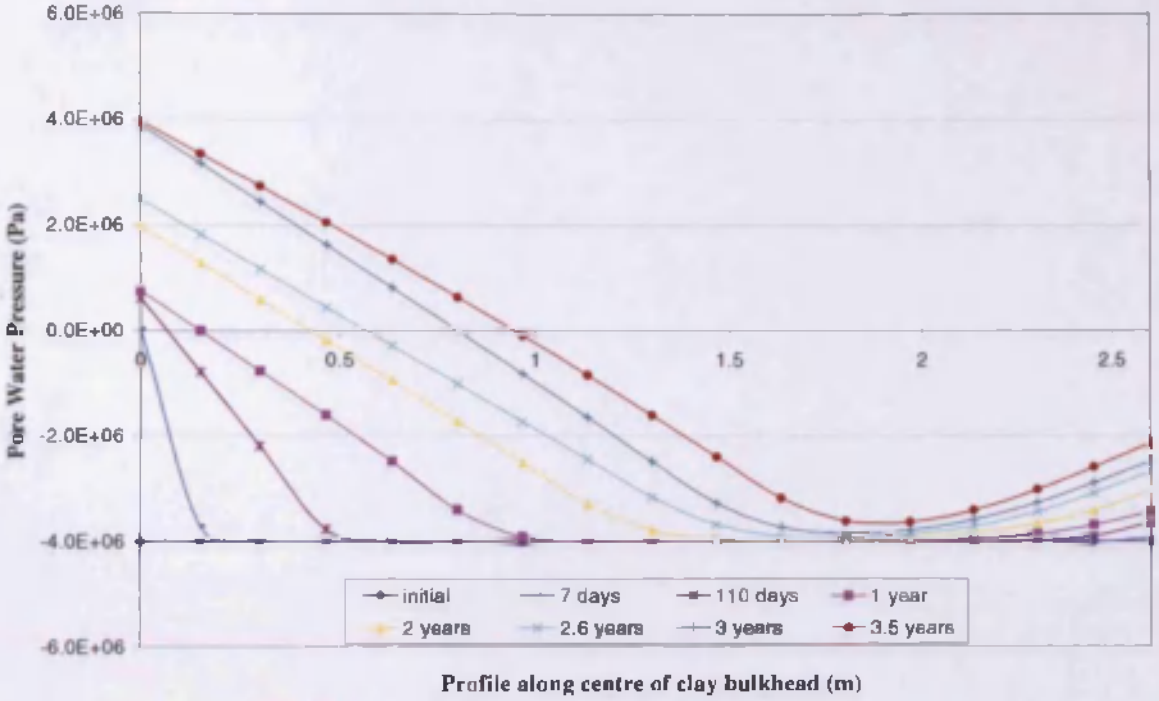

Figure 8.23 Pore Water Pressure profile along the centre line of the clay bulkhead during Phase I from *Analysis_H_2* (section C-C)

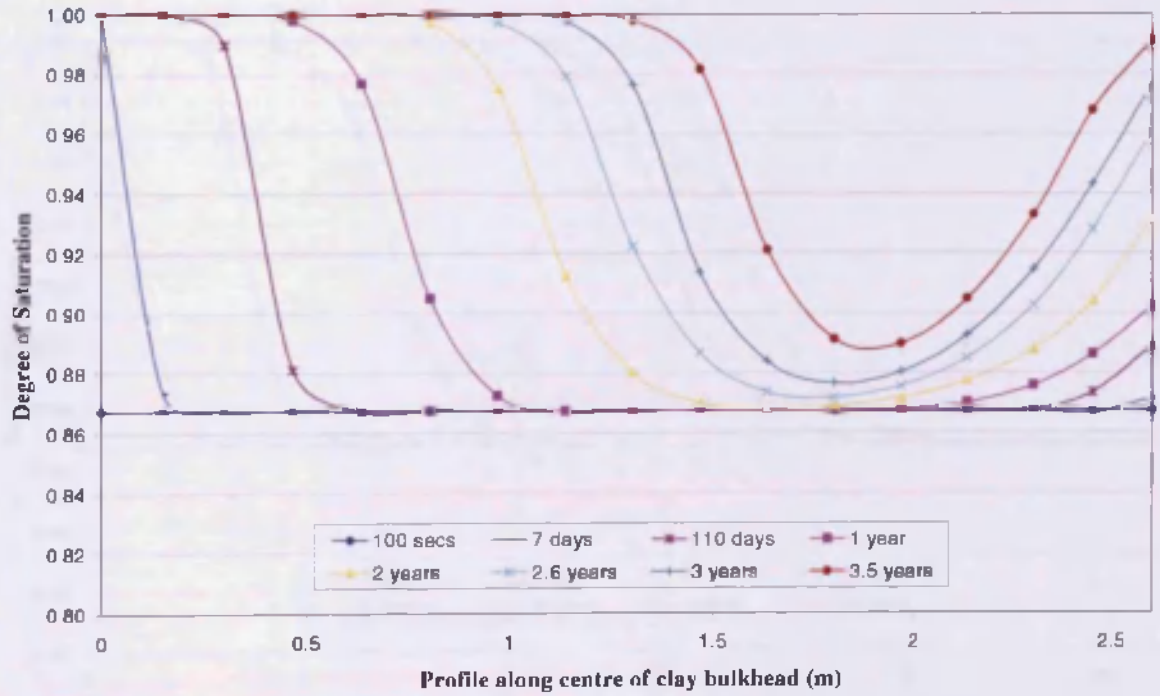

Figure 8.24 Degree of Saturation profile along the centre line of the clay bulkhead during Phase I from *Analysis_H_2* (section C-C)

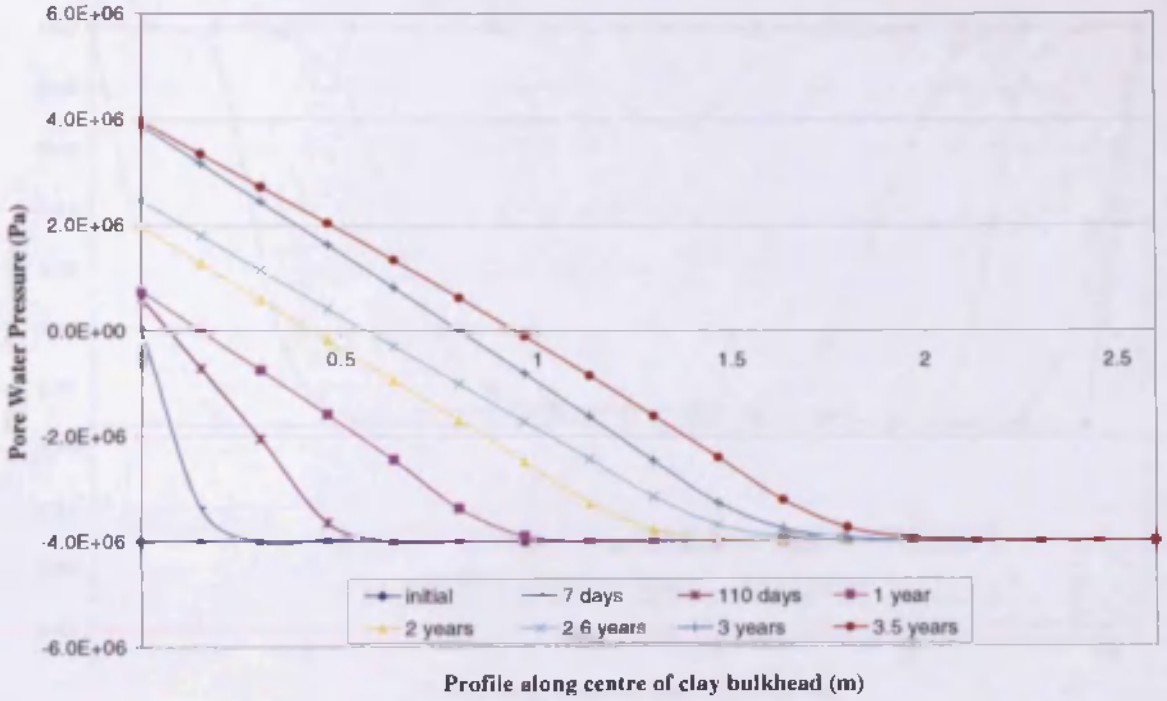

Figure 8.25 Pore Water Pressure profile along the centre line of the clay bulkhead during Phase I from *Analysis_H_3* (section C-C)

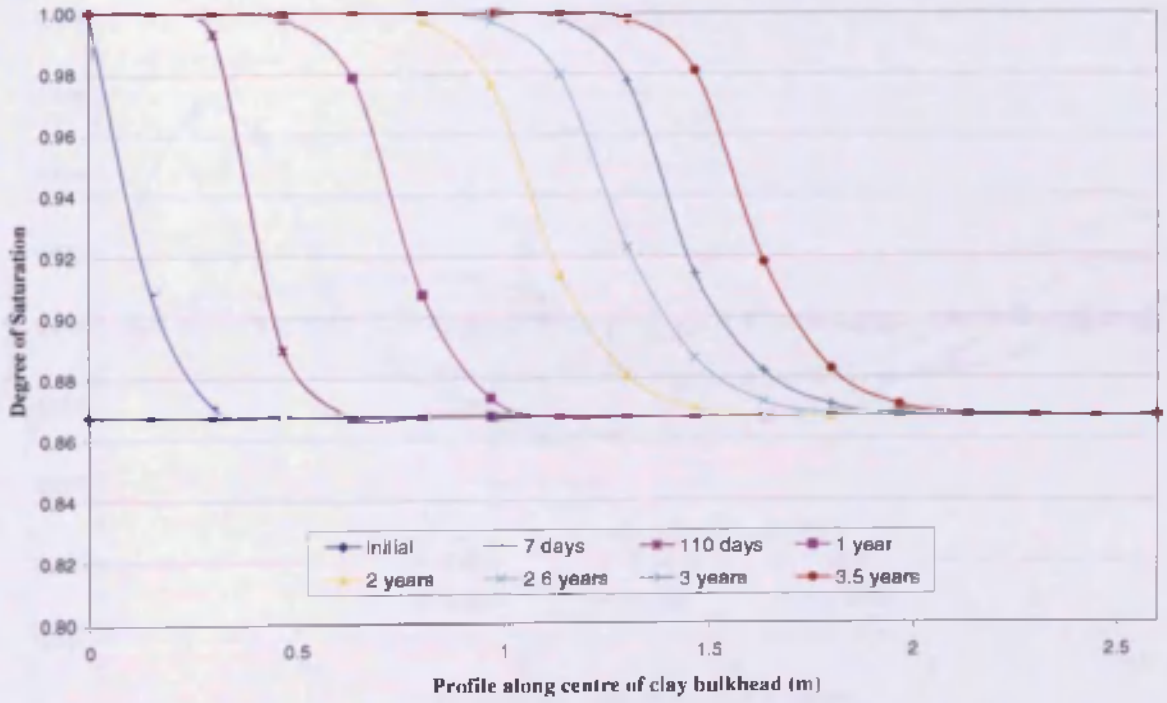

Figure 8.26 Degree of Saturation profile along the centre line of the clay bulkhead during Phase I from *Analysis_H_3* (section C-C)

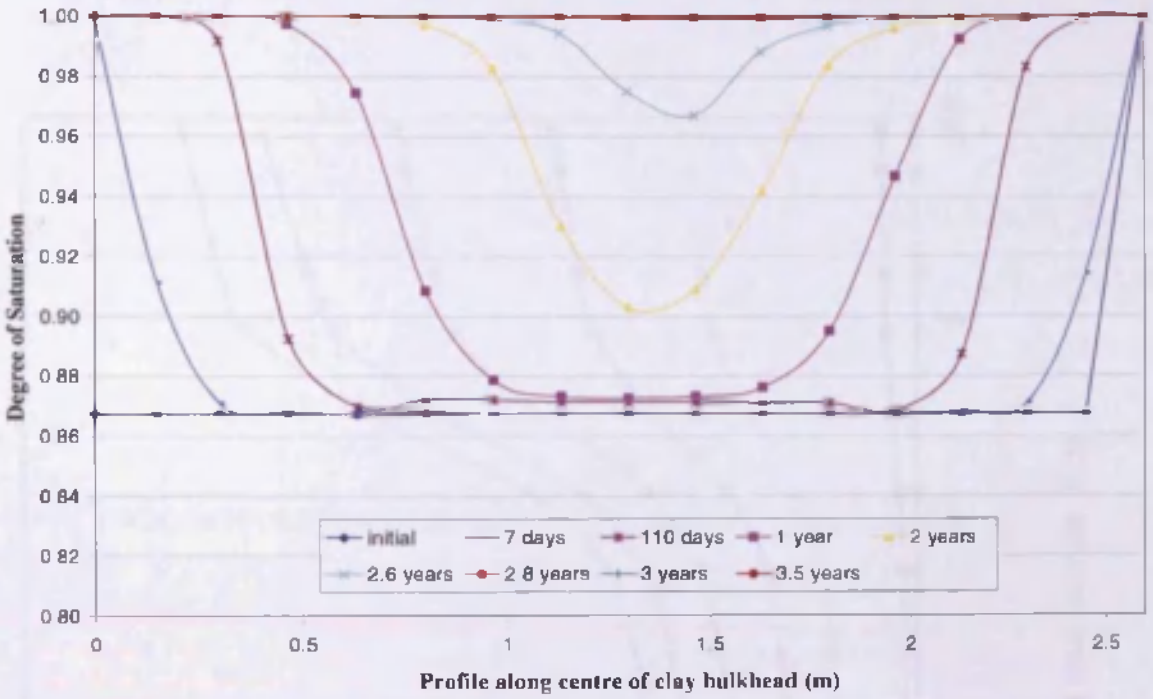

Figure 8.27 Degree of Saturation profile along the centre line of the clay bulkhead during Phase 1 from *Analysis_H-M_1* (section C-C)

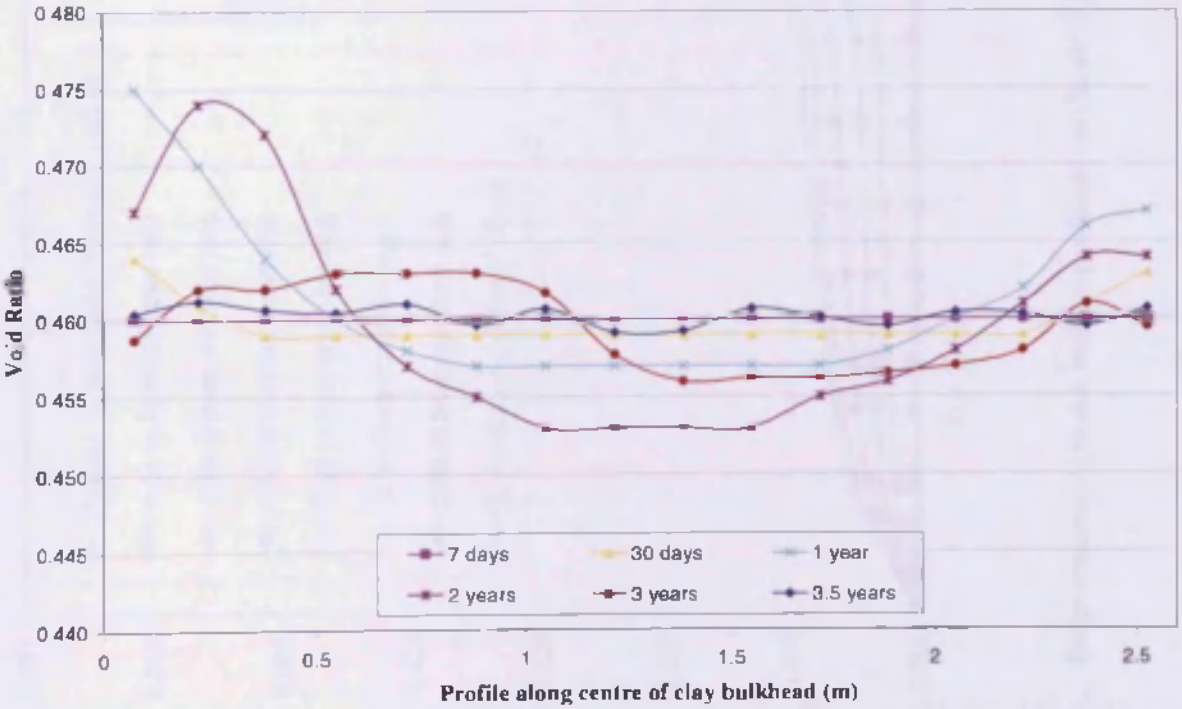

Figure 8.28 Void ratio profile along the centre line of the clay bulkhead during Phase I from *Analysis_H-M_1* (section C-C)

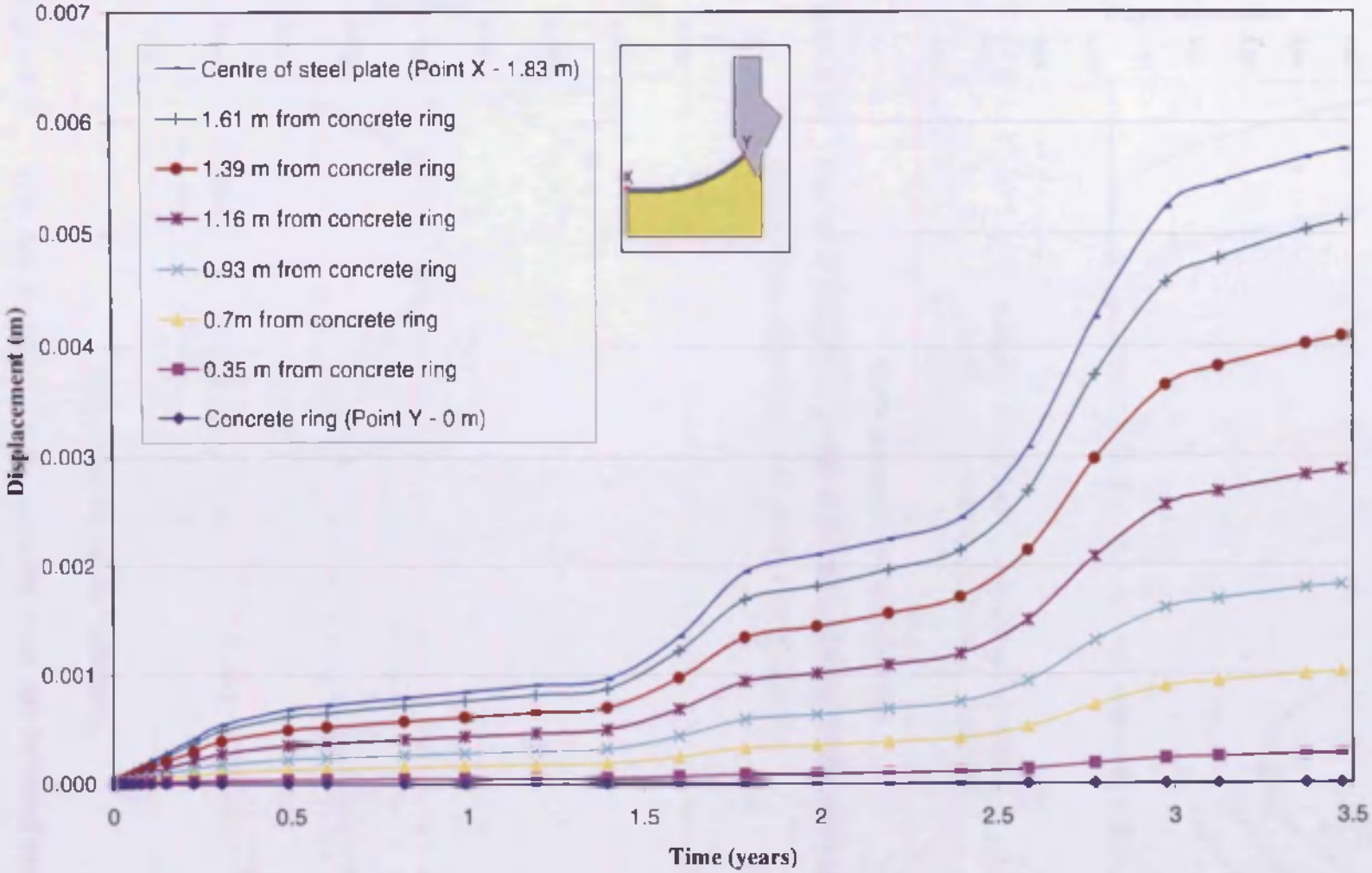

Figure 8.29 Displacement of nodal surface positions on the steel plate during Phase I from *Analysis_H-M_1*

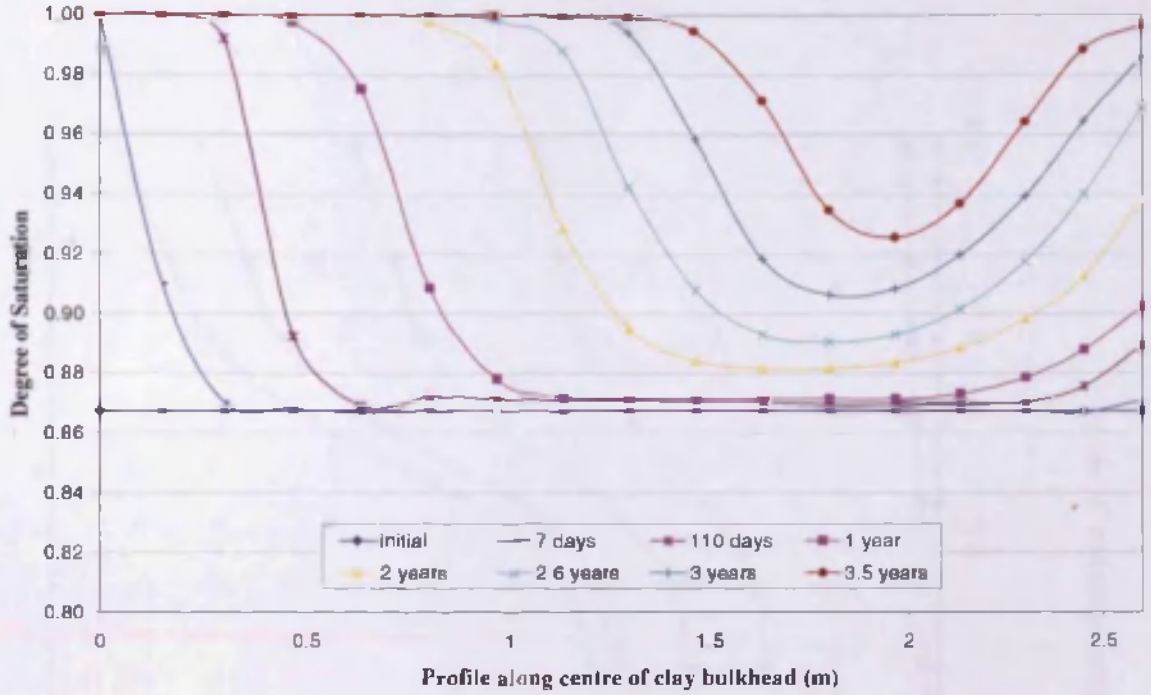

Figure 8.30 Degree of Saturation profile along the centre line of the clay bulkhead during Phase I from *Analysis_H-M_2* (section C-C)

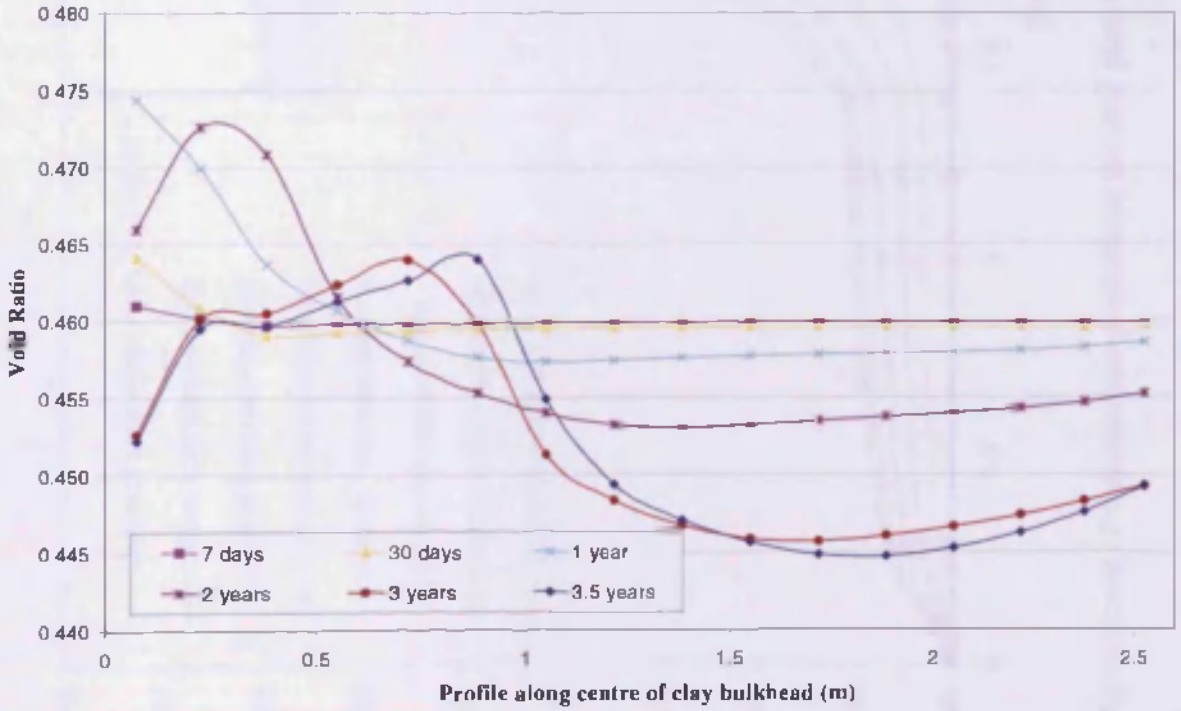

Figure 8.31 Void ratio profile along the centre line of the clay bulkhead during Phase I from *Analysis_H-M_2* (section C-C)

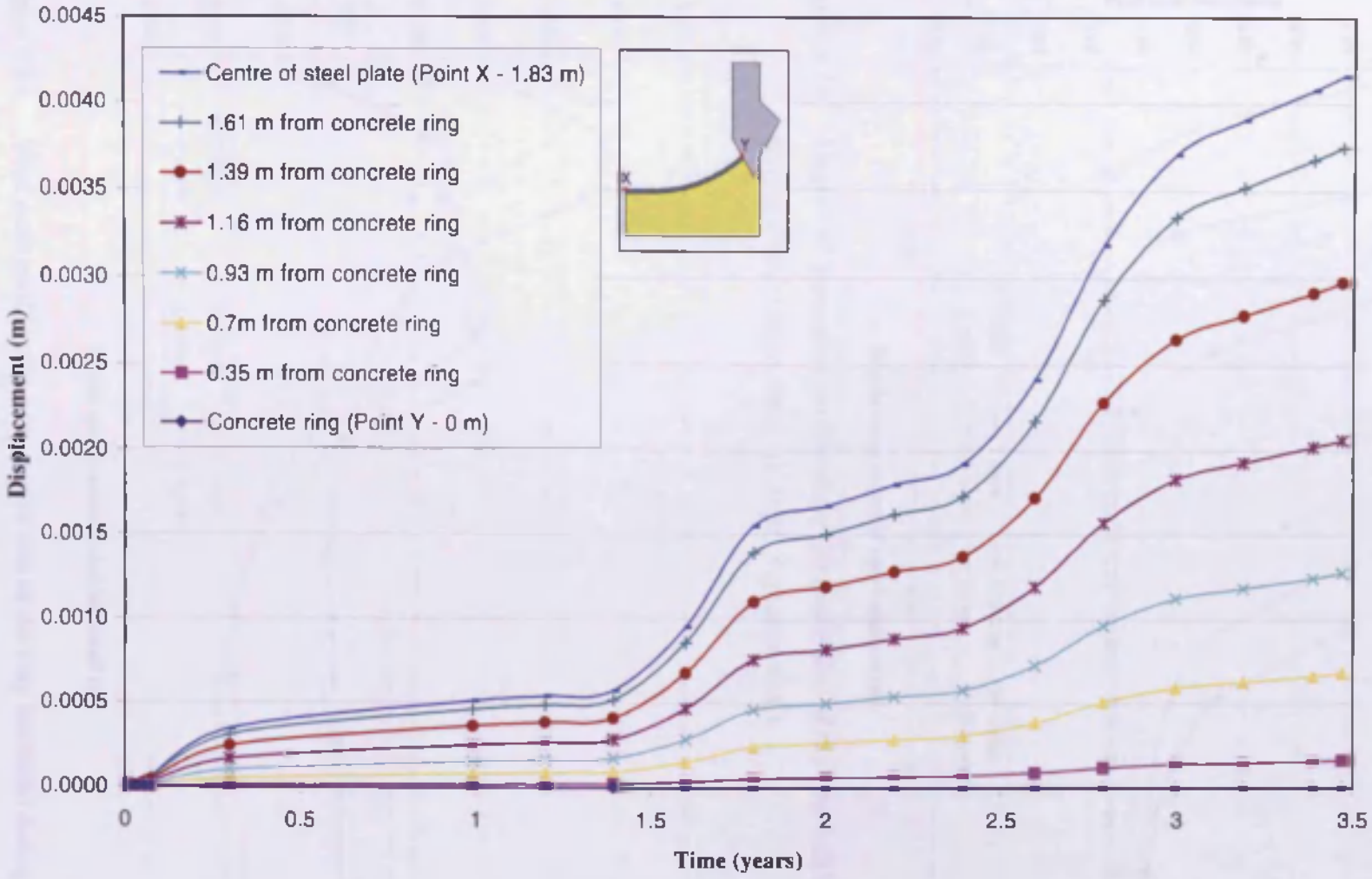

Figure 8.32 Displacement of nodal surface positions on the steel plate during Phase I from *Analysis_H-M_2*

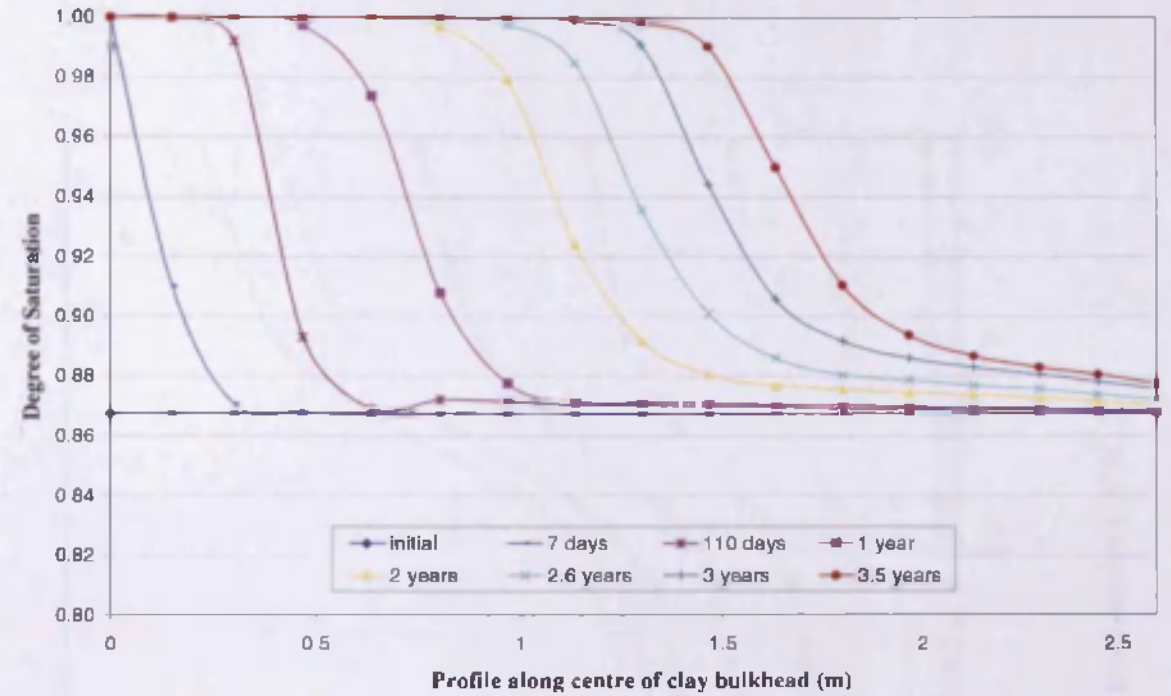

Figure 8.33 Degree of Saturation profile along the centre line of the clay bulkhead during Phase I from *Analysis_H-M_3* (section C-C)

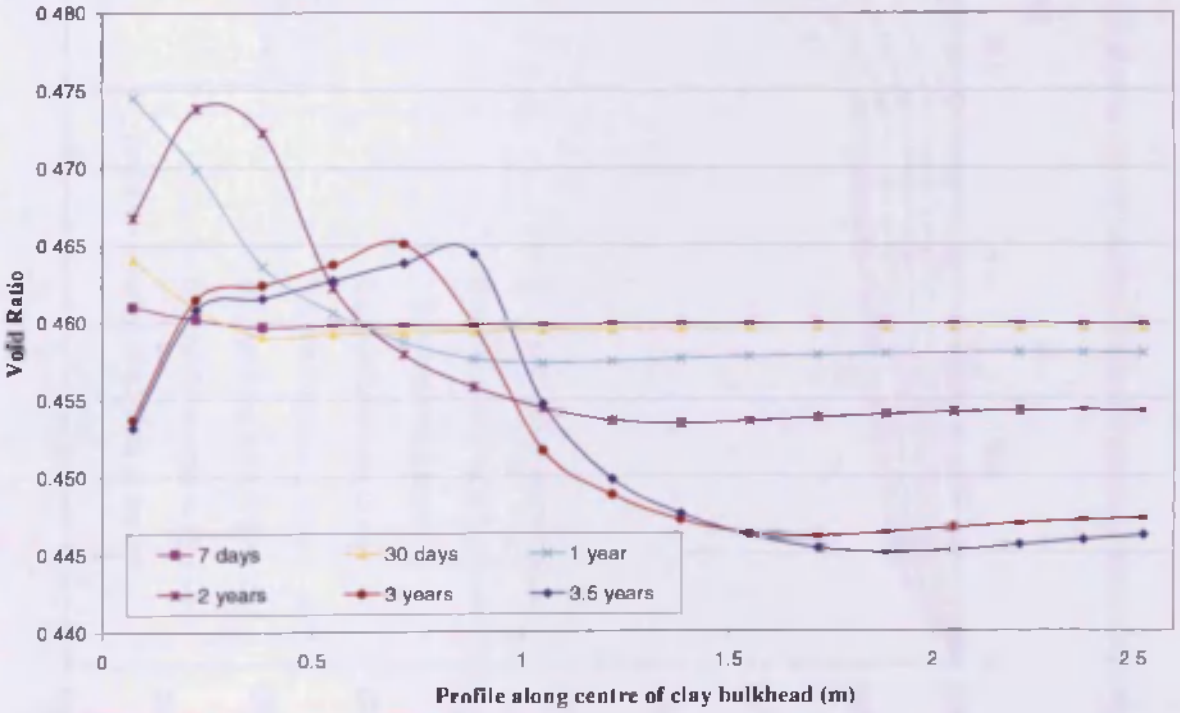

Figure 8.34 Void ratio profile along the centre line of the clay bulkhead during Phase I from *Analysis_H-M_3* (section C-C)

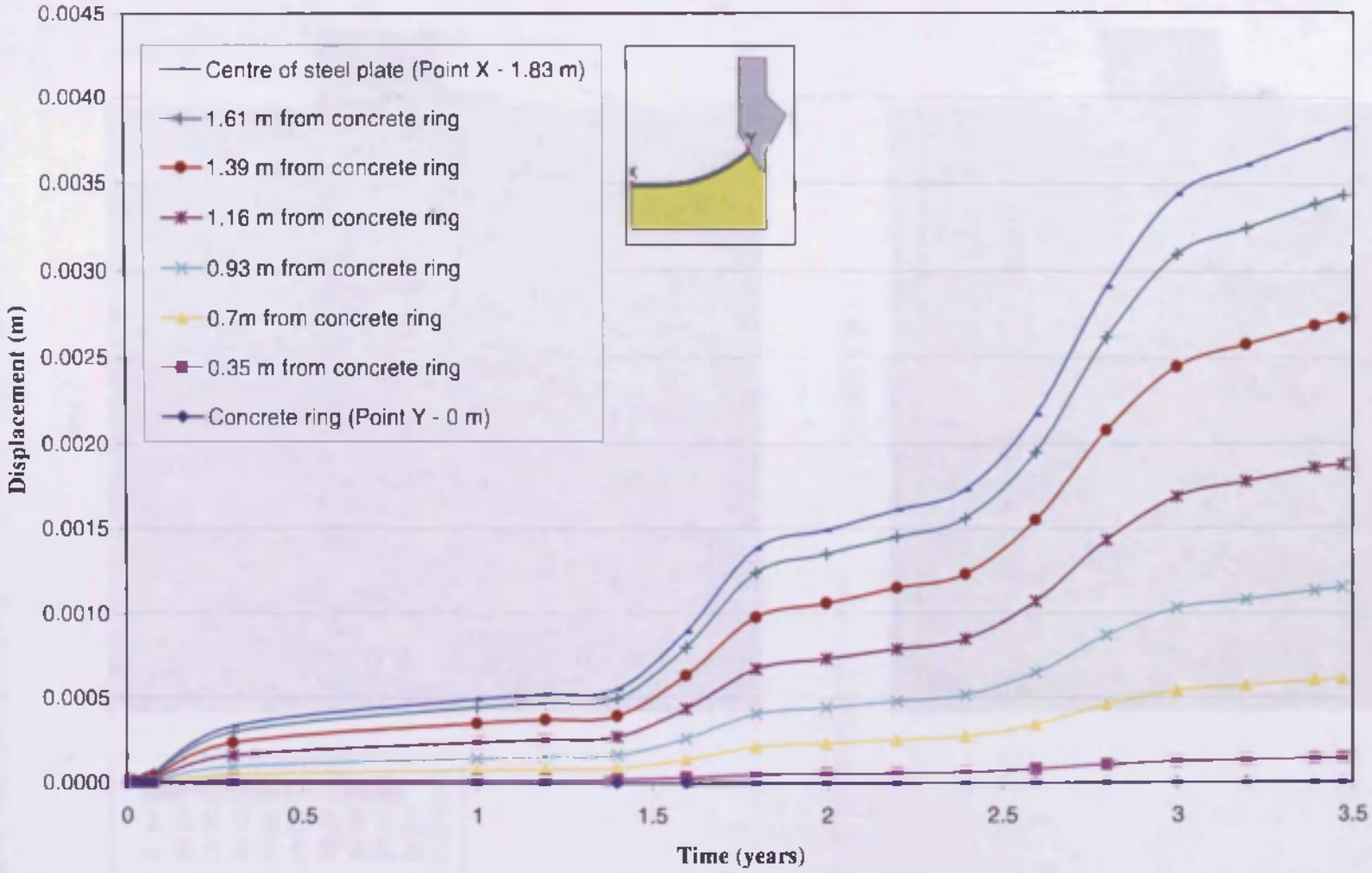

Figure 8.35 Displacement of nodal surface positions on the steel plate during Phase I from *Analysis_H-M_3*

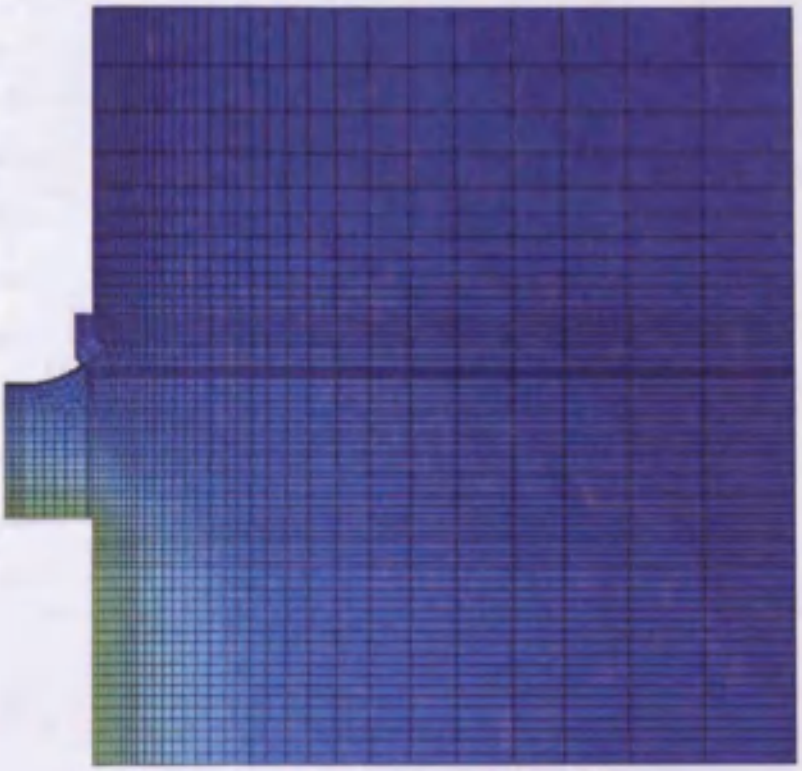

a) 1 year

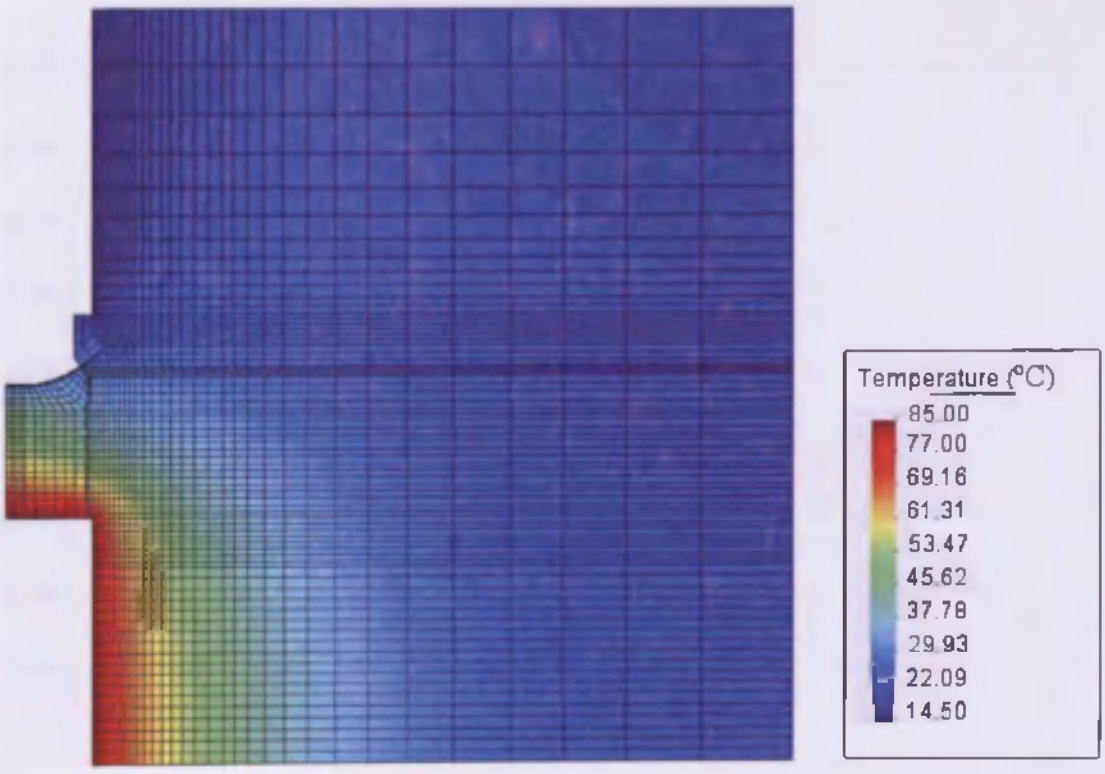

b) 2 years

Figure 8.36 Temperature contour plots in the Tunnel Sealing Experiment for the Thermal analysis of Phase II

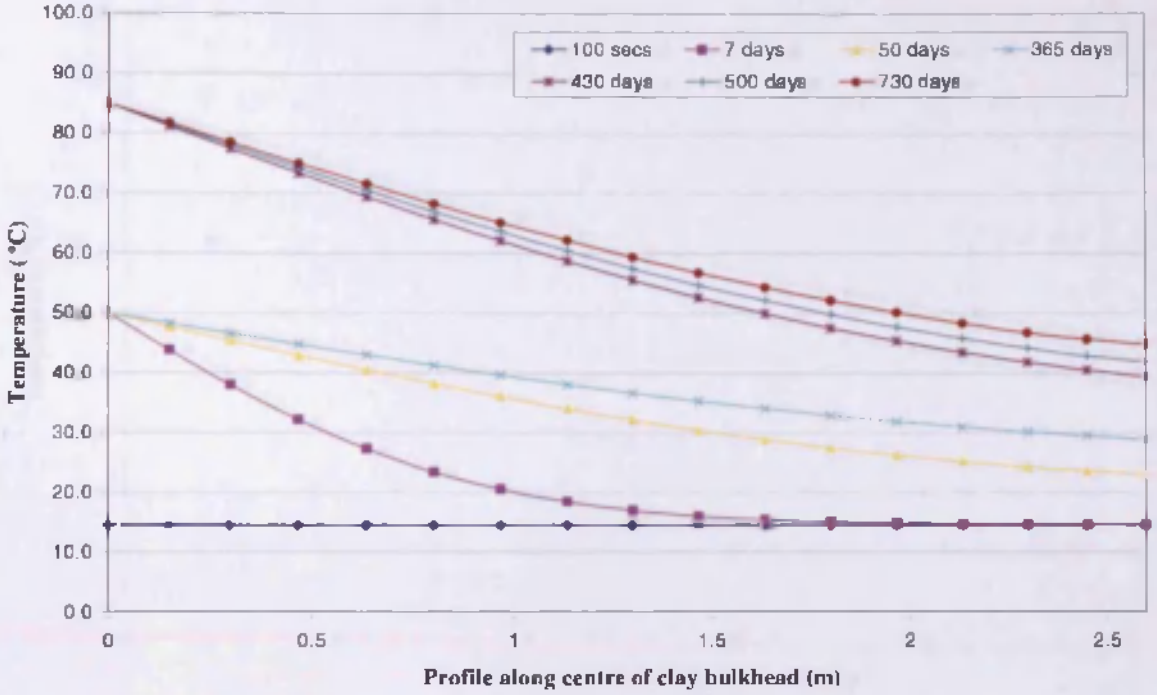

Figure 8.37 Temperature profile through the centre line of the clay bulkhead for the Thermal analysis of Phase II (section C-C)

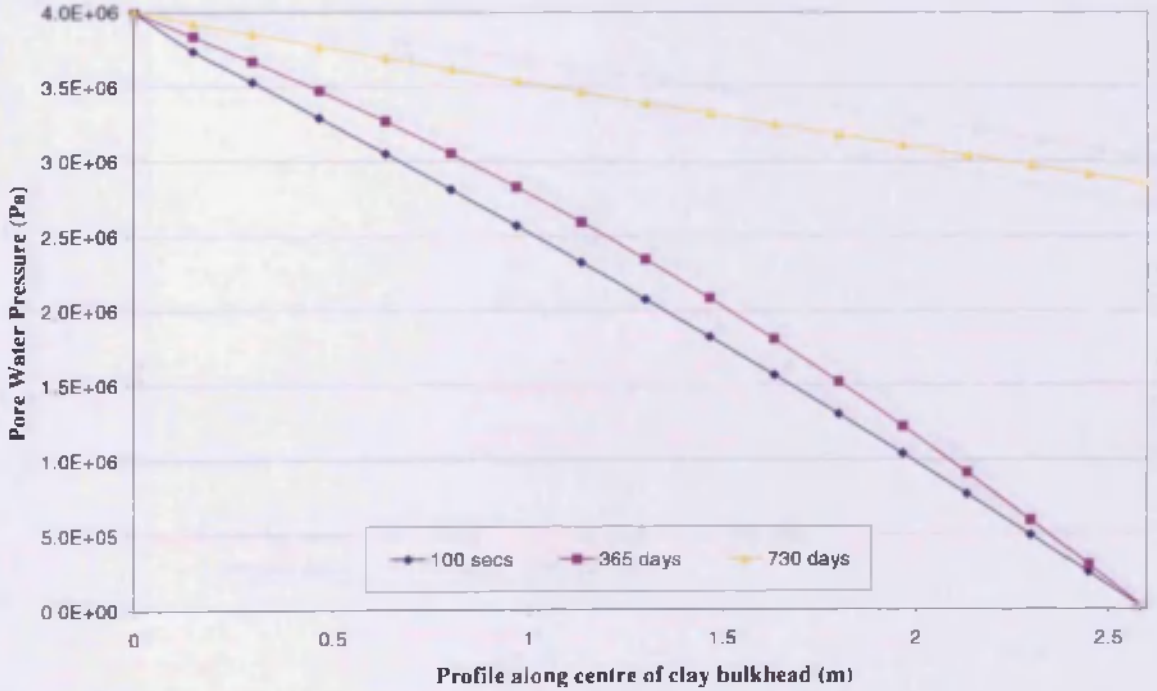

Figure 8.38 Pore water pressure profile through the centre line of the clay bulkhead for the Hydraulic analysis of Phase II (section C-C)

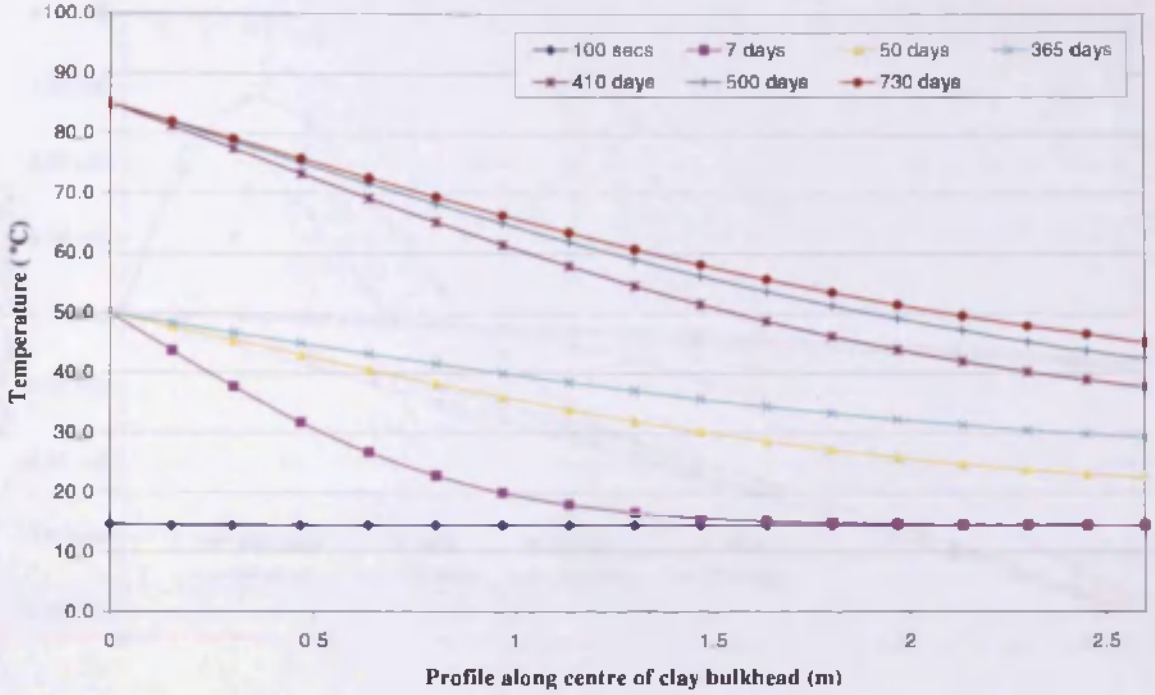

Figure 8.39 Temperature profile through the centre line of the clay bulkhead for the Thermal-Hydraulic analysis of Phase II (section C-C)

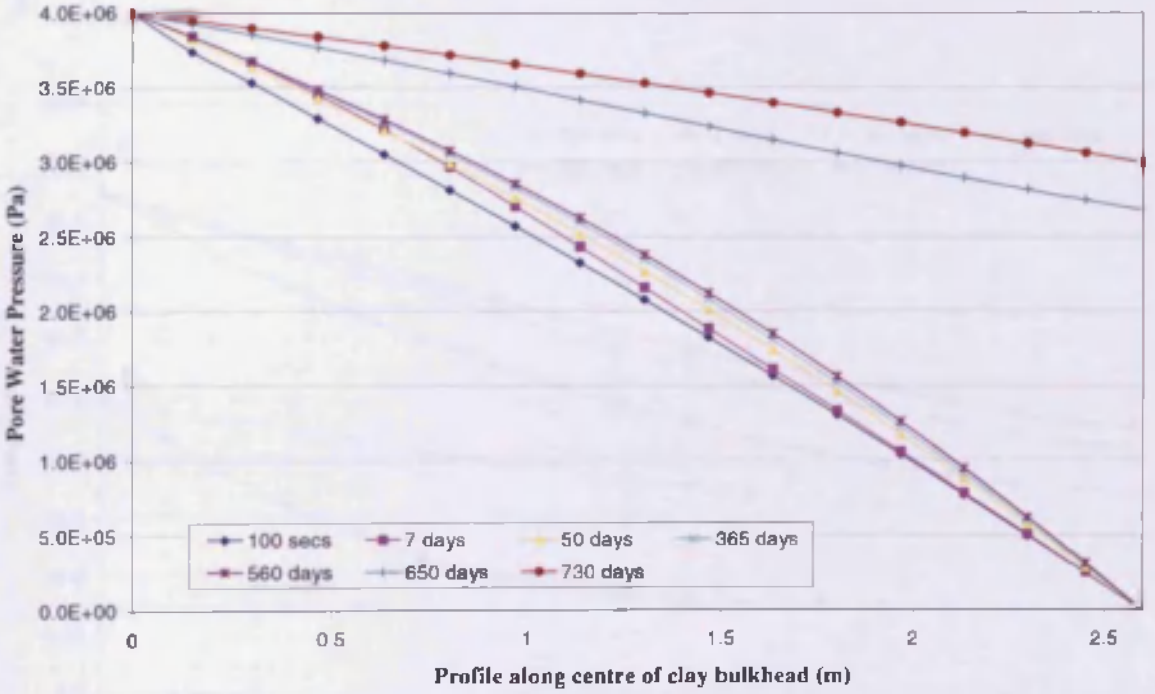

Figure 8.40 Pore water pressure profile through the centre line of the clay bulkhead for the Thermal-Hydraulic analysis of Phase II with the thermal expansion of water not taken into consideration (section C-C)

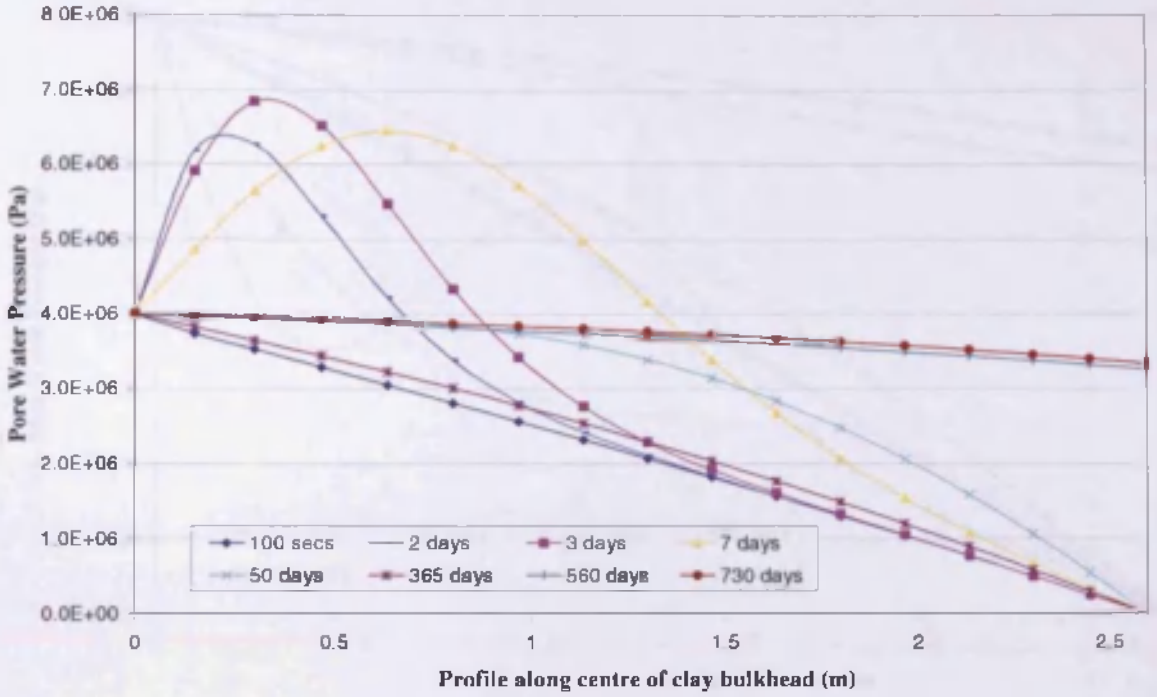

Figure 8.41 Pore water pressure profile through the centre line of the clay bulkhead for the Thermal-Hydraulic analysis of Phase II with the thermal expansion of water taken into consideration (section C-C)

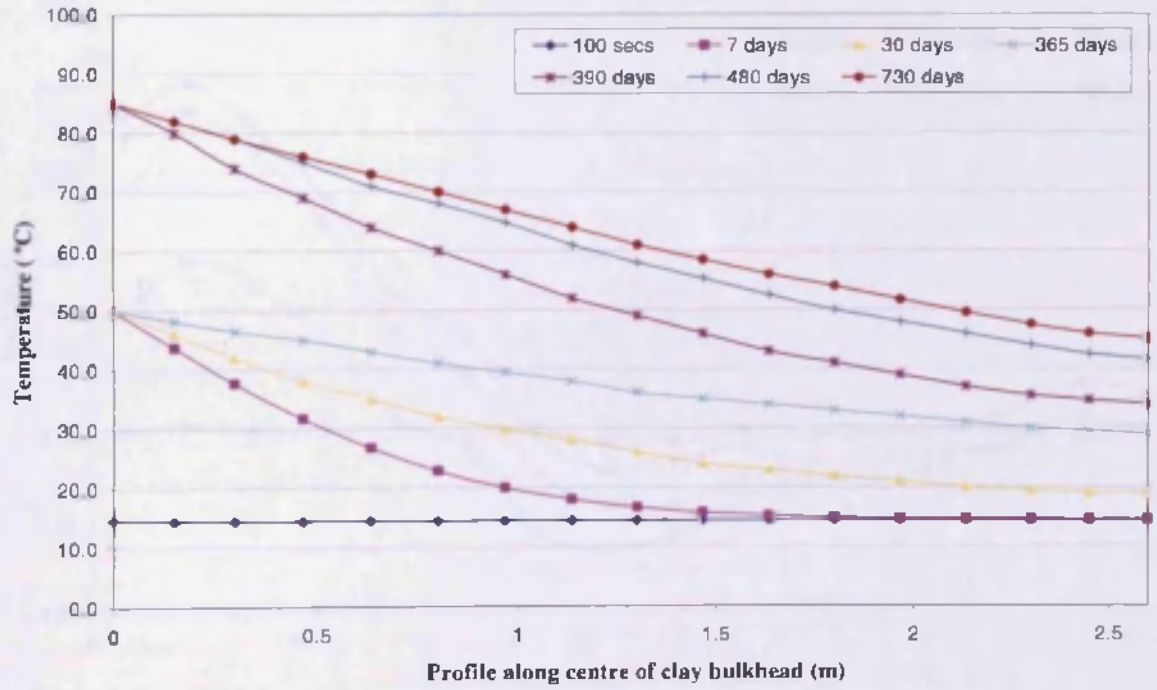

Figure 8.42 Temperature profile through the centre line of the clay bulkhead for the Thermal-Hydraulic-Mechanical analysis of Phase II (section C-C)

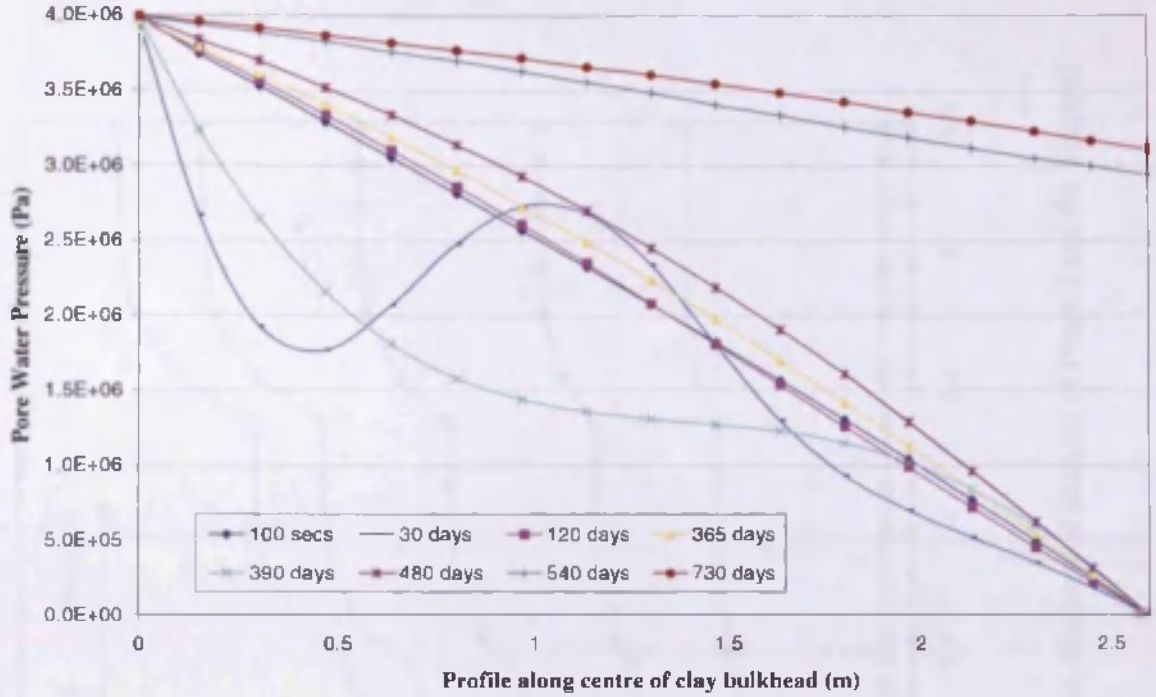

Figure 8.43 Pore water pressure profile through the centre line of the clay bulkhead for the Thermal-Hydraulic-Mechanical analysis of Phase II with the thermal expansion of water taken into consideration (section C-C)

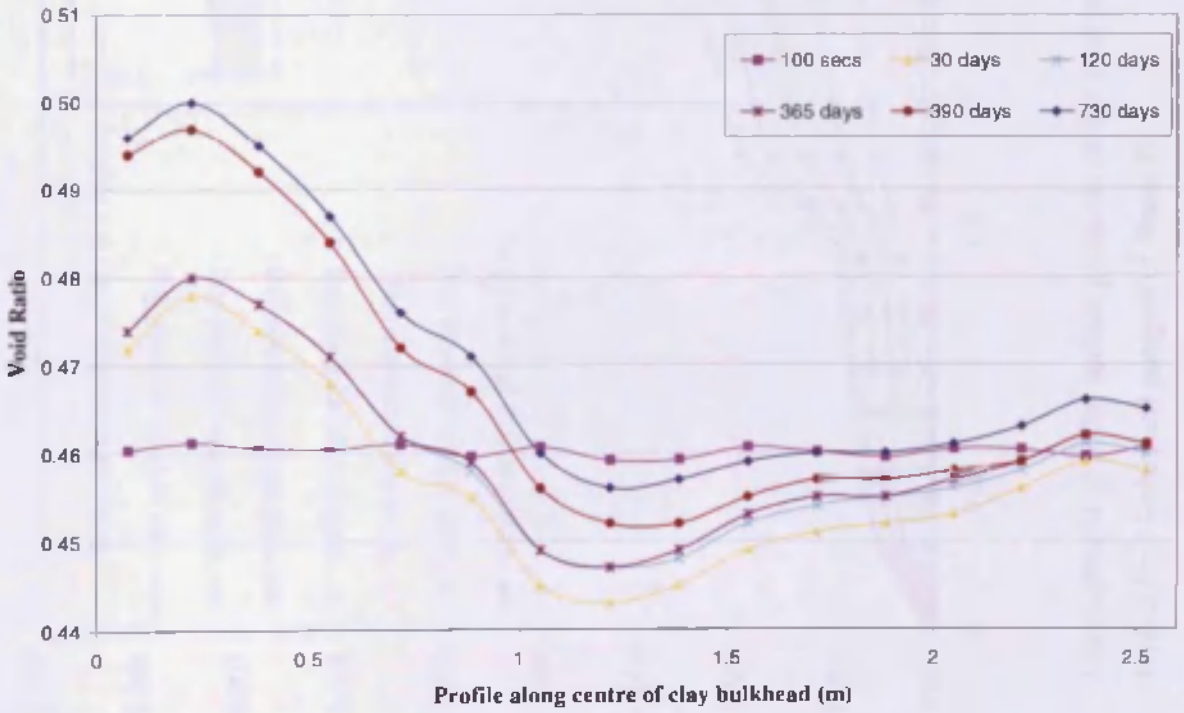

Figure 8.44 Void ratio profile along the centre line of the clay bulkhead for the Thermal-Hydraulic-Mechanical analysis of Phase II (section C-C)

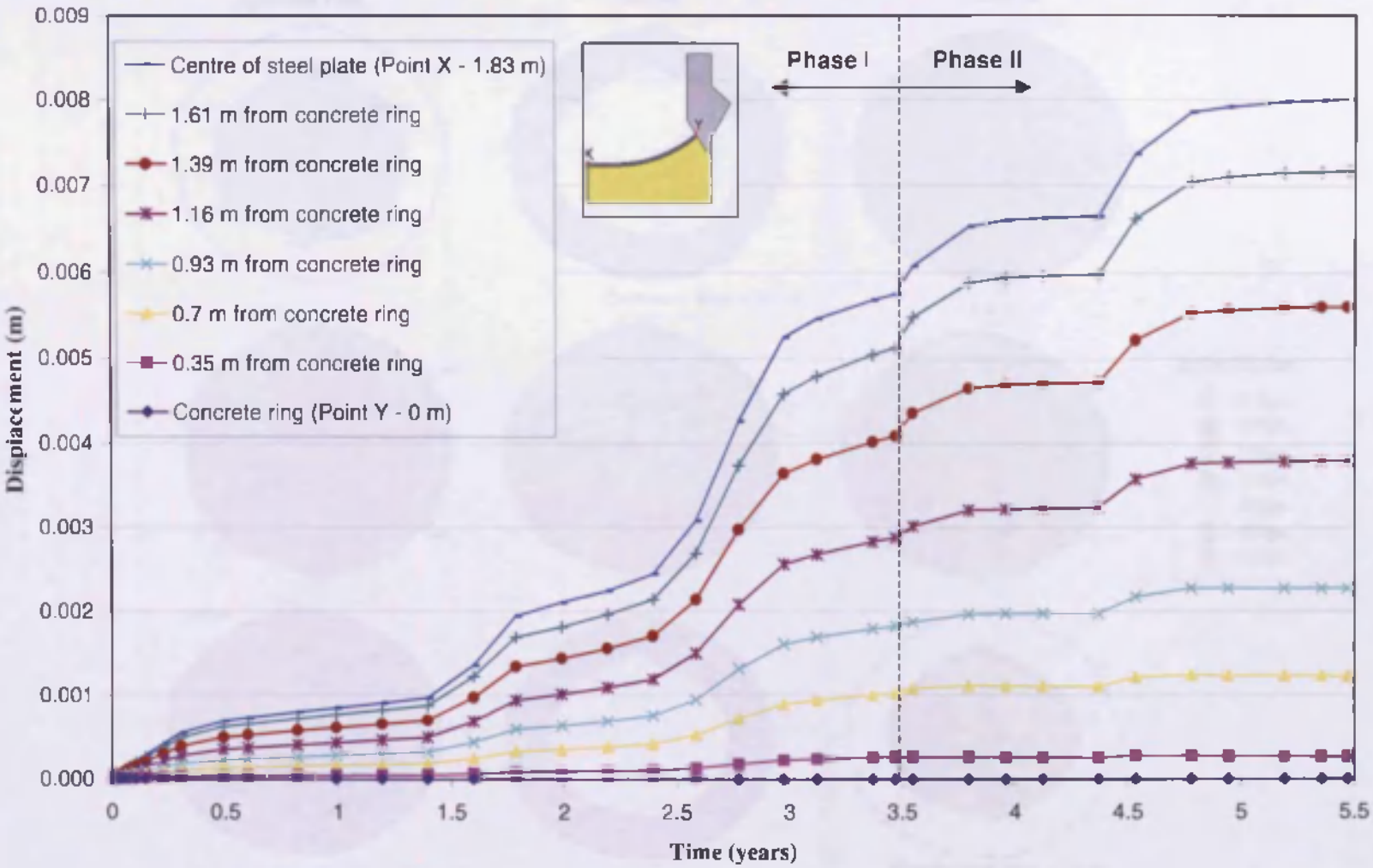

Figure 8.45 Displacement of nodal surface positions on the steel plate for the Hydraulic-Mechanical analysis of Phase I and the Thermal-Hydraulic-Mechanical analysis of Phase II

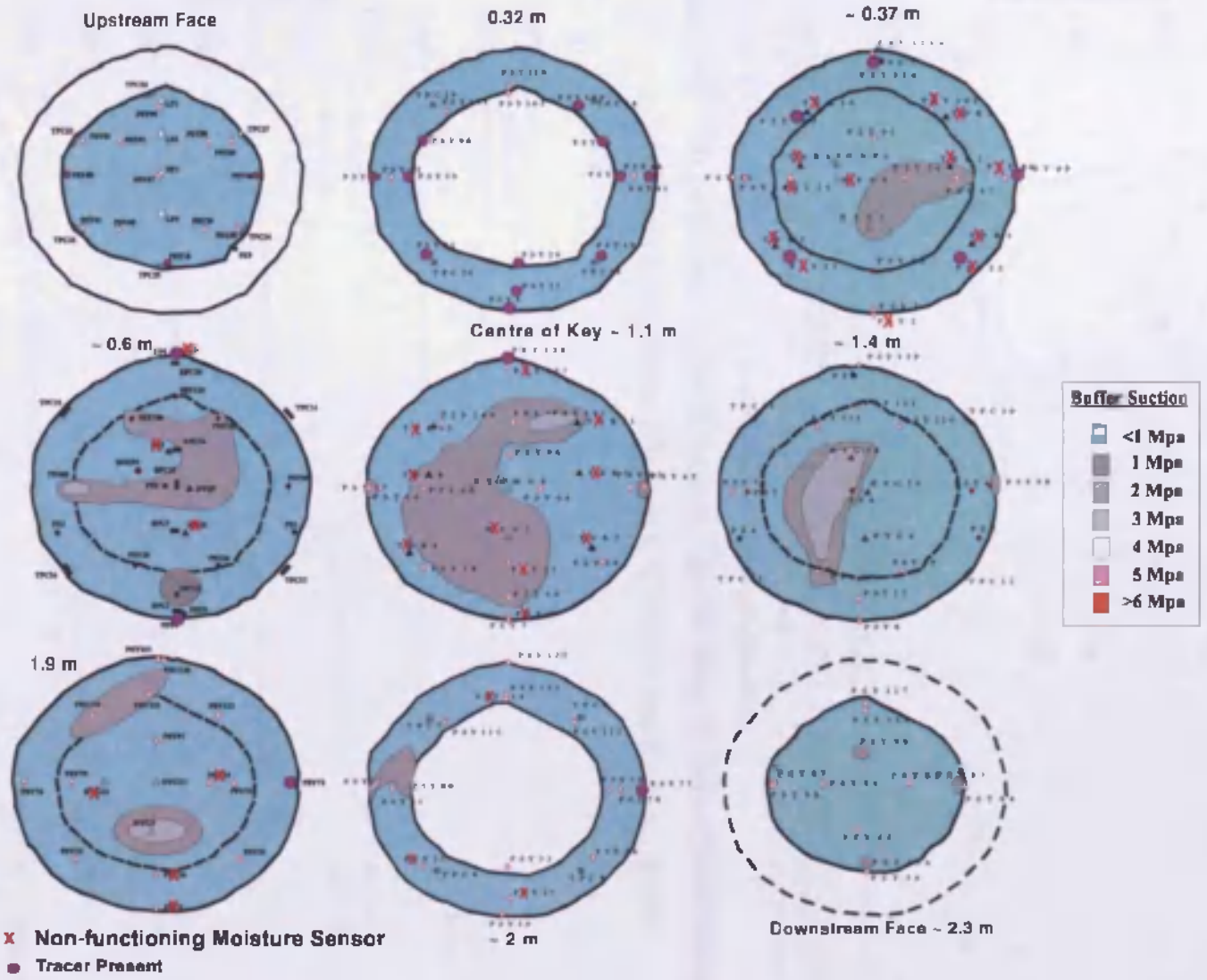

Figure 8.46 Experimental suction profiles within the clay bulkhead after approximately 3 years (AECL, 2001)

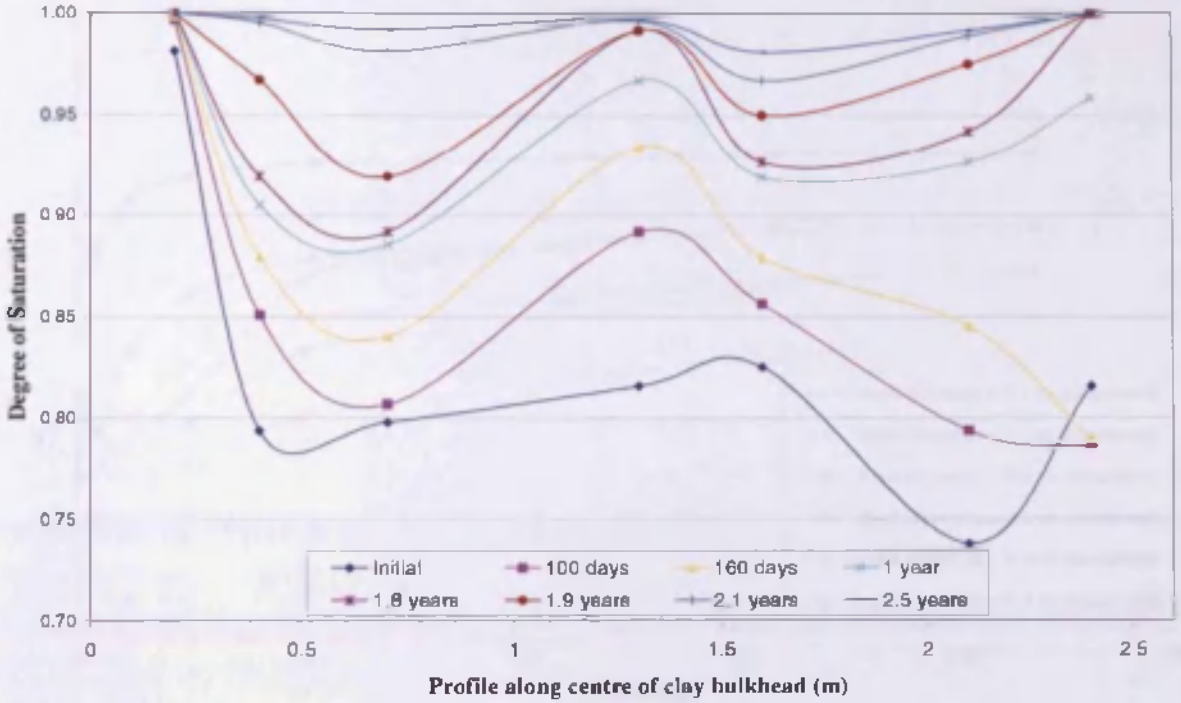

Figure 8.47 Experimental Degree of Saturation profile along the centre line of the clay bulkhead during Phase I (section C-C) (after Chandler et al., 2002b)

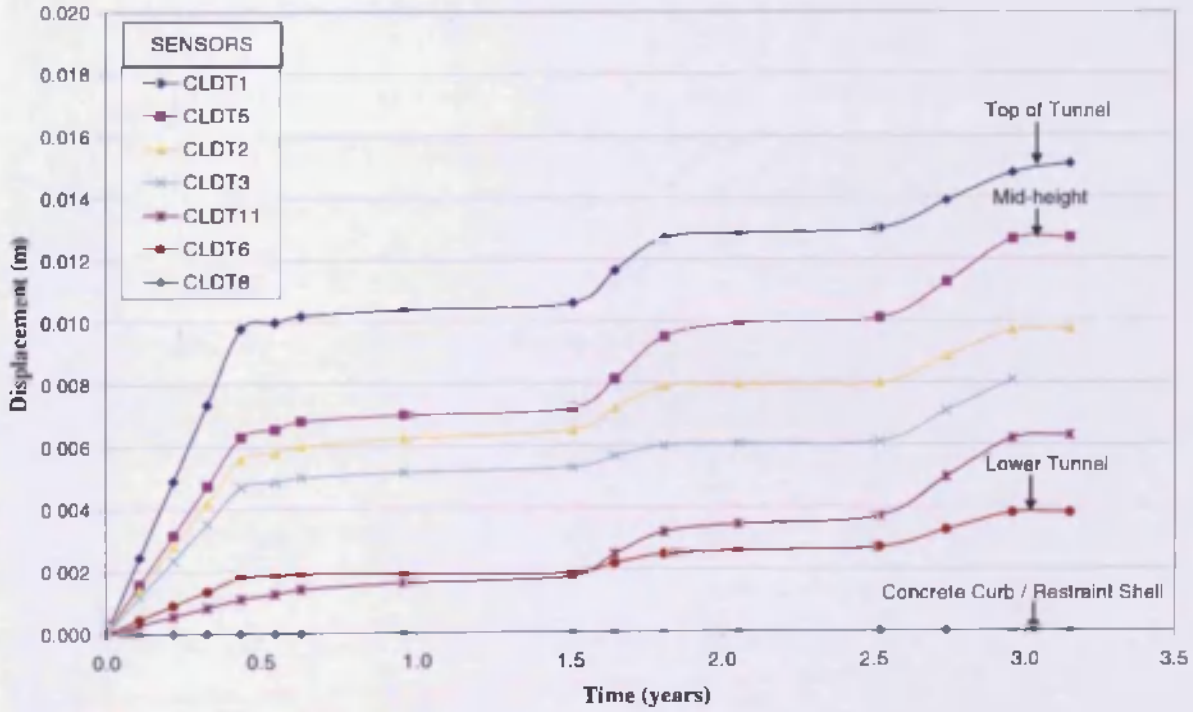

Figure 8.48 Experimentally measured displacement of steel plate during Phase I (AECL, 2001)

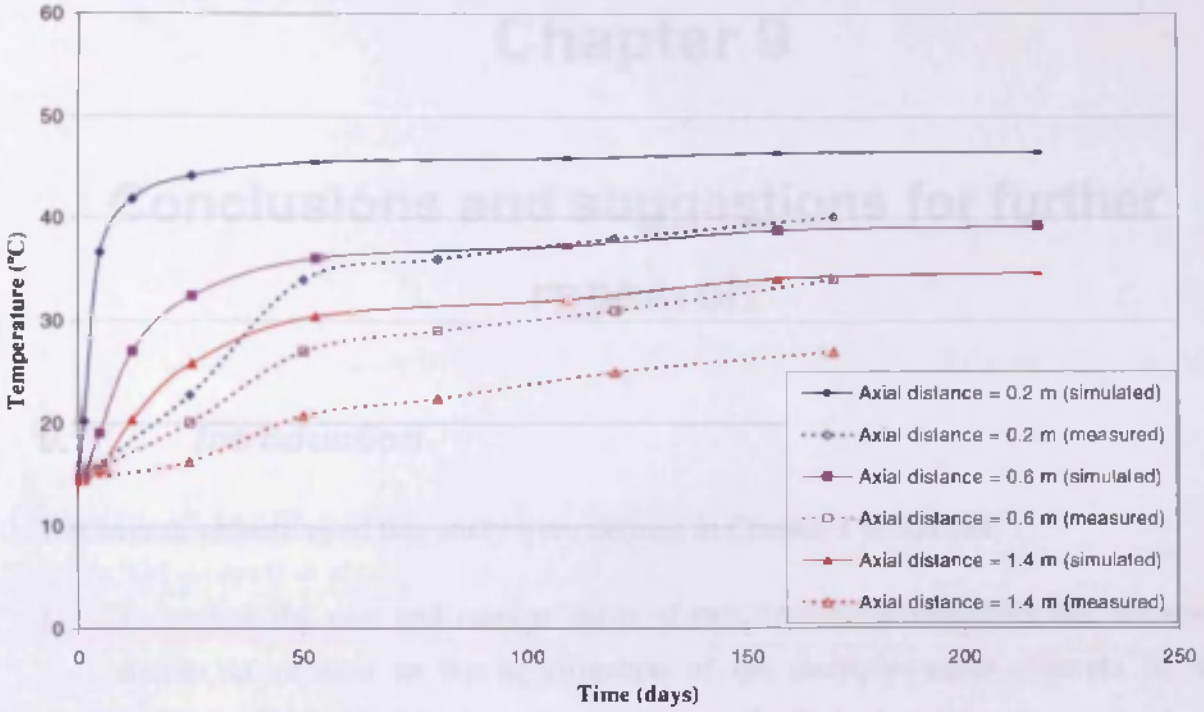

Figure 8.49 Comparison of simulated and measured thermal response of the clay bulkhead at different axial distances during Phase II

Chapter 9

Conclusions and suggestions for further research

9.1 Introduction

The overall objectives of this study were defined in Chapter 1 as follows:

1. To review the past and current status of experimental programmes and numerical studies in relation to the investigation of the multiple-barrier concepts for the disposal of high-level nuclear waste in deep geological repositories.

2. To effectively combine and integrate the numerical code COMPASS with a suitable pre and post-processing piece of software to generate large scale three-dimensional models and finite element meshes.

3. To interface COMPASS with the highly sophisticated three-dimensional visualisation suite recently installed at the Geoenvironmental Research Centre. This is to be used to visualise and interpret results from the large scale numerical analyses investigated in this study.

4. To increase the performance and efficiency of COMPASS to tackle large scale three-dimensional problems via the application of high performance computing techniques and implementation of parallel computing methods.

5. To investigate the three-dimensional thermo/hydro/mechanical behaviour of the buffer, backfill and host rock in the Prototype Repository Experiment and to compare the simulated results to the experimentally measured results.

6. To investigate the fully coupled thermo/hydro/mechanical behaviour of the highly compacted bentonite bulkhead and host rock in the Tunnel Sealing Experiment and make preliminary comparisons with experimental data.

It is claimed that each one of these objectives has been completed successfully during the course of this study.

The following sections review the work presented in this study and summarise the principal conclusions. Finally, suggestions for further work in this area of research are made.

9.2 *Status of research into the disposal of high-level nuclear waste*

Chapter 2 presented a review of both the past and current research work into the disposal of high-level nuclear waste. This research has primarily been focussed within the fields of numerical and experimental investigations. The former research area has developed over many years and has been derived from the need to understand the complex coupled flow and deformation behaviour of partially saturated soils. In the latter case the research has been driven by the need to understand how various engineered barrier materials respond to thermal and hydraulic gradients and stress/strain behaviour.

In recent years there has been a greater emphasis on investigating the performance of engineered clay barriers and natural host rock materials in relation to the multiple-barrier concept proposed for the disposal of high-level nuclear waste. This has become increasingly important as many developed countries have looked at decommissioning nuclear power stations in favour of more renewable, environmentally friendlier options with a view of tackling the ever increasing energy crisis. Of particular interest to this study has been the experimental programmes currently being undertaking by SKB in Sweden and AECL in Canada. These programmes are extremely comprehensive and have investigated not only barrier material performance and behaviour but have also explored new emplacement technologies, tested and validated new instrumentation and analysed the logistical difficulties associated with deep geological disposal.

It is concluded that large scale in-situ experiments such as the Prototype Repository Project and the Tunnel Sealing Experiment have encompassed all of these objectives and provide important information into the feasibility of the multiple barrier concepts for disposal. Furthermore, they also facilitate numerical investigations by providing key information for validation purposes as part of the ongoing research process.

9.3 Combining COMPASS with a pre and post-processor for three-dimensional analyses

As large scale experiments become increasingly more complex there is a requirement for more sophisticated numerical models to represent them more precisely. This enables the complex behaviour to be simulated to a higher degree of accuracy. From the initial outset of this investigation it was obvious that a complex experiment like the Prototype Repository would need to be modelled in three-dimensional space to provide the most representative simulation results. COMPASS, whilst having the capacity to model thermo/hydro/mechanical processes in three-dimensions, had only previously been used for coupled THM analyses in two-dimensions and coupled flow analyses in three-dimensions. Added to this, the existing pre and post-processor, COMPASS GUI, was limited to two-dimensional space. Therefore, the preliminary research involved selecting a suitable pre and post-processor software package with appropriate three-dimensional capabilities and interfacing it successfully with COMPASS.

The software, GiD, developed by the International Centre for Numerical Methods in Engineering (CIMNE) in Spain, was selected for this. GiD was then successfully integrated with COMPASS via a number of interfaces written in FORTRAN 90. This work was extensively tested and verified via a series of small scale tests to ensure that the correct information in the correct format was passed between COMPASS and GiD. This gave confidence in the software and the interface system and allowed increasingly more complex three-dimensional models to be constructed, meshed and analysed. GiD also had the added advantage of a sophisticated post-processor which allowed data interrogation of three-dimensional analyses, albeit on a two-dimensional desktop platform. By providing COMPASS with the additional ability to tackle highly complex three-dimensional numerical simulations the foundation was laid for the successful modelling of the large scale in-situ experiments investigated in this study.

9.4 Interfacing COMPASS with a three-dimensional Visualisation Suite

One of the key areas in three-dimensional modelling is the ability to analyse and interrogate results. In the past this was achieved using post-processing software located on

desktop computers. This has obvious limitations and can potentially lead to misinterpretation of data and numerical errors. In an attempt to overcome these difficulties the Geoenvironmental Research Centre established a three-dimensional virtual reality visualisation platform at Cardiff University in 2002. This system would provide major benefit to the research work presented in this study and hence it was necessary to interface COMPASS with the stereoscopic software, AVS. With input from the AVS technicians, this process was successfully achieved and thus allowed true three-dimensional visualisation of the large scale models presented in this investigation. However it should be noted that due to the time consuming nature of visualising the large finite element meshes on the stereoscopic system and the inherent costs of running it, the system was not used extensively during this study and was used in combination with the visualisation facilities of GiD.

9.5 *Increasing the performance and efficiency of COMPASS*

For the complex numerical modelling conducted in this study it was necessary to increase the performance and efficiency of COMPASS. For small scale coupled one-dimensional and two-dimensional analyses COMPASS performed adequately but as the requirements and complexity of the analyses increased there was a need to improve the proficiency and thus reduce prohibitive computational analyses times. This was achieved via a number of different software measures. Initially, the COMPASS code itself was profiled to determine areas of improvement. As a result it was successfully enhanced and streamlined to improve efficiency and robustness in tackling large analyses. Furthermore, based upon previous research work, suitable iterative solution methods and high-performance computing techniques were effectively implemented into this study. It should be noted that amplifying computational power and performance is an ongoing process and measures have been taken at Cardiff University by the Cardiff Centre for Computational Science and Engineering (CCCSE) to ensure that the most up-to-date hardware is available for increasingly complicated numerical simulations. More recent developments indicate that Grid computing technologies are likely to play a key role in the future of numerical modelling studies.

9.6 *Investigation of the THM behaviour of the Prototype Repository Experiment*

The primary objective of the Prototype Repository Experiment is to investigate at a full scale the integrated performance of engineered barriers and near-field rock for the long-term disposal of high-level nuclear waste. The experiment is currently still ongoing. As part of this international project a series of numerical analyses were performed using the code COMPASS and the simulation results were compared against the experimental results. Many important results were discovered as a consequence of this work and are summarised below.

The key aspect in modelling the complex behaviour of the Prototype Repository Experiment was to represent the complicated geometrical features via a finite element model. Due to the size and configuration of the tunnel and deposition holes this could only be feasibly achieved via the application of a sophisticated three-dimensional model. A less sophisticated two-dimensional model, whilst having many advantages, would not be able to capture the full system-wide behaviour of the experiment. Hence a full three-dimensional finite element model was constructed and when combined with suitable iterative solution methods and high-performance computing techniques it was possible to simulate the coupled flow behaviour of the Prototype Repository Experiment. This proved to be highly advantageous to the research work as it allowed three-dimensional behaviour to be investigated and simulated in a high level of detail.

The first stage of the modelling programme was to simulate the pre-emplacement stage by investigating the hydraulic regime of the host granite rock in response to the excavation of the tunnel and deposition holes. The hydraulic properties of the rock were key to this study as they would control the level and extent of saturation that would take place once the buffer, pellets and backfill were emplaced. It was found that at Äspö the rock mass consisted of a complex array of discrete fractures supplying water at various flowrates. However, due to the limitations of the model it was not possible to represent this complex fracture network in three-dimensions. The alternative method was to include a representative fracture in the finite element model to emulate the fracture that intersected deposition hole 1 in the experiment. The simulated inflow rates were then compared against measured values which allowed a more accurate interpretation of the material parameters of the rock mass. These values were later adopted in the coupled analyses.

Although this was a relatively coarse approximation it did prove successful in these analyses as the simulated results compared favourably with the measured behaviour.

The second stage of the modelling exercise was to simulate the Prototype Repository Experiment following the activation of the heaters in each of the deposition holes in Section I and II. This programme of work entailed the uncoupled thermal analysis of the system, followed by more complex coupled thermal-hydraulic analyses and finally coupled thermal-hydraulic-mechanical analyses. A variety of finite element domains were employed to investigate material parameters, boundary conditions and different phenomena. This study proved to be highly successful and good comparisons were made between the simulated and experimental results.

It was found that the model was able to represent the thermal regime in the buffer, backfill and rock to a high degree of accuracy as a result of using the sophisticated three-dimensional model. This proved to be significant as it showed the importance of using accurate models to capture the behaviour of geometrically complicated experiments over long timescales. The hydraulic response of the system was also captured well, particularly in the drying and wetting rates in the driest deposition hole. This was achieved as a direct result of the calibration of the vapour flow. Key experimental trends were also identified in the simulations, in particular, the regions of highest drying in the buffer above the canisters. This led to greater confidence in the models ability to simulate the Prototype Repository Experiment. The pelletised slot filling material also came under close scrutiny and it was identified that the model over predicted the influence that this zone would have on the resaturation rates in the buffer when compared to experimental observations. Further laboratory testing of this material was recommended in an attempt to ascertain its behaviour under thermal and hydraulic loading.

The mechanical behaviour of the experiment in response to the thermal and hydraulic regimes was investigated via the application of more simplified finite element models. It was found that a fully coupled three-dimensional thermo/hydro/mechanical analysis could not be performed in this study due to the excessive computational requirements required. However, it was identified that the mechanical response of the system could be investigated on a localised scale providing the thermal and hydraulic behaviour was modelled accurately. This allowed a number of analyses to be performed investigating the mechanical material parameters, particularly the deformation characteristics, of the MX-80

pellet material. Following the success of these sensitivity analyses reasonable comparisons were made between the simulated mechanical behaviour and the experimentally measured behaviour.

Overall it can be stated that the results presented in this numerical study were encouraging since they generally provided a good correlation with the experimental data. This gives greater confidence in the ability of the model and theoretical formulation to represent the fully coupled behaviour of unsaturated soils, particularly in the use of engineered barriers for the deep geological disposal of high-level nuclear waste. However, it is acknowledged that this work is continually ongoing and that further numerical investigations are required to coincide with the experimental programme as it advances towards its conclusion.

9.7 *Investigation of the THM behaviour of the Tunnel Sealing Experiment*

AECL conducted the Tunnel Sealing Experiment with the primary objective to investigate the overall performance of two different bulkhead materials, one comprised of highly compacted sand-bentonite blocks and the other constructed using Low-Heat High-Performance concrete. A comprehensive numerical investigation was conducted which constituted a series of predictions on the thermo/hydro/mechanical behaviour of the clay bulkhead during Phase I and II of the experiment. Both two-dimensional and three-dimensional analyses were performed, with the former employed for the more complex coupled simulations.

The results from the hydraulic and hydraulic-mechanical simulations of Phase I showed that the initial conditions on the downstream face of the clay bulkhead had a large influence over the rates of resaturation. Faster resaturation was simulated when recharge occurred from the downstream face. Following the preliminary comparisons with the experimental behaviour this proved significant since recharge had also occurred on the downstream face due to seepage through preferential pathways in and around the clay bulkhead. Therefore a reasonably good correlation was achieved between the numerically modelled results and the experimentally measured data. An additional investigation was performed into the micro/macro behaviour of the clay bulkhead during Phase I and this provided important results. Using a simplified approach it was shown that resaturation

rates could be significantly greater than those simulated using a conventional approach. In light of these findings it is recommended that further experimental and numerical research is conducted into the dual-porosity behaviour of highly swelling clays, particularly for the application of tunnel seals in deep geological repositories.

The deformation behaviour of the bulkhead was also investigated during the saturation phase. This showed that the clay material swelled at the upstream face as the wetting front moved through the bulkhead and consolidated near the downstream face in response. As the hydraulic pressure was further increased during Phase I greater swelling was observed in the bulkhead and incremental displacements were simulated on the steel plate at the downstream end. When this behaviour was compared to the experimentally measured displacements the results were encouraging. Although the model did not capture the initial large displacements, the incremental increases were modelled more quantitatively. This gave confidence in the ability of the coupled stress/strain model to predict overall swelling and deformation in the Tunnel Sealing Experiment.

Phase II of the TSX was modelled via a series of coupled and uncoupled analyses. Since the bulkhead was fully saturated by this stage it was found that the thermal response of the system was largely independent of the hydraulic and mechanical fields. Initial comparisons with the experimentally measured thermal response in the bulkhead showed that the model over predicted the rate of temperature increase and also the magnitude of the temperatures within the bulkhead. This was a result of a simplified thermal boundary condition which assumed an almost immediate thermal response. However, in the experiment this response was delayed due to the presence of the sand chamber. This highlighted the importance of applying representative boundary conditions to model complex experimental patterns.

The thermal expansion of the pore water was investigated and it was found that substantially higher positive pore pressures developed in the bulkhead compared to the hydrostatic pressure. Additional deformation was also identified in the coupled mechanical analysis as a result of thermal expansion of the bulkhead, giving rise to further incremental displacement of the steel plate. Experimental data was unavailable at the time of writing and therefore additional comparisons of the deformation behaviour in Phase II were not made.

Overall it can be stated that the simulation of the Tunnel Sealing Experiment was largely successful and that preliminary comparisons with experimental results were encouraging. A range of phenomena were investigated and different concepts adopted to represent the complex thermo/hydro/mechanical behaviour of the clay bulkhead. The work also highlighted that using simplified models to represent complex three-dimensional behaviour does have many advantages over more sophisticated models. However, this is primarily based on experimental geometry and the adoption of representative boundary conditions.

9.8 General conclusions

The two large scale in-situ experiments investigated in this study are part of an ongoing worldwide research programme and are amongst the most comprehensive ever performed, with the Prototype Repository Experiment planned to run until at least 2021. In particular, the extensive array of instrumentation employed in the Prototype Repository Experiment has meant that valuable experimental data has been available at each stage of the investigation. This has provided a valuable opportunity to test the ability of the numerical model to capture complex coupled behaviour. Therefore, the following general conclusions from this numerical investigation are made.

The three-dimensional modelling of geometrically complex experiments is important for capturing system-wide behaviour. However, there is a computational cost associated with this method and in some cases this can become prohibitive. Less sophisticated finite element models have greater versatility and are less demanding on resources and consequently also have an important role to play in numerical modelling. In conclusion, a comprehensive investigation using both two-dimensional and three-dimensional analyses should be conducted simultaneously to ensure that the model represents the in-situ conditions as closely as possible.

The application of high performance computing and three-dimensional visualisation techniques in this study has meant that complex problems have been analysed in a high level of detail. Without these facilities sophisticated three-dimensional finite element modelling would not have been possible. However, it should be noted that methods of numerical analysis do require further investigation to ensure greater robustness and accuracy for more complex problems. Looking towards the future, as greater processing power becomes available i.e. Grid computing, it is envisaged that more multifaceted

numerical studies will be performed. This is an important criterion since the state of the art needs to development concurrently with experimental programmes to ensure that numerical studies form an integral part on any research activity into the disposal of high-level nuclear waste.

It is imperative that for any modelling programme accurate thermo/hydro/mechanical material parameters are employed. In both numerical studies a range of material and experimental data was made available to ensure accuracy. However, certain parameters required by the model were unavailable and therefore it was necessary to adopt reasonable parameters assumed from similar materials. Therefore, it is important that experimental programmes and numerical studies overlap to ensure that material data is accurate and valid for the computer models.

It was found that the numerical model mostly provided a close correlation with the experimentally measured thermal and hydraulic behaviour. This was observed particularly in the three-dimensional simulation of the Prototype Repository Experiment. The simulation of the coupled stress/strain behaviour proved reasonably successful during the investigations and moderately good correlations were achieved by the model.

9.9 *Suggestions for further research*

It has been shown in this study that the numerical model is capable of representing the coupled thermo/hydro/mechanical behaviour of large scale in-situ experiments for the disposal of high-level nuclear waste. It should be noted however that research into this area is a continually ongoing process and additional development of the model is required. Therefore, the following suggestions are made for further research.

One of the current limitations of the model is that it does not include hysteresis in the relationship between the degree of saturation and suction. This phenomenon may play an important role in the moisture flow behaviour of partially saturated soils and it would be of great benefit to include it in the current formulation. This could potentially be achieved by the application of separate wetting and drying water retention curves.

Further research into the swelling characteristics and micro/macro interaction of bentonitic clays is recommended. This could lead to the development of a dual porosity model

combined with the current theoretical formulation. The current simplified concept could be expanded in greater detail, with small scale laboratory experiments conducted for validation purposes.

Likewise, the vapour flow characteristics of MX-80 buffer and/or similar materials need further research to determine a more precise vapour flow law, particularly for the simulation of the Prototype Repository Experiment. This should be performed concurrently with a series of small scale thermal-hydraulic laboratory experiments. It should be noted that this area of research is currently being performed at the Geoenvironmental Research Centre at Cardiff University.

In both numerical investigations more accurately defined material parameters and relationships would have been of major benefit to the study. Therefore, further experimental study of the MX-80 buffer, MX-80 pellets and backfill under thermal and hydraulic gradients is recommended. In particular, a better understanding of the deformation behaviour of the pelletised region after saturation would be highly valuable.

The heterogeneity of host granitic rock in disposal schemes as illustrated at the Äspö Hard Rock Laboratory needs greater attention in future numerical modelling exercises. This inherent fractured nature could possibly be incorporated into the formulation via a discrete fracture network approach as opposed to a simplified approach. However, further investigation would be required.

There were a number of key developments made during this study into the three-dimensional capabilities of the model i.e. via the application of high-performance computing, parallel processing and visualisation techniques. However, further development is needed to ensure that the model keeps pace with improvements in processing power and new technologies. It is therefore recommended that future computationally demanding analyses benefit from the additional processing power of Grid computing. This could potentially allow complex large scale fully coupled three-dimensional thermo/hydro/mechanical analyses to be performed.

The work presented in this study has not considered the chemical behaviour coupled with the thermo/hydro/mechanical model. It is acknowledged that this in an important area of research in the disposal of high-level nuclear waste in deep geological repositories due to the chemical composition of the granitic water. However, it should be noted that a fully

coupled multi-chemical transport model has recently been developed and validated within the Geoenvironmental Research Centre at Cardiff University.

References

AECL, (2001) "Clay Bulkhead Performance and Status", TSX Progress Meeting #11, Atomic Energy of Canada Limited, *Presentation by D.A. Dixon.*

AECL, (2002) "T-H-M modelling for the TSX", personal communication.

Aggeskog, L. and Jansson, P. (1998) "Finite element analyses of heat transfer and temperature distribution in buffer and rock: general part and case no 1", *SKB*, HRL-98-20.

Aitchison, G.D., (1965) Discussion in Proceedings of the 6th International Conference on Soil Mechanics and Foundation Engineering, **3**, 318-321.

Alonso, E.E., and Alocoverro, J., (1999) "Calculation and testing of behaviour of unsaturated clay as a barrier in radioactive waste repositories (CATSIUS CLAY Project)", *Final Report on Contract*, No. F14W-CT95-0003.

Alonso, E.E., and Alocoverro, J., (2003) "The FEBEX test as a benchmark case for THM modelling", *Proceedings from the Sitges Conference*, Large Scale Field Tests in Granite, Barcelona.

Alonso, E.E., Battle, F., Gens, A., and Lloret, A. (1988) "Consolidation analysis of partially saturated soils – Application to earthdam construction", *Proceedings of the 6th International Conference on Numerical Methods in Geomechanics*, Rotterdam, **2**, 1303-1308.

Alonso, E.E., Gens, A., and Hight, D.W., (1987) "Special problem soils. General report", *Proceedings of the 9th European Conference on Soil Mechanics and Foundation Engineering*, Dublin, **3**, 1087-1146.

Alonso, E.E., Gens, A., and Josa, A., (1990) "A constitutive model for partially saturated soils", *Géotechnique*, **40**, No. 3, 405-430.

Alonso, E.E., Lloret, A., Gens, A., Delahaye, C.H., Vanaut, J. and Volckaert, G., (1995) "Coupled analysis of a backfill hydration test", *Proc. of International Workshop on 'Hydro-Thermo-Mechanics of Engineered Clay Barriers and Geological Barriers'*, Montreal, Quebec, Canada, July 1995 -McGill University.

Alonso, E.E., Vaunat, J. and Gens, A., (1999) "Modelling the mechanical behaviour of expansive clays", *Engineering Geology*, **54**, 173-183.

Axelsson. O., (1972) "A generalised SSOR method", *BIT*, **12**, 443-467.

Axelsson, O., (1985) "A survey of preconditioned iterative methods for linear systems of algebraic equations", *BIT*, **25**, 166-187.

Barden, L., (1965) "Consolidation of compacted and unsaturated clays", *Géotechnique*, **15**, No. 3., 267-286.

Barden, L., Madedor, A.O., and Sides, G.R., (1969) "Volume change characteristics of unsaturated clay", *Journal of Soil Mechanics and Foundation Engineering, American Society of Civil Engineers*, **95**, SM1, 33-51.

Barrett, R., Berry, M., Chan, T., Demmel, J., Donato, J., Dongraa, L, Eijkhout, V., Pozo, R., Romine, C., and Van der Vorst, H., (1995) "Templates, for the solution of linear systems: building blocks for iterative methods", *John Wiley Press, New York.*

Baugh, J.W., and Chadha H.S., (1993) "Network distributed finite element analysis", *Information for technology for civil and structural engineers*, Civ-Comp Press, ISBN 0-948749-16-4, 205-218.

Bernier, F., and Neerdael, B., (1996) "Overview of in-situ thermomechanical experiments in clay: Concept, results and interpretation", *Engineering Geology*, **41**, 51-64.

Biot, M.A., (1941) "General theory of three-dimensional consolidation", *Journal of Applied Physics*, **12(2)**, 115-164.

Bishop, A.W., (1959) "The principle of effective stress", *lecture delivered in Oslo, Norway, in 1955, published in Teknisk Ukeblad*, **106**, No. 39., 859-863.

Bishop, A.W., (1960) "The measurement of pore pressure in the triaxial test", Pore Pressure and Suction in Soils, Publ., Butterworths, London.

Bishop, A.W., and Blight, G.E., (1963) "Some aspects of effective stresses in saturated and partly saturated soils", *Géotechnique*, **13**, No. 3., 177-197.

Bjorstad, P.E., Braekhus, J., and Hvidsten, A., (1990) "Parallel sub-structuring algorithms in structural analysis, direct and iterative methods", *Fourth international symposium on domain decomposition methods for partial differential equations*, 321-340.

Blatz, J.A. and Graham, J., (2000) "A system for controlled suction in triaxial tests", *Géotechnique*, **50**, No. 4, 465-478.

Blatz, J.A. and Graham, J., (2003) "Elastic-plastic modelling of unsaturated soil using results from a new triaxial test with controlled suction", *Géotechnique*, **53**, No. 1, 113-122.

BNFL, (2004) "Nuclear Waste" [WWW] URL:http://www.bnfl.com/index.aspx, [accessed on 13th October 2004]

Bolzon, G., Schrefler, B.A, and Zienkiewicz, O.C., (1996) "Elasto-plastic soil constitutive laws generalise to partially saturated states", *Géotechnique*, **46**, No. 2, 279-289

Bonelli, S., and Poulain, D., (1995) "Unsaturated elasto-plastic model applied to homogeneous earth dam behaviour", *Proceedings of the 1st International Conference on Unsaturated Soils*, Alonso, E.E., and Delage, P., (eds.), Paris, Published by A.A., Balkema, **1**, 265-271.

Börgesson, L., Gunnarsson, D., Johannesson, L.E. and Sandén, T. (2002) "Äspö HRL – Prototype Repository. Installation of buffer, canisters, backfill and instruments in Section 1", *SKB*, IPR-02-23.

Börgesson, L. and Hernelind, J. (1998) "Preparatory modelling for the backfill and plug test – Scoping calculations of H-M processes", *SKB*, IPR-99-11.

Börgesson, L. and Hernelind, J. (1999) "Preliminary modelling of the water saturation phase of the buffer and backfill materials", *SKB*, IPR-00-11.

Börgesson, L., Johannesson, L.E. and Sandén, T. (2001) "Äspö HRL – Prototype Repository. Compilation of Laboratory Data for Buffer and Backfill Materials in the Prototype Repository", *SKB*, IPR-01-34.

Börgesson, L., Johannesson, L.E. Sandén, T. and Hernelind, J. (1995) "Modelling of the physical behaviour of water saturated clay barriers. Laboratory tests, material models and finite element application", *SKB*, TR 95-20.

Börgesson, L., Karnland, O., and Johannesson, L.-E., (1996) "Modelling of the physical behaviour of clay barriers close to water saturation", *Engineering Geology*, **41**, 127-144.

Börgesson, L. and Sandén, T., (2001) "Äspö HRL – Prototype Repository. Report on instrument positions in buffer/backfill and preparation of bentonite blocks for instruments and cables in Section I", *SKB*, IPR-01-20.

Börgesson, L. and Sandén, T., (2003) "Äspö HRL – Prototype Repository. Instrumentation of buffer and backfill in Section II", *SKB*, IPR-03-21.

Britto, A.M., and Gunn, M.G., (1987) "Critical state soil mechanics via finite elements", Ellis Horwood Ltd.

Burland, J.B., (1965) "Some aspects of mechanical behaviour of partly saturated soils", *Moisture Equilibrium and Moisture Changes in Soils Beneath Covered Areas*, Sydney,: Butterworths, 270-278.

Carman, P.C., (1956) "Flow of gases through porous media", Butterworths Scientific Publications, London.

Carter, W.T., Sham, T-L., and Law, K.H., (1989) "A parallel finite element method and its prototype implementation a Hypercube", *Computers & structures*, **31**, No. 6, 921-934.

CATSIUS CLAY Project (1998), *Topical Report*, Stage 3, Contract No. F14W-CT95-003, Doc XII-158-99-EN.

Chandler, N., (2000) "Water inflow calculations for the isothermal buffer-rock-concrete plug interaction test", *Used Fuel Disposal Technology Program Report* 06819-xxxxx-Txx, Ontario Power Generation.

Chandler, N., Martino, J. and Dixon, D., (2002a) "The Tunnel Sealing Experiment", *In Proc. of 6th International Workshop on Design and Construction of Final Repositories*, Session 4, Number 11, Brussels, ONDRAF-NIRAS.

Chandler, N., Cournut, A., Dixon, D., Fairhurst, C., Hansen, F., Gray, M., Hara, K., Ishijima, Y., Kozak, E., Martino, J., Masumoto, K., McCrank, G., Sugita, Y., Thompson, J. Tillerson, P. and Vignal, B., (2002b) "The five year report on the Tunnel Sealing Experiment: an international project of AECL, JNC, ANDRA AND WIPP", Atomic Energy of Canada Limited Report, AECL-12727.

Chang, C.S., and Duncan, J.M., (1983) "Consolidation analysis for partially saturated clay by using an elasto-plastic effective stress-strain model", *International Journal for Numerical and Analytical Methods in Geomechanics*", 7, 30-56.

Chapman, N.A., and McKinley, I.G., (1987) "The geological disposal of nuclear waste", John Wiley and Sons, Chicester.

Chijimatsu, M., Sugita, Y., Fujita, T. and Amemiya, K., (1999) "Coupled Thermo-Hydro-Mechanical Experiment at Kamaishi Mine - experiment results" *Japan Nuclear Cycle Development Institute*, Technical Note 15-99-02 JNC TN8400 99-034.

Chronopoulos A.T., and Gear C.W., (1989) "On the efficient implementation of preconditioned s-step cg methods on multiprocessors with memory hierarchy", *Parallel Computing*, **11**, 37-53.

CIMNE, (2004) "GiD – the personal pre and post processor", [WWW] URL:http://gid.cimne.upc.es/, [accessed on May 28th, 2004].

Cleall, P.J., (1998) "An investigation of the thermo/hydraulic/mechanical behaviour of unsaturated soils, including expansive clays", *Ph.D thesis*, University of Wales, Cardiff, U.K.

Cleall, P. J., Thomas, H.R. and Melhuish, T.A. (2002a) "Vapour transfer in clay based engineered barriers, in high level nuclear waste disposal", Proceedings of Workshop on Clay microstructure and its importance to soil behaviour, Lund, Sweden, pp 58 – 65.

Cleall, P. J., Thomas, H.R., Melhuish, T.A. and Owen, D.H. (2002b) "Simulation of the behaviour of deep geological repositories – some computational challenges", *Proceedings of the 8th International Conference on Numerical Methods in Geomechanics*, Balkema. Numerical Models in Geomechanics - NUMOG VIII, **235 – 240**, ISBN no: 90-5809-359-X.

Coleman, J.D., (1962) "Stress strain relations for partly saturated soil", *Correspondence to Géotechnique*, **12**, No. 4., 348-350.

Collin, F., Li, X.L., Radu, J.P. and Charlier, R., (2002) "Thermo-hydro-mechanical coupling in clay barriers", *Engineering Geology*, **64**, 179-193.

Connell, L.D., and Bell, P.R.F., (1993) "Modelling moisture movement in revegetating waste heaps; Development of a finite element model for liquid and vapour transport", *Water Resources Research*, **29**, No. 5., 1435-1443.

Cook, R.D., (1981) "Concepts and applications of finite element analysis", Wiley, New York.

Couvillion, R.J., and Hartley, J.G., (1986), "Drying front movement near low intensity impermeable underground heat sources", *Journal of Heat Transfer, American Society of Mechanical Engineers*, **108**, 182-189.

Cui, Y.J., and Delage, P., (1996) "Yielding and plastic behaviour of an unsaturated compacted silt", *Géotechnique*, **46**, No. 2, 291-311.

Cui, Y.J., Yahia-Aissa, M, Delage, P. (2002) "A model for the volume change of heavily compacted swelling clays", *Engineering Geology*, **64**, 233-250.

Dahlström, L-O., (1998) "Äspö HRL – Test plan for the Prototype Repository", *SKB*, HRL-98-24.

Dakshanamurthy, V., and Fredlund, D.G., (1981) "A mathematical model for predicting moisture flow in an unsaturated soil under hydraulic and temperature gradients", *Water Resources Research*, **17**, No. 3., 714-722.

Datta, R., Barr, D. and Boyle, W., (2003) "Measuring thermal, hydrologic, mechanical, and chemical responses in the Yucca Mountain Drift Scale Test", *Proceedings from the International Conference on Coupled T-H-M-C Processes in Geo-systems*, GeoProc 2003, Stockholm, Sweden.

Davies, P.B., (1991) "Evaluation of the role of threshold pressure in controlling flow of waste-generated gas into bedded salt at the waste isolation pilot plant", *Technical Report*, SAND-90-3246, Sandia National Laboratories, Albuquerque, New Mexico.

Delage, P., and Graham, J., (1996) "Mechanical behaviour of unsaturated soils: Understanding the behaviour of unsaturated soils requires reliable conceptual models", *Proceedings of the 1st International Conference on Unsaturated Soils*, Alonso E.E., and Delage, P., (eds.), Paris, Published by A.A. Balkema, **3**, 1223-1258.

Delin, P., Sturk, R., and Stille, H., (1995) "Laboratory testing of rock", *SKB*, Technical note 25-95-08v.

de Vries, D.A., (1958) "Simultaneous transfer of heat and moisture in porous media", *Trans. American Geophys. Union*, **39**, No. 5, 909-916.

de Vries, D.A., (1966) "Physics of plant environment", 2nd Edition, North Holland Publishing Company, 215-235.

Dickinson, J.K., and Forsyth, P.A., (1994) "Preconditioned conjugate gradient methods for three-dimensional linear elasticity", *International journal for numerical methods in engineering*, **37**, 2211-2234.

Dixon, D. A. and Gray, M. N., (1985) "The engineering properties of buffer material - research at Whiteshell Nuclear Research Establishment", *In Proceedings of the 19th Information Meeting of the Nuclear Fuel Waste Management Program*, Atomic Energy of Canada Limited, Technical Record, TR-350, Volume III, 513–530.

Edelfsen, N.E., and Andersen, A.B.C., (1943) "Thermodynamics of soil moisture", *Hiigardia*, **15**, No. 2., 31-298.

Edgar, T.V., Nelson, J.D., and McWhorter, D.B., (1989) "Non-isothermal consolidation in unsaturated soils", *Journal of Geotechnical Engineering, ASCE*, **115**, No. 10., 1351-1372.

Ericsson, L.O., (1999) "Geoscientific R&D for high level radioactive waste disposal in Sweden – current status and future plans", *Engineering Geology*, **52**, 305-317.

Ewen, J., (1987) "Combined heat and mass transfer in unsaturated sand surrounding a heated cylinder", *Ph.D. Thesis*, School of Engineering, University College, Cardiff, UK.

Ewen, J., and Thomas, H.R., (1987) "The thermal probe – a new method and its use on an unsaturated sand", *Géotechnique*, **37**, 91-105.

Ewen, J., and Thomas, H.R., (1989) "Heating unsaturated medium sand", *Géotechnique*, **39**, No. 3, 455-470.

Farhat C., and Wilson E., (1987) "A new finite element concurrent computer program architecture", *International journal for numerical methods in engineering*, **24**,1771-1792.

Farhat, C., (1989) "Which parallel finite element algorithm for which architecture and which problem" in R. V. Gradhi *et al* (eds), *Computational structural mechanics and multidisciplinary optimisation*, AD, **16**, ASME, New York, 35-43.

Farhat, C., and Lesoinne, M., (1993) "Automatic partitioning of unstructured meshes for the parallel solution of problems in computational mechanics", *International journal for numerical methods in engineering*, **36**, 745-764.

Felix, B., Lebon, P., Miguez, R., and Plas, F., (1996) "A review of the ANDRA's research programmes on the thermo-hydro-mechanical behaviour of clay in connection with the radioactive waste disposal project in deep geological formations.", *Engineering Geology*, **41**, 35-50.

Forsmark, T. and Rhén, I., (1999a) "Äspö HRL – Prototype Repository. Hydrogeology – Interference test campaign 1 after drill campaign 3", *SKB*, IPR-00-07.

Forsmark, T. and Rhén, I., (1999b) "Äspö HRL – Prototype Repository. Hydrogeology – Drill campaign 3A and 3B", *SKB*, IPR-00-08.

Forsmark, T. and Rhén, I., (2000a) "Äspö HRL – Prototype Repository. Hydrogeology – Injection test campaign 1", *SKB*, IPR-00-20.

Forsmark, T. and Rhén, I., (2000b) "Äspö HRL – Prototype Repository. Hydrogeology – Interference test campaign 2 after drill campaign 3", *SKB*, IPR-00-21.

Forsmark, T., Rhén, I. and Andersson, C., (2001a) "Äspö HRL – Prototype Repository. Hydrogeology – Deposition and lead-through boreholes: Inflow measurements, hydraulic responses and hydraulic tests", *SKB*, IPR-00-33.

Forsmark, T., Rhén, I. and Andersson, C., (2001b) "Äspö HRL – Prototype Repository. Hydrogeology – Injection test campaign 2, flow measurement of DA3575G01, groundwater salinity, groundwater leakage into G, I and J-tunnels", *SKB*, IPR-01-31.

Fredlund, D.G., (1979) "Appropriate concepts and technology for unsaturated soils", *Canadian Geotechnical Journal*, **16**, 121-139.

Fredlund, D.G., (1991) "Seepage in saturated soils. Panel Discussion : Ground water and seepage problems" *Proceedings of the 10th International Conference on Soil Mechanics and Foundation Engineering*, Stockholm, **4**, 629-641.

Fredlund, D.G., and Hasan, J.U., (1979) "One-dimensional consolidation theory: unsaturated soils", *Canadian Geotechnical Journal*, **16**, 521-531.

Fredlund, D.G., and Rahardjo, H., (1993) "Soil Mechanics for Unsaturated Soils", *John Wiley & Sons Inc*, New York.

Fredlund, D.G., and Morgenstern, N.R., (1977) "Stress state variables for unsaturated soils", *Journal of Geotechnical Engineering Division of the American Society for Civil Engineers*, **103**, GT5, 447-446.

Frieg, B., and Vomvoris, S., (1994) "Investigation of hydraulic parameters in the saturated and unsaturated zone of the ventilation drift", *Technical Report* 93-10, Nagra, Baden, Switzerland.

Fuentes-Cantillana, J-L., (2003) "The FEBEX in-situ test: Lessons learned on the engineering aspects of horizontal buffer construction and canister emplacement", *Proceedings from the Sitges Conference*, Large Scale Field Tests in Granite, Barcelona.

Fujita, T., Kobayashi, A. and Börgesson, L., (1996) "Experimental investigation and mathematical simulation of coupled T-H-M processes of the engineered buffer materials, the TC3 problem", *Developments in Geotechnical Engineering*, **79**, 369–392.

Gallipoli, D., Wheeler, S.J. and Karstunen, M., (2003a) "Modelling the variation of degree of saturation in a deformable unsaturated soil", *Géotechnique*, **53**, No. 1, 105-112.

Gallipoli, D., Gens, A., Sharma, R. and Vaunat, J., (2003b) "An elasto-plastic model for unsaturated soil incorporating the effects of suction and degree of saturation on mechanical behaviour", *Géotechnique*, **53**, No. 1, 123-135.

Gens, A., (1995) "Constitutive modelling: application to compacted soils", *Proceedings of the 1st International Conference on Unsaturated Soils*, Alonso, E.E., and Delage, P., (eds.), Paris, Published by A.A., Balkema, **1**, 1179-1200.

Gens, A., and Alonso, E.E., (1992) "A framework for the behaviour of unsaturated expansive clays", *Canadian Geotechnical Journal*, **29**, 1013-1032.

Gens, A., Garcia-Molina, A.J., Olivella S., Alonso, E.E., and Huertas, F., (1998) "Analysis of a full scale *in situ* test simulating repository conditions", *International Journal for Numerical and Analytical Methods in Geomechanics.*, **22**, 515-548.

Gens, A., and Potts, D.M., (1982) "Application of critical state models to the prediction of the behaviour of a normally consolidated low plasticity clay", *Proceedings of the 1st International Symposium on Numerical Modelling and Geomechanics*, Zurich, 312-323.

Gentzschein, B., (1997) "Äspö HRL – Prototype Repository. Hydraulic tests in exploratory holes. Drill campaign 1", *SKB*, IPR-99-27.

Gentzschein, B., (1998) "Äspö HRL – Prototype Repository. Hydraulic tests in exploratory holes. Drill campaign 2", *SKB*, IPR-99-28.

Gentzschein, B., (1999a) "Äspö HRL – Prototype Repository. Hydraulic tests in exploratory holes. Drill campaign 3a", *SKB*, IPR-99-29.

Gentzschein, B., (1999b) "Äspö HRL – Prototype Repository. Hydraulic tests in exploratory holes. Drill campaign 3b", *SKB*, IPR-99-30.

Gentzschein, B., (1999c) "Äspö HRL – Prototype Repository. Hydraulic tests in exploratory holes. Injection tests", *SKB*, IPR-99-31.

Gentzschein, B., (1999d) "Äspö HRL – Prototype Repository. Hydraulic tests in exploratory holes. Interference tests A after drill campaign 3", *SKB*, IPR-99-32.

Gentzschein, B., (1999e) "Äspö HRL – Prototype Repository. Hydraulic tests in exploratory holes. Interference tests B after drill campaign 3", *SKB*, IPR-99-33.

Gentzschein, B., (2001) "Äspö HRL – Prototype Repository. Hydraulic tests in exploratory holes. Injection tests_II", *SKB*, IPR-01-21.

Geraminegrad, M., and Saxena, S., (1986a) "A coupled thermoelastic model for saturated-unsaturated porous media", *Géotechnique*, **36**, No. 4., 539-550.

Geraminegrad, M., and Saxena, S., (1986b) "Finite elements in plasticity: Theory and practice", Pineridge Press Ltd., Swansea.

Goudarzi, R. and Johannesson, L-E., (2003) "Äspö HRL – Prototype Repository. Sensors data report (Period 010917-030901). Report No:7", *SKB*, IPR-03-46.

Graham, J., Chandler, N.A., Dixon, D.A., Roach, P.J., To, T., and Wan, A.W.L., (1997) "The Buffer/Container experiment: Results, synthesis, issues" *Technical Report*, AECL-11746, COG-97-46-I.

Graham, J., Saadat, F., Gray, M.N., Dixon, D.A., and Zhang, Q.-Y., (1989) "Strength and volume change behaviour of a sand-bentonite mixture", *Canadian Geotechnical Journal*, **26**, 292-305.

Green, R.E., and Corey, J.C., (1971) "Calculation of hydraulic conductivity: A further evaluation of some predictive methods", *Proceedings of the Soil Society of America* **35**, 3-8.

Green, R.T. and Painter, S.L., (2003) "Numerical simulation of thermohydrological processes observed at the drift-scale heater test at Yucca Mountain, Nevada", *Proceedings from the International Conference on Coupled T-H-M-C Processes in Geo-systems*, GeoProc 2003, Stockholm, Sweden.

Gunnarsson, D., Börgesson, L. Hökmark, H., Johannesson, L.E. and Sandén, T., (2001a) "Äspö HRL – Report on the installation of the Backfill and Plug Test", SKB, IPR-01-17.

Gunnarsson, D., Johannesson, L-E. and Börgesson, L. (2001b) "Äspö HRL – Prototype Repository. Backfilling of the tunnel in the Prototype Repository. Results of pre-tests. Design of material, production technique and compaction technique", *SKB*, IPR-01-11.

Guo, R., and Chandler, N.A., (2002) "Thermal-Hydraulic Numerical Modelling of the flow of heated water through a sand-filled tunnel in granite", *Proceedings of the 55th Canadian Geotechnical Conference*, Niagara Falls, Ontario, 497-504, Canadian Geotechnical Society.

Guo, R., Chandler, N.A., and Dixon, D., (2002) "Modelling the thermally induced hydraulic and mechanical response for the heated phase of the Tunnel Sealing Experiment", Ontario Power Generation, *Nuclear Waste Management Division*, Report No. 06819-REP-01200-10095-R00.

Guo, R., Chandler, N.A., Martino, J. and Dixon, D., (2003) "Thermo-Hydro-Mechanical Numerical Modelling of the TSX with Comparisons to Measurements During Stage 1 Heating", Atomic Energy of Canada Limited, Report No: 06819-REP-01300-10070-R00.

Guvanasen, V. and Chan, T., (2000) "A three-dimensional numerical model for thermohydromechanical deformation with hysteresis in a fractured rock mass", *International Journal of Rock Mechanics and Mining Sciences*, **37**, 89-106.

Hashm, A.A., (1999) "A study of the transport of a selection of heavy metals in unsaturated soils", *Ph.D. Thesis*, Cardiff University, Wales, UK.

Hökmark, H., (2003) "Temperature Buffer Test – Comparison of modelling results/experimental findings: causes of difference", *Proceedings from the Sitges Conference*, Large Scale Field Tests in Granite, Barcelona.

Hsiung, S.M., Chowdhury, A.H. and Nataraja, M.S., (2003) "Thermal-mechanical modelling of a large-scale heater test", *Proceedings from the International Conference on Coupled T-H-M-C Processes in Geo-systems*, GeoProc 2003, Stockholm, Sweden.

Hueckel, T., and Baldi, G., (1990) "Thermoplasticity of saturated clays. Experimental constitutive study", *Journal of Geotechnical Engineering*, **116**, No. 12, 1778-1796

Huertas, F., Fuentes-Cantillana, J.L., Jullien, F., Rivas, P., Linares, J., Farina, P., Ghorechi, M., Jockwer, N., Kickmaier, W., Martinez, M.A., Samper, J., Alonso, E., and Elorza, F.J. (2000) "Full-scale engineered barriers experiment for a deep geological repository for high level radioactive waste in crystalline host rock (FEBEX project)" *Euratom*.

Jakob, M., (1949) "Heat transfer: Vol 1", Wiley.

Jaky, J., (1948) "Pressure in soils", Proceedings of the 2nd International Conference on Soil Mechanics and Foundation Engineering, **1**, 103-107.

Jennings, J.E., and Burland, J.B., (1962) "Limitations to the use of effective stresses in partly saturated soils", *Géotechnique*, **12**, No. 2., 125-144.

Jing, L., Tsang, C.F., Stephansson, O., and Kautsky, F., (1996) "Validation of mathematical models against experiments for radioactive waste repositories – DECOVALEX experience", *Coupled Thermo-Hydro-Mechanical Processes of Fractured Media, Developments in Geotechnical Engineering*, **79**, 25-56.

Johannesson, L-E. (1999) "Compaction of full size blocks of bentonite for the KBS-3 concept", *SKB*, R-99-66.

Johannesson, L-E., Börgesson, L. and Gunnarsson, D. (2003) "Hydro-Mechanical Properties of Backfill Material", *Proceedings from the Sitges Conference*, Large Scale Field Tests in Granite, Barcelona.

Johannesson, L-E., Börgesson, L. and Sandén, T. (1999) "Äspö HRL – Backfill materials based on crushed rock (part 2). Geotechnical properties determined in laboratory", *SKB*, IPR-99-23.

Jommi, C., and di Prisco, C., (1994) " Un semplice approcio teorico per la modellazione del comportamento meccanico di terreni granulari parcialmente saturi", *Conf. Il ruolo dei fluidi nei problemi di ingegneria geotecnica*, Mondovi, 167-188, (in Italian).

Josa, A., Alonso, E.E., Lloret, A., and Gens, A., (1987), "Stress-strain behaviour of partially saturated soils", *Proceedings of the 9th European Conference on Soil Mechanics and Foundation Engineering*, Dublin, **2**, 561-564.

Josa, A., (1988) "Un modelo elastoplastico para suelos no saturados", *Ph.D. Thesis*, Universitat Politechnica de Catalunya, Barcelona.

Josa, A., Balmaceda, A., Gens, A., and Alonso, E.E., (1992) "An elastoplastic model for partially saturate soils exhibiting a maximum of collapse", *Proceedings of the 3rd International Conference on Computational Plasticity*, Barcelona, **1**, 815-826.

Kanno, T., Fujita, T., Takeuchi, S., Ishikawa, H., Hara, K., and Nakano, M., (1999) "Coupled thermo-hydro-mechanical modelling of bentonite buffer material", *International Journal for Numerical and Analytical Methods in Geomechanics*, **23**, 1281-1307.

Kanno, T., Kato, K., and Yamagata, J., (1996) "Moisture movement under a temperature gradient in highly compacted bentonite", *Engineering Geology*, **41**, 287-300.

Kato, S., Matsuoka, H., and Sun, D.A., (1995) "A constitutive model for unsaturated soil based on extended SMP", *Proceedings of the 1st International Conference on Unsaturated Soils*, Alonso E.E., and Delage, P., (eds.), Paris, Published by A.A., Balkema, **2**, 739-744.

Kaye, G.W.C., and Laby, T.M., (1973) "Tables of physical and chemical constants", 14th Edition, Harlow, Longman.

Khan, A.I. and Topping, B.H.V., (1993) "Parallel finite element analysis using the jacobi-conditioned conjugate gradient algorithm", *Proceedings of the 5th International Conference on Civil Engineering Computing*, Information technology for civil and structural engineering, CIVIL-COMP press, 245-255.

King R.B., and Sonnad. V., (1987) "Implementation of an element-by-element solution algorithm for the finite element methods on a course-grained parallel computer", *Computer methods in applied mechanics and engineering*, **65**, 47-59.

King, S.D., (1991) "A potential based model of coupled heat and moisture transfer in unsaturated soil", *Ph.D. Thesis*, School of Engineering, University of Wales, Cardiff, UK.

Kohgo, Y., Nakano, M., and Miyazaki, T., (1993a) "Theoretical aspects of constitutive modelling for unsaturated soils", *Soils and Foundations*, **33**, No. 4, 49-63.

Kohgo, Y., Nakano, M., and Miyazaki, T., (1993b) "Verification of the generalised elasto-plastic model for unsaturated soil", *Soils and Foundations*, **33**, No. 4, 64-73.

Kornfält, K-A. and Wikman, H., (1988) "The rocks of Äspö Island. Description to the detailed maps of solid rocks including maps of 3 uncovered trenches", *SKB*, Progress report 25-88-12.

Krischer, D., and Rohnalter, H., (1940) "Warmeleitung und Dampfdiffusion in feutchen Gutern", Verein Duet, Ing-Forschungsheft, 402.

Lesoinne, M., Farhat, C., and Geradin, M., (1991) "Parallel/vector improvements of the frontal method", *International journal for numerical methods in engineering*, **32**, 1267-1281.

Lingnau, B.E., Graham, J., and Tanaka, N., (1994) "Isothermal modelling of sand-bentonite mixtures at elevated temperatures", *Canadian Geotechnical Journal.* **32**, 78-88.

Ljunggren, C. and Bergsten, K-Å., (1998) "Äspö HRL – Prototype Repository. Rock stress measurements in KA3579G", *SKB*, HRL-98-09.

Lloret, A., and Alonso, E.E., (1980) "Consolidation of unsaturated soils including swelling and collapse behaviour", *Géotechnique*, **30**, No. 4., 449-477.

Lloret, A., and Alonso, E.E., (1985) "State surfaces for partially saturated soils", *Proceedings of the 11th International Conference of Soil Mechanics and Foundation Engineering*, San Francisco, **2**, 557-562.

Lloret, A., Gens, A., Battle, F., and Alonso, E.E., (1987) " Flow and deformation analysis of partially saturated soils", *Proceedings of the 9th European Conference on Soil Mechanics and Foundation Engineering*, Dublin, **2**, 565-568.

Lloret, A., Villar, M.V., Sánchez, M., Gens, A., Pintado, X. and Alonso, E.E., (2003) "Mechanical behaviour of heavily compacted bentonite under high suction changes", *Géotechnique*, **53**, No. 1, 27-40.

Luikov, A.V., (1966), "Heat and mass transfer in capillary porous bodies", Pergamon Press, Oxford.

Mackerle, J., (1996) "Implementing finite element methods on supercomputers, workstations and PCs", *Engineering Computations*, **13**, No1, 33-85.

Matayas, E.L., and Radhakrishna, H.S., (1968) "Volume change characteristics of partially saturated soils", *Géotechnique*, **18**, No. 4., 432-448.

Millard, A. and Rutqvist, J., (2003) "Comparative analyses of predicted and measured displacements during the heating phase of the Yucca Mountain Drift Scale Test", *Proceedings from the International Conference on Coupled T-H-M-C Processes in Geo-systems*, GeoProc 2003, Stockholm, Sweden.

Mitchell, J.K., (1993) "Fundamentals of soil behaviour" *John Wiley*, New York.

Mitchell, H.P., (2002) "An investigation into the thermo/hydro/mechanical interactions involved in high level nuclear waste disposal" *Ph.D thesis*, University of Wales, Cardiff, U.K.

Navarro, V. and Alonso, E.E., (2000) "Modelling swelling soils for disposal barriers", *Computers and Geotechnics*, **27**, No. 1, 19-43.

NIEeS, (2004) "National Institute for Environmental eScience", [WWW] URL:http://www.niees.ac.uk/index.html, [accessed on June 15th, 2004].

NIREX, (2004) "Background information on radioactive waste", [WWW] URL:http://www.nirex.co.uk/, [accessed on 13th October, 2004].

Notay, I. (1995) "An efficient parallel discrete PDE solver", *Parallel Computing*, **21**, 1725-1748.

Olivella, S., Gens, A. and Gonzalez, C., (2003) "THM analysis of a heating test in a fractured tuff", *Proceedings from the International Conference on Coupled T-H-M-C Processes in Geo-systems*, GeoProc 2003, Stockholm, Sweden.

Ortega, J.M., (1988) "Introduction to parallel and vector solution of linear systems" *Plenum Press*, New York and London, 197-231.

Owen, D.H., (2000) "Preconditioned parallel iterative solution methods for coupled finite element analyses" *Ph.D thesis*, University of Wales, Cardiff, U.K.

Owen, D.R.J., and Hinton, E., (1980) "Finite elements in plasticity: Theory and practice" Pineridge Press Ltd., Swansea.

Partington, J.R., and de Vries, D.A., (1957) "Moisture movement in porous materials under temperature gradients", *Trans. Amer. Geophys. Union*, **38**, No. 2., 222-232.

Patel, S., Dahlström, L-O. and Stenberg, L., (1997) "Äspö HRL – Characterisation of the rock mass in the Prototype Repository at Äspö HRL, Stage 1", *SKB*, HRL-97-24.

Philip, J.R., and de Vries, D.A., (1957) "Moisture movements in porous materials under temperature gradients", *Transactions, American Geophysical Union*, **38**, No. 2, 222-232.

Plischke, B., and Bulgakov, V., (1999) "Application of iterative solvers in geomechanics with special emphasis on petroleum engineering", Submitted for publication.

Pollock, D.W., (1986) "Simulation of fluid and energy processes associated with high level radioactive waste disposal in unsaturated alluvium", *Water Resources Research*, **22**, No. 5., 765-775.

Pool, E.L., Knight, N.R, and Davis, D.D., (1992) "High-performance equation solvers and their impact on finite element analysis", *International journal for numerical methods in engineering*, **33**, 855-868.

Preece, R.J., (1975) "The measurement and calculation of physical properties of cable bedding sands. Part 2; specific thermal capacity, thermal conductivity and temperature ratio across 'air' filled pores", *C.E.G.B. Laboratory Note No.*, RD/L/N 231/74.

Pusch, R., (1998) "Microstructural evolution of buffer clay", In Proceedings of workshop on microstructural modelling of natural and artificially prepared clay soils with special emphasis on the use of clays for waste isolation, Lund, 31-38.

Pusch, R., Karnland, O., and Hokmark, H., (1990) "GMM: a general microstructural model for qualitative and quantitative studies of smectite clays", *Technical Report*, SKB-90-43, Stockholm.

Ramesh, A.A., (1996) "Modelling the thermo/hydraulic/mechanical behaviour of unsaturated soil using an elasto-plastic constitutive relationship", *Ph.D thesis*, University of Wales, Cardiff, U.K.

Rees, S.W., (1990) "Seasonal ground movement effects on buried moisture transfer in unsaturated soil", *Ph.D. Thesis*, School of Engineering, University of Wales, Cardiff, UK.

Rhén, I. and Forsmark, T., (1998a) "Äspö HRL – Prototype Repository. Hydrogeology – Drill campaign 1", *SKB*, HRL-98-12.

Rhén, I. and Forsmark, T., (1998b) "Äspö HRL – Prototype Repository. Hydrogeology – Drill campaign 2", *SKB*, HRL-98-22.

Rhén, I. and Forsmark, T., (2001) "Äspö HRL – Prototype Repository. Hydrogeology – Summary report of investigations before the operation phase", *SKB*, IPR-01-65.

Richards, L.A., (1931) "Capillary conduction of liquids through porous medium", *Journal of Physics*, **1**, 318-333.

Romero, E., Gens, A. and Lloret, A., (2001a) "Laboratory testing of unsaturated soils under simultaneous suction and temperature control", *Proc. 15th Int. Conf. Soil Mech. Geotech. Engng*, Istambul, **1**, 619-622.

Romero, E., Gens, A. and Lloret, A., (2001b) "Temperature effects on the hydraulic behaviour of an unsaturated clay", *Geotechnical and Geological Engineering*, 19, 311-332.

Romero, E., Gens, A. and Lloret, A., (2003) "Suction effects on a compacted clay under non-isothermal conditions", *Géotechnique*, **53**, No. 1, 65-81.

Rutqvist, J., Tsang, C.-F. And Tsang, Y., (2003) "Analysis of stress and moisture induced changes in fractured rock permeability", *Proceedings from the International Conference on Coupled T-H-M-C Processes in Geo-systems*, GeoProc 2003, Stockholm, Sweden.

Saad, Y., (1988), "Preconditioning techniques for nonsymmetric and indefinite linear system", *Journal of computational and applied mathematics*, **24**, 89-105.

Saadat, F., Graham, J., and Kjartanson, B.H., (1992) "Finite element deformation analysis of a sand-bentonite liner for radioactive waste containment", *Innovation, Conservation and Renovation,* Proceedings of the 45th Canadian Geotechnical Society Conference, Innovation Q94/00234.

Sansom, M.R., (1995) "A fully coupled numerical analysis of mass, air and heat transfer in unsaturated soil", *Ph.D. Thesis*, School of Engineering, University of Wales, Cardiff, UK.

Seetharam, S.C., (2003) "An investigation of the thermo/hydro/chemical/mechanical behaviour of unsaturated soils" *Ph.D. Thesis*, Cardiff University, Wales, UK.

Selvadurai, A.P.S., (1996) "Heat-induced moisture movement in a clay barrier I. Experimental modelling of borehole emplacement", *Engineering Geology*, **41**, 239-256.

Shih, T.M., Hays, L.J., Minkowyez, W.J., Yang, K.T., and Aung, W. (1986) "Parallel computations in heat transfer", *Numerical heat transfer,* **9**, 639-662.

Sivakumar, V., (1993) "A critical state framework for unsaturated soil", *PhD thesis*, University of Sheffield, UK.

SKB, (2002) "MX-80 material parameters", personal communication.

SKB, (2004a) "High-level waste – Quantity and hazard level", [WWW] URL:http://www.skb.se/templates/SKBPage____3331.aspx, [accessed on March 2nd, 2004].

SKB, (2004b) "Clab – Central interim storage facility for spent nuclear fuel", [WWW] URL:http://www.skb.se/templates/SKBPage____3333.aspx, [accessed on March 2nd, 2004].

SKB, (2004c) "Äspö Hard Rock Laboratory - Projects", [WWW] URL:http://www.skb.se/templates/SKBPage.aspx?id=3352, [accessed on March 4th, 2004].

Sloper, N.J. (1997) "The development of a new three dimensional numerical model for fully coupled heat, moisture and air flow in unsaturated soil incorporating scientific visualisation and parallel computing techniques", *PhD Thesis,* University of Wales, Cardiff, UK.

Sonneveld, P., (1989) "CGS, a fast laczos-type solver for non-symmetric linear systems", *SIAM J. Sci. Stat. Comput.,* **10**, No1, 36-52.

Stenberg, L., (1994) "Manual for field work in the TBM tunnel. Documentation of the geological, geohydrological and groundwater chemistry conditions in the TBM tunnel", *SKB*, Progress report 25-95-13.

Stephansson, O., Tsang, C.F., and Kautsky, F., (2001) "Foreword", *International Journal of Rock Mechanics and Mining Sciences*, **38**, 1-4.

Stigsson., M., Outters, N. and Hermansson., J., (2001) "Äspö HRL – Prototype Repository. Hydraulic DFN Model No. 2", *SKB*, IPR-01-39.

Stille, H., and Olsson, P., (1996) "Summary of rock mechanical results from the construction of Äspö Hard Rock Laboratory", *SKB*, HRL-96-07.

Sultan, N., Delage, P., and Cui, Y.J., (2002) "Temperature effects on the volume change behaviour of Boom Clay", *Engineering Geology*, **64**, 135-145.

Svemar, C. and Pusch, R., (2000) "Äspö HRL – Prototype Repository. Project description", FIKW-CT-2000-00055, *SKB*, IPR-00-30.

Terzaghi, K., (1936) "The shearing resistance of saturated soils and the angle of plates between the planes of shear", *Proceedings of the 1st ICSMFE*, Harvard, Mass., **1**, 54-56.

Terzaghi, K., (1943) "Theoretical soil mechanics", Wiley, New York.

Thomas, H.R., (1980) "Finite element analysis of shrinkage stresses in building materials", *Ph.D. Thesis*, University College, Swansea, U.K.

Thomas, H.R., (1985) "Modelling two-dimensional heat and moisture transfer in unsaturated soils, including gravity effects", *International Journal of Analytical Methods in Geomechanics*, **9**, 573-588.

Thomas, H.R., (1987) "Non-linear analysis of heat and moisture transfer in partly saturated soil", *Journal of Engineering Mechanics, American Society of Civil Engineering*, **113**, 1163-1180.

Thomas, H.R., (1988a) "A non-linear analysis of two-dimensional heat and moisture transfer in partly saturated soil", *International Journal of Analytical Methods in Geomechanics*, **12**, 31-44.

Thomas H.R., (1988b) "The influence of non-linear thermal parameters on moisture content distributions in unsaturated soil", *International Journal of Analytical Methods in Engineering*, **26**, 263-279.

Thomas, H.R., and Cleall, P.J., (1997) "Chemico-osmotic effects on the behaviour of unsaturated expansive clays", *Geoenvironmental engineering, Contaminated ground: fate of pollutants and remediation*, Yong, R.N. and Thomas, H.R., eds., Thomas Telford, London, 272-277.

Thomas, H.R., and Cleall, P.J., (1999) "Inclusion of expansive clay behaviour in coupled thermo hydraulic mechanical models", *International Journal of Engineering Geology*, **54**, 93-108.

Thomas, H.R. and Cleall, P.J., (2000) "A validation exercise for THM modelling in unsaturated soil", *Proc. of European Congress on Computational Methods in Applied Sciences and Engineering*, ECCOMAS 2000, Barcelona.

Thomas, H.R., Cleall, P.J., Chandler, N., Dixon, D. and Mitchell, H.P., (2003a) "Water infiltration into a large-scale in-situ experiment in an underground research laboratory", *Géotechnique*, **53**, No. 2, 207-224.

Thomas, H.R., and Ferguson, W.J., (1999) "Fully coupled heat and mass transfer model incorporating contaminant gas transfer in an unsaturated porous medium", *Computers and Geotechnics*, **24**, No. 1., 65-87.

Thomas, H.R., and He, Y., (1994) "An elasto-plastic analysis of the thermo/hydraulic/mechanical behaviour of unsaturated soil", *Proceedings of the 8th International Conference on Computer Methods and Advances in Geomechanics*, Morgantown, Siriwardane, H.J. and Zaman, M.M. eds., Balkema, Rotterdam, 1171-1176.

Thomas, H.R., and He, Y., (1995) "Analysis of coupled heat, moisture and air transfer in a deformable unsaturated soil", *Géotechnique*, **45**, No. 4., 677-689.

Thomas, H.R and He, Y., (1998) "Modelling the behaviour of unsaturated soil using an elasto plastic constitutive relationship", *Géotechnique*, **48**, No. 5., 589-603.

Thomas, H.R., He, Y., and Onofrei, C., (1998a) "An examination of the validation of a model of the hydro/thermo/mechanical behaviour of engineered clay barriers", *International Journal of Numerical and Analytical Methods in Geomechanics*, **22**, 49-71.

Thomas, H.R., He, Y., Ramesh, A., Zhou, Z., Villar, M.V., and Cuevas, J., (1994a) "Heating unsaturated clay – An experimental and numerical investigation", *Proceedings of the 3rd International Conference on Numerical Methods in Geotechnical Engineering*, Manchester, *Numerical Methods in Geotechnical Engineering*, Smith, I.M., (eds.), A.A. Balkema, Rotterdam, 181-186.

Thomas, H.R., and King, S.D., (1991) "Coupled temperature/capillary potential variations in unsaturated soil", *Journal of Engineering Mechanics*, American Society of Civil Engineers, **117**, No. 11, 2475-2491.

Thomas, H.R., and Li, C.L.W., (1991) "A parallel computing solution of coupled flow processes in soil", *Journal of Computing in Civil Engineering*, American Society of Civil Engineers, **5**, No. 4, 428-443.

Thomas, H.R., and Rees, S.W., (1988) "The use of Lee's algorithm in the analysis of some ground heat and mass transfer problems", *Proceedings of the 6th International Conference on Numerical Methods in Geomechanics*, Innsbruck, Austria.

Thomas, H.R., and Rees, S.W., (1990) "An examination of the performance of a 3-level time stepping algorithm – Coupled heat and mass transfer computing", *Proceedings of the 1st International Conference, Advances in Computer Methods in Heat Transfer*, Southampton, U.K.

Thomas, H.R., and Rees, S.W., (1993) "The numerical simulation of seasonal soil drying in an unsaturated clay soil", *International Journal of Numerical and Analytical Methods in Geomechanics*, **17**, No. 1, 119-132.

Thomas, H.R., Rees, S.W., and Sloper, N.J., (1998b) "Three-dimensional heat, moisture and air transfer in unsaturated soils", *International Journal of Numerical and Analytical Methods in Geomechanics*, **22**, No. 2, 75-95.

Thomas, H.R., and Sansom, M.R., (1995) "A fully coupled analysis of heat, moisture and air transfer in unsaturated soil", *Journal of Engineering Mechanics, American Society of Civil Engineering*, **12**, No. 3., 392-405.

Thomas, H.R., Sansom, M.R., Volckaert, G., Jacobs, P., and Kumnam, M., (1994b) "An experimental and numerical investigation of the hydration of compacted powdered Boom clay", *Proceedings of the 3rd International Conference on Numerical Methods in Geotechnical Engineering*, Manchester, *Numerical Methods in Geotechnical Engineering*, Smith, I.M., (eds.), A.A. Balkema, Rotterdam, 135-142.

Thomas, H.R., Yang, H.T., and He, Y., (1997) "A sub-structuring based parallel solution of coupled thermo-hydro-mechanical modelling of unsaturated soil". *Engineering computations*, **16**, No.4, 428-442.

Thomas, H.R., Yang, H.T., He, Y. and Cleall, P.J., (2003b) "A multi-level parallelised substructuring frontal solution for coupled thermo/hydro/mechanical problems in unsaturated soil", *International Journal for Numerical and Analytical Methods in Geomechanics*, **27**, 951-965.

Thomas, H.R., and Zhou, Z., (1995) "A comparison of field measured and numerically simulated seasonal ground movement in unsaturated clay", *International Journal for Numerical and Analytical Methods in Geomechanics*, **19**, 249-265.

Thomas, H.R., Zhou, Z., and He, Y., (1992) "Analysis of consolidation of unsaturated soils", *Proceedings of the 2nd Czechoslovak Conference on Numerical Methods in Geomechanics*, Prague, Dolezalova, M., eds., **1**, 242-247.

Thorstenson, D., and Pollock, D.W., (1989) "Gas transport in unsaturated zones: Multicomponent systems and the adequacy of Fick's laws", *Water Resources Research*, **25**, No. 3., 477-507.

Truesdell, C., and Toupin, R., (1960) "Classical field theories", *Encyclopaedia of Physics*, Flugge, S., (eds.), III/1, Springer-Verlag, West Berlin.

Tsang, C-F., Stephansson, O., Kautsky, F. And Jing, L., (2003) "An overview of the DECOVALEX Project on coupled THM processes in fractured rock-bentonite systems", *Proceedings from the International Conference on Coupled T-H-M-C Processes in Geo-systems*, GeoProc 2003, Stockholm, Sweden.

Tullborg, E-L., (1995) "Mineralogical and chemical data on rocks and fracture minerals from Äspö", *SKB*, Technical note 25-95-07g.

United Nations, (1992) "United Nations Framework Convention on Climate Change"

Van der Vorst, H.A., (1989) "High performance preconditioning", *SIAM, J. Sci. Stat. Comput.* **10**, No. 6, 1174-1185.

Van der Vorst, H.A., (1992) "Bi-CGSTAB: A fast and smoothly converging variant of Bi-CG for the solution of non-symmetrical linear systems", *SIAM J. Sci. Stat. Comput.*, **13**, No. 2, 631-644.

Van der Vorst, H.A., (1994) "Recent developments in Hybrid CG methods", *Lecture notes in computer science 797*, High performance computing and networking, international conference and exhibition, Munich, Germany, April, Proceedings, Volume II: Networking and Tools. ISBN 3-540-57981-8.

Villar, M.V., (1999) "Investigation of the behaviour of bentonite by means of suction-controlled oedometer tests", *Engineering Geology*, **54**, 67-73.

Villar, M.V., Cuevas, J., and Martin, P.L., (1996) "Effects of heat/water flow interaction on compacted bentonite: Preliminary results", *Engineering Geology*, **41**, 257-267.

Volckaert, G., Imbert, C., Thomas, H.R., and Alonso, E.E., (1996) "Modelling and testing of the hydration of clay backfilling and sealing materials", *End of Contract Report on CEC*, Contract No. F12W-CT90-0033.

Wan, A.W.L., Gray, M.N., and Graham, J., (1995a) "On the relations of suction, moisture content, and soil structure in compacted clays", *Proceedings of the 1st International Conference on Unsaturated Soils*, Paris, France, June 6-8, 1995, 215-222.

Wan, A.W.L., Gray, M.N., and Chandler, N., (1995b) "Tracking in situ moisture transients in heated clay", *Proceedings of the 1st International Conference on Unsaturated Soils*, Paris, France, June 6-8, 1995, 925-932.

Wang, C., (1953) "Applied Elasticity", McGraw-Hill Book Co.

Wang, J., (2000) "Transient and dynamic thermo/hydraulic/mechanical behaviour of partially saturated soil", *Ph.D thesis*, University of Wales, Cardiff, U.K.

Welsh e-Science Centre (WeSC), (2004) "The Internet Bytes Back. Grid research at the Welsh e-Science Centre", *Annual Research Review*, Cardiff University, UK.

Wheeler, S.J., and Karube, D., (1996) "Constitutive modelling", *Proceedings of the 1st International Conference on Unsaturated Soils*, Alonso E.E., and Delage, P., (eds.), Paris, Published by A.A. Balkema, **3**, 1323-1356.

Wheeler, S.J., Sharma, R.S. and Buisson, M.S.R., (2003) "Coupling of hydraulic hysteresis and stress-strain behaviour in unsaturated soil", *Géotechnique*, **53**, No. 1, 41-54.

Wheeler, S.J., and Sivakumar, V., (1995) "An elasto-plastic critical state framework for unsaturated soil", *Géotechnique*, **45**, No. 1., 35-53.

Whitaker, S., (1977) "Simultaneous heat, mass and momentum transfer in porous media: A theory of drying", *Advances in Heat Transfer*, **14**, 119-203.

Wikman, H., Kornfält, K-A., Riad, L., Munier, R. and Tullborg, E-L., (1988) "Detailed investigations of the drillcores KAS 02, KAS 03 and KAS 04 on Äspö Island and KLX 01 at Laxemar", *SKB*, Progress report 25-88-11.

Winberg, A., Andersson, P., Poteri, A., Cvetkovic, V., Dershowitz, W., Hermanson, J., Gómez-Hernández, J.J., Hautojärvi, A., Billaux, D., Tullborg, E.V., Holton, D., Meier, P. and Medina, A., (2003) "Final report of the TRUE Block Scale project. 4. Synthesis of flow, transport and retention in the block scale", SKB, TR-02-16.

Wood, D.M., (1990) "Soil behaviour and critical state soil mechanics", Cambridge University Press, Cambridge.

Yang, D.Q., Rahardjo, H., Leong, E.C., Choa, V., (1998) "Coupled model for heat, moisture, air flow and deformation problems in unsaturated soils", *Journal Engineering Mechanics*, **124**, No.12, 1331-1338

Yong, R.N., Japp, R.D., and How, G., (1971) "Shear strength of partially saturated clays", *Proceedings of the 4th Asian Reg. Conference on Soil Mechanics and Foundation Engineering*, Bangkok, **2**, No. 12, 183-187.

Yong, R.N., and Mohamed, A.-M.O., (1996) "Evaluation of coupled heat and moisture flow parameters in a bentonite-sand buffer material", *Engineering Geology*, **41**, 269-286.

Yuen, C.K., (1997) "Parallel programming - A critique", *Parallel communication*, **23**, 369-380.

Zakaria, I., (1995) "Yielding of unsaturated soil", *PhD thesis*, University of Sheffield, UK.

Zhou, Y., (1998) "Non-linear Thermo-Hydro-Mechanical behaviour of saturated and unsaturated porous media", *PhD. Thesis*, University of Manitoba, Canada.

Zhou, Y., Rajapakse, R.K.N.D., Graham, J. (1998) "Coupled heat-moisture-air transfer in deformable unsaturated media", *Journal of Engineering Mechanics*, **124**, no. 10, 1090-1099.

Zienkiewicz, O.C., and Morgan, K., (1982) "Finite elements and approximations", *John Wiley and Sons Ltd*, USA

Zienkiewicz, O.C., and Taylor, R.L., (1989) "The finite element method", *McGraw Hill*, 4th edition.